Design and synthesis of modified peptide antibiotics of the vancomycin family

A thesis presented by

Philip Andrew Bone

Submitted in accordance with the requirements for the degree of

Doctor of Philosophy

The University of Leeds

School of Chemistry

March 2008

The candidate confirms that the work submitted is his own and that appropriate credit has been given where reference has been made to the work of others.

Acknowledgements

I would like to thank my supervisors Prof. A. Peter Johnson and Dr Colin W.G. Fishwick for giving me the opportunity to work on such an interesting and demanding PhD Project. Their endless supply of ideas and suggestions has been inspiring and their input throughout the course of my PhD has been invaluable.

I would like to thank Tanya Marinko-Covell for all the mass spectrometer data, Simon Barrett for the NMR data, Jacqui Colley and Jim Titchmarsh for analytical and preparative HPLC.

I would also like to thank Dr Julieanne Bostock for performing the MIC determinations and Dr Alison Ashcroft for her help designing and performing the nanoelectrospray ionisation – mass spectrometry experiments.

Thanks are also due to all the past and present members of the Johnson and Fishwick synthetic group and the members of ICAMS. Particularly Shane Weaver for helping me learn to use SPROUT and Gilbert Besong for helping me to get started in the lab.
I would also like to thank all the researchers in lab G39a, who have all helped to make it a great place to work.

Particular thanks must be given to Laura Johnson, whose encouragement and support has helped me get through the most difficult parts of this project and who suffered the unenviable task of proof reading my thesis and is largely responsible for helping me make this document readable. Further thanks must go to Dan Clarke, who has been a good friend through-out my studies in Leeds, and shared the unenviable task of proof reading this document. All the errors that remain are my own.

A final thanks goes to the EPSRC who paid for all of this!

Abstract

The ability of bacteria to constantly evolve new methods of resistance to antibacterial therapies represents a constant challenge in medicine. Emergence of strains of enterococci and *S. Aureus* that show resistance to vancomycin is an alarming phenomenon, as vancomycin represents the last line of defence against pathogens with a significant level of resistance to all other available therapies, methicillin resistant *S. Aureus* (MRSA) being a prime example of such a pathogen.

Vancomycin has a number of significant advantages as a drug therapy. It exploits a target that is not found in the host cells, the cell wall. It does this by inhibiting transpeptidation, which blocks murein biosynthesis, destabilising the cell wall and allowing the internal osmotic pressure of the cell to cause the cell membrane to rupture, killing the cell. The target of vancomycin is on the outside of the cell, so it is not affected by the membrane bound efflux pumps that induce multi-drug resistance. Therefore the only mechanism of resistance available is alteration of the target. Two such resistance mechanisms exist and if these can be overcome, the analogues of vancomycin that achieve this should be less prone to drug resistance than any other existing therapy.

This work represents the first step towards such a goal, and is the first example of the application of rational drug design to complex natural product drugs, like vancomycin. This project used an X-ray crystal structure of vancomycin complexed to a mimic of the cell wall peptide. This structure was used in conjunction with the *de novo* design program SPROUT as the basis for molecular design, in order to create analogues of vancomycin that were predicted to offer increased affinity for the tripeptide cell wall mimic. Five such designed molecular templates were created and assessed for synthetic feasibility. One of these templates was selected and synthesised. This analogue prompted a second design phase which produced a further three molecular templates, two of which were also synthesised. The efficiency of these modified vancomycins to bind the target tripeptide was assessed using nanoelectrospray ionisation – mass spectrometry. It was found that all the analogues produced offered increased binding efficiency as compared to vancomycin tested under the same conditions. This work paves the way to exploring the use semi-synthetic derivatives of vancomycin as novel therapeutic agents.

Contents

Table of Figures

Table of Tables

Abbreviations

Ac	acetyl
AcCl	acetyl chloride
AcOH	acetic acid
ADP	adenosine diphosphate
Ala, A	alanine
ATP	adenosine triphosphate
*p*ABA	*p*-aminobenzoic acid
Bn	benzyl
BOC	*tert*-butoxycarbonyl
^{t}Bu	*tert*-butyl
c	concentration
CDP	crystalline degradation product
clogP	log of partition coefficient between octanol/water
DAP	diaminopimelic acid
DBU	1,8-diazabicyclo[5.4.0]undec-7-ene
DCC	*N*,*N*'-dicyclohexylcarbodiimide
DCE	dichloroethane
DCM	dichloromethane
DCU	dicyclohexylurea
DHF	dihydrofolic acid
DHFR	dihydrofolate reductase
DHFS	dihydrofolate synthase
DHP	dihydropteroic acid
DHPPP	7,8-dihydropterin-pyrophosphate
DHPS	dihydropteroate synthase
DIPEA	diisopropylethylamine (Hünig's base)
dis	disconnection
DL-DAP	*meso*-diaminopimelic
DMAP	*para*-dimethylaminopyridine
DMF	*N*,*N*-dimethylformamide
DMSO	dimethylsulphoxide
DNA	deoxyribonucleic acid
EDC	1-ethyl-3-(3-dimethylaminopropyl)-carbodiimide

	hydrochloride
EF	elongation factors
eq.	equivalent (s)
Et	ethyl
Et_3N	triethylamine
Ether	diethyl ether
EtOAc	ethyl acetate
EtOH	ethanol
ESI	electrospray ionisation
GDP	guanidine diphosphate
GTP	guanidine triphosphate
HATU	*O*-(7-aabenzotriazol-1-yl)-*N*,*N*,*N*',*N*`-tetramethyluronium hexafluorophosphate
HBTU	*O*-benzotriazol-1-yl-*N*,*N*,*N*',*N*'-tetramethyluronium hexafluorophosphate
Hex	hexapeptide
HOBt	1-hydroxybenzotriazole
HPLC	high performance liquid chromatography
Hrs	hours
IF	initition factors
lac	lactate
LCMS	liquid chromatography – mass spectrometry
Lys, K	lysine
Me	methyl
MIC	minimum inhibitory concentration
Mp	melting point
mRNA	messenger ribonucleic acid
MRSA	methicillin resistant *Staphylococcus Aureus*
MS	mass spectrometry
NADPH	nicotinamide adenine dinucleotide phosphate
NAM	*N*-acetylmuramic acid
NMR	nuclear magnetic resonance
Nts	nucleotides
PBP	penicillin binding protein
Ph	phenyl

ppm	parts per million
RF	release factors
RNA	ribonucleic acid
rRNA	ribosomal ribonucleic acid
RT	room temperature
SEM	β-trimethylsilylethoxymethyl
Ser, S	serine
SPR	surface plasmon resonance
THFA	tetrahydrofolic acid
THF	tetrahydrofuran
TFA	trifluoroacetic acid
TLC	thin layer chromatography
TMS	trimethylsilyl
TMSE	trimethylsilylethyl
tRNA	transfer ribonucleic acid
UDP	uridine diphosphate
UDP-NAG	*N*-acylglucosamine uridine diphosphate
UDP-NAM	*N*-acetylmuramic acid uridine diphosphate
UV	ultraviolet
VISA	vancomycin intermediate *S. aureus*
VRE	vancomycin resistant enterococci

Chapter One

Project Introduction

1.1 Introduction

In order to design good drug treatments, it is important to understand the nature of the disease processes involved. This is as true in the field of antibiotics, as it is in any other area of medicinal chemistry. Therefore an understanding of the structure of bacteria and their biochemistry is a crucial tool in antibacterial drug design. In particular, knowledge of the inherent differences between pathogenic bacterial cells and cells of their mammalian hosts is invaluable when attempting to produce drugs that are able to selectively damage bacterial cells, whilst minimising disruption to the host cell's biochemistry.

1.2 Bacteria

Bacteria are probably the most abundant form of life on the planet and billions live on the skin and in the intestinal track of every animal. Most of these are benign and even beneficial, helping in digestion. Occasionally, they are pathogenic and infection causing. This may be the result of bacteria normally present growing out of control, like the enterococci in *Pseudomembranous colitis*, or by introduction of a pathogenic species such as *E. coli*, which causes food poisoning or *S. aureus*, which infects wounds. Bacteria are prokaryotic and all share a similar cell construction. Shown below is a depiction of a typical bacterial cell (Figure 1.1).

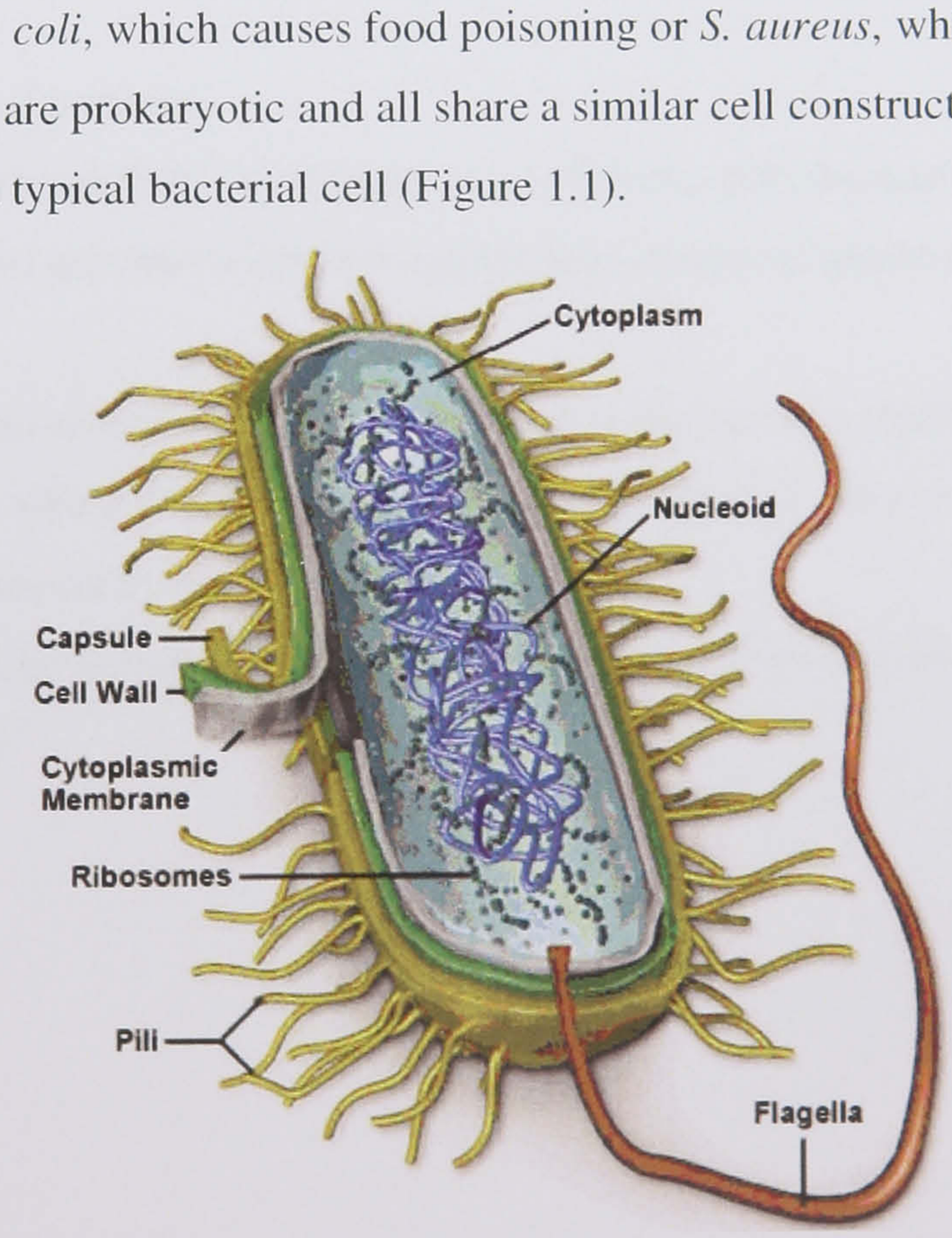

Figure 1.1. A typical cell.

Some of these features are highly variable like the pili and flagella, but most are highly conserved. The more conserved structures are of more interest as antibacterial targets.[1]

The most highly conserved portions are:

The nucleoid, this is the condensed form of the bacterial chromosome. It is a single double helix of DNA, that codes for all the major structures of the bacteria. There are secondary DNA elements called plasmids, which are present in most bacteria, which code for extra features and are very important in bacterial resistance. This is significantly different to humans who have 46 chromosomes and cannot make plasmids.

Ribosomes, these freely-floating structures are responsible for protein synthesis.

Cytoplasm, this is predominantly water and contains nutrients and additional components.

The cell membrane encloses the cytoplasm and controls movement of material in and out of the cell. There maybe one or two of these depending on the type of bacteria.

The cell wall, provides mechanical stability to the cell, preventing lysis by osmotic pressure when the cell is in a solution that is more dilute than the cytoplasm (a hypotonic solution).[1]

The least conserved portions:

The capsule, also termed the slime layer, is a gelatinous polysaccharide layer that encases the cell and provides a defence against the immune response of higher organisms.

Pili, are used in cell-to-cell recognition, allowing conjugation, a simplified from of sexual interaction where DNA is transferred but reproduction does not occur. They also allow invading bacteria to attach to the host cells.

Flagella, these whip-like appendages facilitate motion and more than one maybe present on the cell.[1]

1.3 Potential targets and existing therapies

1.3.1 Nucleic acid synthesis

The nucleic acid structure is significantly different in bacteria and mammalian cells. However, the genetic information needed to code for cell structures is stored as DNA and utilises transcription to RNA and translation to proteins as in eukaryotic cells.

Although the processes are similar in both cell types, there are considerable differences as prokaryotic bacterial cells have different enzymes to construct and manipulate their DNA and RNA.

These differences can be exploited in order to target pathogenic bacterial cells whilst having a minimal effect on the eukaryotic cells of the host. The two major opportunities for interfering with the nucleic acid synthesis in bacteria utilise these enzymatic differences between prokaryotic and eukaryotic cells. The first is direct interference with the enzymes responsible for RNA and DNA synthesis. The second involves indirectly interfering with nucleic acid synthesis by inhibition of folic acid production. Folic acid is an important co-factor in nucleic acid synthesis, but it is also important in many other cell functions and is therefore discussed in detail later.

1.3.1.1 DNA replication[2,3]

DNA replication occurs during mitotic cell division, where one bacterial cell copies its chromosome and divides into two daughter cells. It also takes place during plasmid replication whilst in conjugation to a second bacterial cell. Both of these processes rely on a large number of enzymes, but are subtly different and as conjugation is not vital for cell viability, only the effects on chromosome replication are considered here.

Of the many enzymes involved in DNA replication, two can be exploited as targets for inhibition of nucleic acid synthesis, they are: Topoisomerase II (also known as DNA gyrase, T-II) and Topoisomerase IV (T-IV).[4-7]

T-II is responsible for the negative supercoiling of DNA within the chromosome during replication.[4-6] This is an ATP dependent process, where one strand of the DNA helices

being produced is broken transiently to allow the other double helical strand to be passed through it, the helix is then rejoined without disruption to its genetic sequence. This relieves the strain produced in the newly formed DNA chains, a strain that arises due to the action of helicases, which unwind the double stranded helix into single stranded DNA allowing base pairing for replication. Once fully replicated, the intertwined DNA intermediates are freed from the enzyme and are described as catenated, this means that the two daughter DNA chromosomes are physically interlocked.

T-IV is responsible for decatenation,[7] which is also an ATP dependent process where one double strained helix is transiently cleaved and the other double stranded DNA helix is passed through the gap. The first strand is then rejoined and the two chromosomes are entirely separate. They can then be moved apart into the forming daughter cells, thus allowing the completion of cell replication.

1.3.1.2 Inhibitors of DNA replication

Novobiocin is an antibiotic derived from *Streptomyces niveus*. It binds to T-II and prevents hydrolysis of ATP. As ATP hydrolysis is a crucial step in the enzymatic pathway providing the energy for the enzyme to perform its function, this inhibits T-II blocking enzyme activity and terminating DNA replication (Figure 1.2).[6]

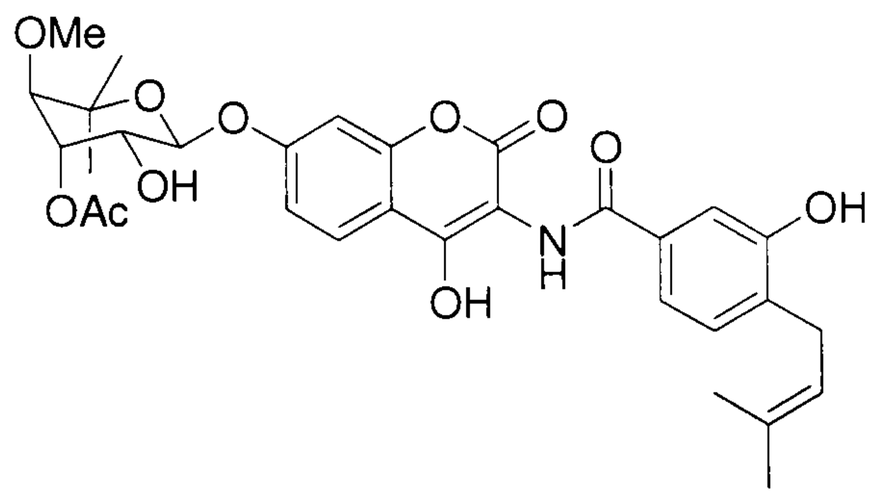

Figure 1.2. Novobiocin.

Another important class of drugs are the fluoroquinolones, which act by inhibiting either T-II or T-IV. Their specific activity depends on their structure and on the bacterial species; two members of this drug family are ciprofloxacin and sparfloxacin (Figure 1.3). Ciprofloxacin's primary mode of action is inhibition of T-II in Gram-negative pathogens and T-IV in Gram-positive pathogens, yet sparfloxacin, which is only slightly different in structure, inhibits T-IV as its primary mode of action in Gram-

positive bacteria.[5] In all cases these drugs work by stabilising the complex between the enzyme and the cleaved DNA strand, enhancing their ability to cleave DNA and thus turning the enzyme into a physiological poison.

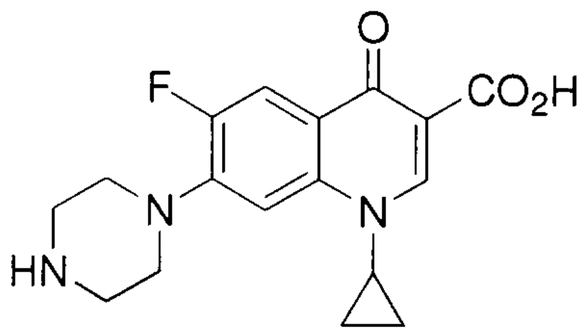

Ciprofloxacin

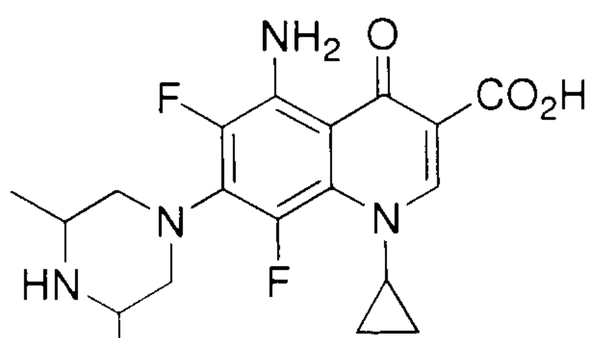

Sparfloxacin

Figure 1.3. Fluoroquinolone antibacterials.[5]

1.3.1.3 RNA synthesis[8,9]

RNA synthesis is a fundamental step in the cell cycle. It is intimately involved in the production of proteins and inhibition of RNA synthesis leads to rapid cell death by depletion of critical cell proteins. There are three predominant types of bacterial RNA: ribosomal RNA (rRNA), transfer RNA (tRNA) and messenger RNA (mRNA). These are also utilised in mammals and in both cases they are vital in the processes of transcription and translation, converting DNA into RNA and then RNA into proteins. However there are again enzymatic differences that can be exploited. In eukaryotic cells there are at least three RNA polymerases, for example human cells produce five, whereas bacterial cells posses only one. RNA polymerases are the enzymes responsible for joining one RNA base to the next to produce an RNA chain. The single RNA polymerase (RNAp) of bacteria is structurally similar to RNA polymerase I (RNAp-I) of eukaryotes. They have similar functions, as they are both DNA dependant RNA polymerases. Despite this, there are sufficient differences in their structures, which means that drug therapies which inhibit one have a minimal effect on the other.

1.3.1.4 Inhibitors of RNA synthesis

One inhibitor of the bacterial RNAp is rifampicin (Figure 1.4). Rifampicin works by blocking the channel that the elongating RNA proceeds along in the enzyme active site, thus preventing the elongation stage of RNA synthesis. This forces the release of the RNA strand after only two RNA bases have been joined.[10] This effectively terminates RNA synthesis and as a result protein production.

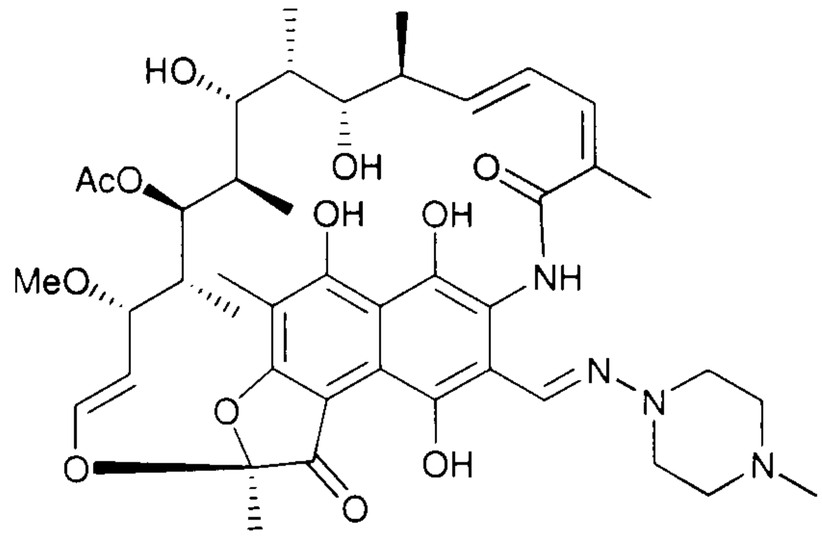

Figure 1.4. Rifampicin.[11]

1.3.2 Protein synthesis

Protein synthesis is one of the most significant aspects of the bacterial life cycle and in fact the life cycle of any cell, prokaryotic or eukaryotic. However this is significantly accentuated by the rapid growth of bacteria and the consequential high demand for protein production. In addition to their involvement in the cell structure, enzymes are proteins that catalyse essentially all cellular reactions and they are associated with the cell membranes to allow the uptake of nutrients, the expulsion of wastes and cell-to-cell interactions. Therefore any interruption to their production is highly damaging to cell growth.[12,13]

1.3.2.1 Ribosomes

Protein synthesis is facilitated by ribosomes, which are structures that are freely-floating in the bacterial cytoplasm and are composed of two subunits, each of which is a combination of ribosomal RNA and polypeptide chains. The significance of protein synthesis can be demonstrated by the prevalence of these structures in the bacterial cell. *E. coli* typically contain some 15 to 20 thousand of these structures, approximately 15% of the cell mass. [12,13]

The subunits are described as 30S and 50S and associate to give the complete ribosome, which is 70S. In this instance S stands for Svedberg unit, which is a measure of sedimentary velocity and is an expression of the particles density. It describes how fast a given particle will precipitate by centrifugation.[12,13]

The 30S subunit is smaller than the 50S component and contains one strand of rRNA, 16S, and 21 peptide chains. The 50S subunit contains two strands of rRNA, one 5S and

one 23S, and has 34 peptide chains. In both cases these components arrange in a highly organised way to produce the specific shape of each type of sub-unit. The distinct 3D shape of each sub-unit is highly conserved. This is crucial as the active site for translation is formed at the interface of these two subunits when they associate (Figure 1.5).[12,13]

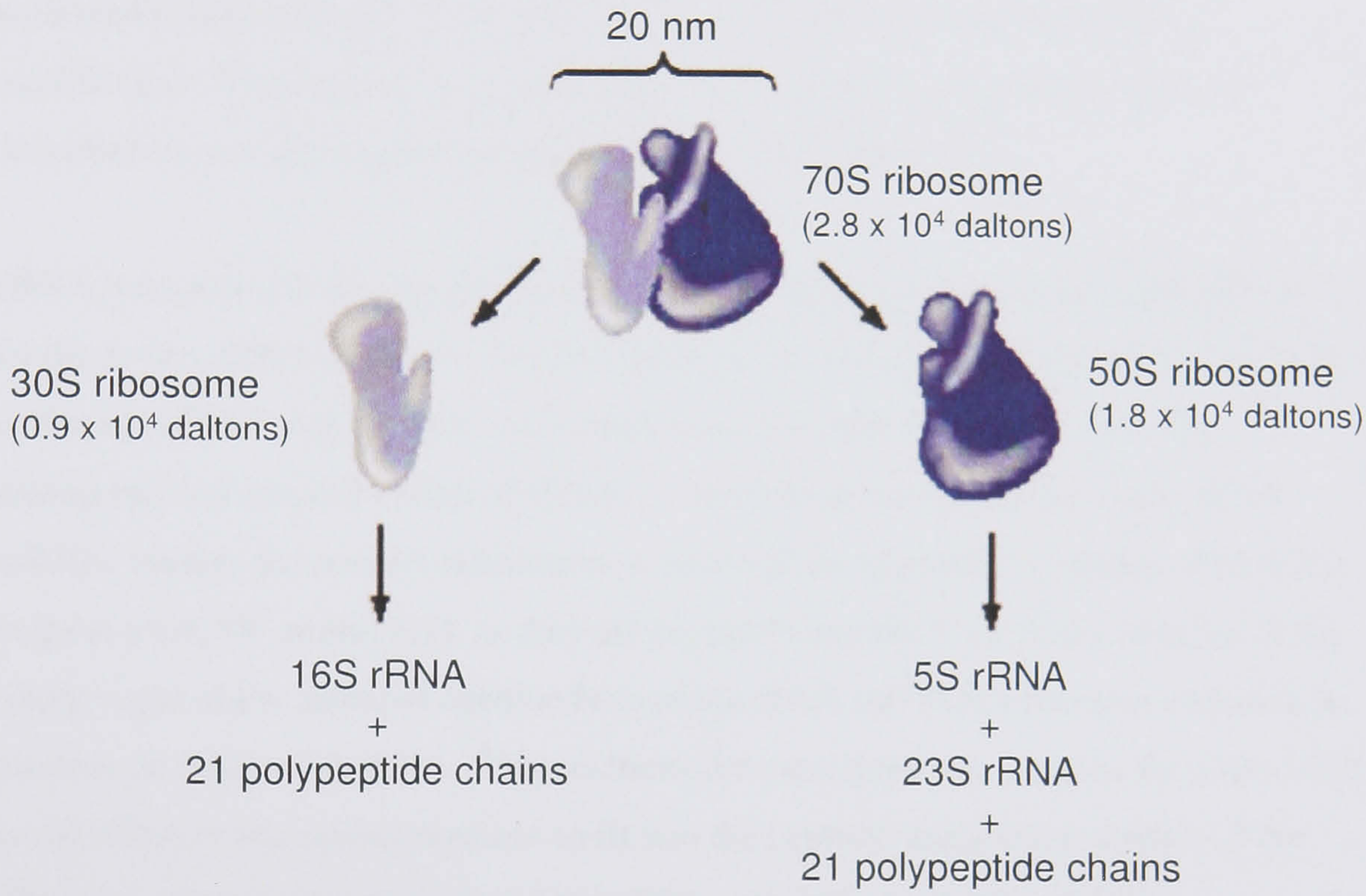

Figure 1.5. The 70S ribosome and its constituents.[12]

1.3.2.2 The synthetic sequence

The sequence of protein synthesis can be described as a three step series. It begins with initiation, the assembly of mRNA, the ribosome and an initiator. It then progresses through elongation, where the codon sequence is read sequentially and the corresponding amino acid assembled, and finishes with termination where the assembled protein is released and the mRNA and ribosome disengage from each other. However, before these sequences can be explained it is necessary to describe some important features of tRNA and mRNA.[12,13]

mRNA is essentially the blue-print of a protein, describing the linear structure of a protein. It works via codons; which are specific sequences of three adjacent base pairs that code for a single amino acid. They are read from the 5' end of the mRNA and code the protein from the *N*-terminus to the *C*-terminus. Three bases are necessary for each

codon as this leads to 64 possible combinations of base sequences (2 bases would give only 16 possibilities), this allows the system to code for the twenty different amino acids with some remaining codes to start and stop the process. Each of the amino acids have at least one distinct codon that codes for it in mRNA, but some are encoded by multiple codons. However any codon will only ever code for one amino acid. There is one codon for initiation (AUG), which also codes for methionine. All proteins begin with methionine although this maybe removed by post-translational protein modification. There are three codons that do not code for amino acids, these are described as stop and cause termination of peptide synthesis.[12,13]

tRNA is responsible for the positioning of amino acids in conjunction with mRNA. To facilitate this, tRNA possesses an anti-codon which is the reciprocal code to that of the codon on mRNA. Again, each anti-codon codes for only one amino acid. The arrangement of the anti-codon of tRNA, so that it base pairs with the codon of the mRNA, ensures the correct orientation of amino acids in peptide synthesis. The tRNA helps activate the amino acid, as they are acylated onto the 3'-hydroxy position of the ribose sugar of the terminal adenine base of the tRNA (all tRNA finish in adenine), to produce an aminoacyl-tRNA. This positions the ester bond that couples the amino acid to the tRNA in the correct position to fit into the peptidyl transferase domain of the ribosome, where it is activated and the tRNA can easily be displaced.[12,13]

Initiation

Initiation (shown in Figure 1.6) begins with the 30S sub-unit binding *N*-formylmethionyl-tRNA (fMet-tRNA), the interface of this complex presents the anti-codon of the tRNA and the 3' end of the 16S rRNA, together these form a binding site for the mRNA, the first codon pairs with the anti-codon of the tRNA. This pairing is usually AUG for the codon and gives UAC as the corresponding anti-codon on the tRNA, but it can also be GUG giving CAC as the anti-codon. The 50S subunit then binds to this to form the active ribosome-mRNA complex.[12,13] There are extra proteins involved in this sequence called initiation factors (IF) and these help to control the sequence of binding, in prokaryotes there are three of these, in eukaryotes there are more. They are numbered 1-3 in prokaryotes; IF-3 prevents binding of the 50S and 30S subunits before mRNA binding and promotes correct binding of the mRNA. IF-2 binds guanidine tri-phosphate (GTP) and fMet-tRNA directing the attachment of the fMet-tRNA to the 30S sub-unit and displacing IF-3. IF-1 appears to direct the addition of the

50S sub-unit, which results in the hydrolysis of GTP to guanidine di-phosphate (GDP). IF-1 then permits the loss of IF-2 and GDP to from the complete 70S ribosome-mRNA complex.[12,13]

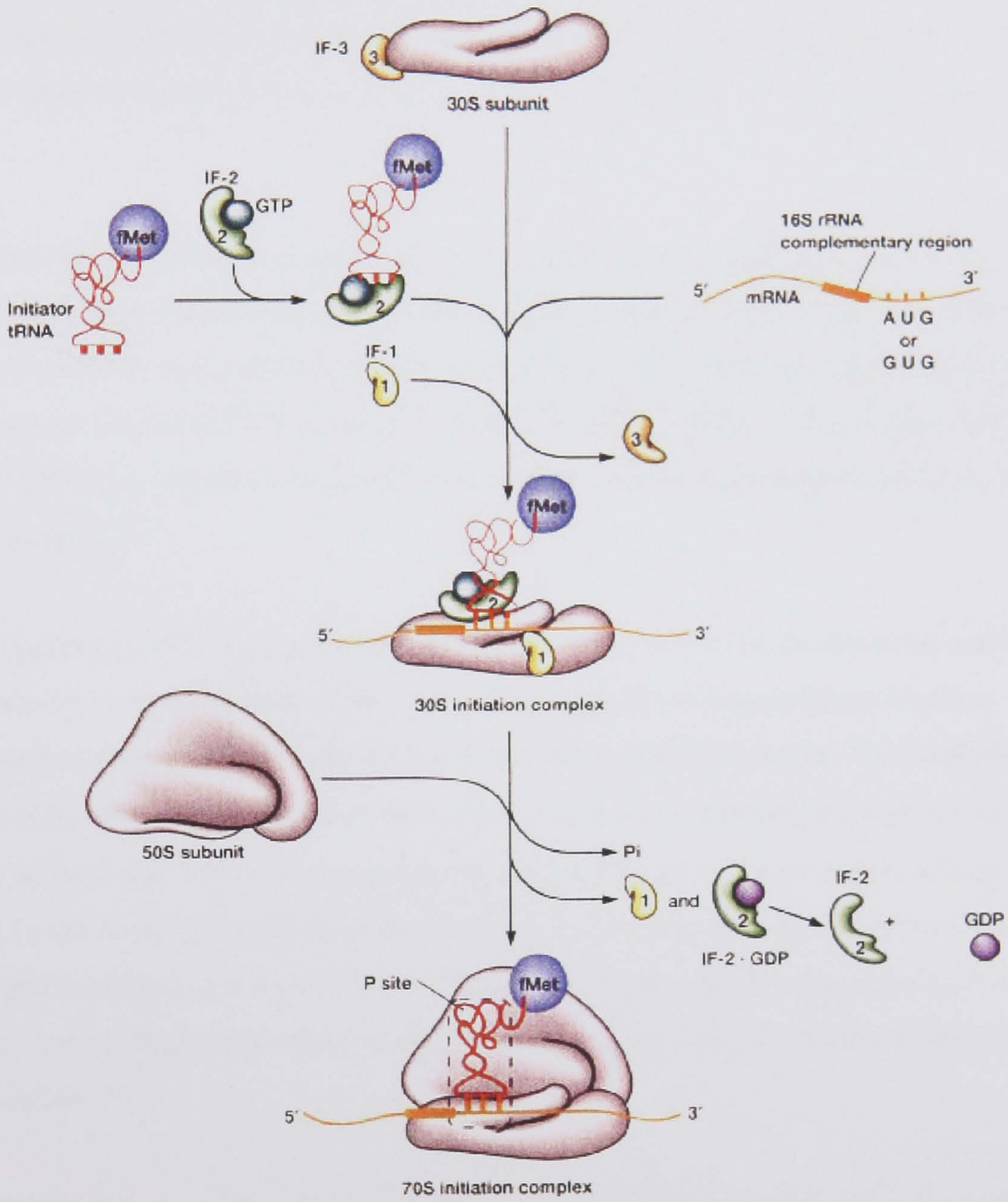

Figure 1.6. The initiation of protein synthesis.[12]

Elongation

Elongation is a cyclic process consisting of three steps, aminoacyl-tRNA binding, transpeptidation and translocation, which are repeated until every amino acid of the peptide has been added, as shown in Figure 1.7. These steps also rely on protein co-factors which are referred to as elongation factors (EF).[12,13]

Aminoacyl-tRNAs can be bound in three sites on the ribosome-mRNA complex, they are described as the peptidyl site (P site), the aminoacyl site (A site) and the exit site (E site) respectively. The tRNA carrying the growing peptide chain is always in the P site at the beginning of any elongation cycle (or fMet-tRNA if it's directly after initiation), the A site then takes the incoming aminoacyl-tRNA. For all cases the anti-codon of the tRNA must be complementary to the codon on the mRNA, ensuring the correct amino acid is delivered to the peptidyl transferase domain. The E site is unoccupied at this stage.

The binding of an aminoacyl-tRNA to the ribosome is made possible by EF-Tu, this co-factor binds GTP and an aminoacyl-tRNA and delivers them to the A site, where the aminoacyl-tRNA base pairs to the mRNA. This results in hydrolysis of the GTP to GDP and releases the EF-Tu GDP complex. The EF-Tu GDP complex is then regenerated to EF-Tu GTP by a second co-factor EF-Ts and binds another aminoacyl-tRNA ready for the next cycle.[12,13]

The appropriate tRNA now occupies both the P and the A sites of the ribosome and the second step of the elongation cycle begins. This stage is a transpeptidation reaction catalysed by the peptidyl transferase domain found on the 50S subunit. This catalytic site activates the α-carboxyl group of the amino acid that is forming the acyl link to the tRNA in the P site. This is then attacked by the α-amine group of the amino acid on the tRNA in the A site. This displaces the 3'-hydroxy of the ribose sugar, breaking the ester bond and forming a new peptide bond. This results in the peptide being one amino acid longer, and attached to the tRNA in the A site. The tRNA in the P site has no bound amino acids.[12,13]

Translocation is the final step in the elongation cycle. This step moves the ribosome one codon along the mRNA in the 3' direction. The tRNA that was in the P site now moves to the E site and leaves the ribosome, the tRNA bound to the peptide chain is transferred from the A site to the P site and this leaves the A site free for the next aminoacyl-tRNA. This complicated process is reliant on the co-factor EF-G, which is bound to another GTP and again the energy required is derived from the cleavage of an inorganic phosphate from the GTP to give GDP.[12,13]

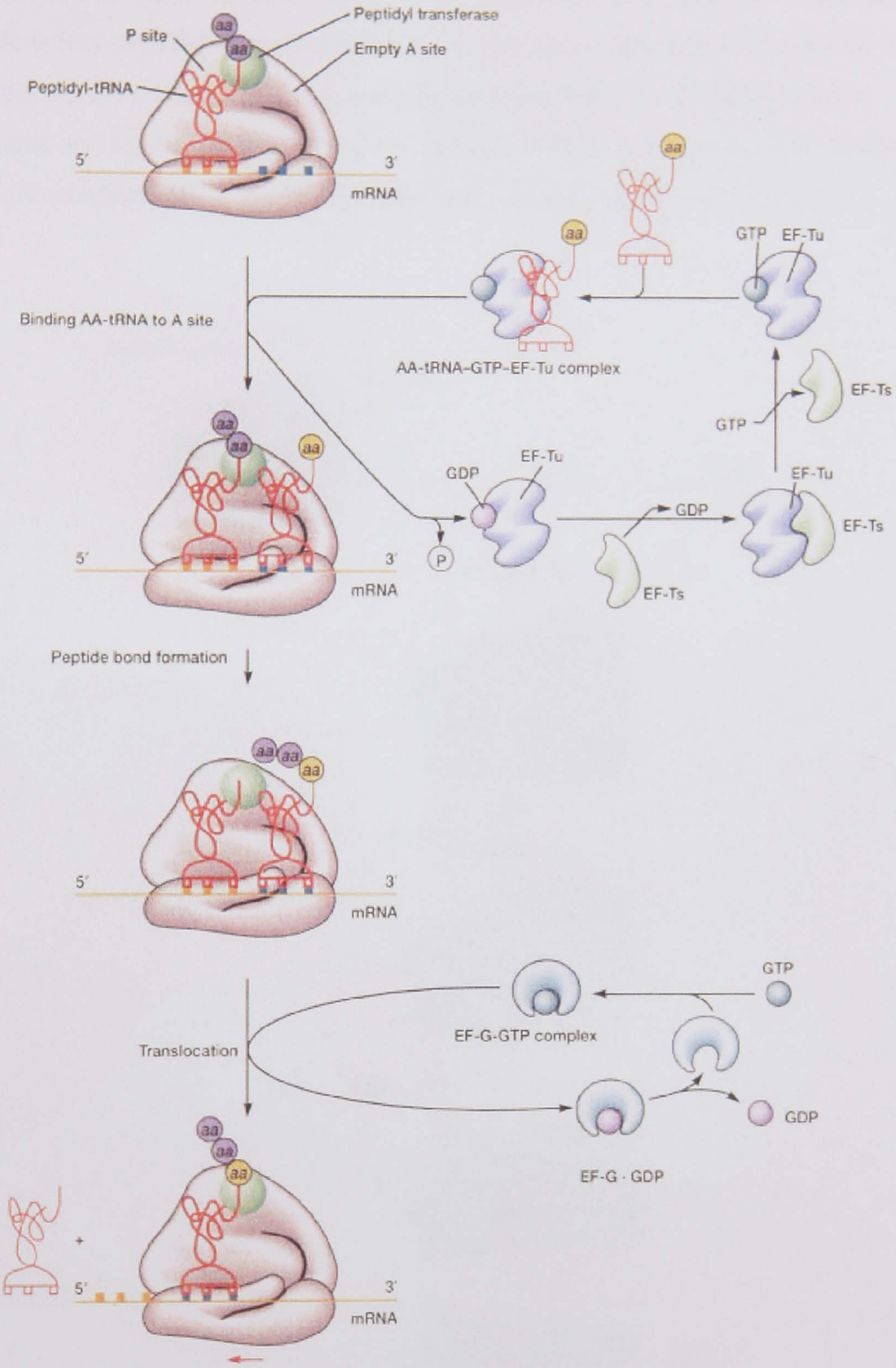

Figure 1.7. The elongation cycle.[12]

Termination

Termination (Figure 1.8) occurs when all the codons have been read, all the amino acids added and a nonsense codon enters the A site, these are UAA, UAG or UGA. At this point further protein co-factors are involved. These are the release factors 1 to 3 (RF-1, RF-2 and RF-3). These help recognise the stop codon and stimulate the cleavage of the

peptide from the tRNA in the P site by the peptidyl transferase domain. At this point the peptide is free and folds into the final tertiary structure of the protein and the tRNA is moved from the P site to the E site and released. The 50S and 30S subunits then dissociate and release the mRNA. At this point IF-3 binds again to the 30S subunit to block its association with the 50S sub-unit until another mRNA is in place.[12,13]

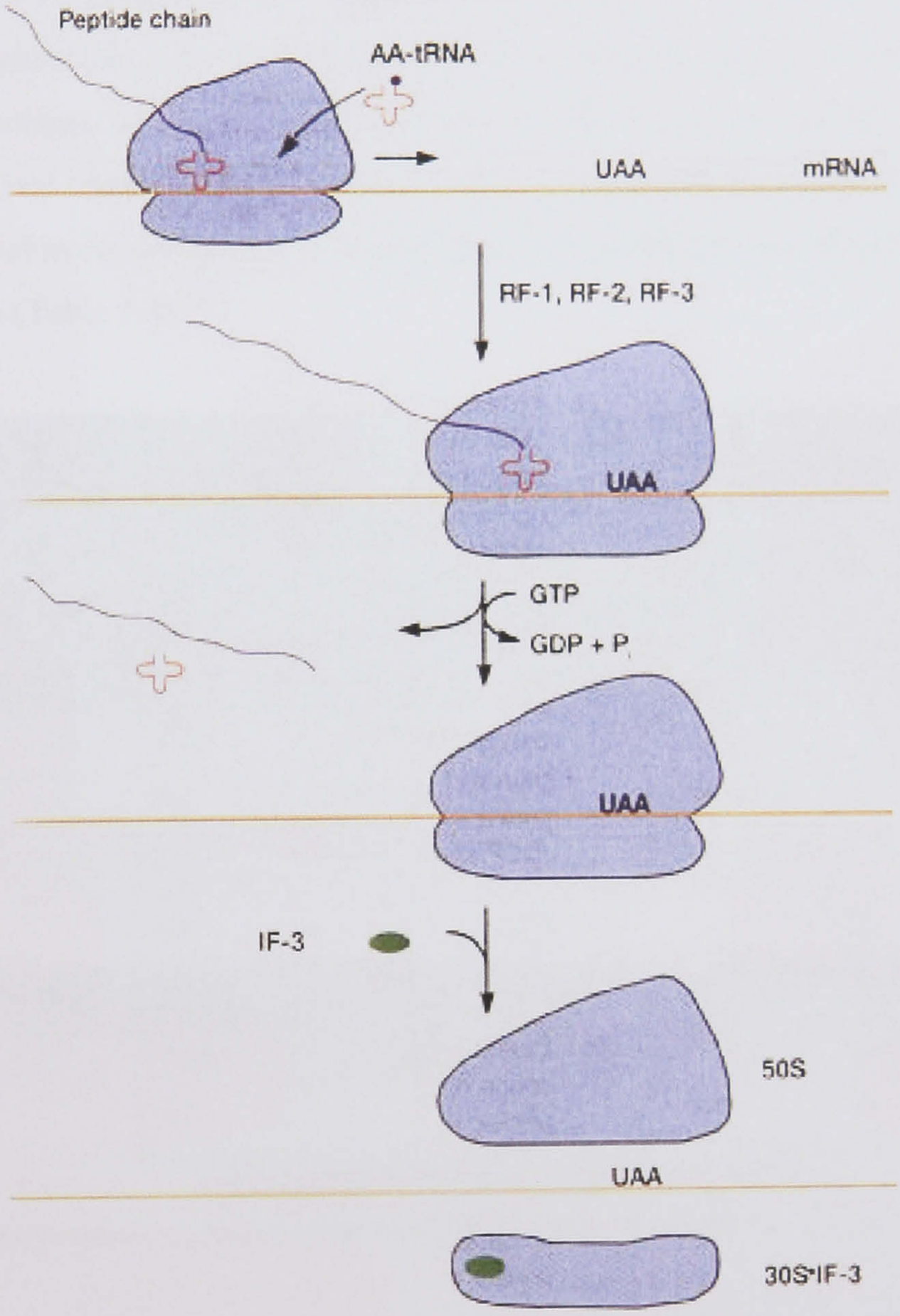

Figure 1.8. Termination of protein synthesis.[12]

1.3.2.3 Selectivity

As described at the beginning of this section, proteins are highly significant to all aspects of the cell and disruption to their production inhibits cell growth. The processes of translation are similar in both eukaryotes and prokaryotes and both are reliant upon mRNA, aminoacyl-tRNA and ribosomes. This introduces the possibility of toxicity if the host protein synthesis is inhibited by the antibacterial therapy. However, at the ribosome level differences can be observed. Prokaryotes have a single type of ribosome whereas eukaryotes have three types, cytosolic ribosomes which are 80S, membrane bound ribosome, which are also 80S but are attached to the endoplasmic reticulum and mitochondrial ribosomes, which are 55S. The cytosolic and membrane bound ribosome are identical in composition and can therefore be consider as one class of the 80S ribosomes (Table 1.1).[12-14]

Comparison of ribosome structure in prokaryotes, eukaryotes, and mitochondria						
	Bacterial (70S)		**Eukaryotic (80S)**		**Mitochondrial (55S)**	
Large Subunit	**50S**		**60S**		**39S**	
rRNAs (1 of each)	23S 5S	2904 nts 120 nts	28S 5S 5.8S	4700 nts 120 nts 160 nts	16S	1560 nts
Proteins	33		~49		48	
Small Subunit	**30S**		**40S**		**28S**	
rRNA	16S	1542 nts	18S	1900 nts	12S	950 nts
Proteins	21		~33		29	

Table 1.1. Ribosomes types and their properties.

(nts = nucleotides; ~ indicates these are typical values for peptides – variable upon species)[14]

Table 1.1 highlights potentially exploitable differences between these three ribosome types and these are sufficient enough to offer a high degree of selectivity. This selectivity is vital in order to minimise disruption to the host's protein synthesis. The bacterial ribosomes and the mitochondrial ribosomes show the greatest similarity, which is the origin of the most side-effects displayed by protein synthesis inhibitors. These side-effects are produced by inhibition of both the ribosomes of the pathogen and those of the host's mitochondria.[12-14]

1.3.2.4 Inhibitors of protein synthesis

There are a large number of drugs that inhibit protein synthesis. There are four main classes; the aminoglycosides, the macrolides, the tetracyclines and the oxazolidinones. There are also a number of individual compounds that also inhibit protein synthesis. The most significant of these is chloramphenicol. Of these only the aminoglycosides are bactericidal drugs, the others are bacteriostatic at therapeutic concentrations.

The aminoglycoside antibiotics are structurally related polycationic compounds containing at least two amino sugars. There is more than one binding site for these drugs in the 70S ribosomes. Streptomycin was one of the first drugs of this class to be discovered and hence is the most well studied. Streptomycin binds to the 30S sub-unit, whereas kanamycin has binding sites on both the 50S and the 30S subunit (Figure 1.9). The streptomycin binding site on the 30S ribosome appears to be unique, as there is no competition between streptomycin and the other aminoglycosides for this binding site. In addition, mutations of the 30S ribosome that offer resistance to streptomycin do not confer resistance to the other aminoglycosides, which reinforces the idea of different binding sites.[13]

Regardless of the binding site, the aminoglycosides all cause the misreading of the mRNA codons and induce the introduction of incorrect amino acids into the proteins that are synthesised whilst these drugs are bound to the ribosome. This produces proteins that have altered actions or are completely without function. It appears that many of these miscoded proteins become embedded in the cell membrane and change its permeability which maybe a significant contribution to the bactericidal activity of this class of compounds.[13]

It has also been noted that high concentrations of streptomycin can induce complete inhibition of protein synthesis by binding to the mRNA-70S ribosome complex either during or just after initiation and thus preventing the elongation cycle from occurring.[13,15]

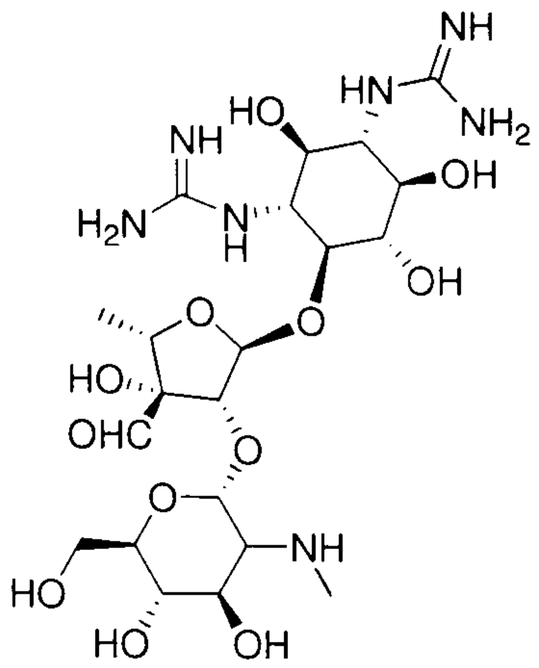

Streptomycin

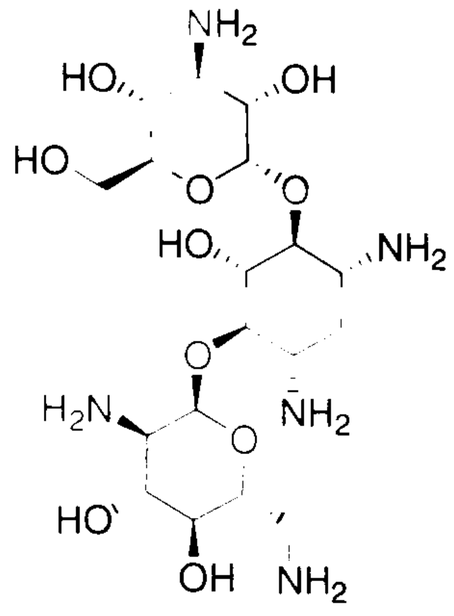

Kanamycin

Figure 1.9. Some aminoglycoside antibacterials.

The macrolides are macrocyclic lactones which inhibit protein synthesis by binding to the 50S ribosome near the peptidyl transferase site in the entrance of a tunnel that allows the egress of the newly formed peptide from the ribosome. This prevents the progress of the peptide through the tunnel and causes the premature release of the peptidyl-tRNA complex and terminates peptide synthesis. There are both natural and semi-synthetic macrolides, erythromycin is probably the most extensively used natural macrolide. However, many of the semi-synthetic macrolides exhibit greater activity, the semi-synthetic macrolide azithromycin is 2-8 fold more active (Figure 1.10).[16]

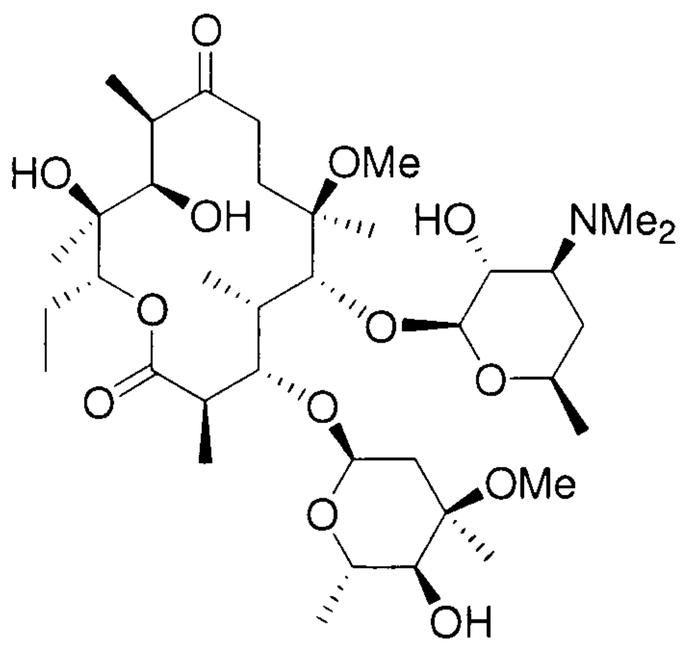

Erythromycin

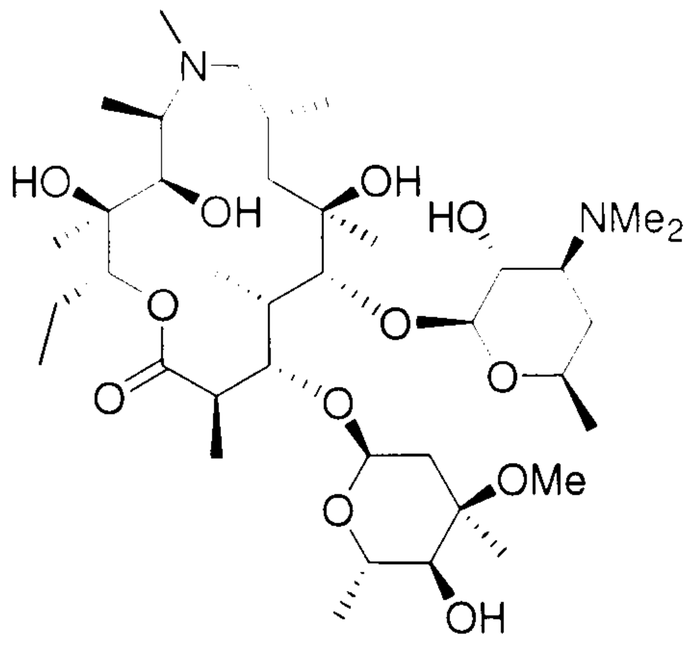

Azithromycin

Figure 1.10. Some macrolide antibacterials.

The tetracyclines are a series of compounds based around a linear fused ring system that incorporates both aromatic and non-aromatic rings. Tetracycline was the first discovered and lends its name to the whole class, 6-deoxy-demethyltetracycline is not a clinically significant antibiotic, but it possesses the minimum pharmacophore necessary for antibacterial activity (Figure 1.11). These compounds bind to the 30S ribosome sub-

unit and in the 70S ribosome, thus blocking the A site and preventing the binding of aminoacyl-tRNA, which terminates peptide synthesis.[17]

Tetracycline 6-Deoxy-demethyltetracycline

Figure 1.11. Some tetracycline antibacterials.

The oxazolidinones are unique in that they are totally synthetic drugs, unlike most other antibacterials. They bind to the 50S ribosome near to the peptidyl transferase domain but do not inhibit its action. They do however block the formation of the 70S ribosome, if they bind before the association of the 50S and 30S subunits. Alternatively, if binding occurs after association, they prevent the translocation of the peptidyl-tRNA from the A site to the P site. They posses relatively simple structures. Linezolid was the first of this class of drugs and is effective primarily against Gram-positive bacteria, ranbezolid is a newer oxazolidinone and shows activity against both Gram-positive and Gram-negative bacteria (Figure 1.12).[18,19]

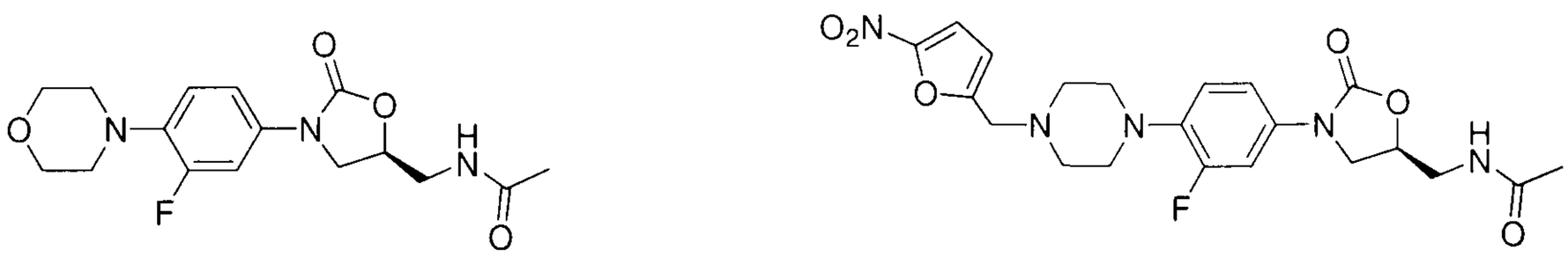

Linezolid Ranbezolid

Figure 1.12. Some oxazolidinones antibacterials.

Chloramphenicol is also produced synthetically but was originally isolated from *Streptomyces venezuelae*, it has a very simple structure and yet has a very broad range of activity (Figure 1.13). It prevents peptidyl transferase from linking the aminoacyl-tRNA in the A site to the nascent peptide on the tRNA in the P site by binding close to the peptidyl transferase domain on the 50S sub-unit and disrupting the binding of the aminoacyl portion of the aminoacyl-tRNA. It has no effect on the codon – anti-codon interaction.[13]

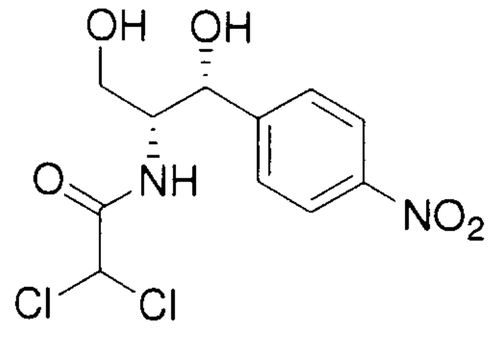

Figure 1.13. Chloramphenicol.

1.3.3 Folic acid synthesis

Reduced forms of folic acid are a crucial co-factor in a multitude of enzymes that are vital to cell growth. These enzymes rely on transfer of a single carbon and reduced folic acids act as the source of this carbon. Both RNA and DNA synthesis are reliant upon this co-factor, as the purine bases and thymidine are synthesised using reduced folic acid as a source of carbon. It is also a co-factor in the synthesis of glycine and methionine and therefore has a double impact upon protein synthesis as it is crucial for both access to amino acids and to the template (mRNA) from which the protein is synthesised.[13,20,21]

Bacteria must synthesise folic acid as they do not have the active transport proteins necessary to import it into their cells, in contrast mammals can not synthesise folic acid and must gain it from their diet.

Bacteria synthesise reduced folic acids in three steps from *p*-aminobenzoic acid, pteridine and glutamate. The first step is the addition of *p*-aminobenzoic acid (*p*ABA) and the pteridine, 7,8-dihydropterin-pyrophosphate (DHPPP), to give dihydropteroic acid (DHP). This is catalysed by dihydropteroate synthase (DHPS). The next step is addition of glutamate to give dihydrofolic acid (DHF) and this is catalysed by dihydrofolate synthase (DHFS). The final step is catalysed by dihydrofolate reductase (DHFR) and converts dihydrofolic acid to tetrahydrofolic acid (THFA) (Figure 1.14).[13,20,21]

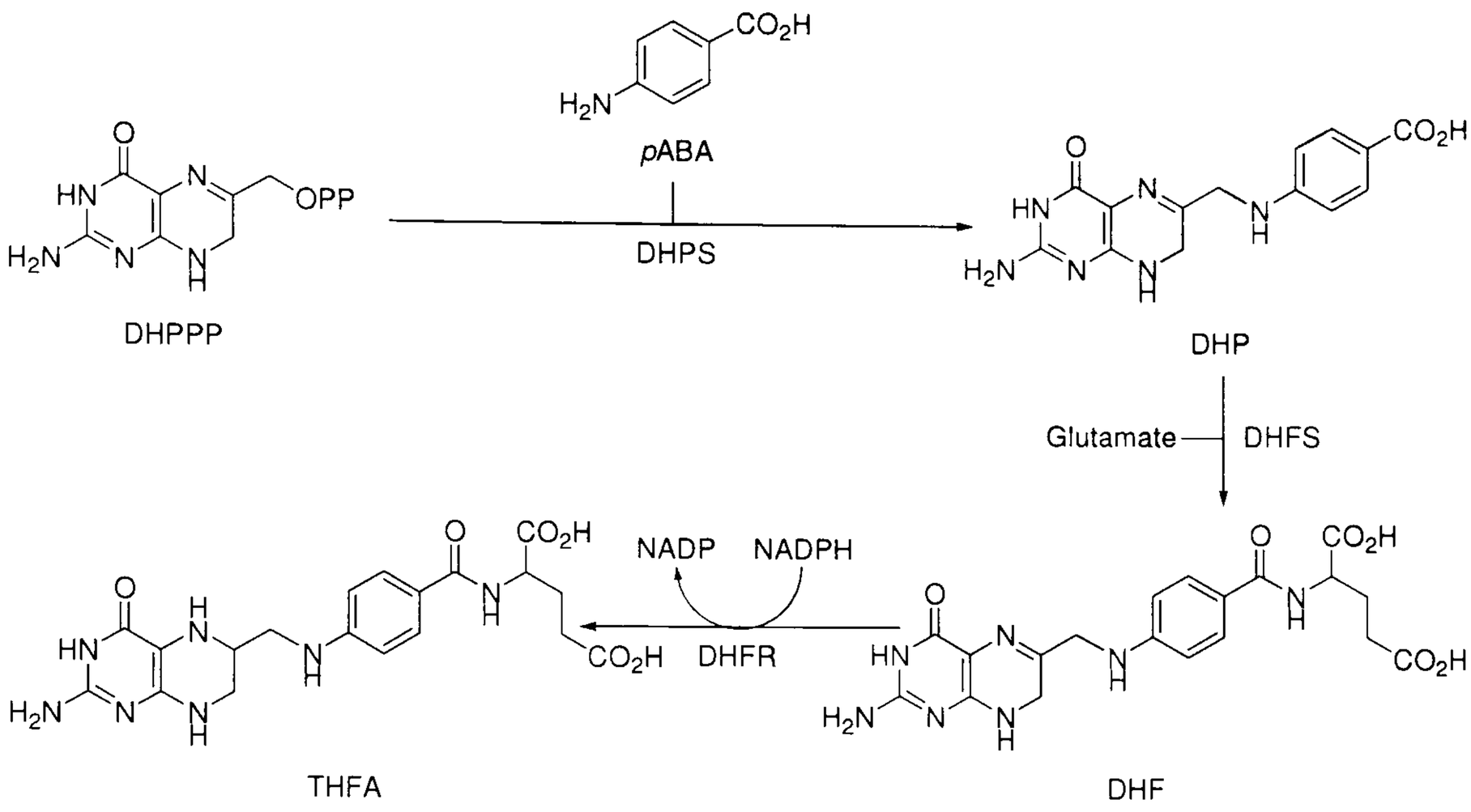

Figure 1.14. Synthesis of reduced folates.

1.3.3.1 Inhibitors of folic acid synthesis

Neither DHPS nor DHFS are present in mammalian cells and are therefore excellent targets for inhibition. However there are no clinically significant DHFS inhibitors. DHPS is inhibited by the sulfonamides, which are clinically significant drugs, used to treat urinary tract infections. They are mimics of *p*ABA and act by competitive inhibition of dHPS. Sulfamethoxazole is the major antibiotic of this type (Figure 1.15).[13,20,21]

Trimethoprim (Figure 1.15) inhibits DHFR and mimics the structure of the pteridine fragment of dihydrofolate. It also acts as a competitive inhibitor. It has a 60,000-fold selectivity for bacterial DHFR and is therefore selectively toxic, inhibiting only the bacterial enzyme at therapeutic levels.

Inhibition of either of these enzymes is sufficient to block DNA, RNA and protein synthesis, but this could only produce a bacteriostatic effect. Trimethoprim and sulfamethoxazole are routinely prescribed together and have a synergistic action, usually producing a bactericidal effect.[13,20,21]

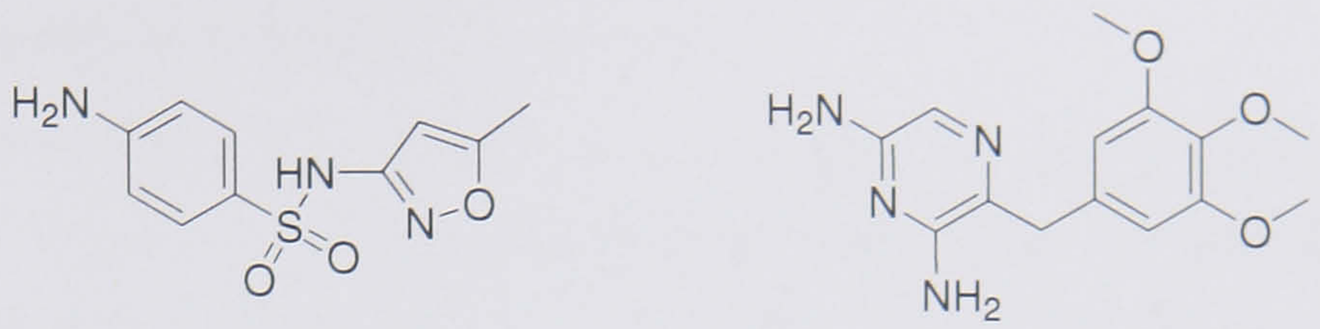

Sulfamethoxazole

Trimethoprim

Figure 1.15. Sulfamethoxazole and Trimethoprim.[13,20,21]

1.3.4 The cell membrane

The cell membrane of bacterial cells is a bi-layer of phospholipids; it follows the fluid mosaic model that is the standard arrangement in all cell membranes. This means that the polar phosphate heads of the phospholipids point toward the cell cytoplasm on one face of the bi-layer and toward the aqueous environment of the exterior of the cell on the other. This arrangement places the hydrophobic fatty acid tails of the phospholipids in a central layer and excludes water. The combined effects of the polar layers sandwiching the lipophilic layer creates a semi-permeable membrane, which is effective in controlling the movement of solutes in and out of the cell. Proteins, glycoproteins and cholesterol are incorporated into the bi-layer. Proteins control the uptake of desired solutes and facilitate the removal of cellular by-products and wastes, glycoproteins are involved in cellular recognition and cholesterol helps to maintain the fluidity of the membrane (Figure 1.16).

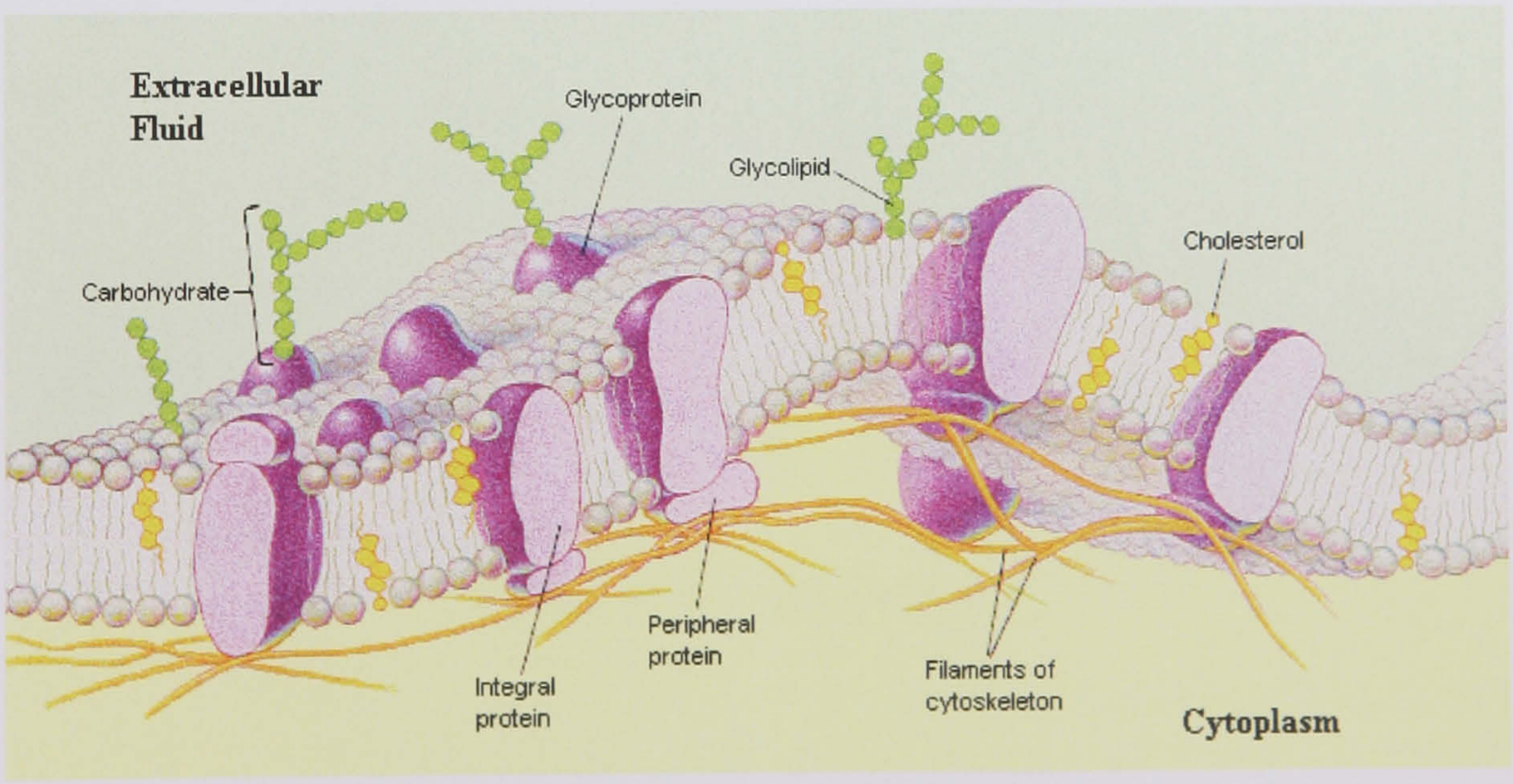

Figure 1.16. A depiction of the cell membrane.[22]

1.3.4.1 Membrane disruption therapies

Despite its complexity the cell membrane offers a challenging target for antibacterial therapies, as it is common to all organisms. There are differences in the proteins and glycoproteins present, but so far there are no clinically significant therapies that offer selective disruption of bacterial membranes without damage to the host organism. There are however a number of compounds that are clinically used despite their apparent lack of selectivity. They are effective with limited toxicity by virtue of being applied topically. By administering to the surface of the skin, compounds that would be highly toxic if taken internally are useful as antiseptics and they have few side effects, as the outer layers of the skin are already dead.

Two typical members of this antibacterial class are polymyxin B and gramicidin A, they both work by disrupting the bi-layer of the cell membrane, increasing its permeability to polar molecules and thus allowing vital nutrients to escape from the cells resulting in cell death. They are used topically to prevent wound infections and to treat infections of the eye (Figure 1.17).[13,23,24]

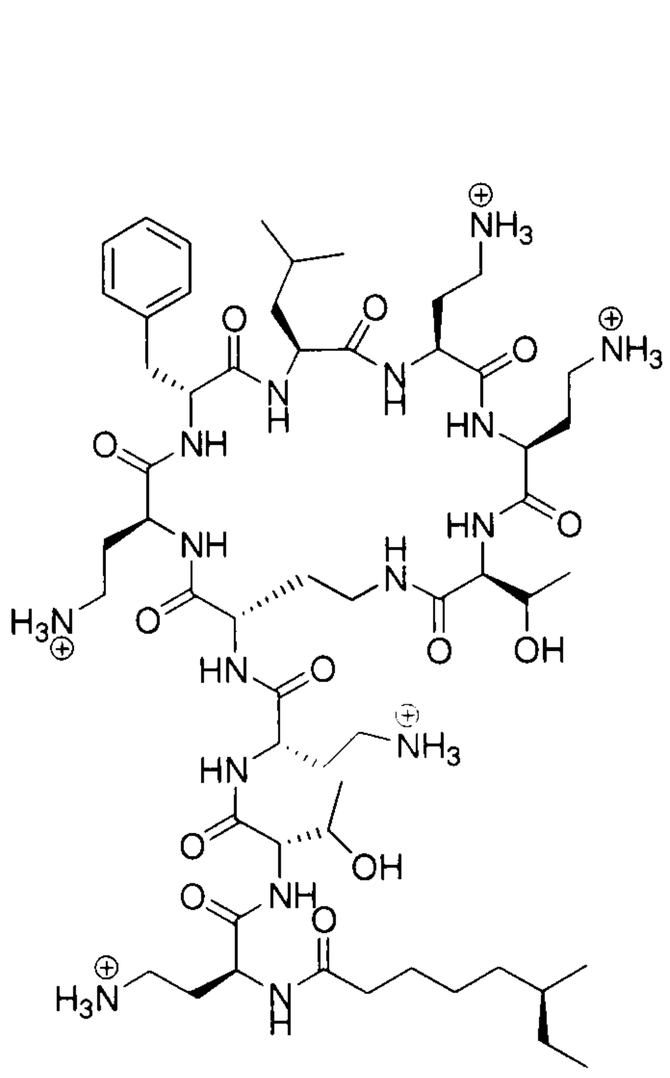

Polymyxin B

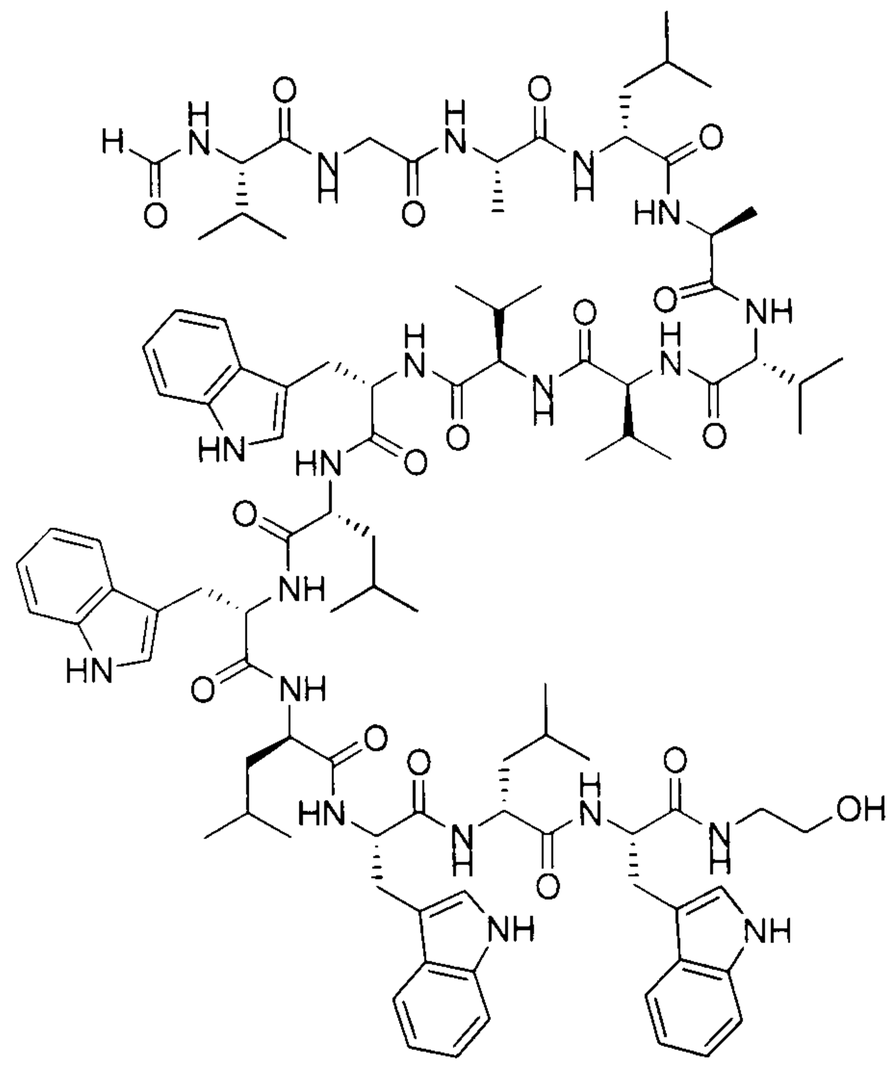

Gramicidin A

Figure 1.17. Two topical antibiotics[13]

1.3.5 The cell wall[25-28]

The cell wall prevents osmotic lysis of the cell membrane whilst the bacteria are in a hypotonic environment. There are two distinct organisations of the cell wall structure and these have been traditionally used to subdivide bacteria into two classes dependent upon their response to a staining agent developed by Christian Gram in 1884.[29] These are termed Gram-positive and Gram-negative. Gram-positive cells are stained by crystal violet and once fixed by the mordent, iodine, are not decolourised by ethanol, staying blue or purple. Whereas Gram-negative bacteria initially stain but are decolourised when washed with ethanol. An adaptation of this technique utilises sarfranin as a counter stain. This dyes the Gram-negative cells pink or red. As the cell wall structures of each cell type were elucidated, the understanding of these observations increased and the reasons for the differential staining became obvious (Figure 1.18).

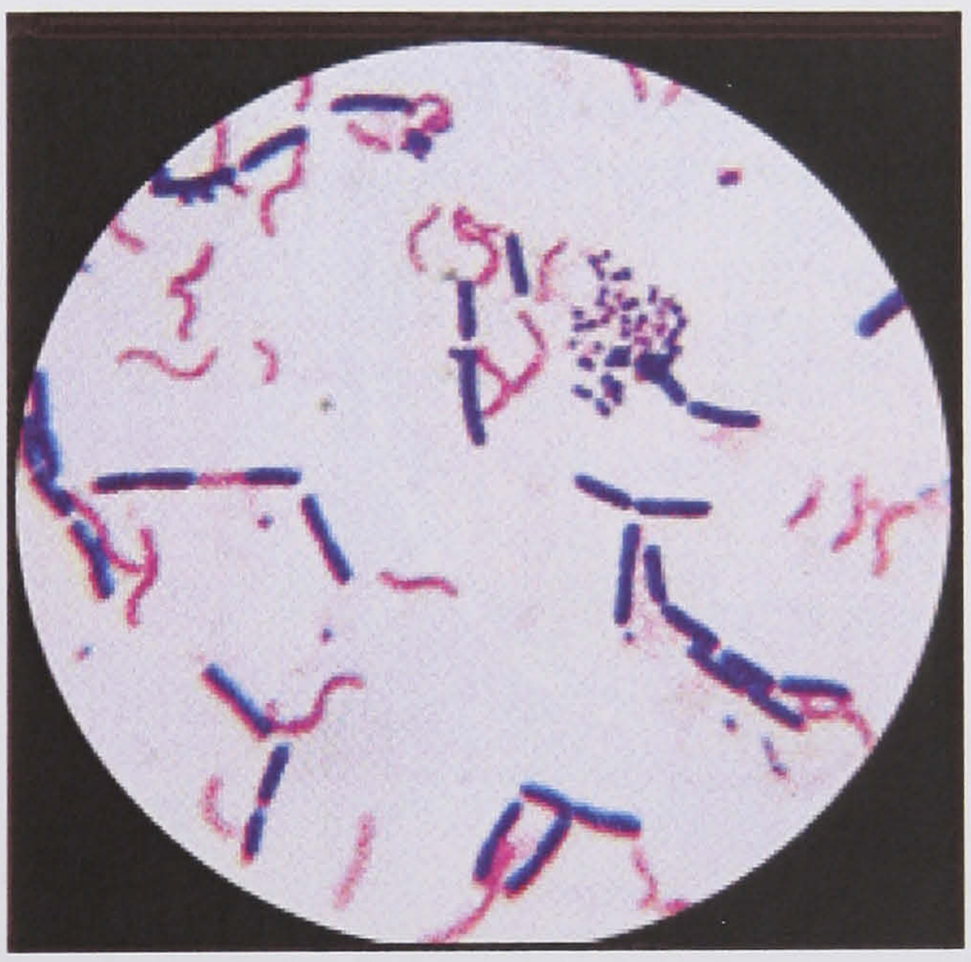

Figure 1.18. A stained bacterial sample, pink cell are Gram-negative and blue cells are Gram-positive.[30]

Gram-positive cells have a cell membrane surrounded by a layer of peptidoglycan (murein) between 20 and 80 nm in thickness. Gram-negative bacteria again have a cell membrane but this is surrounded by a thinner peptidoglycan layer only 7 to 8 nm thick, this is then surrounded by a further outer membrane. Both cell walls provide rigidity to the cell but the extra membrane of the Gram-negative bacteria prevents access to the peptidoglycan layer by a range of external compounds, such as crystal violet stain. The dye sticks to the surface of the membrane initially staining the cell but is then washed off, but in the Gram-positive cells it diffuses into the peptidoglycan and once treated

with iodine becomes insoluble and stains the cell even after washing with ethanol. This demonstrates the effect of the outer membrane of Gram-negative cells as a molecular barrier and this has significant impact upon the effect of certain antibiotics (Figure 1.19).

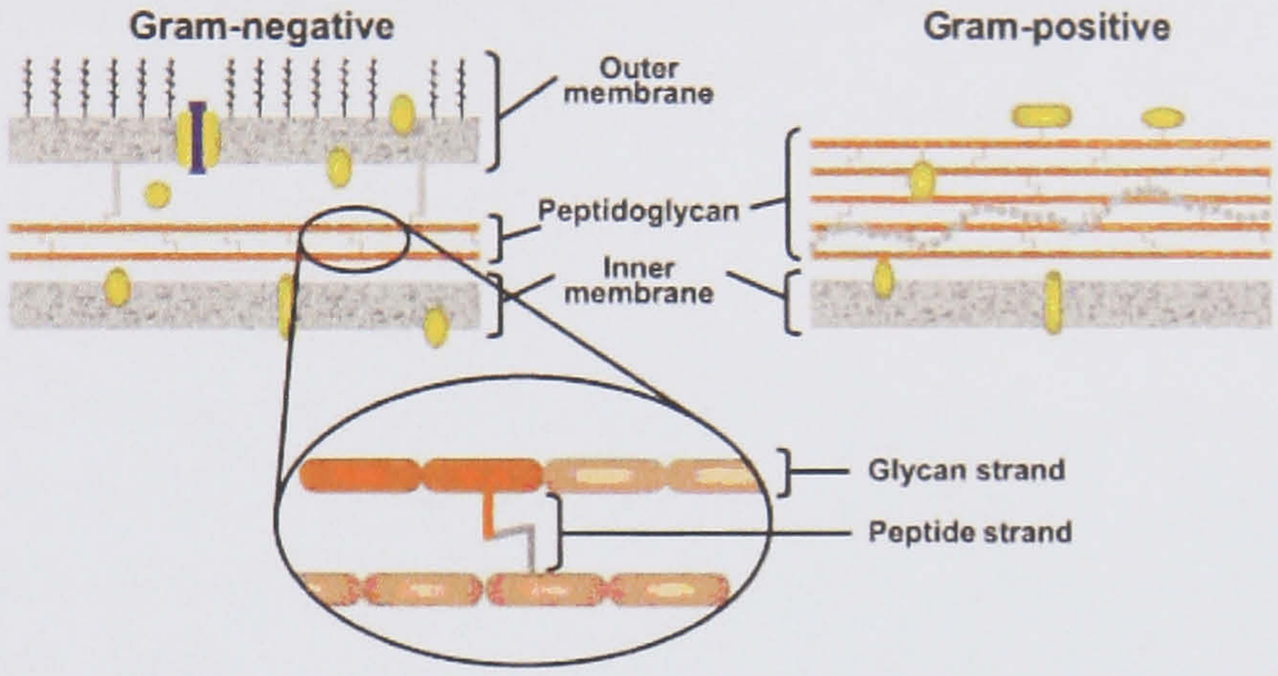

Figure 1.19. The cell wall arrangements in Gram-positive and negative species.[31]

In both cases the cell wall is complex and contains a multitude of compounds, but peptidoglycan has offered the most significant targets for antibacterial therapy to date. The basic structure of peptidoglycan is the same throughout all bacterial species and is comprised of a series of glycosidic chains cross-linked by short peptides (Figure 1.20).

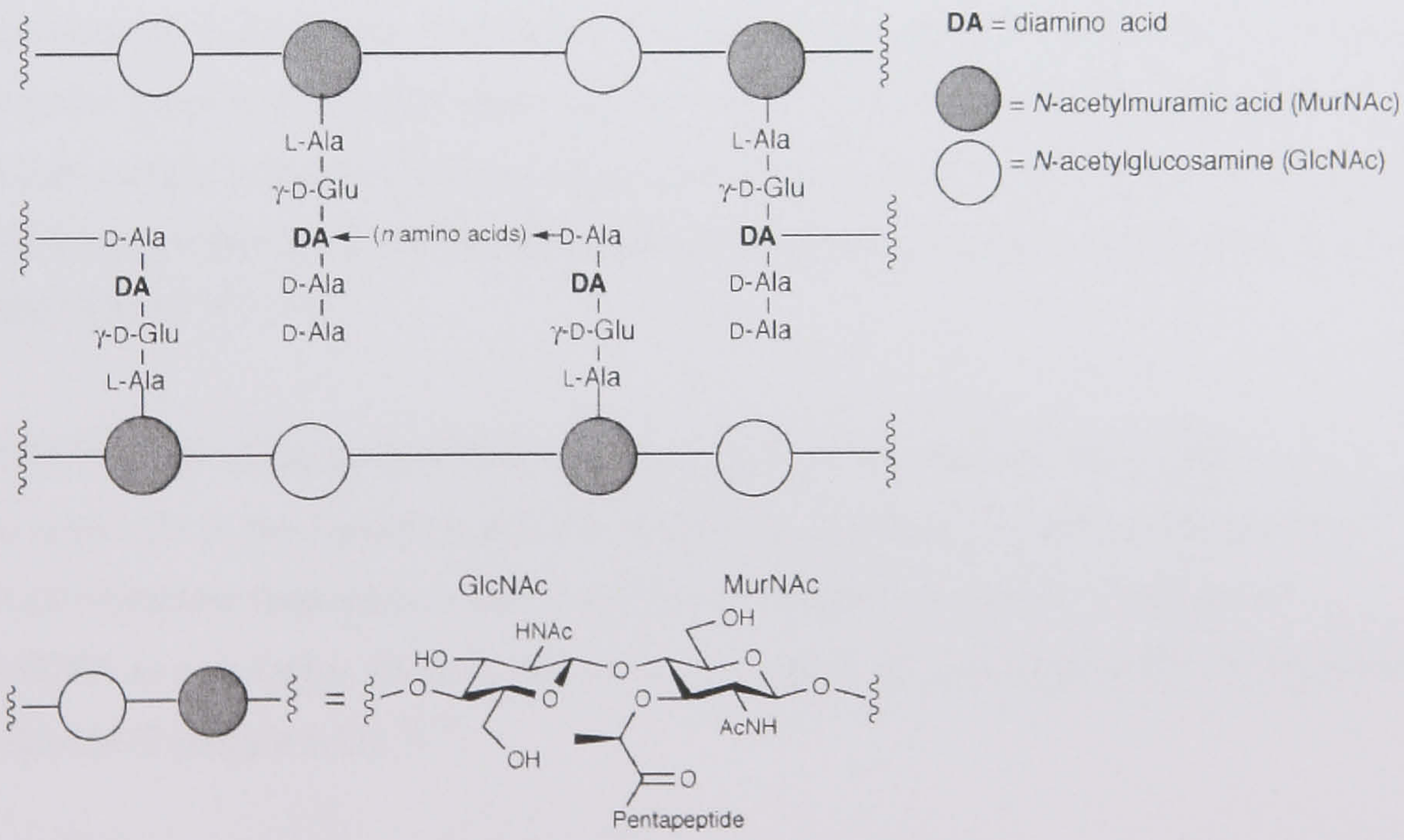

Figure 1.20. The primary structure of peptidoglycan.[32]

Peptidoglycan synthesis is a multi-step process, which is carried out by an extensive array of enzymes, in a synthetic sequence that spans the cell membrane of the bacteria. Steps occur in the cell cytoplasm, the cell membrane and also outside the cell. This can be used as a basis to subdivide this sequence into three phases, they are; the cytoplasmic synthesis, membrane associated synthesis and extra cellular polymerisation and tailoring.

1.3.5.1 Cytoplasmic synthesis[26,28,32-34]

There are several crucial reactions that take place in the cytoplasm, they are; the synthesis of *N*-acylglucosamine uridine diphosphate (UDP-NAG), the synthesis of *N*-acetylmuramic acid uridine diphosphate (UDP-NAM), the synthesis of the D-amino acids, glutamate and alanine and the synthesis of *meso*-diaminopimelic acid or lysine. Finally these substrates are assembled into the UDP-NAM pentapeptide.

Substrate synthesis[26,28]

UDP-NAG is synthesised in four successive steps beginning from D-fructose-6-phosphate. The first reaction is catalysed by GlmS transferase (L-glutamine: D-fructose-6-phosphate amidotransferase), this enzyme catalyses the hydrolysis of glutamine to glutamate and utilises the released ammonia to convert D-fructose-6-phosphate to glucosamine-6-phosphate. The second step utilises phosphoglucosamine mutase, which converts glucosamine-6-phosphate to glucosamine-1-phosphate. The bi-functional enzyme GlmU synthase catalyses the last two steps, acylation of the amine on the sugar and then the transfer of uridine diphosphate (UDP) to the 1 position of the sugar to give UDP-NAG.[26,28,32,34-36]

UDP-NAM is synthesised in two steps from UDP-NAG. The first stage adds enolpyruvate to the 3 position of UDP-NAG; this is catalysed by MurA transferase. MurB reductase then catalyses the reduction of the pyruvate double bond, using NADPH as a co-factor. Overall, this involves addition of lactic acid to the 3 position of UDP-NAG (Figure 1.21).[32,34]

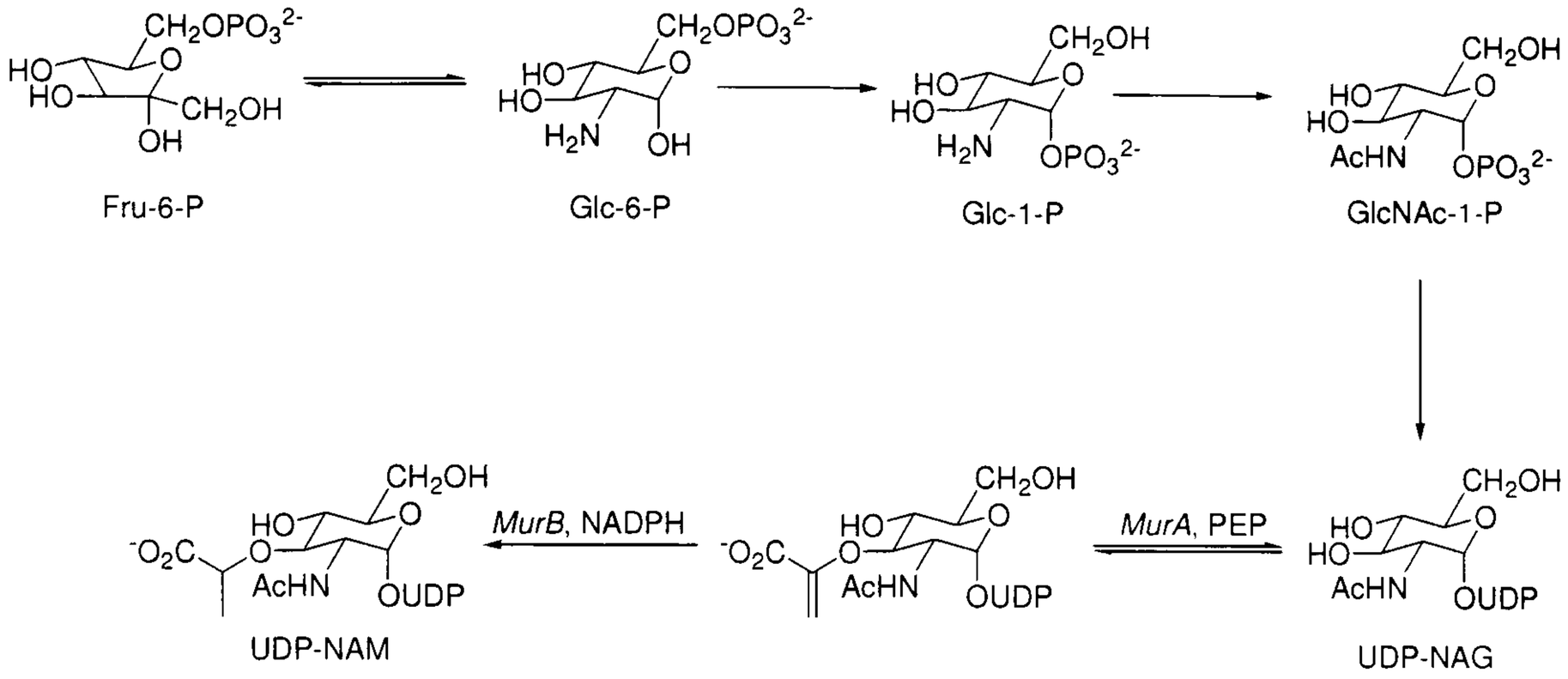

Figure 1.21. Synthesis of UDP-NAG and UDP-NAM.[34]

D-alanine is produced by the epimerisation of L-alanine, which is catalysed by alanine racemase. There is evidence that there maybe two distinct forms of alanine racemase, however both have the same responses to alanine, both rely on pyridoxal-5-phosphate as a co-factor and are inhibited by the same antibiotics.[30-32]

D-Alanine is then utilised by a further enzyme in the cytoplasm, D-ala-D-ala ligase. This takes two alanine molecules and activates the carboxyl group of one as the mixed phosphate anhydride using ATP as the source of the phosphate and producing ADP as a by-product. Then the amino group of the second alanine displaces the phosphate to form a D-ala-D-ala dipeptide (Figure 1.22).[32-34]

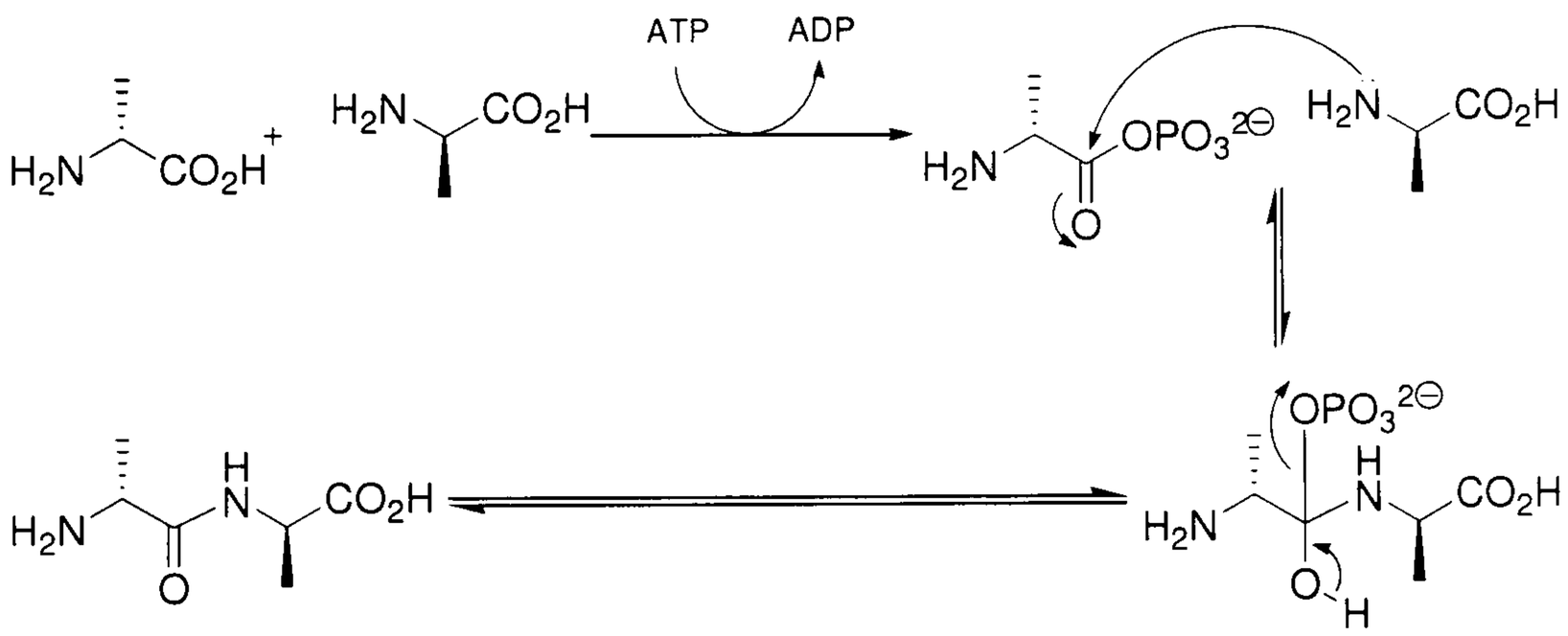

Figure 1.22. The mechanism of D-ala-D-ala ligase.[34]

D-Glutamic acid is produced by the action of D-amino acid aminotransferase in the majority of bacteria. This enzyme removes the amino group from D-alanine and transfers it to α-keto-glutarate. This yields D-glutamic acid and pyruvate. In many of

the lactic acid bacteria, D-glutamic acid is also produced by the action of glutamate racemase on L-glutamic acid.[32,34]

Meso-diaminopimelic acid (DL-DAP) is synthesised by the action of diaminopimelate epimerase on LL-diaminopimelic acid. Diaminopimelic acid may then be converted to lysine by diaminopimelate decarboxylase or it maybe incorporated into the UDP-NAM pentapeptide, this depends on the bacterial species (Figure 1.23).[34]

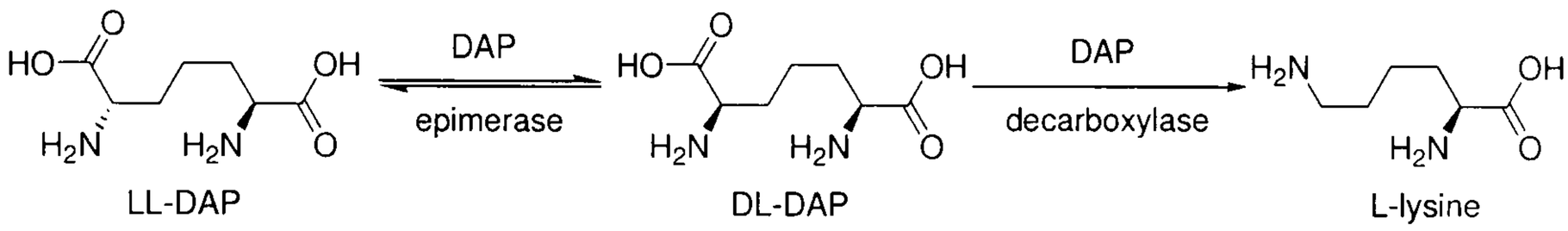

Figure 1.23. The synthesis of *Meso*-diaminopimelic acid and L-lysine.[34]

UDP-NAM pentapeptide synthesis

This stage of cell wall synthesis involves the sequential addition of five amino acids to the carboxyl terminus of the lactic acid of UDP-NAM. This is an unusual occurrence as it involves peptide synthesis removed from the ribosome and without the involvement of mRNA. This process is controlled by the Mur synthase enzymes, which activate the carboxyl group as a phosphate mixed anhydride, whilst hydrolysing ATP to ADP. The carbonyl group of the mixed anhydride is then attacked by the amine of the amino acid being added to give a tetrahedral intermediate. This intermediate then collapses to release the newly generated amide and an inorganic phosphate Figure 1.24).[28,34]

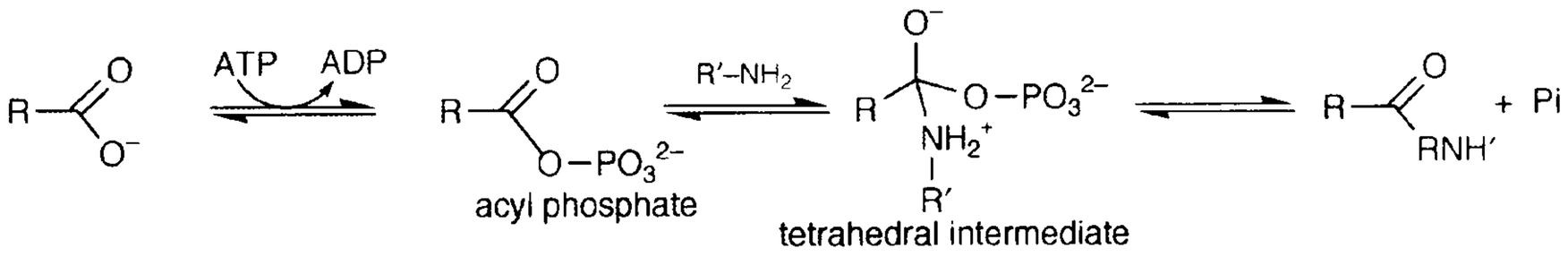

Figure 1.24. A general mechanism for the addition of amino acids as catalysed by the Mur synthase enzymes.[32]

MurC synthase is the first enzyme in this sequence and is responsible for the addition of L-alanine to the carboxyl of the lactic acid of UDP-NAM. In some species it can add either glycine or L-serine but these are much less common.[32,34,37]

MurD adds D-glutamic acid and is a highly specific enzyme as little variation has been observed in this position. Some bacteria show that the α–carboxylic acid can be

converted into a primary amide. However it is not clear whether this is due to addition of an altered monomer or whether this occurs after the pentapeptide is formed.[32,34,37]

MurE is responsible for the addition of the diamino acid to the third position of the peptide chain; this is the least specific enzyme in the sequence as the third position shows the largest variation in the amino acid. The amino acid added is always added to the γ-position of the glutamic acid, a motif not normally seen in peptides synthesised on ribosomes.

The only observed residue in Gram-negative bacteria is *meso*-diaminopimelic acid (*m*-DAP),[27] in Gram-positive bacteria the predominant amino acids are *m*-DAP or L-lysine. In all cases the *m*-DAP is incorporated by addition of the amine of the L-stereocentre, as apposed to the D-stereocentre and therefore mirrors the addition of L-lysine.
However, there are numerous other possibilities for this residue at this position in Gram-positive bacteria; L-ornithine, LL-diaminopimelic acid, *meso*-2,6-diamino-3-hydroxy-β-pimelic acid and L-hydroxy-lysine have all been observed. There are also amino acids found in this position that have the distant amine acetylated or only have one amine group; 4-acetylamino-2-amino-butyric acid, L-homoserine, L-alanine or L-glutamate. This leads to the conclusion that there must be a second mode of cross-linking in the bacteria that does not involve the distant amine of the amino acid in the third position and this is indeed the case. In a limited number of bacteria the cross-linking (discussed in detail below) is between the glutamate in the 2 position and the alanine in the 4 position.[32,34,37]

MurF is the last enzyme in this sequence and is responsible for the addition of the two remaining amino acids of the pentapeptide as a dipeptide. This dipeptide is normally the D-ala-D-ala produced by D-alanine ligase, although there are a number of variations observed here as well. In some cases the terminal D-alanine is replaced by D-serine and may also be replaced by D-lactate to give a depsipeptide that is incorporated into the pentapeptide. In both these cases the D-alanine in the fourth position is conserved and there appears to be very little variation in that position. These variations of the ultimate amino acid are important resistance mechanisms to the glycopeptide antibiotics, particularly the D-lactate presenting mutant and are discussed below in greater detail.[32,34,37]

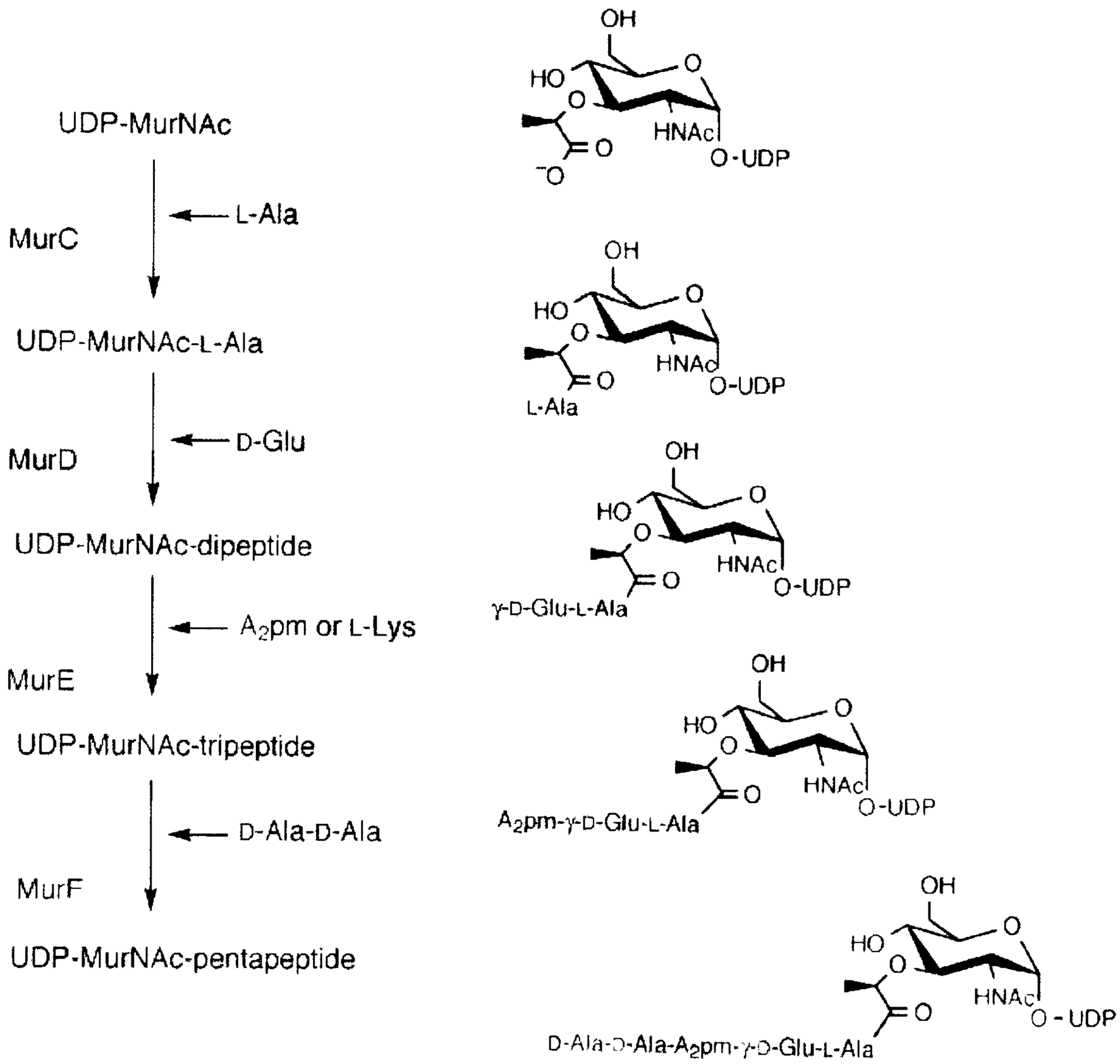

Figure 1.25. A summary of UDP-NAM pentapeptide synthesis.[32]

1.3.5.2 Inhibitors of cytoplasmic synthesis[13,26]

Fosfomycin inhibits the transfer of enolpyruvate, the first step in the synthesis of UDP-NAM from UDP-NAG, the reaction catalysed by MurA synthase. It mimics phosphoenol-pyruvate, the natural substrate of the enzyme, and is able to enter the active site. One of the catalytic cysteine residues of the active site then ring opens the epoxide. This results in a stable covalent bond between the enzyme and the antibiotic, preventing enzymatic catalysis and therefore depleting UDP-NAM, thus preventing the synthesis of the cell wall.

D-Cycloserine inhibits alanine racemase and D-ala-D-ala ligase. It acts as a mimic of D-alanine and binds competitively to the active site of the effected enzymes thus preventing synthesis of D-ala-D-ala and therefore preventing cell wall synthesis.

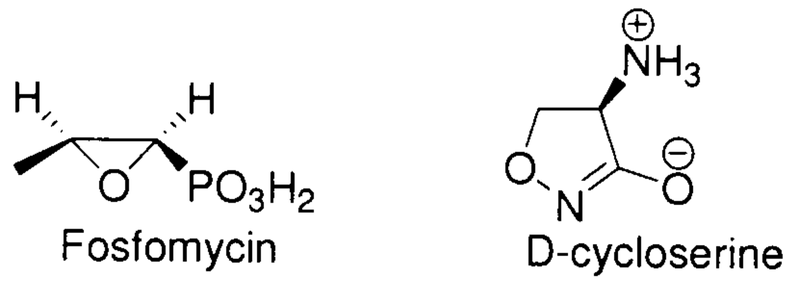

Figure 1.26. Inhibitors of cytoplasmic cell wall synthesis.[13,26]

1.3.5.3 Membrane associated synthesis[38-41]

There are two reactions on the inner surface of the cell membrane and these produce a monomer (lipid II), which is transported across the membrane to the outside of the cell, where it can be polymerised into the peptidoglycan cell wall. Neither of the enzymes seem to have a great degree of specificity in regard to the pentapeptide chain, as there is little evidence for mutants of these enzymes in bacteria that present altered amino acid sequences. Heijenoort and co-workers[42] report that MraY transferase will accept peptides with altered length (dipeptides to heptapeptides), pentapeptides with altered sequences and pentapeptides with dansyl or acetyl substitutents. Ha *et al.*[43] show that MurG is slightly more specific than MraY, it requires that the pentapeptide be present, but it is known that this enzyme will tolerate modification of the pentapeptide, as the D-serine or D-lactate presenting mutants that are resistant to glycopeptides do not contain altered versions of this enzyme.

Lipid I synthesis[38-41]

Lipid I (undecaprenyl diphospho-NAM-pentapeptide) is synthesised by the enzyme MraY transferase. This enzyme is a phospho-*N*-acetylmuramoyl-pentapeptide transferase. This means that it catalyses the cleavage of the pyrophosphate between UDP and NAM whilst catalysing the formation of a second pyrophosphate between NAM and undecaprenyl phosphate with UMP as a side product. Undecaprenol is a 55-carbon molecule that is highly unsaturated and linear in shape, this makes it ideal for embedding in the phospholipid bi-layer of the cell membrane. It acts to anchor the amino-sugar and its pentapeptide substitutent to the membrane, both initially on the inner face and then after it has been transferred to the cell exterior.

Lipid II synthesis[38-41]

In the second step of the membrane bound sequence MurG transferase (N-acetylglucosamine transferase) catalyses the transfer of NAG to NAM with release of UDP, thus forming the β-1,4-glycosidic linkage observed in cell walls.

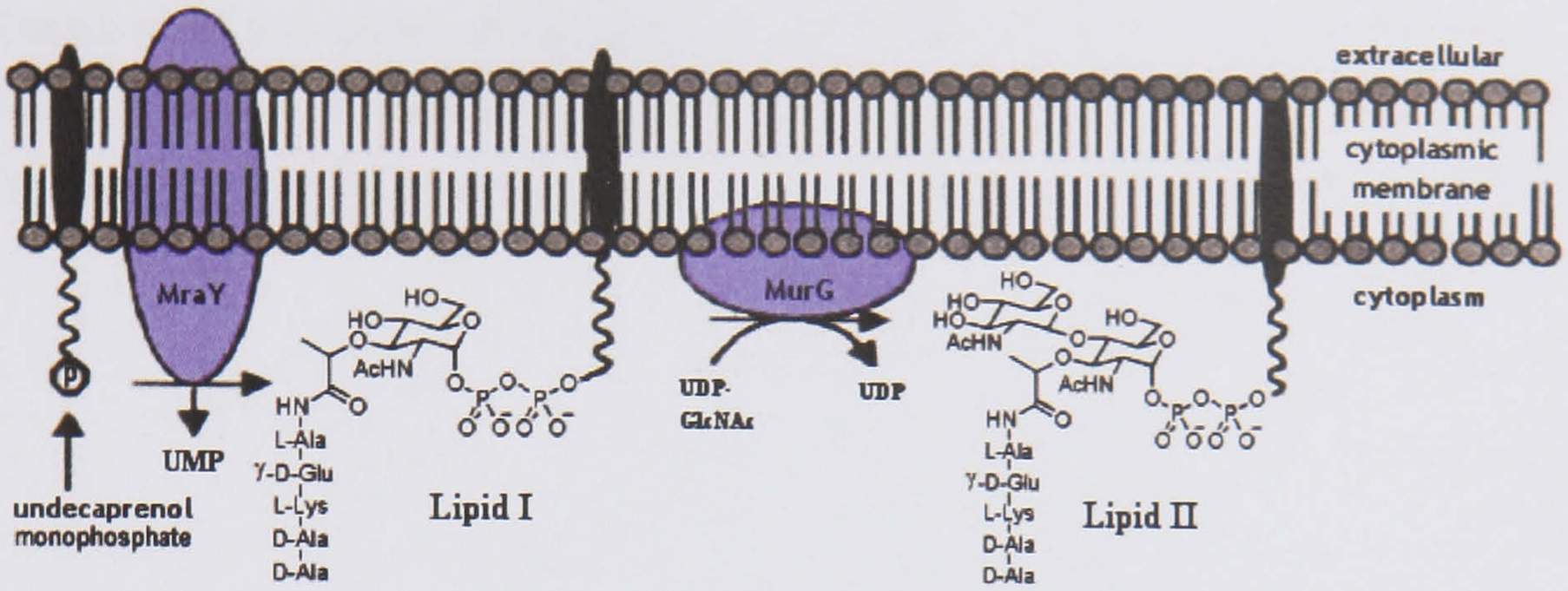

Figure 1.27. The steps of membrane bound synthesis[41]

In some bacterial species the distant amine of the diamino acid in position 3 of the pentapeptide is extended at this point. This is accomplished by the sequential addition of amino acids to the amine terminus; the amino acids added are activated as they are bound to tRNA. The amine terminus therefore reacts with the tRNA-activated amino acid and forms an amide bond whilst releasing tRNA. The number and type of amino acid added depends on the bacterial species.

1.3.5.4 Inhibitors of lipid I synthesis[13,26]

Bacitracin inhibits the dephosphorylation of undecaprenol pyrophosphate by stabilising the complex it forms with the membrane bound phosphatase that cleaves it. This is on the cell exterior but has a considerable impact on these internal processes as it prevents the recycling of the undecaprenol and therefore prevents the formation of lipid I.

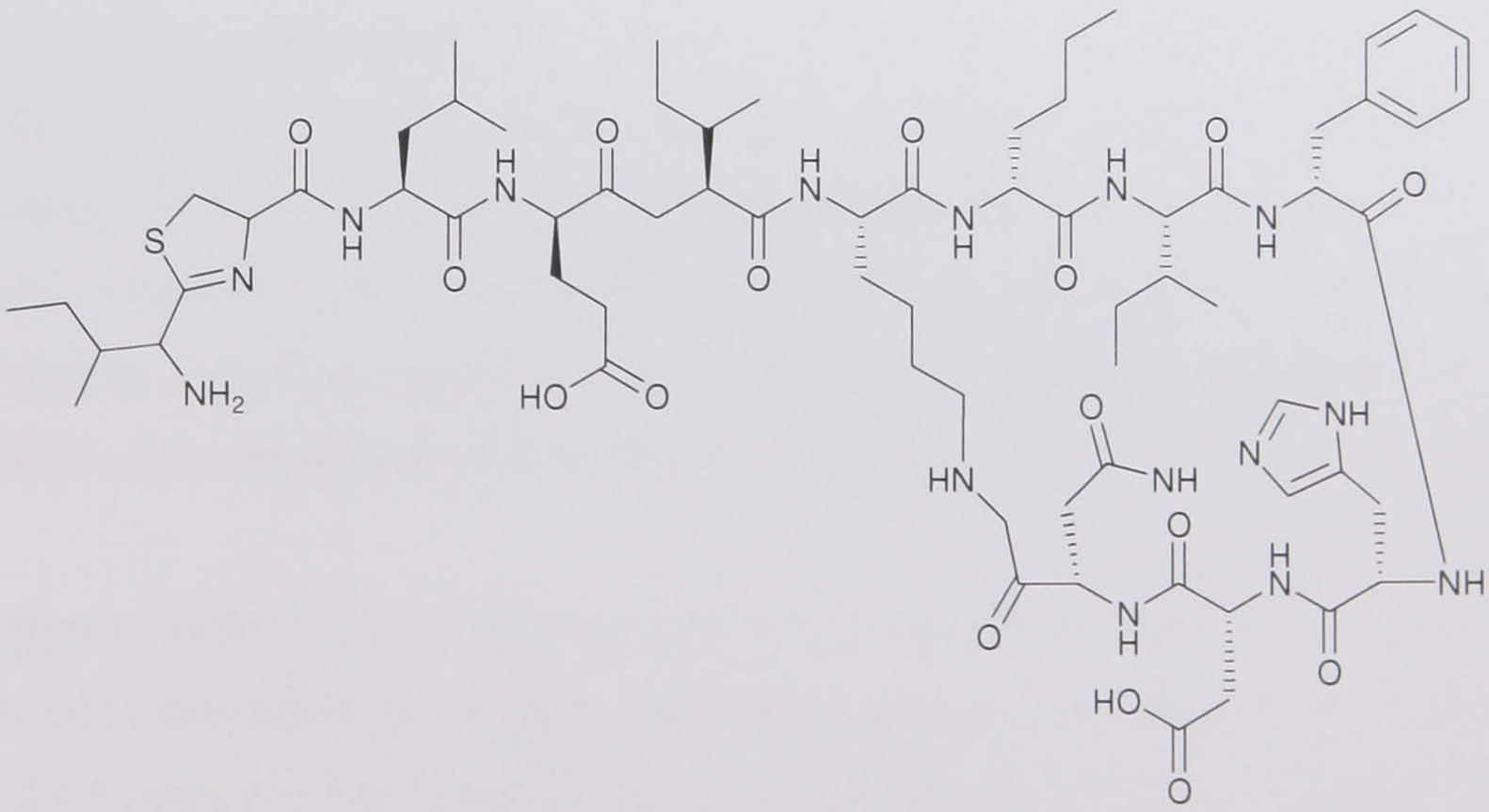

Figure 1.28. Bacitracin.

Tunicamycin also inhibits the synthesis of lipid I, but it acts by inhibition of phospho-*N*-acetylmuramoyl-pentapeptide transferase, preventing it from catalysing the transfer of NAM-pentapeptide to undecaprenol phosphate.

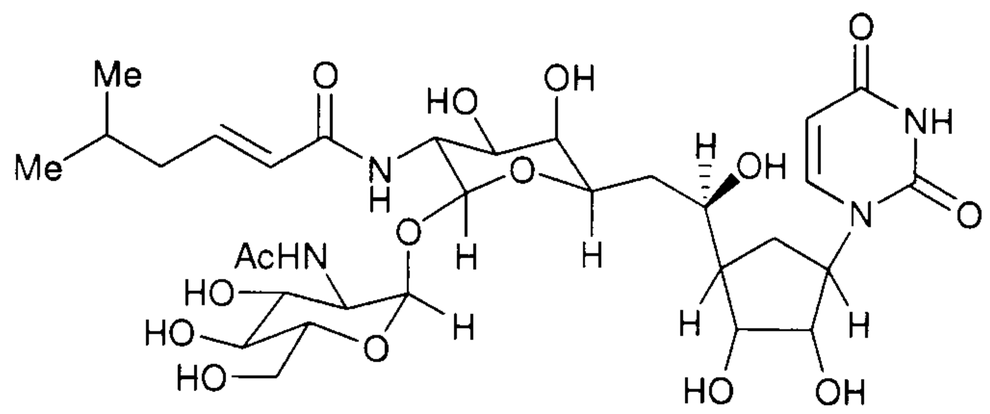

Figure 1.29. Tunicamycin.

1.3.5.5 Extra-cellular polymerisation[38-41]

The lipid II monomer is inverted in the membrane, transferring the NAG-NAM pentapeptide to the outer surface of the membrane. The mechanism for this and the protein responsible for this action are as yet unknown. After this transfer the monomeric units are exposed to two further enzymatically-catalysed reactions that convert a series of these monomers into the characteristic polymeric glycopeptide cell wall.

There is a range of enzymes that are membrane associated and described as penicillin binding proteins (PBP's). These enzymes affect the polymerisation steps. Their nature and functions vary greatly as does their size and degree of expression across bacterial species. They are split into two groups, high molecular weight PBP's and low molecular weight PBP's.

High molecular weight PBP's[41]

High molecular weight PBP's control transglycosylation and transpeptidation. There is a wide range of these PBP's and they are all multi-modular, largely consisting of a lipophilic anchor that embeds in the cell membrane, a non-penicillin binding domain that is usually a transglycosylase and then a penicillin binding domain that is a penicilloyl serine transferase, which catalyses transpeptidation.

Transglycosylation is a reaction where the NAG-NAM pentapeptide from lipid II is transferred to the extending cell wall. Depending on the bacterial species this is either by the displacement of the pyrophosphate from lipid II with 4-hydroxy group of the *N*-acetylglucosamine of the elongating glycan chain (arrow 2, Figure 1.30) or the inverse the 4-hydroxy group of the *N*-acetylglucosamine displaces the pyrophosphate of the

elongating glycan chain (arrow 1, Figure 1.30). Either way, undecaprenol is released as the pyrophosphate, which is dephosphorylated and re-absorbed into the bacteria to be re-used. Little else is known about this enzymes mechanism, particularly the key interactions between the enzyme and the substrate, although steps have been taken to attempt to identify which PBP's are critical to cell function using knockout studies.[41]

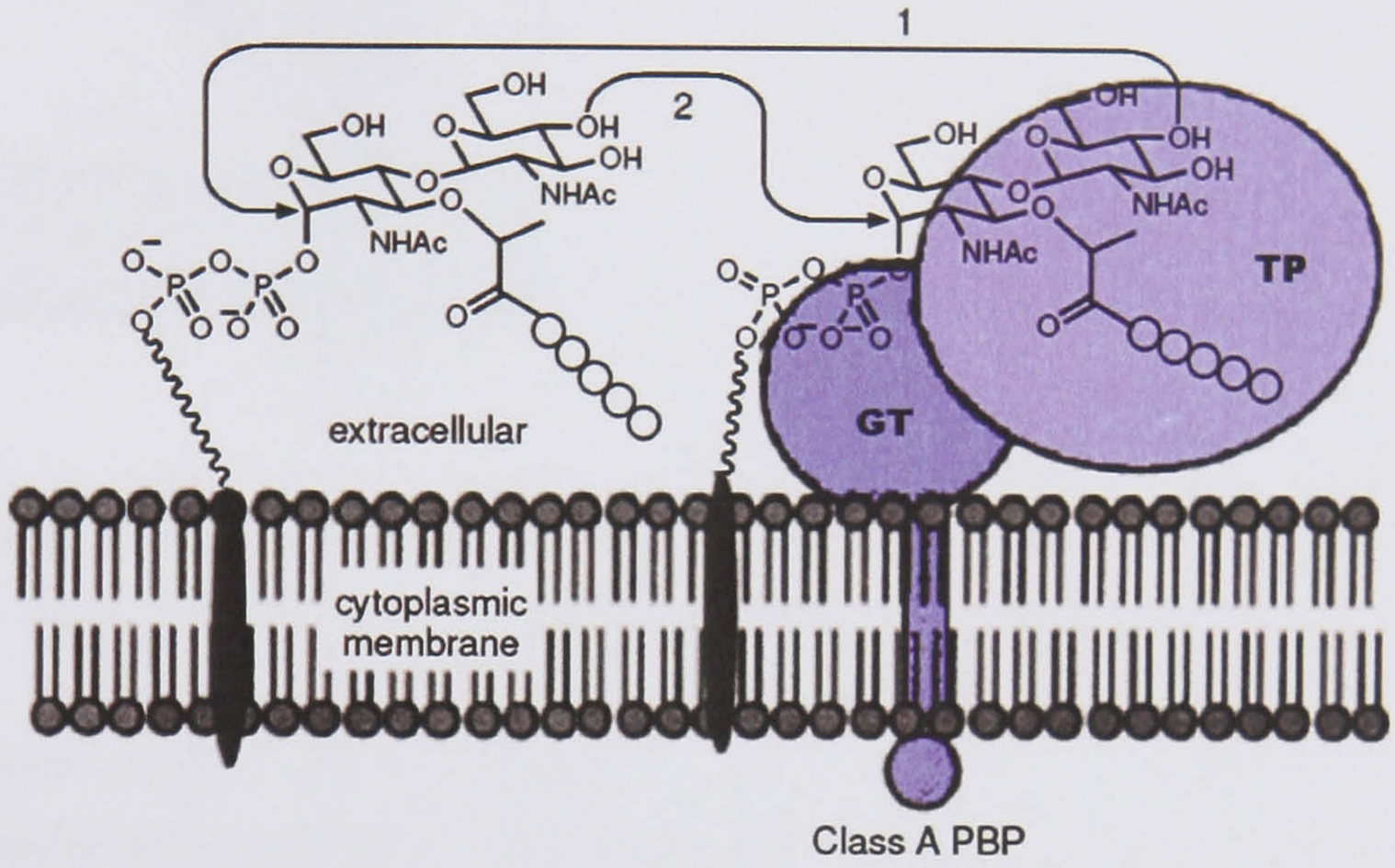

Figure 1.30. Transglycosylation one of the extra-cellular steps in glycopeptide synthesis.[41]

Transpeptidation is the cross-linking step between the peptide side-chains of adjacent glycan strands. There are a number of different types of cross-links possible; the majority of these are formed by displacement of the terminal D-amino acid residue with either the distant amine of the diamino acid in the third position of the pentapeptide, or by displacement with an inter-peptide bridge extending from the distant amine. This inter-peptide bridge is yet another source of diversity in the cell wall structure, the number of residues and the amino acid composition is highly variable and dependent upon the bacterial species. The simplest form of transpeptidation is shown in Figure 1.31 A and B.

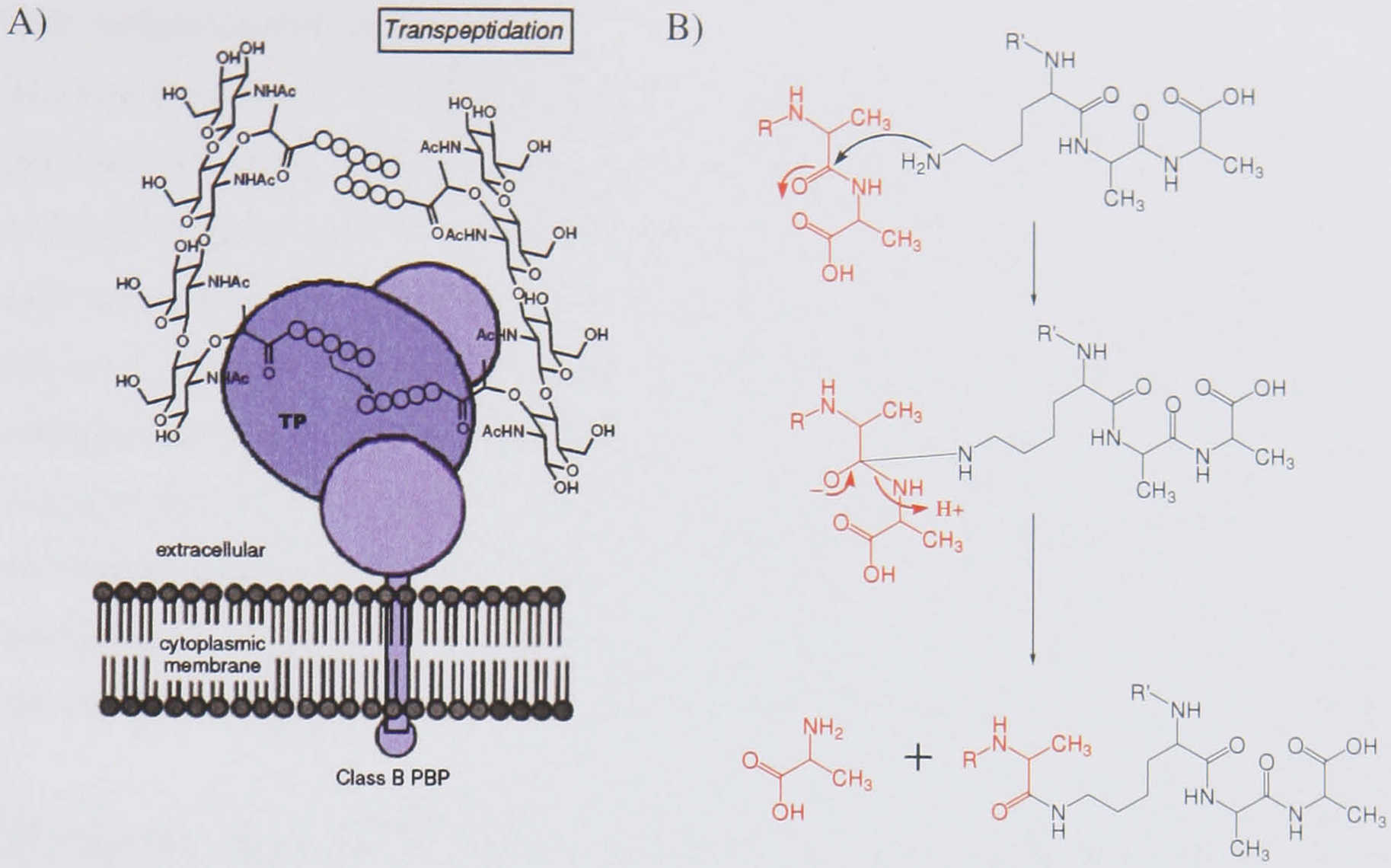

Figure 1.31. Simple transpeptidation: A) shown in an extra-cellular context.[41] B) shown as a synthetic scheme.

As mentioned above a limited number of bacteria display cross-linking between the glutamate in the 2 position and the alanine in the 4 position, this necessitates the inclusion of a diamino acid in the inter-peptide bridge. This is linked to the α-carbonyl of the glutamate residue by its α-amine and then displaces the terminal D-alanine of the adjacent chain with its distant amine or the *N*-terminus of an extending residue attached to that amine.

This variation in the mode of linking and the nature of the inter-peptide bridge may go some way to explaining why there are multiple copies of the PBP's in the bacterial world, yet this does not explain why multiple copies should be expressed in a single organism, a trait that is very common. It is likely that they are more deeply involved in the life cycle of the bacteria than just the initial synthesis of peptidoglycan. There is already a large body of evidence that shows that these enzymes are critical in the division to daughter cell during reproduction and that they are crucial in determining cell morphology. However, it is only as more is becoming clearly understood about these enzymes, that it may be possible to show exactly which particular enzyme is responsible for peptidoglycan synthesis in each part of the bacterial cells life cycle.

Low molecular weight PBP's[41]

The low molecular weight PBP's are smaller enzymes, which have been shown to have peptidase activities. There are two types of low molecular weight PBP's, DD-carboxypeptidases and DD-endopeptidases, both are involved in further tailoring of the exposed chemical functionality on the peptidoglycan. The DD-carboxypeptidases remove D-alanine terminal residues and so limit the amount of cross-linking. The DD-endopeptidases cleave internal DD-dipeptide bonds in the peptidoglycan layer, for example, those in between the D-centre of diaminopimelic acid and D-alanine of the cross-links between the peptide side chains. This opens up the peptidoglycan layer and allows the growth of the cell. DD-endopeptidases are also involved in the recycling of the cell wall fragments that were cleaved to allow cell expansion.

The number and type of PBP present is dependant upon the species of bacteria, but all the enzymes that have a penicillin-binding domain are serine transferases and share a common mechanism of action, that was described by Ghuysen and co-workers. [38]

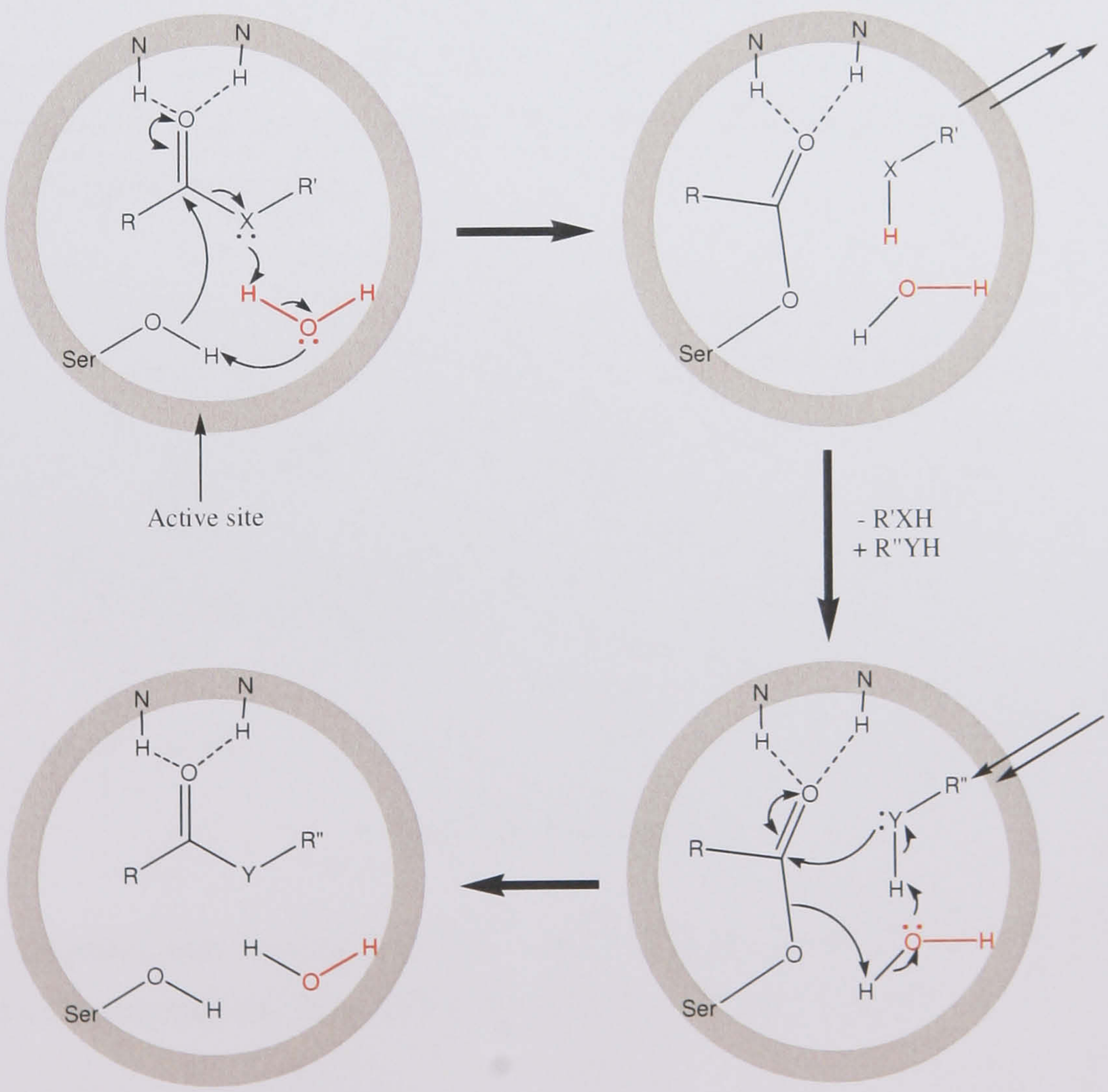

Figure 1.32. A depiction of the active site and the reaction mechanism of the serine transferases.[38]

The carbonyl donor is bound into the active site and the carbonyl group activated by H-bonding to two amines, the water molecule (shown in red in Figure 1.32) acts as a proton transfer agent removing a proton from the serine residue allowing it to attack the carbonyl group. The water accepts a proton from serine and also donates a proton that is accepted by R'X, forming R'XH which diffuses from the active site to be replaced by R"YH. The process is then reversed. Water accepts a proton from R"YH which attacks the carbonyl displacing the serine residue which extracts a proton from the water. Thus giving RC(O)YR" which is released from the active site. X can be O or NH depending on the species of bacteria. For peptidases R"YH is water and for transpeptidase R"YH is an amino acid.

1.3.5.6 Inhibition of transglycosylation and transpeptidation[13,26,38,41]

As yet there are no effective inhibitors available for clinical use that specifically target transglycosylation. However a natural product, moenomycin (Figure 1.33), is a potent inhibitor of the transglycosylase (non-penicillin binding) domain of PBP's, thus preventing addition of the NAG-NAM sugars to the growing cell wall. Although moenomycin is too toxic for clinical use, it is hoped that it can be used to gain a greater understanding of the mechanism of transglycosylation and thus allow the production of clinically significant inhibitors.[41]

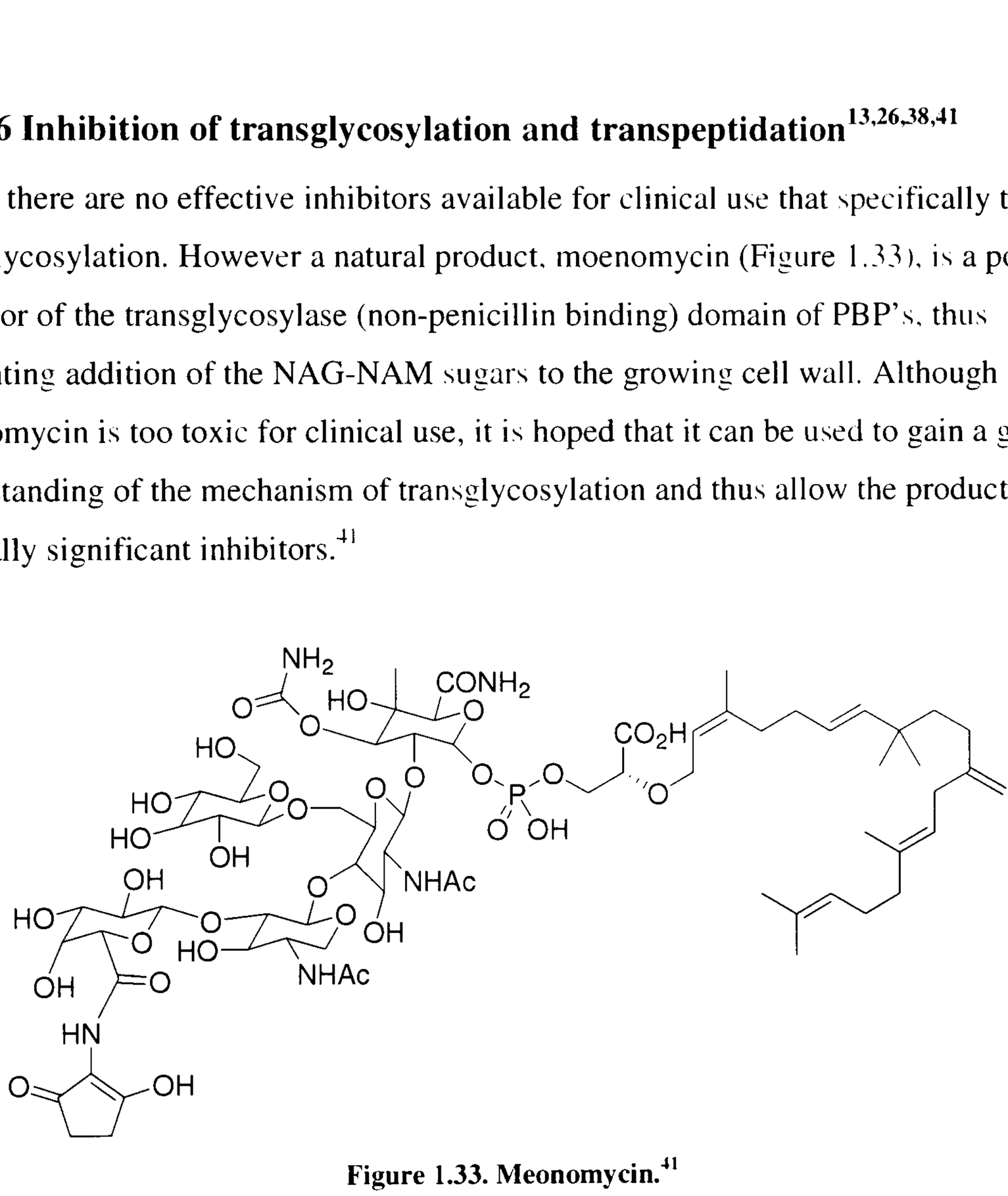

Figure 1.33. Meonomycin.[41]

Glycopeptides, like vancomycin or ristocetin, do inhibit transglycosylation, but also inhibit transpeptidation. They are discussed below in detail (section 4).

The foremost class of antibacterials to date has been the β-lactams. There are many groups of molecules which posses this structure, including penicillins, cephalosporins, carbapenems and monobactams (aztreonam is the only monobactam in use). They are all clinically useful antibiotics that inhibit the transpeptidase (penicillin binding) domain of PBP's (Figure 1.34).

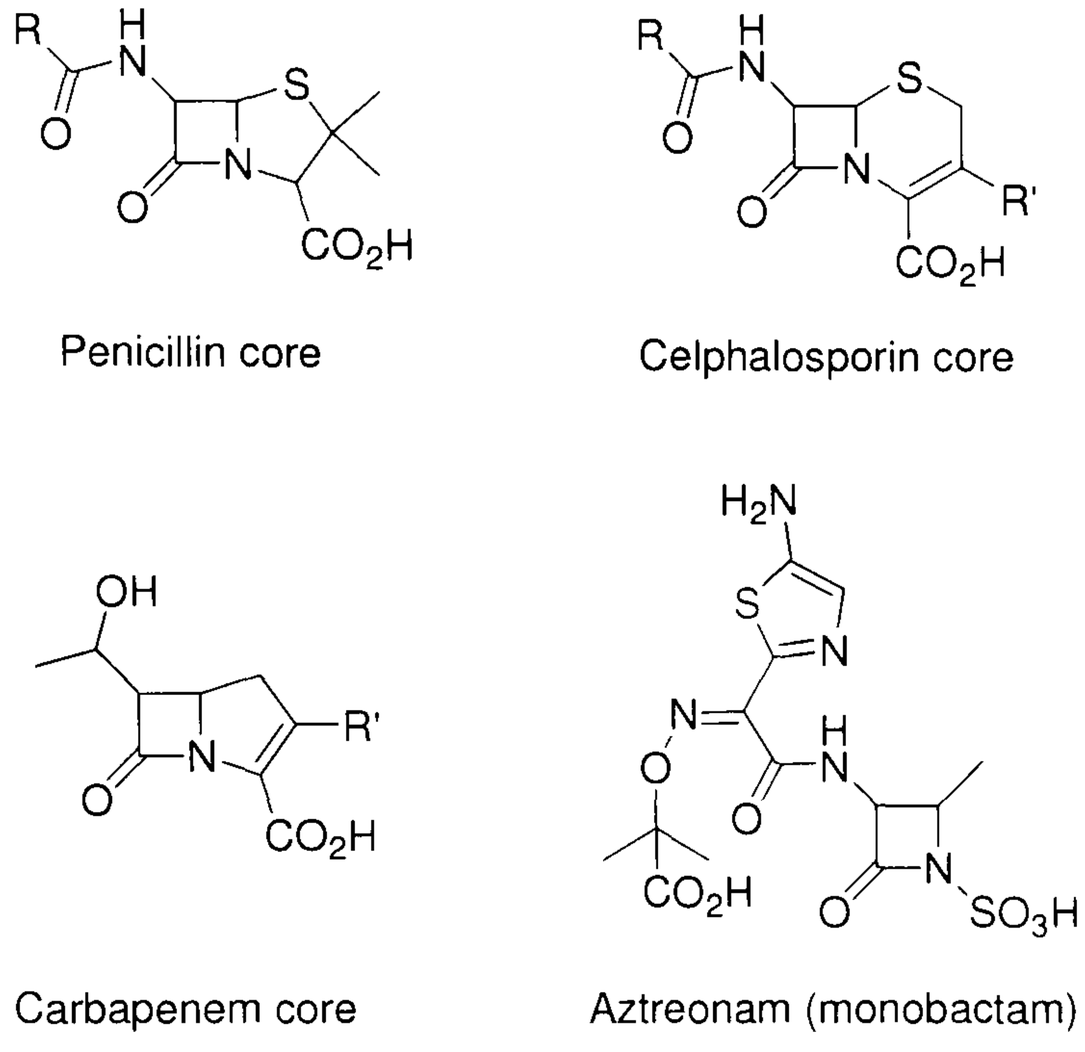

Figure 1.34. The core structures of the β-lactam containing antibiotics.[13]

All β-lactams work by mimicking the structure of the D-ala-D-ala terminus of the pentapeptide and in so doing, they act as a competitive inhibitor for the active site of transpeptidase. They have a significant advantage as they are already locked in the appropriate conformation to bind into the active site. In comparison, the D-ala-D-ala terminus is freely rotating and therefore must adopt the correct conformation to bind, thus slowing binding and incurring an entropic penalty for the loss of free rotation. This overall means β-lactams have a higher affinity for transpeptidase than D-ala-D-ala. Once in the active site, the amide of the β–lactam is cleaved, this is analogous to the cleavage of the D-ala-D-ala amide that frees one of the D-alanines. However, the β-lactam ring is cyclic, therefore cleavage of the amide does not release the remainder of the structure, and this acts as a steric block preventing access of a nucleophile (R"YH) to the acetylated serine of the enzyme. This means that hydrolysis of the acylated enzyme is very slow, it has a turn over rate of one or less per hour and the enzyme is effectively inhibited by covalent irreversible inhibition (Figure 1.35).[26,38]

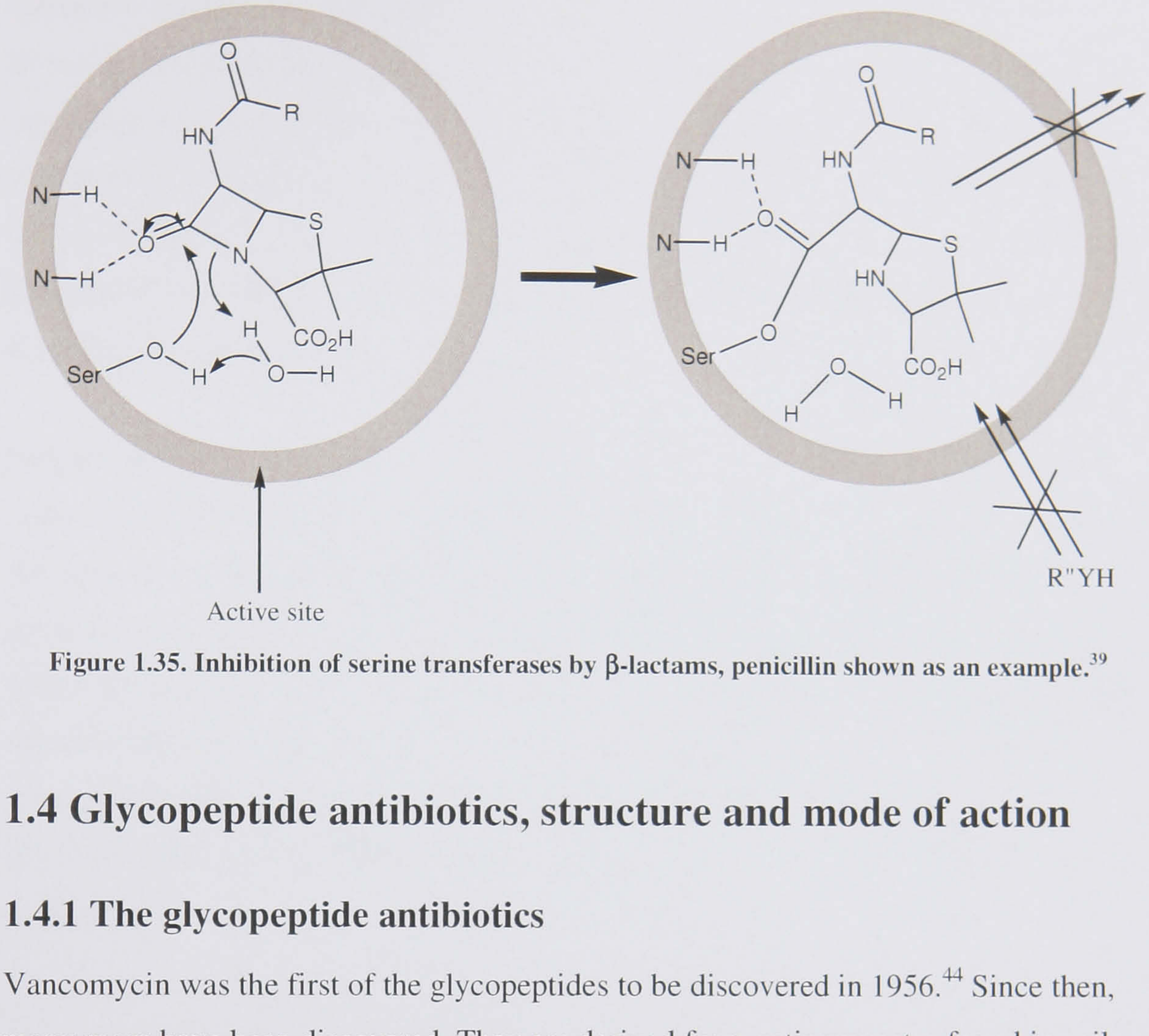

Figure 1.35. Inhibition of serine transferases by β-lactams, penicillin shown as an example.[39]

1.4 Glycopeptide antibiotics, structure and mode of action

1.4.1 The glycopeptide antibiotics

Vancomycin was the first of the glycopeptides to be discovered in 1956.[44] Since then, many more have been discovered. They are derived from actinomycetes found in soil samples.[45] Only two of the glycopeptides, vancomycin and teicoplanin, are currently in clinical use in humans. Both are antibacterials used to treat Gram-positive bacterial infections. They are not transported across the outer membrane of Gram-negative bacteria and therefore cannot reach their site of action in the cell wall and thus have no effect on Gram-negative pathogens.[45] Vancomycin is the last resort treatment for post-surgical infections with methicillin resistant *Staphylococcus aureus* (MRSA).[46]

1.4.2 Structure of the glycopeptide antibiotics

Glycopeptides share the common construction suggested by their name, i.e. they are composed of both glycosides (sugars) and a peptide. The sugars are highly variable and some are unique to these antibiotics. However, the aglycones, the peptide portion of the drug available after removal of the sugars, show much less variation. The first attempt at the characterisation of these structures involved the use of chemical methods. Marshall[47] was the first to publish the combustion analysis of vancomycin in 1965. Quoted as C, 54.01; H, 5.68; Cl, 4.71; N, 8.88; O, 27.13, which is remarkably close to the predicted

values for vancomycin, which are C, 54.70; H, 5.22; Cl, 4.89; N, 8.70; O, 26.50. However, the derivation of the empirical formula was incorrect, $C_{148}H_{185}C_{l4}N_{21}O_{56}$ was suggested, whereas $C_{66}H_{75}Cl_2N_9O_{24}$ is now known to be the formula.[48,49] This paper also describes the preparation of two crystalline degradation products, CPD-I and II, CPD-I is discussed below. Marshall's work[47] began the task of uncovering the complete structure by identifying a number of phenolic residues and identifying the presence of *N*-methyl-D-leucine. However, the complete structure was not proposed.

Further chemical studies were undertaken,[50-53] but the next significant breakthrough came from Williams *et al.* and NMR studies of vancomycin in 1977.[54] In this work, all the elements of the vancomycin structure were accounted for and evidence was presented from assignment of the 270 MHz H^1NMR spectrum, and the use of nuclear Overhauser effects. The nature of the backbone (the presence of secondary amides) and the stereochemistry of the sugars were elucidated. Although the total carbon skeleton was accounted for, the total structure was not assigned at this point. The work of Sheldrick and Williams in the following year, was the first to offer a complete structural assignment.[55]

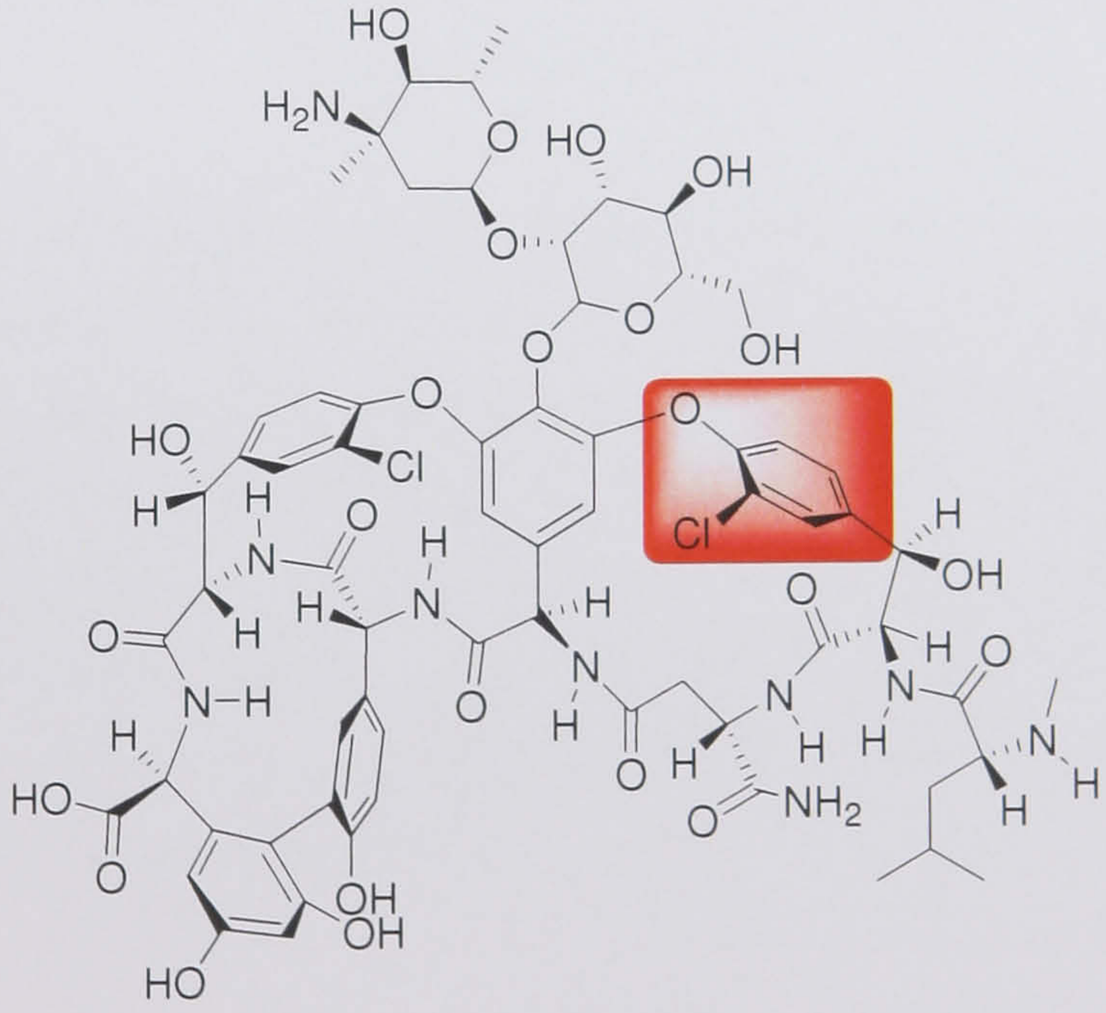

Figure 1.36. Structure as determined by Sheldrick *et al.*[55]

Further work by Williams *et al.* [56] in 1981 refined this total structure by comparison of the nuclear Overhauser effect difference spectra of vancomycin and crystalline degradation product 1 (CDP-I), and the X-ray crystal structure of CDP-I. Marshall[47] was the first to produce CPD-I by heating vancomycin in aqueous HCl (pH 4.2) for 40

hrs at 60 – 70 °C. This produced a brown crystalline solid but Marshall did not suggest a structure for the compound produced. The work of Williams allowed the assignment of the stereo-configuration of the chlorine substitutent of the ring that is highlighted in Figure 1.36 to be revised. It was shown to be pointing backwards in vancomycin (Figure 1.37), whereas it is pointing forward in CDP-I.[56]

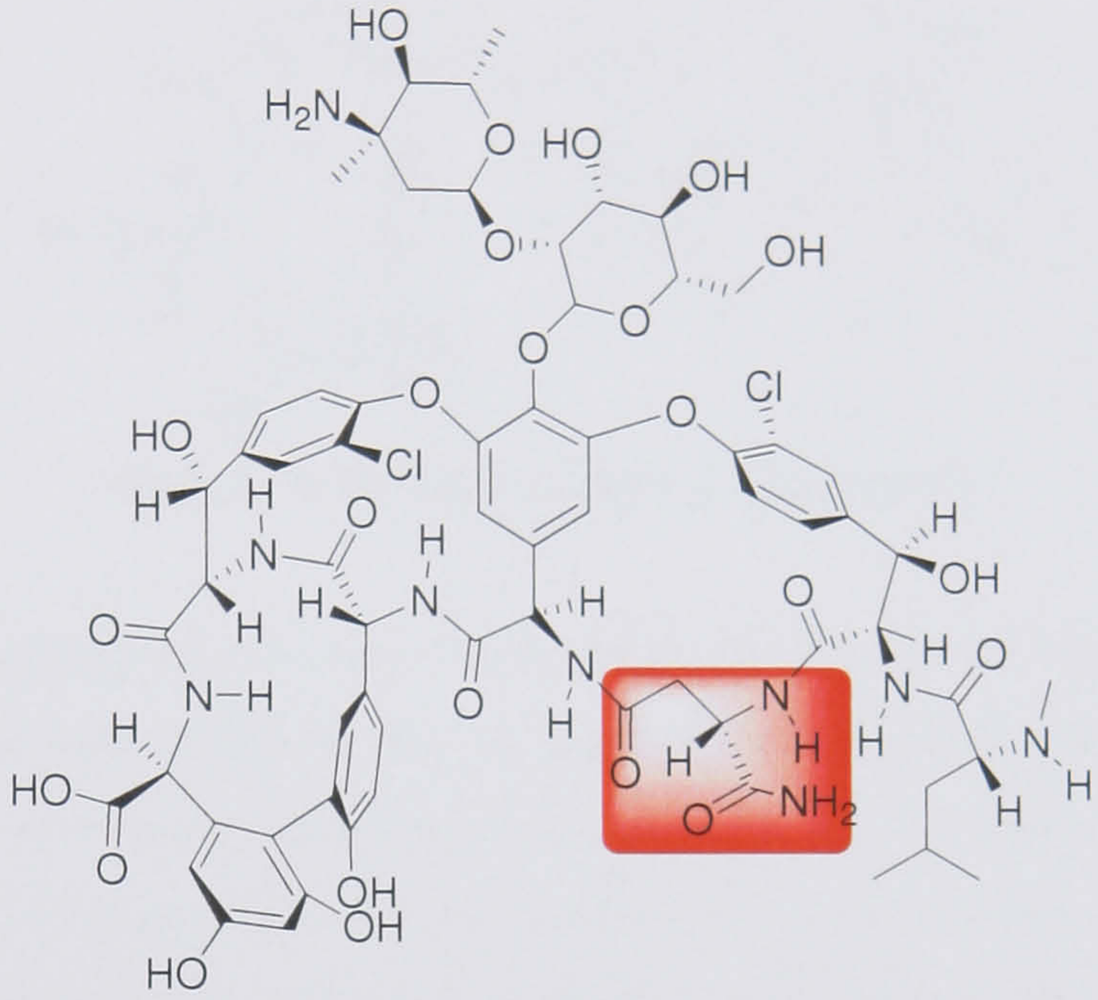

Figure1.37. The proposed structure of vancomycin, the highlighted area indicates the arrangement of residue 3.[56]

This structure was then refined by Harris and Harris (1982-1983).[48,49] They postulated that the unusual arrangement of residue 3, as an iso-asparagine (highlighted in Figure 1.37), was unlikely and that it was probable that the iso-aspartic acid present in the crystalline degradation product was derived *via* the cleavage and re-arrangement of an asparagine present in the vancomycin structure. The presence of the asparagine residue was then confirmed through a series of chemical tests on vancomycin. This lead to an amendment to the proposed structure of vancomycin, to give the structure below. This is the final structure of vancomycin (Figure 1.38).[48,49]

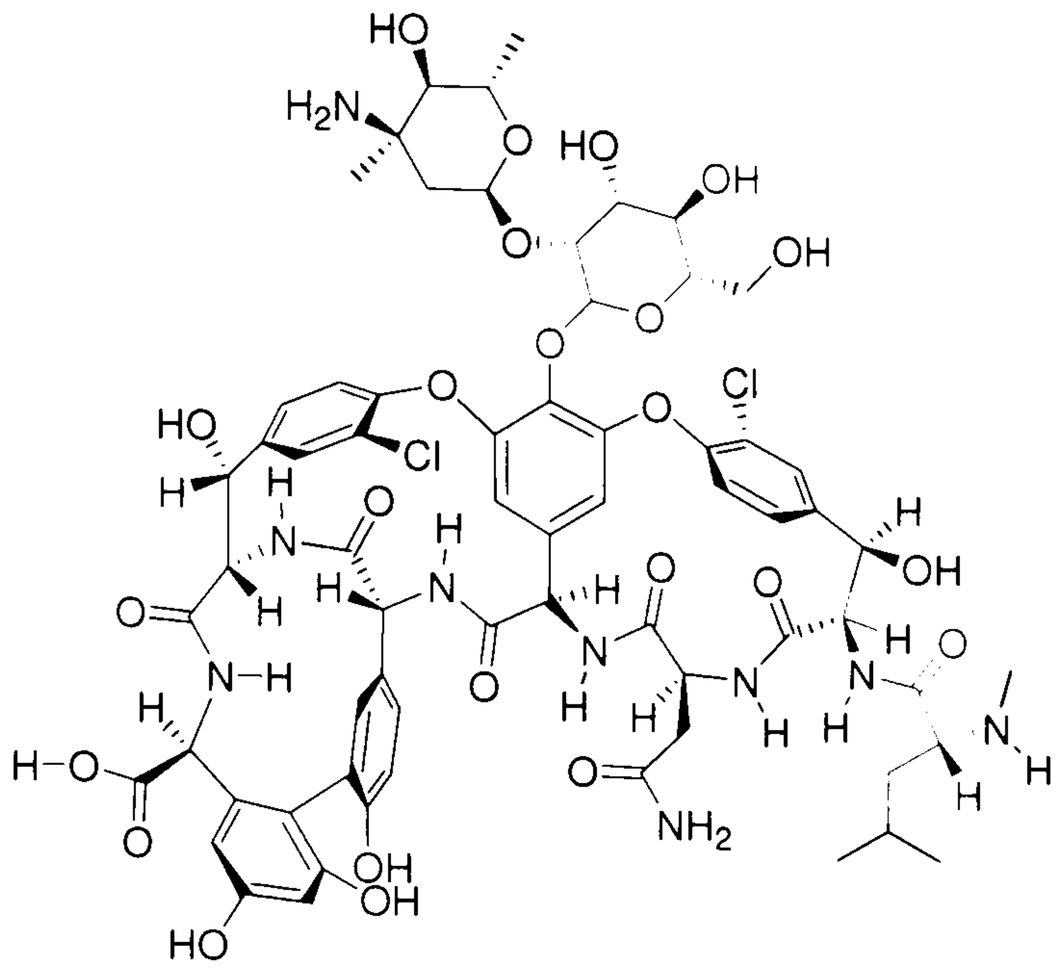

Figure 1.38. The final structure of vancomycin.[48,49]

Although most of the work carried out to elucidate the structures of the glycopeptides was preformed on vancomycin itself, or its derivatives, it was obvious at the time that vancomycin did not share its aglycone with most of the other glycopeptides that had been discovered.[57] There are two possible variations of the aglycone in the glycopeptides; one is displayed by vancomycin and the other by ristocetin. Ristocetin is not used clinically, as it causes aggregation of platelets in the blood.

The determination of the structure of ristocetin (Figure 1.40) was also quite involved and took a number of years and the input of many research groups. However the complete assignment of vancomycin accelerated this process.[58-63]

Following the elucidation of both the vancomycin and ristocetin structure, it was observed that all the glycopeptides are heptapeptides (seven residue) which display identical stereo-configuration along the peptide backbone, which is D-D-L-D-D-L-L.[31] They all have either the aglycone displayed by vancomycin or ristocetin.[45] Complestatin is an exception to these rules and its structure is shown below (Figure 1.39).

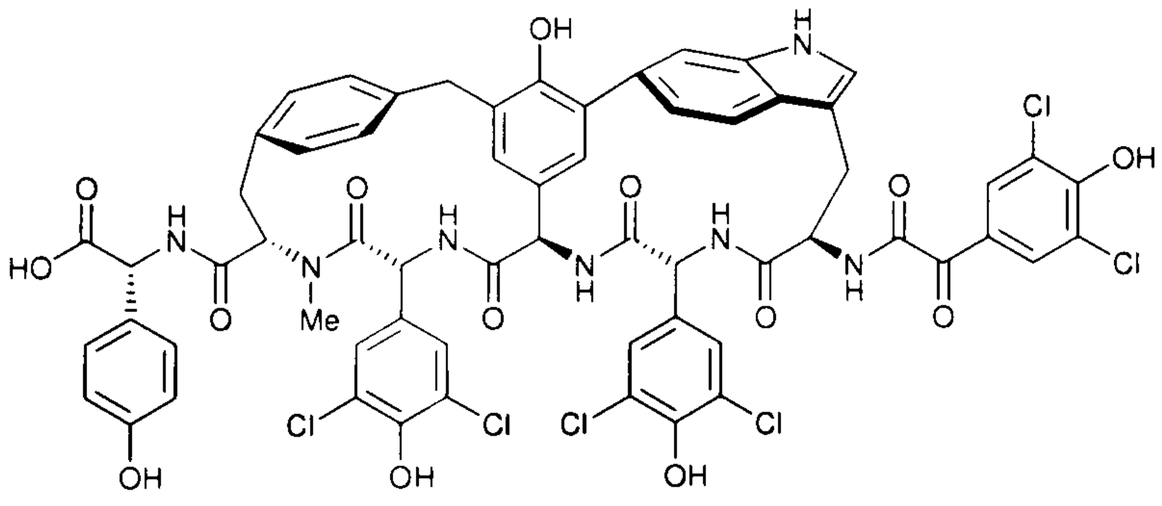

Figure 1.39. Complestatin.[31]

Chloreremomycin, balhimycin and orienticin C share the vancomycin aglycone. Five out of the seven amino acid bear aromatic residues (residue 2 and residues 4-7). These aromatic residues are cross-linked, residue 2 linked to 4, which is also linked to 6, and residue 5 is linked to 7. The remaining two amino acids bear aliphatic residues, asparagine at position 3 and *N*-methyl-D-leucine at position 1, and these are not cross-linked. These structural elements combine to give three fused rings that form a bowl shaped cradle that is distinctive in all glycopeptides.

Teicoplanin, avoparcin, actaplanin and A47934 share the ristocetin aglycone. This has all seven amino acids with aromatic side chains and in addition to the cross-links displayed in the vancomycin aglycone, has a further cross-link between the aromatic residues 1 and 3. Thus there are four fused rings and these also fold into the characteristic glycopeptide cradle.[31]

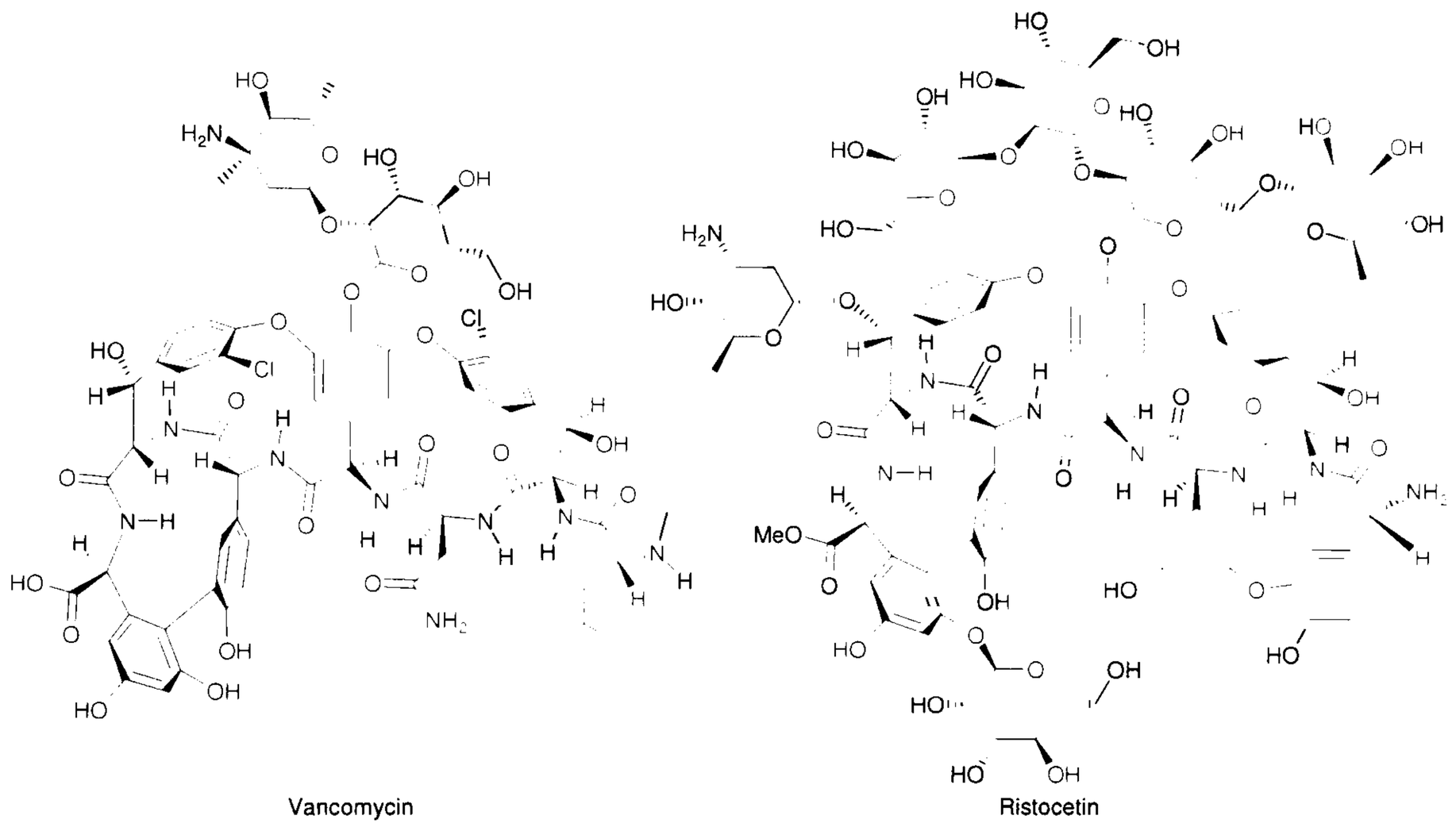

Figure 1.40. Vancomycin and ristocetin, exemplifying the two peptide cores of glycopeptides.[31]

1.4.3 Mode of action

The cradle-like structure adopted by the peptide portion of the glycopeptides is crucial to their mode of action.[45] The cleft this conformation creates allows the binding of the terminal D-alanyl-D-alanine portion of the intermediates used to synthesise the cell wall. Both lipid II and immature cell walls display these D-ala dipeptide termini and are therefore sequestered by vancomycin. When vancomycin binds to lipid II it prevents

access of both the transglycosylase and the transpeptidase. This stops the formation of new cell wall. When vancomycin binds to the immature peptide that has already undergone transglycosylation, transpeptidation is blocked, thus preventing the cross-linking of the amino acid side chains. The result of this is that the balance between the hydrolysis of the cell wall and the addition of new cell wall is destroyed and the cell wall loses its mechanical stability. The bacterial cell is then lysed by osmotic pressure if it enters a hypotonic solution.[45]

The molecular basis for the ability of vancomycin to sequester the D-ala-D-ala dipeptide terminus was determined by Williams *et al.*[64] It was shown that a dipeptide, acetyl-D-ala-D-ala fits into the cleft in the surface of vancomycin, so that its carboxyl terminus points at the *N*-terminus of vancomycin. This allows the formation of a hydrogen bonding network between the amide backbones of the dipeptide and vancomycin, as well as a salt bridge between the *C*-terminal carboxylate of the dipeptide and the cationic nitrogen of the *N*-methyl-D-leucine. This binding model was then refined in a later paper, [65] where the isobutyl group of the terminal *N*-methyl-D-leucine was shown to wrap over the dipeptide and exclude water from the binding pocket, thus re-enforcing the hydrogen bonding. These investigations allowed the production of a model of the binding site for the dipeptide and the antibiotic, shown below in Figure 1.41.

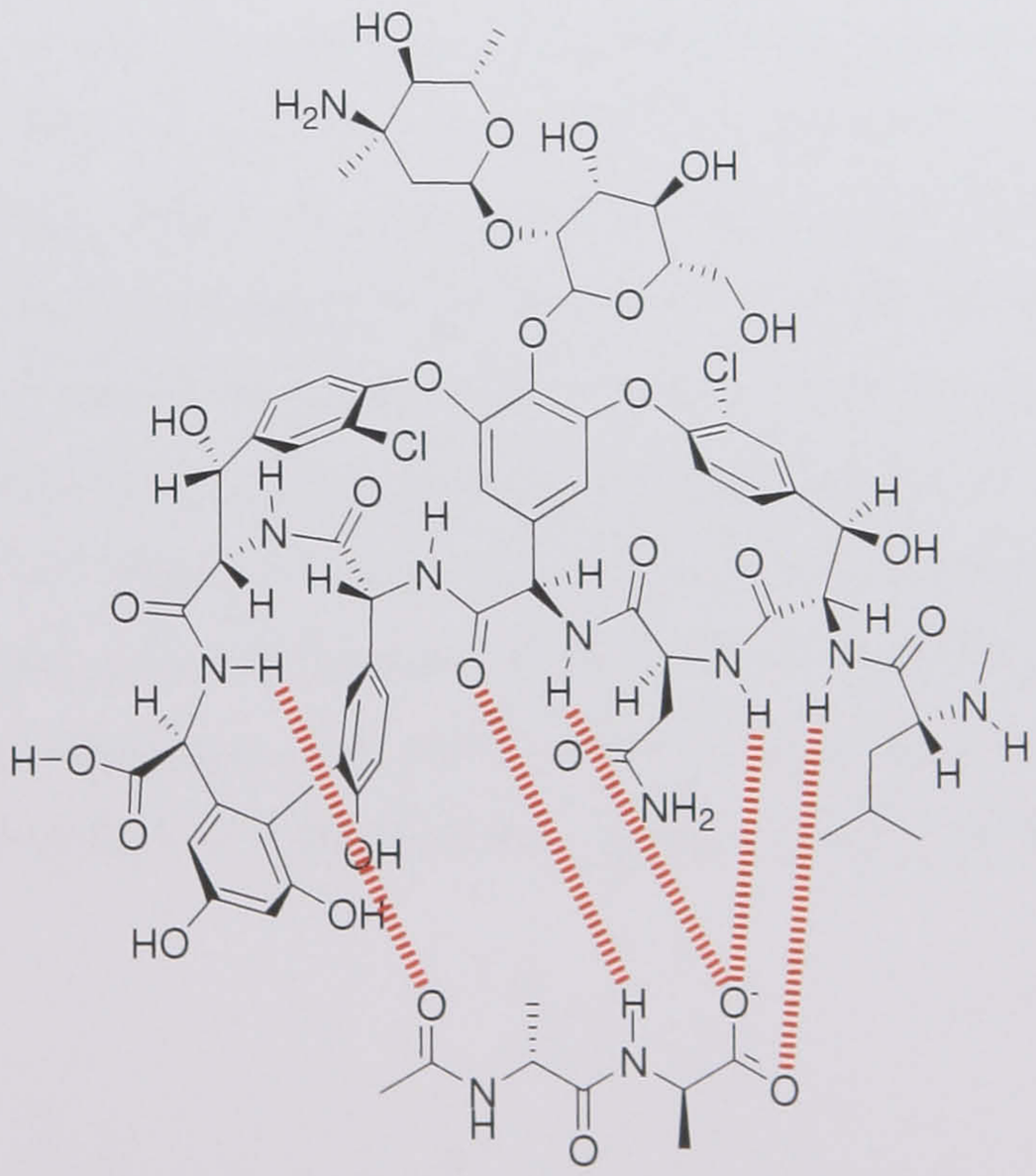

Figure 1.41. An exploded view of vancomycin and D-ala-D-ala dipeptide indicating the H-bond network.[31]

Williams *et al.*[66] then went on to consider the energetics of complex formation, which led to the conclusion that the mobility of residues one and three was an advantage in binding. Movement of these residues allow the partial association of the dipeptide and the antibiotic. This is followed by a re-arrangement that displaces solvent from the reminder of the structure and allows the completion of the binding interactions.[66]

Further work advanced the binding model using diacetyl-L-lys-D-ala-D-ala and other D-ala-D-ala containing peptides. The aglycone and some semi-synthetic analogues of vancomycin were also considered in these studies. These studies helped to define the role of the chlorine substituents and the *N*-terminal amino acid in the binding of the dipeptide containing cell wall analogues.[67-70]

A further development in the understanding of the binding process came from the observation that the dimerisation of these antibiotics is significant in the mode of action and this is discussed in detail in Section 1.5.

In addition to antibiotic action brought about by inhibition of transpeptidation, a number of studies have provided evidence that there is an additional mechanism for antibiotic activity in some glycopeptides. Kahne and co-workers[71] developed a series of compounds that showed binding of the cell wall peptide is not actually necessary to produce biological activity. They produced disaccharides (glucose and vancosamine) which had been alkylated on the amino sugar with a lipophilic chlorobiphenyl chain. This moiety produced a measurable minimum inhibitory concentration (MIC) against both sensitive and resistant strains of *E. faecium* and *E. faecalis* and thus they concluded that there must be an alternative mode of action for this compound, as it lacked the binding pocket needed to bind D-ala-D-ala or D-ala-D-lac based cell wall peptides. It was suggested that this inhibition was mediated through a direct interaction between the disaccharide and some of the enzymes involved in cell wall biosynthesis. The compounds are shown in Figure 1.42 and the MICs for one of them and vancomycin are shown in Table 1.2 (N.B. Van A and Van B are phenotypes of resistance, see Section 1.6).

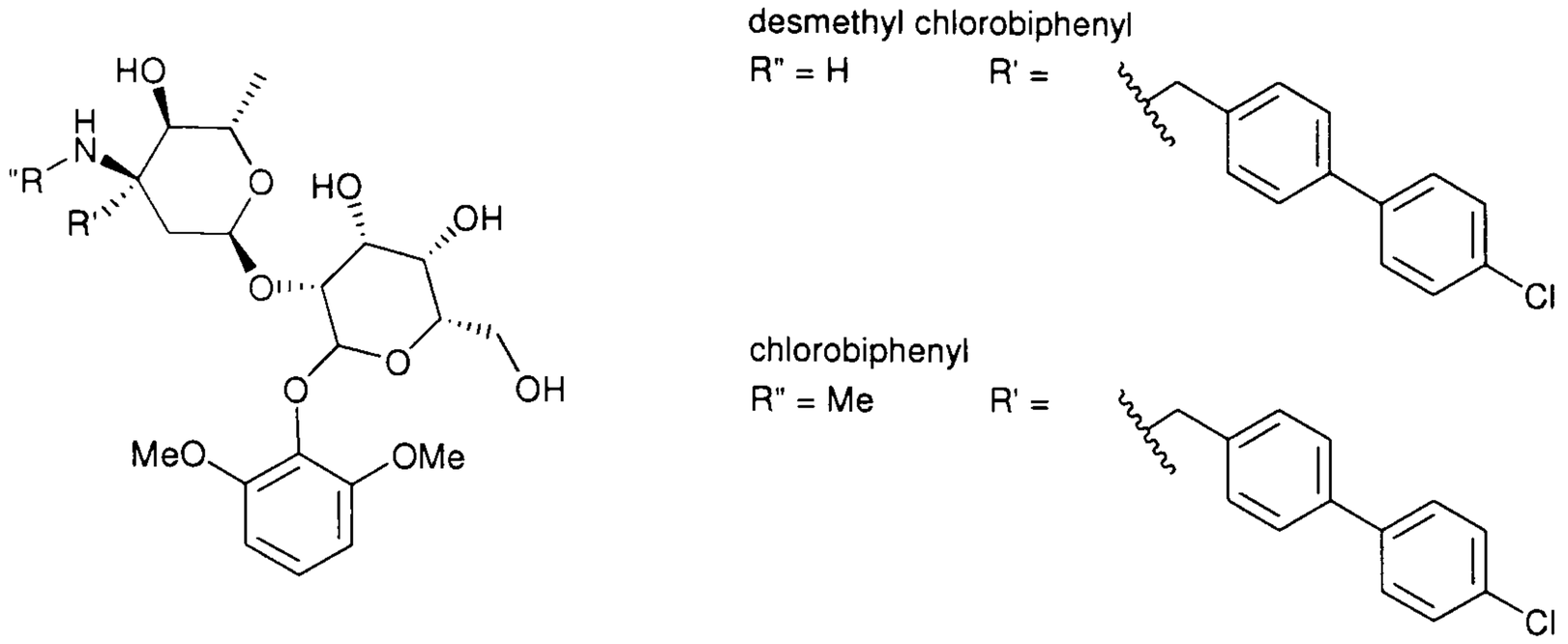

Figure 1.42. Two disaccharides produced by Kahne and co-workers.[71]

Compound	MIC (μg/ml)			
	E. faecium		*E. faecalis*	
	Sensitive	Resistant (Van A)	Sensitive	Resistant (Van B)
vancomycin	1	2048	4	2048
chlorobiphenyl disaccharide	128	128	128	128

Table 1.2. MIC's for the chlorobiphenyl disaccharide and vancomycin from Kahne and co-workers[71]

Kahne and co-workers[72] also produced a number of compounds with variations of the sugars seen in vancomycin, where hydrophobic chains had been added to the sugars and alternative links to the peptide portion of vancomycin were also employed. By comparing the differences these novel sugars had when coupled to either the hexapeptide, which cannot effectively bind the cell wall peptide, or to the heptapeptide which can bind the cell wall peptide, they were able to confirm that alternate binding mode and were able to understand it more fully. The first series has sugar variations coupled to the 4th amino acid residue, as shown in Figure 1.43 and their MIC data are shown in Table 1.3.

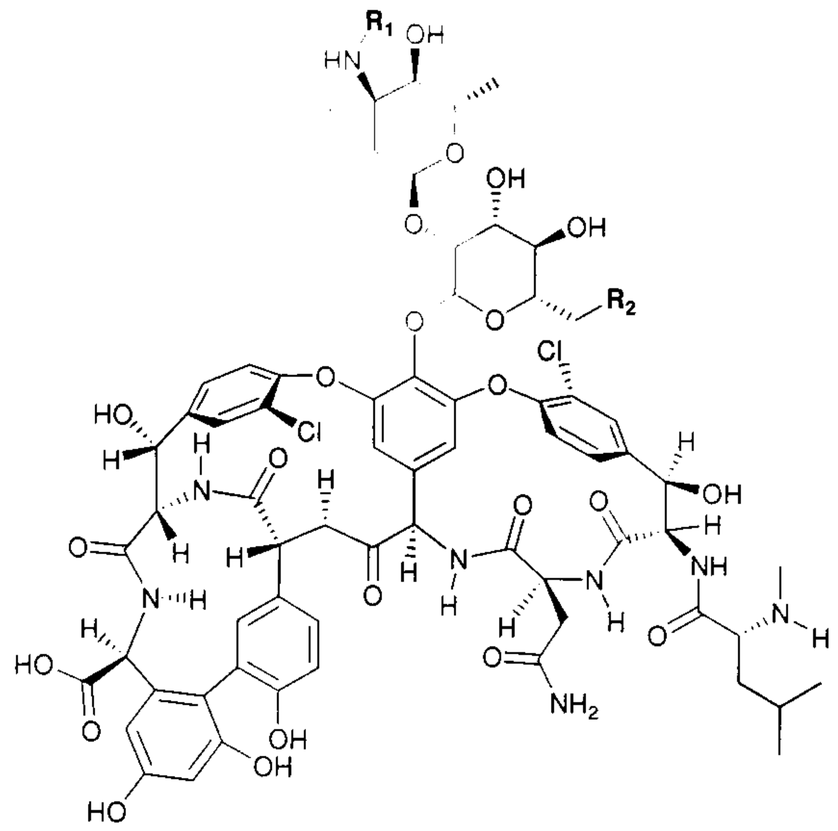

1 R_1 = -H R_2 = -OH

2 R_1 = $-CH_2-C_6H_3Cl-C_6H_4Cl$ R_2 = -OH

3 R_1 = -H R_2 = $-NHCH_2-C_6H_3Cl-C_6H_4Cl$

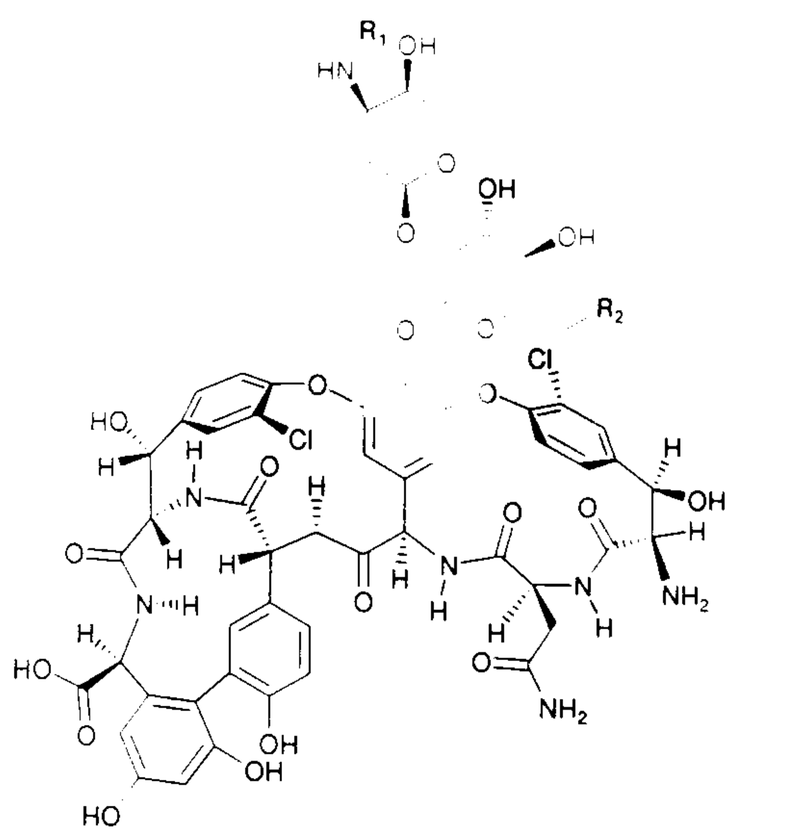

2a R_1 = $-CH_2-C_6H_3Cl-C_6H_4Cl$ R_2 = -OH

3a R_1 = -H R_2 = $-NHCH_2-C_6H_3Cl-C_6H_4Cl$

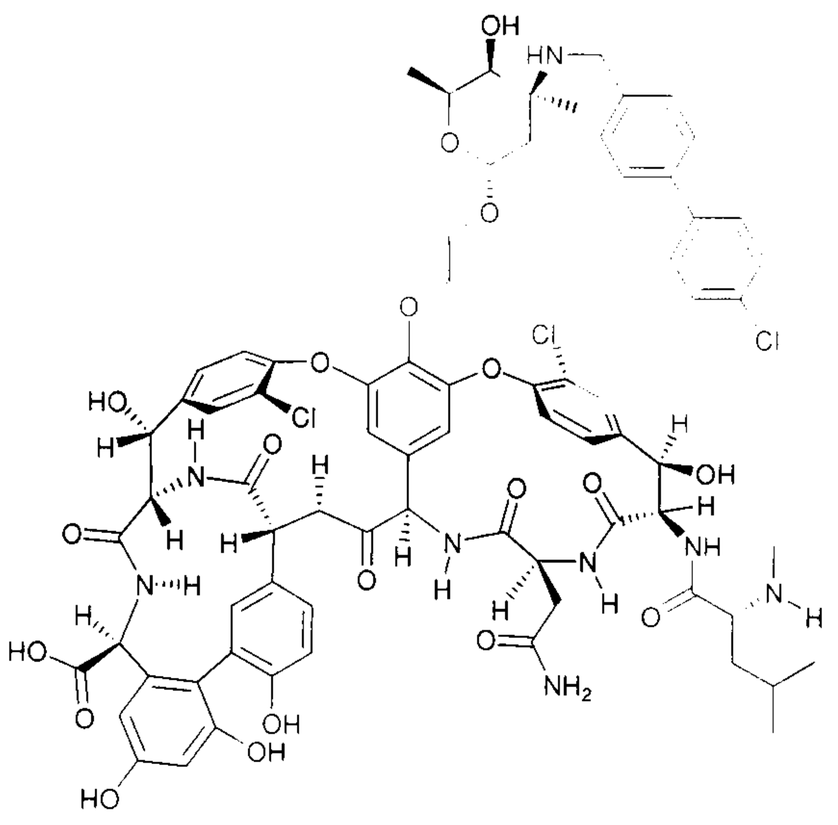

4

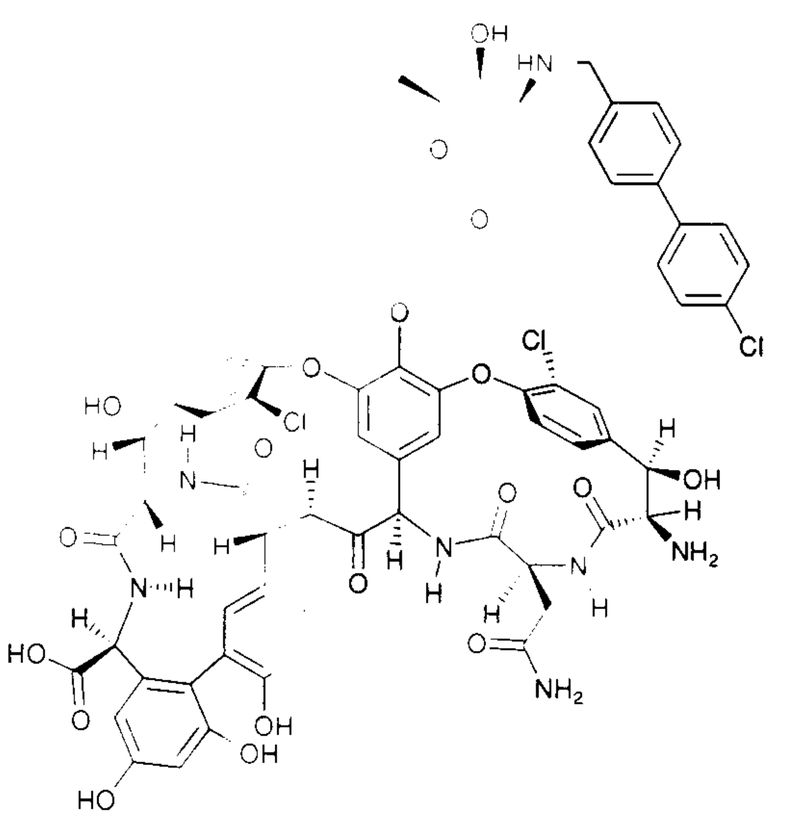

4a

Figure 1.43. Kahne and co-workers compounds with altered sugars.[72]

Compound	MIC (μg/ml) *E. faecium*	
	Sensitive	Resistant (Van A)
Vancomycin (1)	2	2048
2	<0.025	12.5
3	<0.03	16
4	0.8	63
2a	10	40
3a	64	1024
4a	50	>200

Table 1.3. MIC data for compounds with altered sugars produced by Kahne and co-workers.[72]

This series showed both sugars are important for binding (compare 4/4a to 2/2a) and that the activity produced by binding D-ala-D-ala containing cell wall intermediates is

more important than the activity produced by the novel binding mechanism (compare compounds 2-4 to compounds 2a-4a). It does however show that there is a significant level of activity retained in compound 2a which can not effectively bind D-ala-D-ala containing cell wall intermediates and thus this secondary binding mode has some importance in the search for compounds active against resistant strains of bacteria. The marked loss of activity of 3a compared to 2a shows that the placement of the hydrophobic chain is crucial in the activity of these compounds.

Kahne and co-workers[72] also produced a pair of compounds where the position at which the sugars were attached was altered, these are shown in Figure 1.44 and their MIC data is shown in Table 1.4.

Compound	MIC (μg/ml) *E. faecium*	
	Sensitive	Resistant (Van A)
Vancomycin	2	2048
Residue 4 linked	<0.01	63
Residue 7 linked	0.16	16

Table 1.4. MIC data for compounds with altered point of sugar attachment produced by Kahne and co-workers.[72]

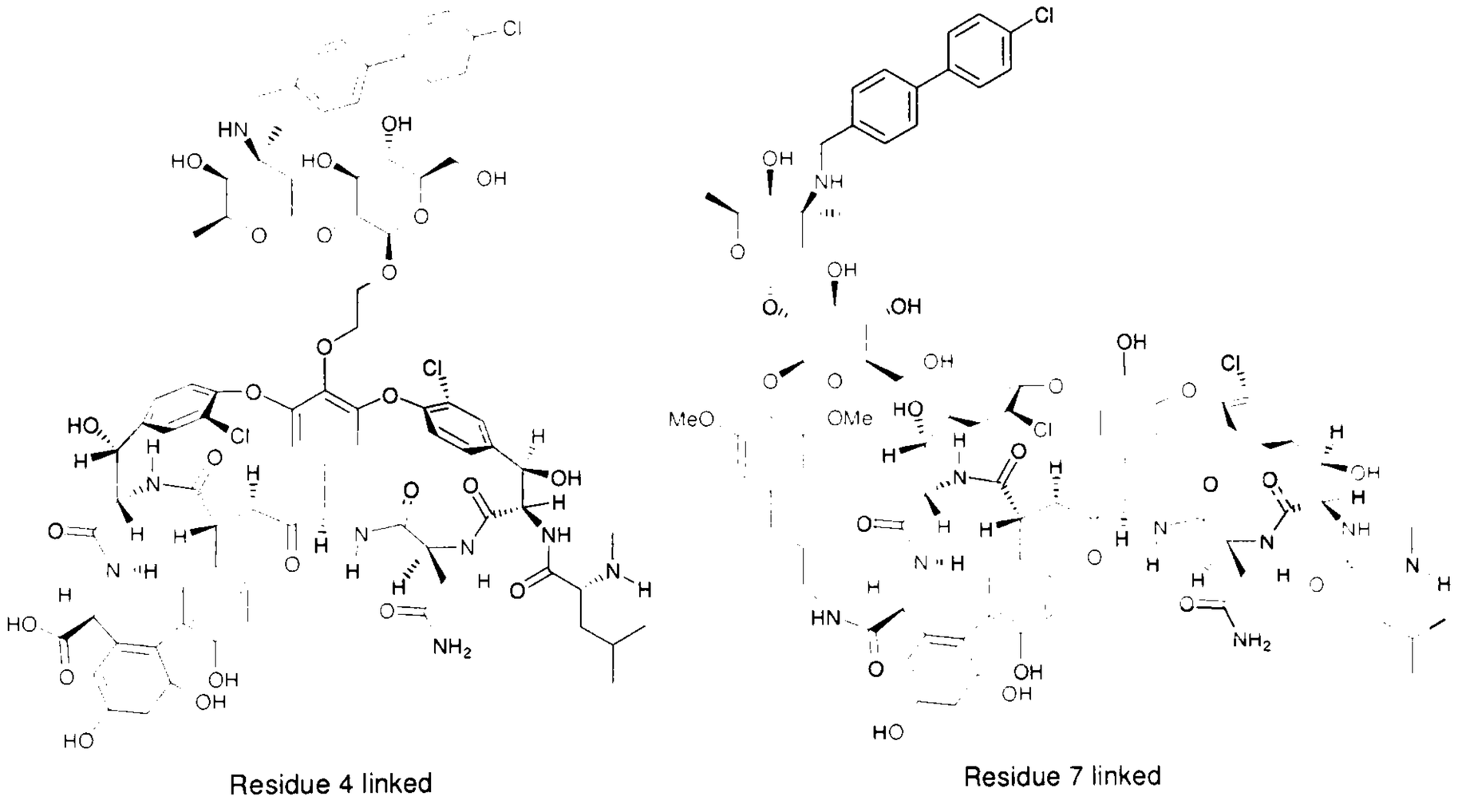

Figure 1.44. Compounds with altered point of sugar attachment produced by Kahne and co-workers.[72]

A comparison of MIC data for these compounds showed that the compound with the sugars linked through residue 7 had the best activity against the resistant strain, though both compounds had good activity. Kahne and co-workers[72] conclude that the altered

binding found in these kinds of compounds are probably the result of inhibition of transglycosylation, but they did not feel that the data generated was sufficient to be certain that this was their mode of action.

Kahne and co-workers[73] further strengthened the hypothesis that there is a secondary mode of action for some glycopeptides by producing and comparing a series of glycopeptides with and without the damaged binding pockets. They used vancomycin, chlorobiphenyl vancomycin, teicoplanin and dalbavancin. They showed that while the parent compounds with intact binding pockets have similar values for both MIC and IC_{50} in a transglycosylase assay with penicillin binding protein 2 (PBP2), there is a marked difference in the activities of the compounds with damaged pockets (Table 1.5). The chlorobiphenyl vancomycin and dalbavancin analogues were still able to produce measurable MIC's and IC_{50}'s (transglycosylase), but the vancomycin and teicoplanin analogues could not. Kahne and co-workers[73] reasoned that this could only occur if these compounds exhibited a second mode of action that was independent of binding the cell wall peptide.

Compound	**MIC (μg/ml)** *S. aureus 29213*	**IC_{50} (μm)** *S. aureus* **PBP2**
vancomycin	3.2	1.7
teicoplanin	3.2	1.2
chlorobiphenyl vancomycin	0.1	2.7
dalbavancin	0.1	1.1
vancomycin damaged pocket	>264	>500
teicoplanin damaged pocket	>100	>500
chlorobiphenyl vancomycin damaged pocket	4.8	3.5
dalbavancin damaged pocket	50	70

Table 1.5. MIC's and IC_{50}'s for a range of compounds studied by Kahne and co-workers.

Roy *et al.*[74] built on this hypothesis by producing affinity columns with lipophilic glycopeptide anchored to solid supports, which were then used to chromatograph solubilised *E. coli* membranes. This produced very interesting results as it showed that a number of cell wall biosynthetic enzymes were bound to the column and could be isolated and characterised. They also carried-out similar experiments with glycopeptides that had no lipophilic side chains anchored to solid supports and found that they had no specific binding interactions with the membrane enzymes. Thus this supported the hypothesis of Kahne and co-workers[71] that there was a further mode of action for glycopeptides with hydrophobic side chains.

1.5 Dimerisation

Dimerisation, an important phenomenon in the glycopeptide antibiotics, is the spontaneous association of two molecules of glycopeptide into a complex that is stabilised by a network of hydrogen bonds. It is most often observed in the presence of an appropriate ligand but the more strongly dimerising glycopeptides will associate even when a ligand is not present.[75]

This phenomenon was first reported by Waltho and Williams[76] when they observed and quantified the dimerisation of complexes formed by ristocetin A and its pseudoaglycone in the presence of diacetyl-L-lys-D-ala-D-ala. They calculated that the dimerisation constant for ristocetin-diacetyl-L-lys-D-ala-D-ala dimer was ~2000 M^{-1}.

Further work by Williams and co-workers[77] went on to measure the dimerisation constants of a range of glycopeptides, including vancomycin (700 M^{-1}), and gave a greater understanding of the mechanism of dimerisation and its effects. They showed that the dimerisation in ristocetin is a back-to-back, head-to-tail arrangement as shown in Figure 1.45.

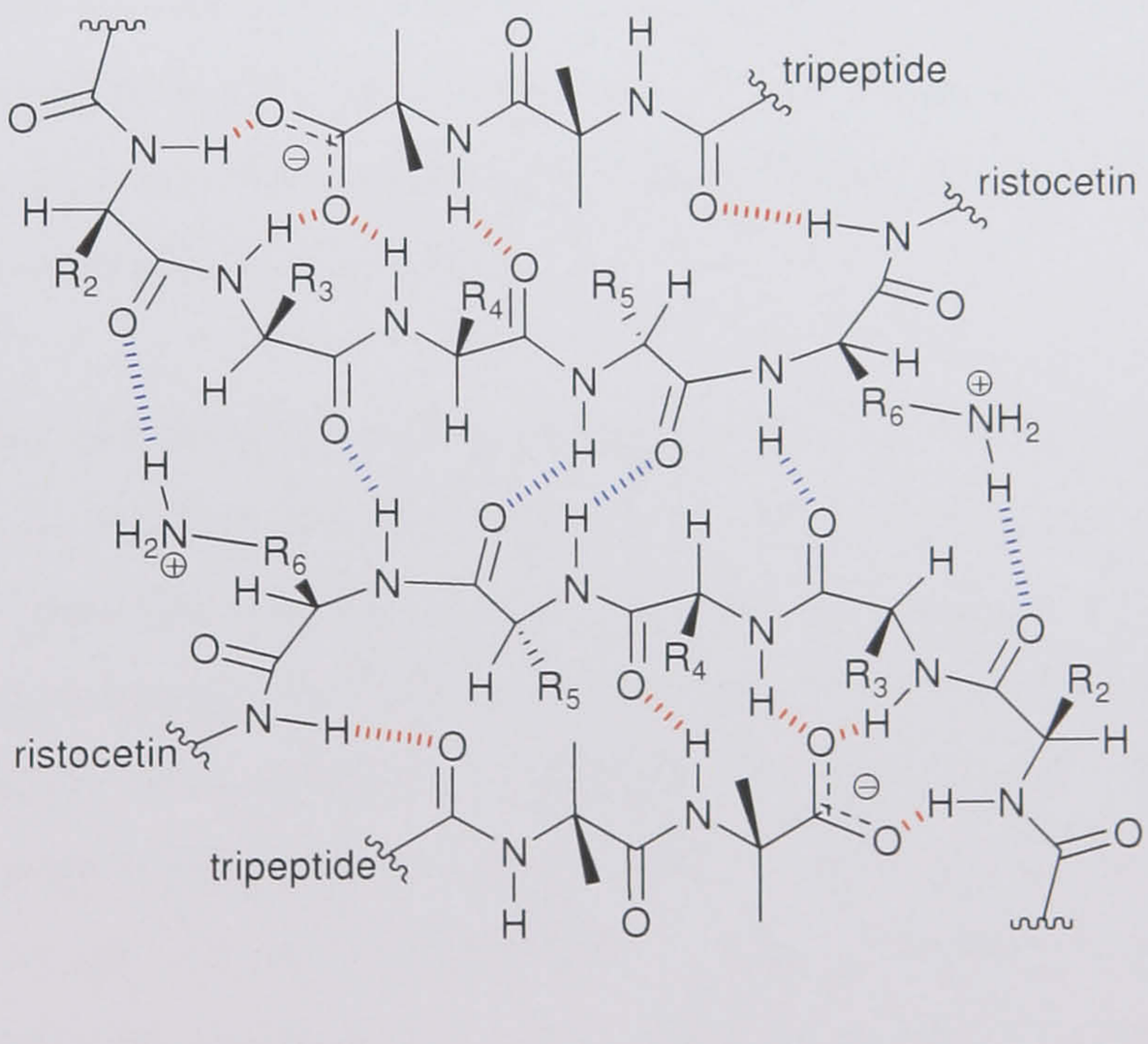

Figure 1.45. A representation of the dimer formed between two ristocetin tripeptide complexes.[77] The red dashed bonds indicate the hydrogen bonding normally observed in complex formation and the blue dashed bonds show the hydrogen bonds of the dimer.

Williams and co-workers[77] explained that dimerisation is favourable because it is a cooperative process, which strengthens and shortens the hydrogen bonds between both the two glycopeptides and also between the glycopeptides and the tripeptide that mimics the cell wall.

There are a number of ways that dimerisation may help improve the antibacterial properties of these compounds *in vivo*. Firstly, because of its cooperative nature, once the dimer is formed and binds to two cell wall intermediates each set of hydrogen bonding interactions are re-enforced. Therefore, it becomes less likely that either one of the cell wall intermediates would dissociate or that the glycopeptides would dissociate from each other, thus the complex formed should be longer lived than that of the monomeric form. In addition, once one cell wall peptide is bound it becomes more likely that a second cell wall peptide will be bound. This is because the dimer is held in close association with the bacterial cell wall and thus the dimer is effectively tethered by the first complex (between the cell wall peptide and glycopeptide), the formation of the second complex is effectively an intramolecular process, and thus is favoured over the analogous process where a monomeric glycopeptide approaches the cell wall and has to bind in an intermolecular process. The formation of the second complex is also preferred because the unoccupied binding site is already pre-organised into the correct conformation by the hydrogen bonds to the occupied glycopeptide and therefore has already paid the entropic plenty for this part of the binding event, thus further favouring binding of a second cell wall intermediate.

The amino-sugar extending from residue 6 of ristocetin adds an extra stability to the complex dimer, as it hydrogen bonds to the carbonyl group of the backbone amide in residue 2 in the other ristocetin (shown in Figure 1.45). This sugar is also present in another of the glycopeptides studied in this work, eremomycin, which also exhibits a high dimerisation constant $\geq 10000\ M^{-1}$. Ristocetin, eremomycin and vancomycin all exhibit the same back-to-back dimer arrangement, yet vancomycin has a lower dimerisation constant. Williams and co-workers[77] suggest thtat the absence of this particular sugar in vancomycin provides an explanation for the lower dimerisation constant observed in vancomycin.

Williams and co-workers[78] carried out further experiments to assess the importance of dimerisation in the antibacterial activity of glycopeptides. The antibacterial properties of

three antibiotics with a range of dimerisation constants, teicoplanin A_3-1 (which does not dimerise), vancomycin (which dimerises weakly), and eremomycin (strongly dimerising) were tested by measuring the inhibition of growth of *B. subtilis* with varying amounts of diacetyl-L-lys-D-ala-D-ala as an exogenous antagonist. In these experiments the antibiotics which dimerised most strongly were expected to be the most difficult to antagonize with exogenous ligand. This is because their binding would be initially bimolecular (intermolecular) and thus strongly effected by the exogenous ligand, but then unimolecular (intramolecular) and thus weakly effected by the exogenous ligand. Whereas, the weakly dimerising glycopeptide would always bind by a bimolecular (intermolecular) fashion and thus be strongly effected by the exogenous ligand. Their experiments proved this to be true, as 1 μg teicoplanin A_3-1 needed only 5 μg of ligand to prevent a zone of inhibition forming, 1 μg of vancomycin took 50 μg to prevent a zone of inhibition forming and eremomycin still showed inhibition despite the presence of 50 μg of ligand. This strengthens the hypothesis that the more strongly a glycopeptide antibiotic dimerises, the more likely it is to have good antibacterial activity. Figure 1.46 gives a simple schematic that illustrates why a dimeric form is more strongly bound. However this is a simplification as there are numerous factors that contribute to the antibacterial properties of these compounds.

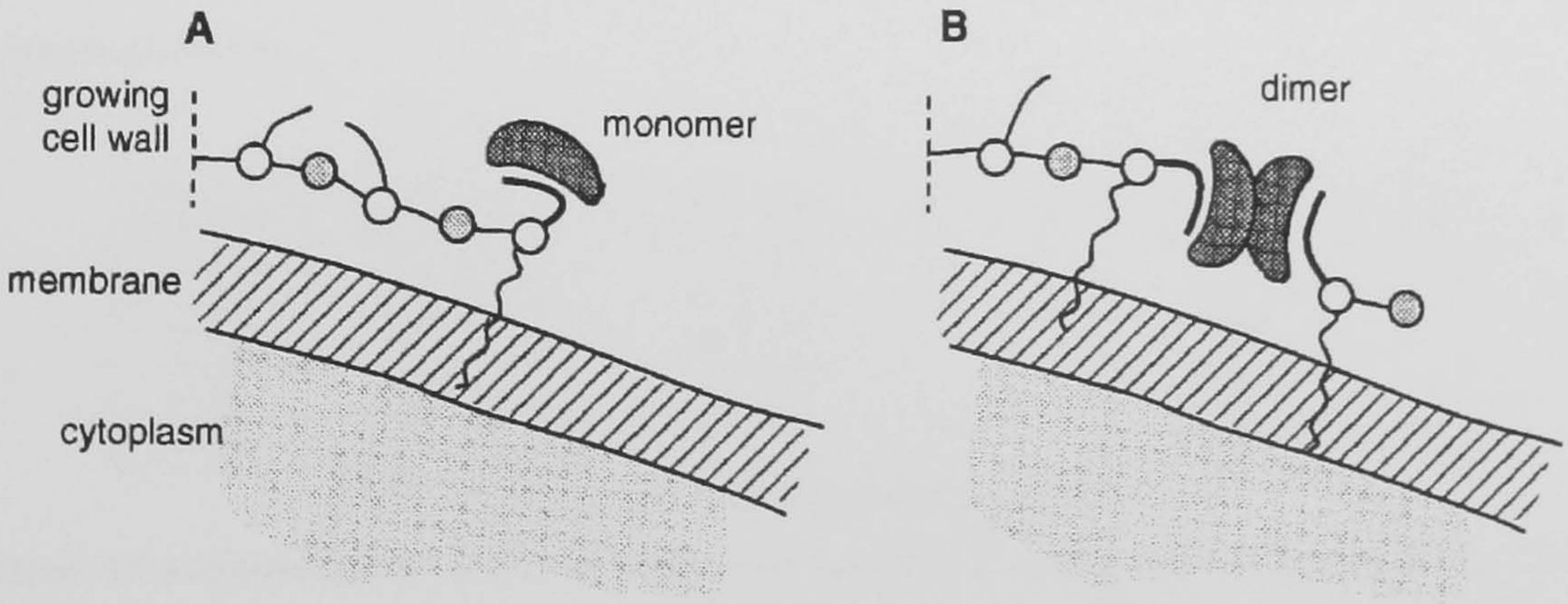

Figure 1.46. A) Shows the weakly bound monomeric glycopeptide. B) Shows the more strongly bound dimeric glycopeptide. Adapted from Williams and co-workers.[78]

Sheldrick and co-workers[79] solved a crystal structure for vancomycin where the dimer had bound an acetate ion. This displayed the back-to-back dimerisation that had been suggested from the NMR data of earlier studies and confirmed this hypothesis.

Try *et al.*[75] examined the effect that dimerisation has upon binding when the complex of the glycopeptide is in close association with a surface. They used micelles of sodium dodecyl sulphate (SDS) or vesicles of phosphatidylcholine (PC) which had a range of cell wall mimic peptides bound into them with deconyl chains. They found that the PC vesicles with a deconyl pentapeptide gave a system that was qualitatively similar to binding near the surface of the bacteria and that they observed an approximate 100-fold enhancement of binding compared to the unanchored system.

Loll *et al.*[80] also solved a crystal structure for vancomycin, again with a bound acetate ligand, that shed further light on its dimerisation. They were able to measure the bond length and angles for the hydrogen bonds of the dimer interface (shown in Table 1.6). From this data they concluded that the increase in affinity for the bound ligand was due to increased polarisation in the amide bonds of the backbone residues that form the dimer interface. They also suggest that the reason why ristocetin, eremomycin and other compounds that contain an amino-sugar attached to the 6th amino acid residue have greater dimerisation constants, is that the amino-sugar is charged and forms a further hydrogen bond at each end of the dimer interface. This not only increases the number of hydrogen bonds, but since the amine on the amino-sugar is a cation, the polarisation induced by its hydrogen bonding is greater than that of the hydrogen bonds of the backbone amides. This agrees with the observations of Williams and co-workers[77] mentioned above.

Donor	Acceptor	O---H Distance (Å)	C=O---H Angle (deg)
V2:6	V1:3	2.29	170
V1:5	V2:5	2.14	149
V2:5	V1:5	2.03	163
V1:6	V2:3	2.22	164

Table 1.6. Hydrogen bonding in the dimer interface.[80]

Where V2:6 indicates that the donor or acceptor is on the 6th amino acid of the second monomer.

Further work by Loll and co-workers[81] showed that the sugar residues of vancomycin play a significant role in the formation of the dimer, in that they provide a steric constraint which reduces the motility of the peptide portion of the compound. They compared crystal structures of vancomycin and aglucovancomycin and found that there was a greater degree of conformational heterogeneity in the crystal structure of the aglucovancomycin as four distinct conformations were observed in the crystal structure.

Lehman *et al.*[82] solved four crystal structures for balhimycin and degluco-balhimycin. Balhimycin is a closely related glycopeptide and differs in structure to vancomycin by having only glucose attached to the residue of amino acid 4 and an amino-sugar attached to the residue of amino acid 6. In these structures they again observed the characteristic back-to-back dimer, but they also observed a face-to-face dimerisation. They postulated that this form of dimerisation may be significant in binding events *in vivo* because this dimer traps the two peptides within the complex. However, this face-to-face dimerisation has not been observed in solution studies, so may not be particularly important.

Williams and co-workers[83] effectively combined many aspects from the studies of dimerisation by examining the data generated by solution NMR studies and the published crystal structures of a range of glycopeptides that covered the spectrum of dimerisation strength. They found that there was a correlation between the interfacial distance of the dimer measured in the crystal structures, the shift of the X_4 proton (Figure 1.47), measured by NMR, and the dimerisation constants observed for each glycopeptide. They found that when a compound has a high dimerisation constant, the interfacial distance measured in the crystal structure was smaller, and the X_4 proton was shifted further downfield in the NMR spectra. From this, Williams and co-workers[83] reasoned that the stronger the dimerisation, the shorter (and thus stronger) the hydrogen bonds between the dimer pairs and the more rigidly held the dimer is. The shift of proton X_4 is dependent upon the dimer strength because the tightening of the dimer interface shortens the hydrogen bonds and brings this proton into close association with two of the backbone carbonyl groups that form part of the hydrogen bond network between the two glycopeptides of the dimer, shown in Figure 1.47.

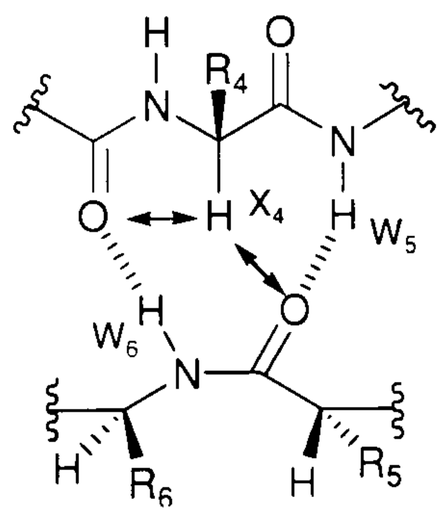

Figure 1.47. Section of the dimer interface of two glycopeptides of the vancomycin family showing the proximity of X_4 to two amide carbonyls that results from the formation of the dimer hydrogen bond network.[83]

1.5.1 Synthetic variants which exploit dimerisation

The observed dimerisation of glycopeptides opened up new ways for improving the antibacterial properties of these compounds. A number of groups have attempted to make synthetic analogues where two glycopeptides are covalently linked and could exploit the favourable cooperative binding which results from dimerisation.

Rao and Whitesides[84] produced a dimer where two vancomycin molecules were linked through their *C*-terminus to each other using *p*-xylenediamine as a linking fragment (Figure 1.48). They used *p*-xylenediamine because it was rigid and thus would not introduce an entropic penalty, through loss of bond rotations, when the synthetic dimer bound to ligands. They decided to link through the *C*-terminus as previous studies showed that modification here had minimal effects on the binding characteristics of the compound. Rao and Whitesides[84] also produced a covalently linked dimer of the tripeptide cell wall mimic (Figure 1.48). To do this they linked two α-acetyl-L-lys-D-ala-D-ala tripeptides through there ε-amines of lysine using succinic acid as the linking fragment. They examined these in competitive fluorescence and affinity capillary electrophoresis assays and determined the dissociation constant for the divalent complex. These results indicated that the divalent complex had an enhancement of ~1000-fold relative to the corresponding monomeric complex.

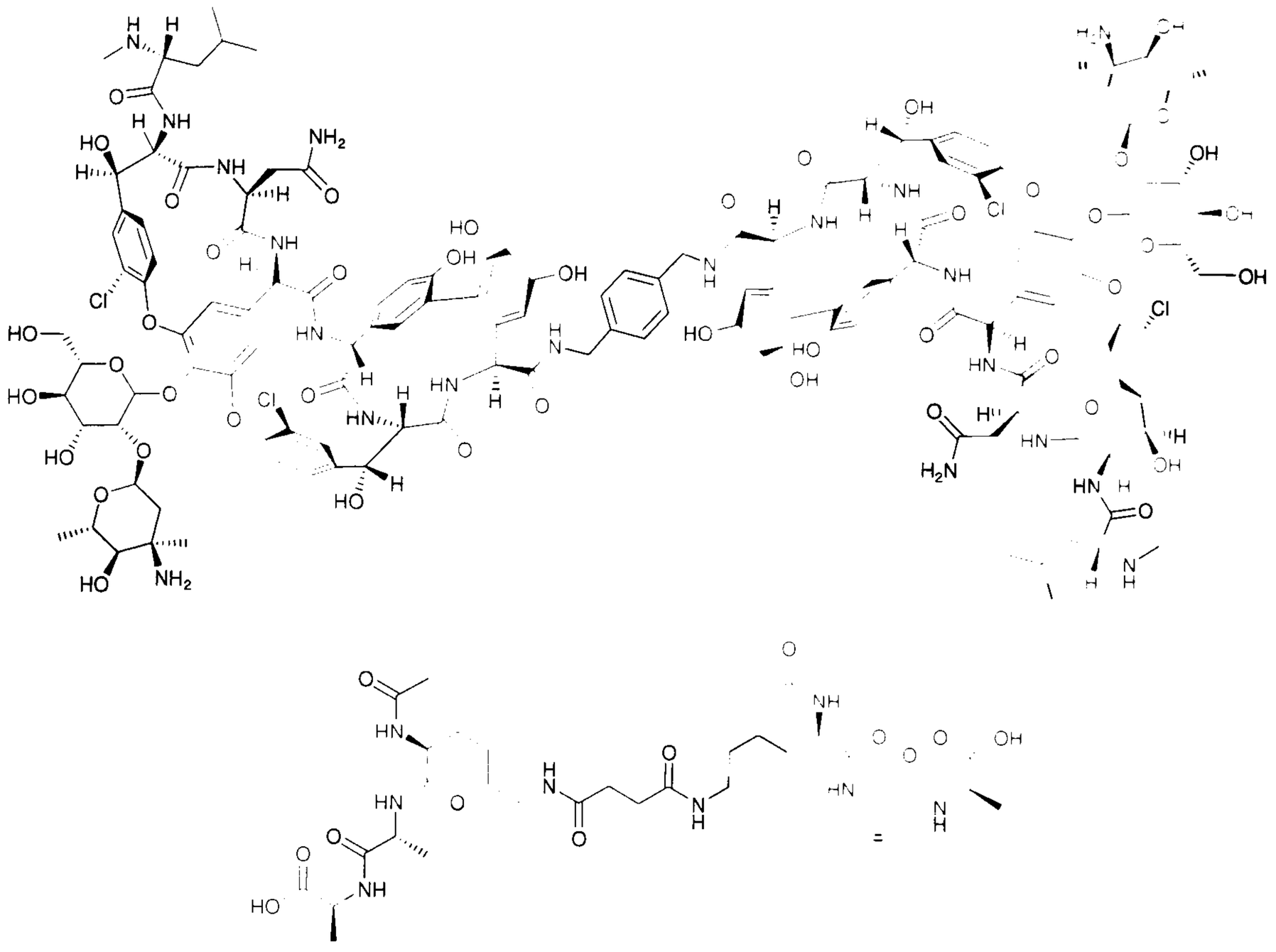

Figure 1.48. The vancomycin and ligand covalently linked dimers of Rao and Whitesides.[84]

Staroske and Williams[85] produced covalently bound dimers of vancomycin that were linked from the *N*-terminus of one vancomycin to the *C*-terminus of the other, called a head-to-tail dimer. They produced two variations of this type of dimer, one that used β-alanine as a linking fragment and a second that used 6-aminohexanoic acid as the linking fragment. Staroske and Williams[85] reasoned that these dimers would be more active than the head-to-head (*C*-terminus to *C*-terminus) compounds produced Rao and Whitesides[84] because they would more effectively form a tetrameric arrangement that utilises the back-to-back dimerisation seen in the monomeric form of vancomycin. They believed that the cooperative strengthening of the complex, that would be expected with dimerisation should lead to an improvement in the compounds activity against vancomycin-resistant enterococci. Figure 1.49 shows a schematic that demonstrates the differences in the tetrameric arrangements of the head-to-head and the head-to-tail dimers.

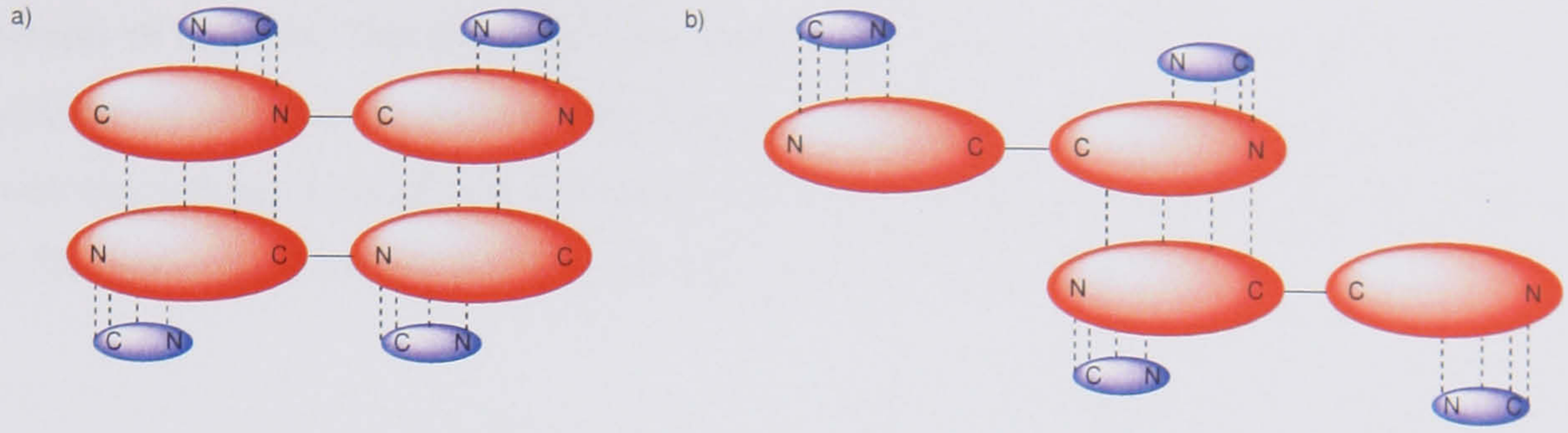

Figure 1.49. a) shows tetrameric complex as postulated for the head-to-tail covalent dimer, b) shows the tetrameric complex as postulated for the head-to-head covalent dimer. [85]

As can be seen in Figure 1.49, the tetrameric form postulated for the head-to-tail covalent dimer (a) places all four vancomycins in such a way that they can form two back-to-back dimers and thus strongly bind four ligands. The tetrameric form of the head-to-head covalent dimer (b) allows only one back-to-back dimer to form and therefore would result in two strongly bound ligands and two more weakly bound ligands.

Nicolaou *et al.*[86,87] made as series of covalently linked dimers through a process of target-accelerated combinatorial synthesis. To achieve this a selection of vancomycin analogues were made, these analogues were alkylated on the amine of the vancosamine sugar with varying chain lengths of fragments that terminated in either a double bond or a sulphide. These compounds were then mixed and dimerised *in situ* with the ligand present and because olefin metathesis and disulphide formations are both reversible an equilibria was formed between all the possible complexes of dimers that the mixed chain length monomers could produce.

The compounds that formed the most stable complexes were favoured in these circumstances because they would be bound to the ligands and pre-organised to react with each other. Thus, pairs of analogues that were able to form dimers would be rapidly reacted to form covalent dimers and would then also be much more likely to stay bound to a ligand. Whereas, pairs of analogues that formed weakly associated dimers would not be in stable complexes and thus would not be cross-linked and could freely dissociate to form better pairs and thus be converted to more strong associated dimers. The process would thus, in theory, equilibrate to a distribution of covalent dimers with a chain lengths that are ideal to orientate them to form stable back-to-back dimers. As strong dimerisation correlates to good antibacterial activity, it was thought that this process should select for potent compounds with good activity against resistant

strains of bacteria. This technique was both successful and prolific, producing a vast number of compounds, most of which had activities that were equal to or greater than vancomycin in all the strains of bacteria that were evaluated in the MIC studies. Figure 1.50 shows the common structure for this sequence of compounds.

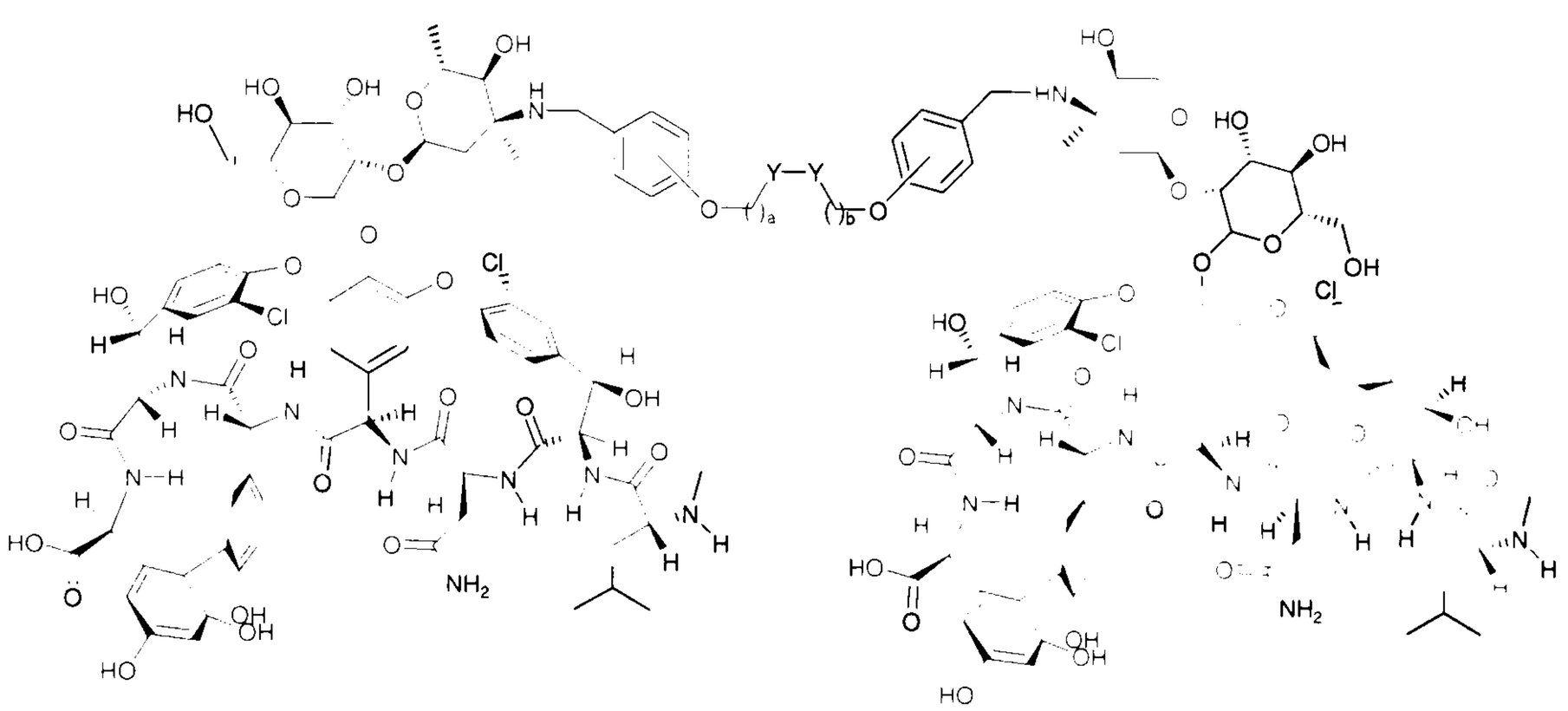

Figure 1.50. The covalent dimers produced by Nicolaou *et al.* Where Y-Y is S-S or C=C and a and b are 1-8.[86,87]

1.6 Resistance to glycopeptides

As the use of glycopeptides slowly increased during the 1980s, it became inevitable that resistance would eventually occur.[88] This was finally observed in 1986 in *Enterococcus faecium*.[89] The molecular basis for this resistance was elucidated by Walsh and co-workers[90] who showed that it is the result of replacement of the terminal D-alanine residue on the cell wall intermediate lipid II that confers resistance. They showed that *Enterococcus faecium* mediated this change through the use of two enzymes, *VanH* and *VanA*, which reduce pyruvate to D-lactic acid (*VanH*) and then form a depsipeptide with D-alanine and the D-lactate (*VanA*). Further work by Walsh *et al.*[91] showed three further proteins were necessary to mediate this action; *VanX* a zinc dependant D,D dipeptidase, that selectively cleaves D-ala-D-ala dipeptides, showing a 1010 fold preference for the dipeptide over the depsipeptide[92] and *VanS* and *VanR*, which form a two-component regulatory system, where *VanS* is a sensor protein and embeds in the cell membrane and *VanR* is a cytoplasmic response regulator that activates transcription of the DNA encoding *VanA*, *VanH* and *VanX*.[91]

Following this, more evidence of resistance was observed in enterococci and there are now at least six known phenotypes of resistance to glycopeptides.[92] These are classified depending upon the breadth and level of resistance and whether the resistance is inducible, *i.e.* presence of the drug triggers the resistance mechanism, or constitutive, present whether drug is present or not. However, the mechanisms all rely on the replacement of the terminal D-alanine residue of the peptidoglycan building block with an alternate residue. The mechanism described by Walsh is now known as the VanA phenotype, the remainder are listed below in Table 1.7.

Phenotype	Peptidoglycan Terminus	Resistance (MIC in µg/mL)	Source	Induction	Organism
VanA	D-ala-D-lac	Vanc (≥64) Teic (≥16)	Acquired	Inducible	*E. faecium* E. faecalis
VanB	D-ala-D-lac	Vanc (≥4)	Acquired	Inducible	*E. faecium* E. faecalis
VanC	D-ala-D-ser	Vanc (≥2)	Intrinsic	Constitutive & Inducible	*E. gallinarium* E. casseliflavus
VanD	D-ala-D-lac	Vanc (≥16) Teic (≥2)	Intrinsic	Constitutive	*E. faecium*
VanE	D-ala-D-ser	Vanc (16)	Acquired	Inducible	E. faecalis
VanG	D-ala-D-ser?	Vanc (16)	?	?	E. faecalis

Table 1.7. Phenotypes of glycopeptide resistance.[92]

These six resistance paths can be divided into two subtypes based on the nature of the residue that replaces the terminal alanine. The first type of resistance involves the replacement of the terminal alanine by a D-lactate (phenotypes VanA, VanB and VanD). VanA encodes two further proteins *VanY* and *VanZ*, *VanY* is a membrane bound carboxypeptidase that can cleave both D-ala-D-ala dipeptides and D-ala-D-lac depsipeptides, and is analogous to the low molecular weight PBP's discussed above. *VanZ*'s purpose is as yet unknown but it is also membrane bound and appears to be significant in teicoplanin resistance. VanB resistance phenotype also relies on *VanH*, *VanA* and *VanX* enzymes and the two-component regulatory system of *VanS* and *VanR*, however these sensor proteins have a low homology with the VanA phenotype, which may explain why VanB is sensitive to teicoplanin but VanA is not. Kahne and co-

workers[93] offered a further explanation of this fact, by demonstrating that the aglycones of either vancomycin or teicoplanin would induce resistance in bacteria with the VanB phenotype. However if either of the aglycones were glycosylated with the sugar from teicoplanin that carries a lipophilic residue the resistance mechanism is not induced and the drugs are able to inhibit cell wall synthesis. This suggests that the sugar is in someway countering the effect of the resistance by preventing the recognition of teicoplanin by *VanS*.

VanD phenotype presents the D-lactate precursor whether glycopeptides are present or not and is therefore resistant to both vancomycin and teicoplanin. Consequently *VanS* and *VanR* are unimportant in this phenotype as the production of the lactate intermediate does not need to be induced.[92]

The affect on the molecular interactions between the cell wall intermediate and the glycopeptides is profound, altering the two terminating residues so that they are now linked by an ester where there would be an amide linkage in the wild type. This produces a 1000 fold drop in the binding affinity.[92] When the ester presenting cell wall intermediate is placed in the same binding position as the wild type intermediate there would be an unfavourable interaction between the carbonyl of the amide that connects amino acids 3 and 4 of vancomycin and the oxygen of the ester in the depsipeptide. There is an electrostatic repulsion between the lone pairs on the oxygens, where originally there would have been a hydrogen bond (Figure 1.51).[92]

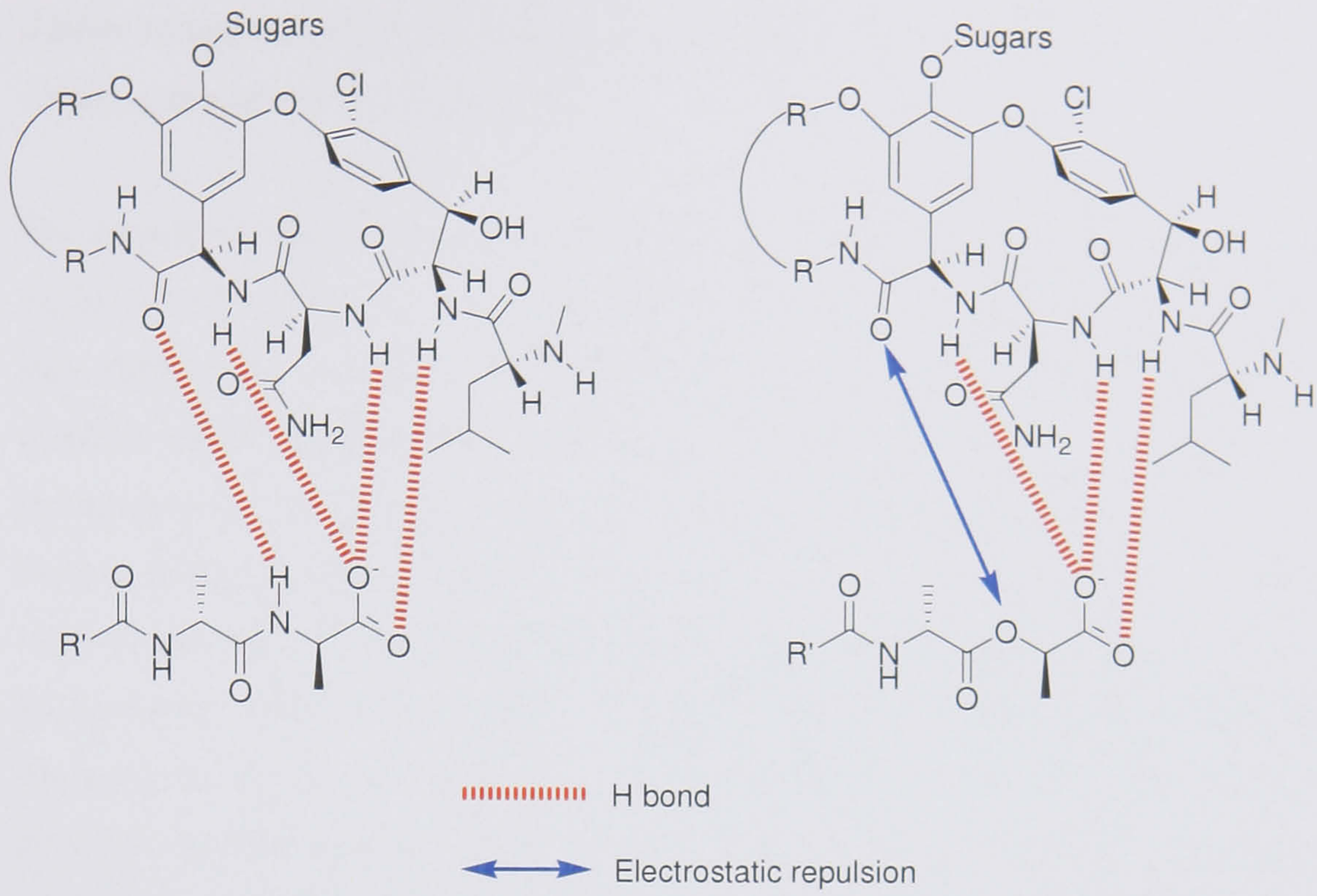

Figure 1.51. Comparison of binding, in the wild type versus lactate containing intermediate.[94]

The effects of both the loss of the hydrogen bond and of the electrostatic repulsion combine to produce such a dramatic loss in activity. Recent work by Boger and co-workers[94] quantified the relative effects of each of these phenomena, by using a tripeptide mimic where the nitrogen of the amide joining the two terminal amino acids had been substituted for a methylene group to give the structure shown in Figure 1.52.

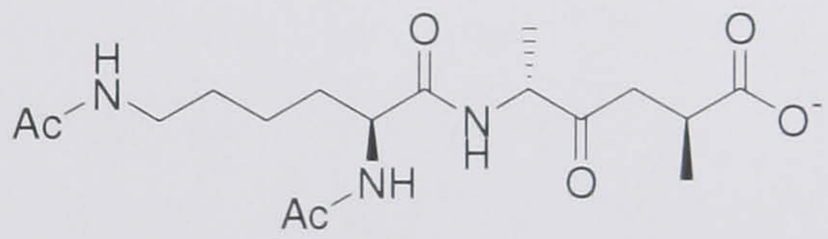

Figure 1.52. Boger's novel binding probe.[94]

This novel compound was used to quantify the loss of a hydrogen bond by comparing the binding affinities of vancomycin and aglucovancomycin to this and to the natural cell wall mimic D-ala-D-ala. It was found that in both cases the binding affinity was ten times lower for the novel binding probe than D-ala-D-ala.[94] The process was then repeated, but this time comparing the binding of the binding probe and D-ala-D-lac to both glycopeptides, here the binding affinity of D-ala-D-lac was found to be a 100 fold lower than that of the binding probe. It was therefore reasoned that the repulsive effect contributed a 100 fold reduction to the binding of D-ala-D-lac and the loss of the H-bond contributed a ten fold reduction in the binding affinity.[94] This was confirmed by a

further compound where the carbonyl on the backbone of vancomycin was removed, which is discussed later in Section 1.7.2.

The second category of resistance relies upon the bacteria replacing the terminal D-alanine with D-serine, as seen in the phenotypes: VanC, VanE and VanG. All three phenotypes rely on three enzymes to produce the resistant cell wall intermediates, similar to the lactate presenting phenotypes.[92] The first is *VanXY* is a D-ala-D-ala dipeptidase and it functions as *VanX* does, however it can also act as a carboxypeptidase, like *VanY*, and shows the same specificity. This means it can cleave UDP-NAM D-ala-D-ala pentapeptide, but it cannot cleave UDP-NAM D-ala-D-ser pentapeptide. The second enzyme, *VanT*, is a membrane-bound racemase, which takes the naturally occurring L-serine and converts it to the D-isomer. The third, *VanC*, *VanE* or *VanG*, depending on the phenotype, is similar to the natural ligase, but has altered specificity, in order to promote the formation of D-ala-D-ser dipeptides. VanE, VanG and some VanC phenotypes are inducible and have the two-component *VanR* and *VanS* sensor kinases, the constitutive VanC phenotypes do not require these.[92]

VanC is exceptionally selective in its ability to synthesise dipeptides of the D-ala-D-ser form, it shows a 400 fold selectivity in the selection of D-ser in the terminal position.[95]

Alteration of the terminal D-ala to D-ser confers resistance because serine has a CH_2OH as its side chain, whereas alanine has a CH_3 (Figure 1.53). As a result this altered cell wall intermediate has increased steric bulk close to the crucial C-terminus and this prevents it from binding in the same way as the wild type.[92]

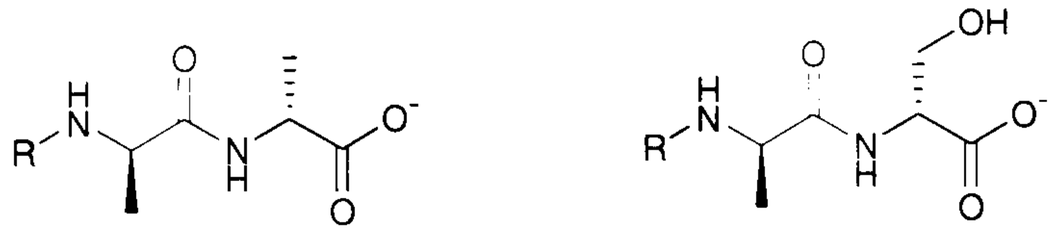

Figure 1.53. A comparison of C-terminus of D-ala-D-ala and D-ala-D-ser presenting cell wall intermediates.

In addition, the OH group makes serine a hydrophilic residue and will therefore not satisfy the hydrophobic binding of this area, further decreasing the binding affinity. This is quite important because the entropic effects of this hydrophobic interaction make a substantial contribution to the overall binding energy. Cristofaro *et al.*[70] quantified the effect of loss of this hydrophobic interaction by measuring the association constants between diacetyl-L-lys-D-ala-D-ala and a vancomycin derivative that was missing the

isobutyl side-chain from the terminal amino acid. They found that the loss of this group reduced the association constant from 1.6 x 10^6 to 7.7 x 10^4. The combined effects of the increase in steric bulk and the loss of the hydrophobic interaction mean vancomycin has a binding affinity 6 times lower for this substrate than for the natural substrate.[92]

1.7 Previous modifications of vancomycin

There have been numerous attempts to modify vancomycin and other related glycopeptides. Many of the papers referenced above in the elucidation of the vancomycin or ristocetin structures (Section 1.4.2), which were the basis for the study and classification of glycopeptides, used modifications of the natural drug to help discover the structure and mode of action. Most of these modifications do not increase the binding of the modified drug, and so will not be discussed in detail here.

There have been numerous studies which have attempted to modify the structure of vancomycin in order to increase its ability to bind to the cell wall intermediates and ultimately its efficacy as a drug. Three groups of these modifications are discussed below; hydrophobic derivatives, derivatives including internal modifications of the binding pocket and derivatives modified at the *N*-terminus.

1.7.1 Hydrophobic derivatives

There are a number of reported naturally occurring glycopeptides which have lipophilic chains attached. Some of these exhibited increased antibacterial activity as compared to vancomycin.[46,96] The discovery of these has prompted many research groups to investigate semi-synthetic derivatives that incorporate similar hydrophobic chains.

Nagarajan and co-workers[46,97-99] produced over a hundred such synthetic derivatives by varying the position of attachment of the hydrophobic chain (either on the amine of the amino sugar or the *N*-terminal amine or both) and the nature of the hydrophobic chain (both aryl and aliphatic chains were used). These studies showed that mono alkylation of the amino sugars with benzyl and benzyl derivatives substituted in the *para* position produced the greatest increase in antibacterial activity when measured *in vitro*.[97] The two compounds with the lowest MIC's are shown in Figure 1.54. The MIC data for the compounds and some reference glycopeptides are shown in Table 1.8.

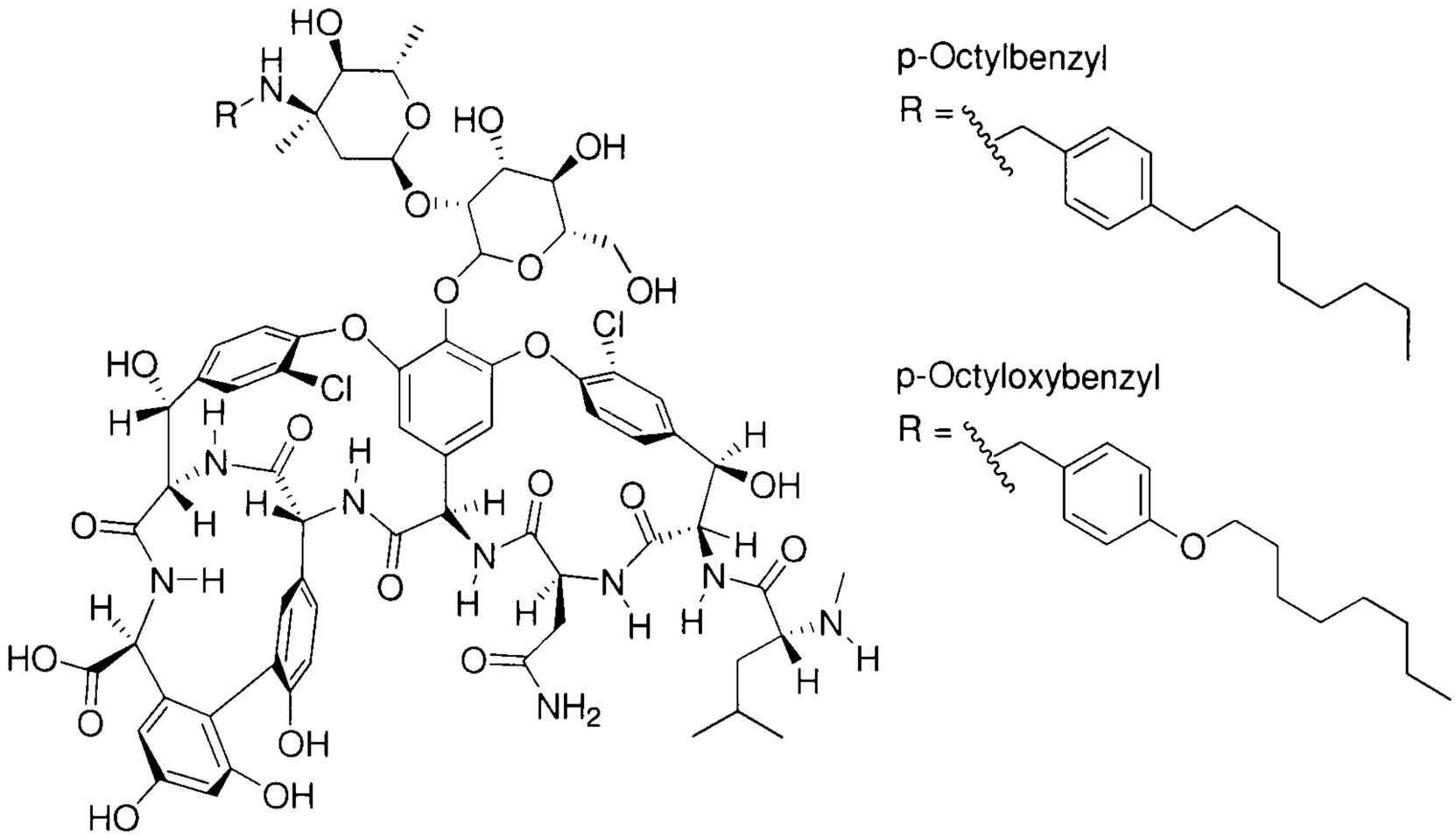

Figure 1.54. The two analogues produced by Nagarajan and co-workers with the lowest MIC.[97]

Compound	MIC (μg/ml)
vancomycin	128, 256_3, 512, 1,024
teicoplanin	16, 64, 128_4
ristocetin	514_4, 1024, 2048
p-octylbenzyl	1_2, 2_2, 4, 8
p-octyloxybenzyl	0.5, 2, 4_2, 8_2,

Table 1.8. MIC data for the compounds of Nagarajan and co-workers with some reference glycopeptides against 4 *E. faecium* and 2 *E. faecalis* isolates (the subscripts indicate the number of times a value was observed).[97]

Allen *et al.*[100-102] reported a series of compounds that are hydrophobic derivatives of a glycopeptide that is closely related to vancomycin, bearing an additional *epi*-vancosamine sugar on the sixth residue of the peptide and where the vancosamine of vancomycin was replaced with *epi*-vancosamine. They were produced by alkylating on the amine of the *epi*-vancosamine sugar (the one on residue 4, Figure 1.55, the residues are numbered from the *N*-termnus) with chains containing one or two phenyl rings. The analogues show that there is good agreement between the clogP of the compound, its propensity to dimerise or become membrane bound and antibacterial activity. They showed that as clogP increased for a compound, so did its propensity to dimerise, the likelihood of it becoming membrane bound and the antibacterial activity as measured by MIC. The two compounds with the lowest MIC's are shown in Figure 1.55. The MIC data and binding constant to diacetyl-L-lys-D-ala-D-ala (Ac_2KAA) and diacetyl-L-lys-D-ala-D-lactate (Ac_2KAlac) are shown in Table 1.9 for the compounds and vancomycin.

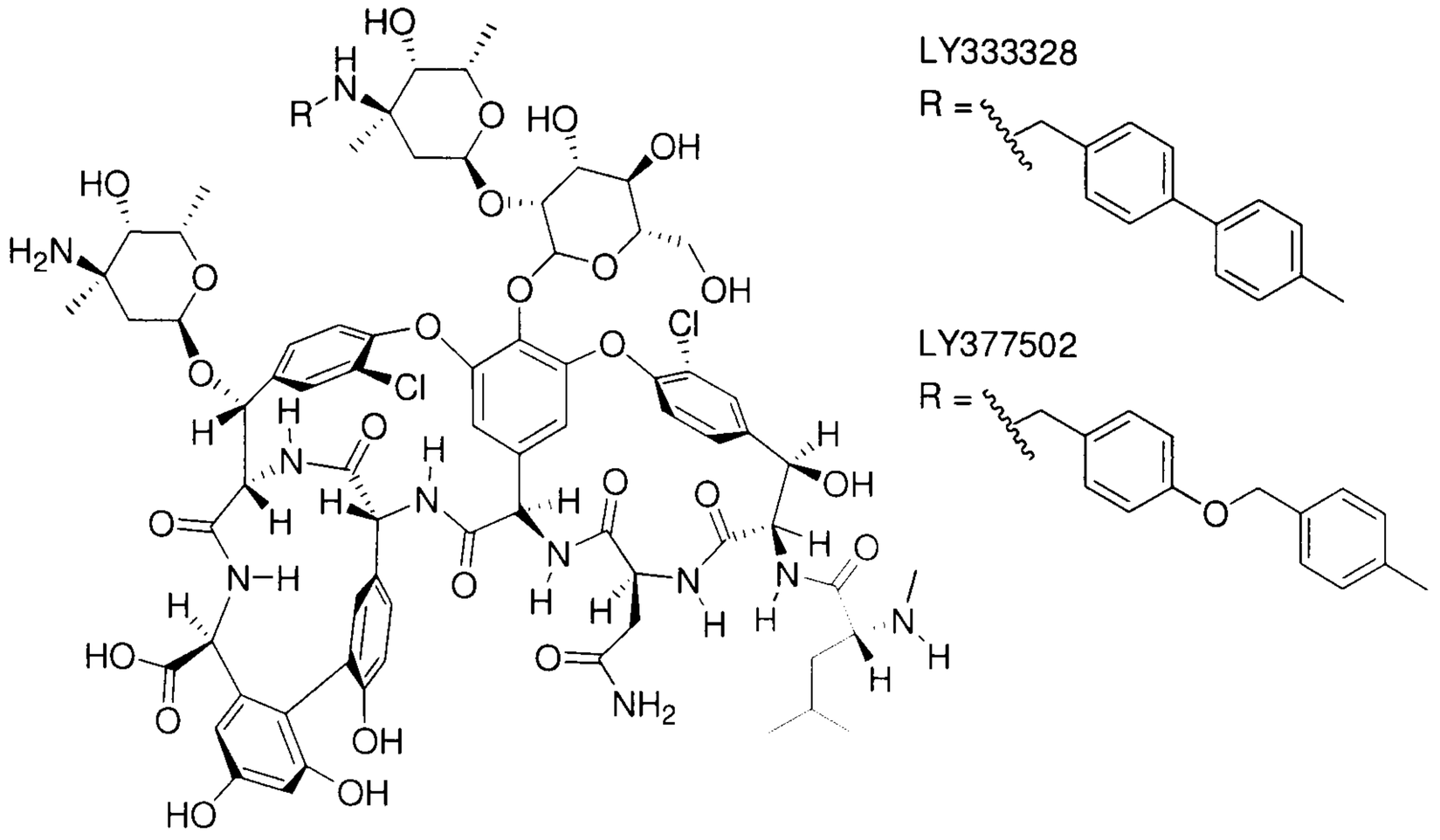

Figure 1.55. LY333328 and LY377502, the two most potent analogues produced by Allen *et al.*[101]

Compound	MIC (μg/ml) *M. luteus* (ATCC9341)	K_b Ac_2KAA	K_b Ac_2KAlac
vancomycin	0.26	$4.1x10^{5}$	$0.41x10^{3}$
LY333328	0.0011	$2.6x10^{5}$	$0.24x10^{3}$
LY377502	0.00072	$4.4x10^{5}$	$0.37x10^{3}$

Table 1.9. MIC and binding constants for vancomycin, LY333328 and LY377502 from Allen *et al.*[101]

In one of the papers Allen *et al.*[102] reiterate an argument put forward by Williams *et al.*[78,103] that suggested an explanation for the increased affinity seen in these hydrophobic derivatives. The explanation states that the increase was the result of a combination of cooperativity of binding produced by dimerisation of the glycopeptide and from membrane anchoring *via* the lipophilic side chain.

The dimerisation offers an increased binding affinity to the cell wall peptides by forming homo-dimers of the glycopeptide, where the hydrogen-bonding network that is formed in dimerisation re-enforces the hydrogen-bonding network that forms on complexation with the ligand.

The lipophilic chains acting as membrane anchors fix the glycopeptide to the surface of the bacterial cell. This means that ligand complexation is in-effect an intramolecular process as both the glycopeptide and glycan strands are anchored to the membrane, as opposed to an intermolecular process, as in un-substituted glycopeptides that do not

possess a lipophilic membrane anchor. The intramolecular process is energetically favoured over the intermolecular process and this re-enforces the effect of the dimerisation. Allen *et al.* confirmed this theory by testing two compounds LY264826 and an analogue produced by alkylating LY264826 on the amine of one of the *epi*-vancosamine sugars with *para*-chlorobenzylaldehyde to give LY191145. They found that the alkylated compound LY191145 had a lower MIC, dimerised more strongly and had a greater inhibition of transglycosylation. The two compounds are shown in Figure 1.56. The MIC data and binding constant to Ac_2KAA and Ac_2KAlac are shown in Table 1.10 for the compounds and vancomycin.

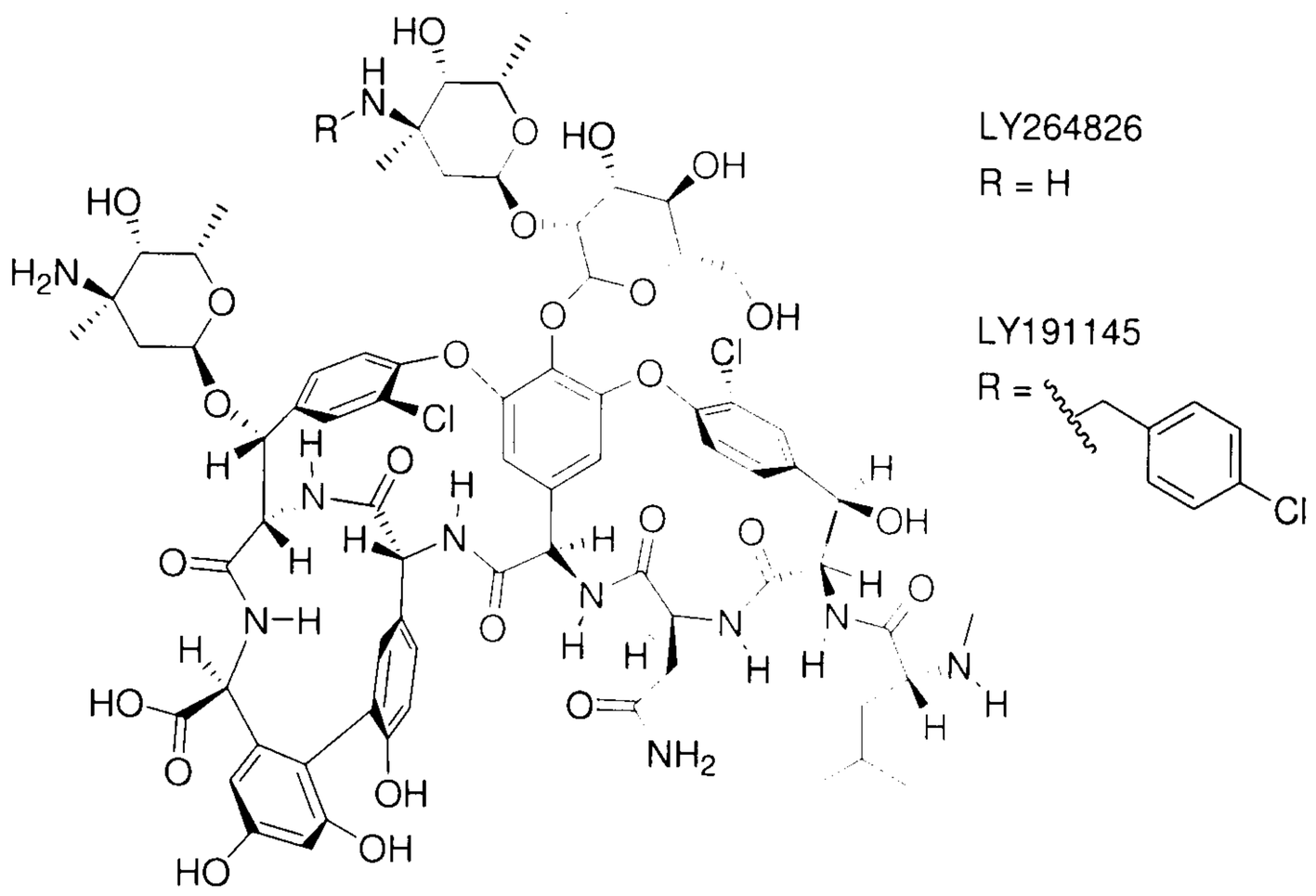

Figure 1.56. LY264826 and LY191145.[102]

Compound	MIC (μg/ml) *M. luteus* (ATCC9341)	K_b Ac_2KAA	K_b Ac_2KAlac
Vancomycin	0.26	$4.1x10^5$	$5.1x10^3$
LY264826	0.063	$1.5x10^5$	$1.4x10^3$
LY191145	0.023	$4.0x10^5$	$1.8x10^3$

Table 1.10. MIC and binding constants for vancomycin, LY264826 and LY191145 from Allen *et al.*[102]

1.7.2 Derivatives including internal modifications of the binding pocket

There have been limited attempts to modify the binding pocket of glycopeptides like vancomycin. The aim of these efforts was to re-engineer the binding pocket in order to remove the repulsive interaction that occurs when glycopeptides try to bind the lactate presenting resistant cell wall peptide and thus increasing the spectrum of activity for

these compounds. However, these undertakings were limited because the glycopeptide core is composed of interlinked peptide macro-cycles, which make modification to the deep seated peptide residues very challenging.

Malabarba *et al.*[104] produced two analogues of the teicoplanin aglycone where the first and third residues were replaced, one had L-lysine at position 3 and D-lysine at position 1, the other had L-phenylalanine at position 3 and D-lysine at position 1 (Again, the residues are numbered from the *N*-termnus). Both of these compounds show a marginal increase in antibacterial activity, as compared to vancomycin, over a range of sensitive and resistant species. This is a surprising result as the aglycones of all of the glycopeptides are significantly less active than their parent compounds.

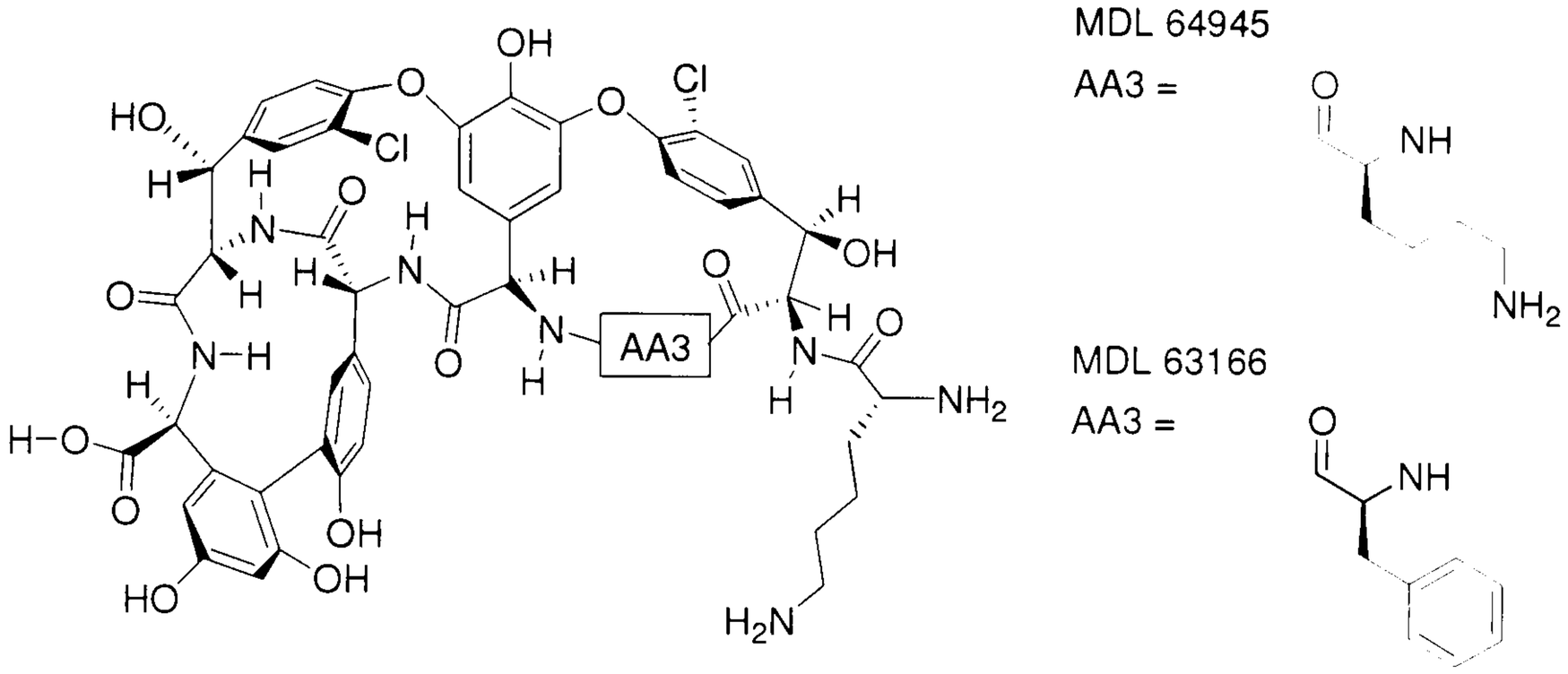

Figure 1.57. Two analogues of the teicoplanin aglycone produced by Malabarba *et al.*[104]

Compound	MIC (μg/ml)				
	S. aureus (Tour)	*S. haemolyticus* (L602)	*S. pyogenes* (C203)	*E. faecalis* (ATCC7080)	*E. faecalis* (L526 (VanA))
teicoplanin	0.125	8	0.125	0.125	>128
vancomycin	0.25	1	0.25	0.5	>128
MDL 63166	0.125	0.25	0.25	0.5	16
MDL 64945	0.063	0.063	0.5	0.5	>128

Table 1.11. Comparison of MIC data for teicoplanin, vancomycin and the two compounds produced by Malabarba *et al.*[104]

Boger and co-workers[105] produced a series of vancomycin analogues that varied in the presence or absence of sugar and the degree of methylation, but contained a L-β-cyanoalanine at the 3 position, and compared them to the equivalent vancomycin with the original L-asparagine at the three position. They found that these tended to have

lower MIC's than vancomycin for a range of both resistant and susceptible bacteria. However, one analogue was as good or better than the equivalent vancomycin analogue and better than vancomycin itself against all the tested strains.

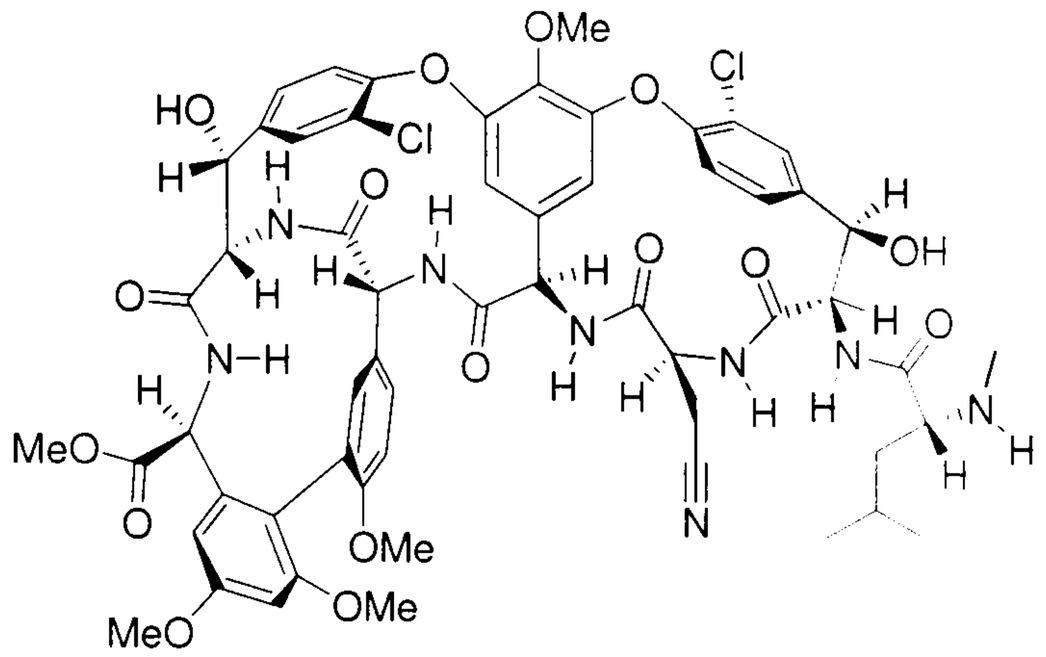

Figure 1.58. The most potent cyanoalanine analogue produced by Boger and co-workers.[105]

Compound	MIC (μg/ml)					K_a	
	S. aureus ATCC 25923	*E. faecium*		*E. faecalis*		Ac_2KAA ($x10^{-5}$)	Ac_2KAlac ($x10^{-2}$)
		ATCC 35667	vancomycin resistant	Van A BM4166	Van B ATCC 51299		
vancomycin	1.25	2.5	500	2000	125	2.3 – 3.9	3.3
aglucovancomycin	0.625	2.5	160	640	80	5.8	2.1
cyanoalanine analogue	0.625	1.25	40	40	2.5	9.9	3.3

Table 1.12. Comparison of K_a and MIC data for vancomycin, aglucovancomycin and the cyanoalanine analogue produced by Boger and co-workers.[105]

Crowley and Boger[106] re-engineered the vancomycin binding pocket at the critical location of the repulsive interaction with the altered lactate presenting cell wall precursor. However, to effect such a deep seated modification of the pocket it was necessary to resort to the total synthesis of the molecule. They successfully synthesised the aglycone of vancomycin where the amide carbonyl between residues 4 and 5 of the heptapeptide had been replaced by a methylene group, to leave an amine joining the two residues instead of an amide. This resulted in a 35-fold drop in affinity to the D-ala-D-ala cell wall mimic, but an increase in affinity of 40-fold against D-ala-D-lac cell wall mimic. This produced an analogue with balanced affinities against both the lactate and the alanine presenting cell wall mimics and showed increased antibacterial activity against VanA resistant *E. faecalis*, when compared to vancomycin, as measured by MIC.

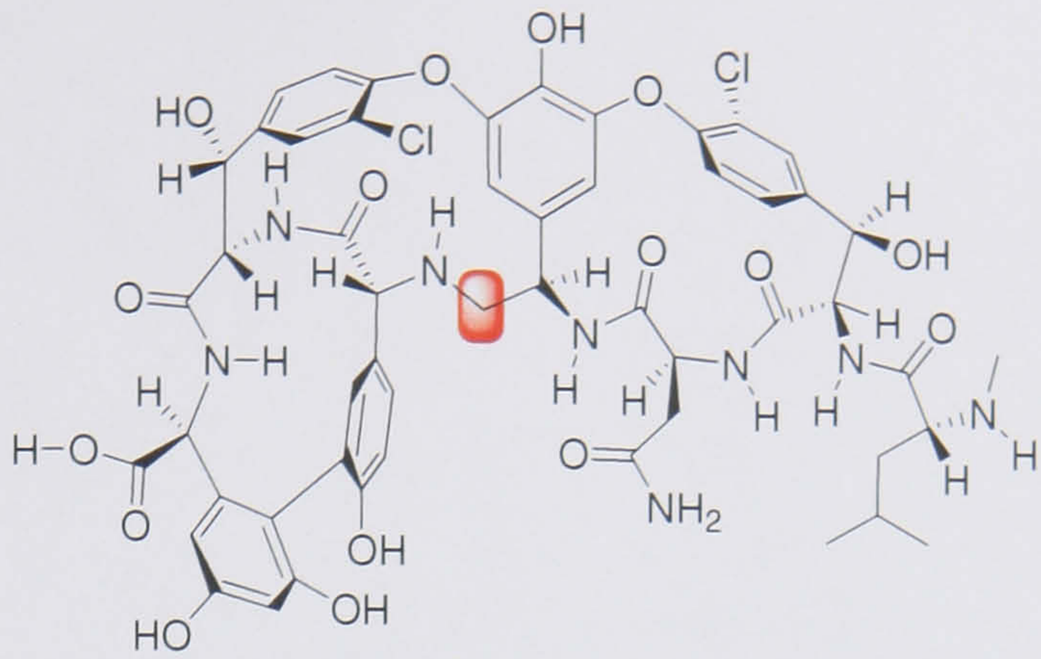

Figure 1.59. Vancomycin analogue with re-engineered portion highlighted in red.[106]

Compound	MIC (μg/ml)	K_a	
	E. faecalis BM4166	Ac_2KAA	Ac_2KAlac
vancomycin	>500	2.0×10^{-5}	1.8×10^{-2}
aglucovancomycin	>500	1.7×10^{-5}	1.2×10^{-2}
re-engineered analogue	31	4.8×10^{-3}	5.2×10^{-3}

Table 1.13. Comparison of K_a and MIC data for vancomycin, aglucovancomycin and the re-engineered analogue produced by Crowley and Boger.[106]

1.7.3 Derivatives modified at the *N*-terminus

There are a small number of reports of modification at the *N*-terminus of vancomycin with limited success.

Williams and co-workers[107] attempted to introduce sp^2 centres at the *N*-terminus by replacing the terminal amine of *N*-demethylvancomycin with a ketone and then reacting this with hydroxylamine, benzyl hydroxylamine or malononitrile to produce an oxime, a benzyl oxime and a malononitrile derivative. They also reduced the ketone to yield a sp^3 alcohol, effectively replacing the amine of *N*-demethylvancomycin with an alcohol. However, all of these derivatives had a lower affinity for diacetyl-L-lys-D-ala-D-ala. This loss in affinity is attributed to the sp^2 centre forcing a conformation where the hydrophobic side chain that remains of the terminal leucine residue points away from the tripeptide losing a crucial hydrophobic interaction. The alcohol also had a lower affinity for diacetyl-L-lys-D-ala-D-ala, but the loss of activity was not as severe. This reduction probably results from a loss of the Coulumbic interaction between the amine and the *C*-terminus of the tripeptide, because the amine would be positively charged at physiological pH, whereas the alcohol would not.

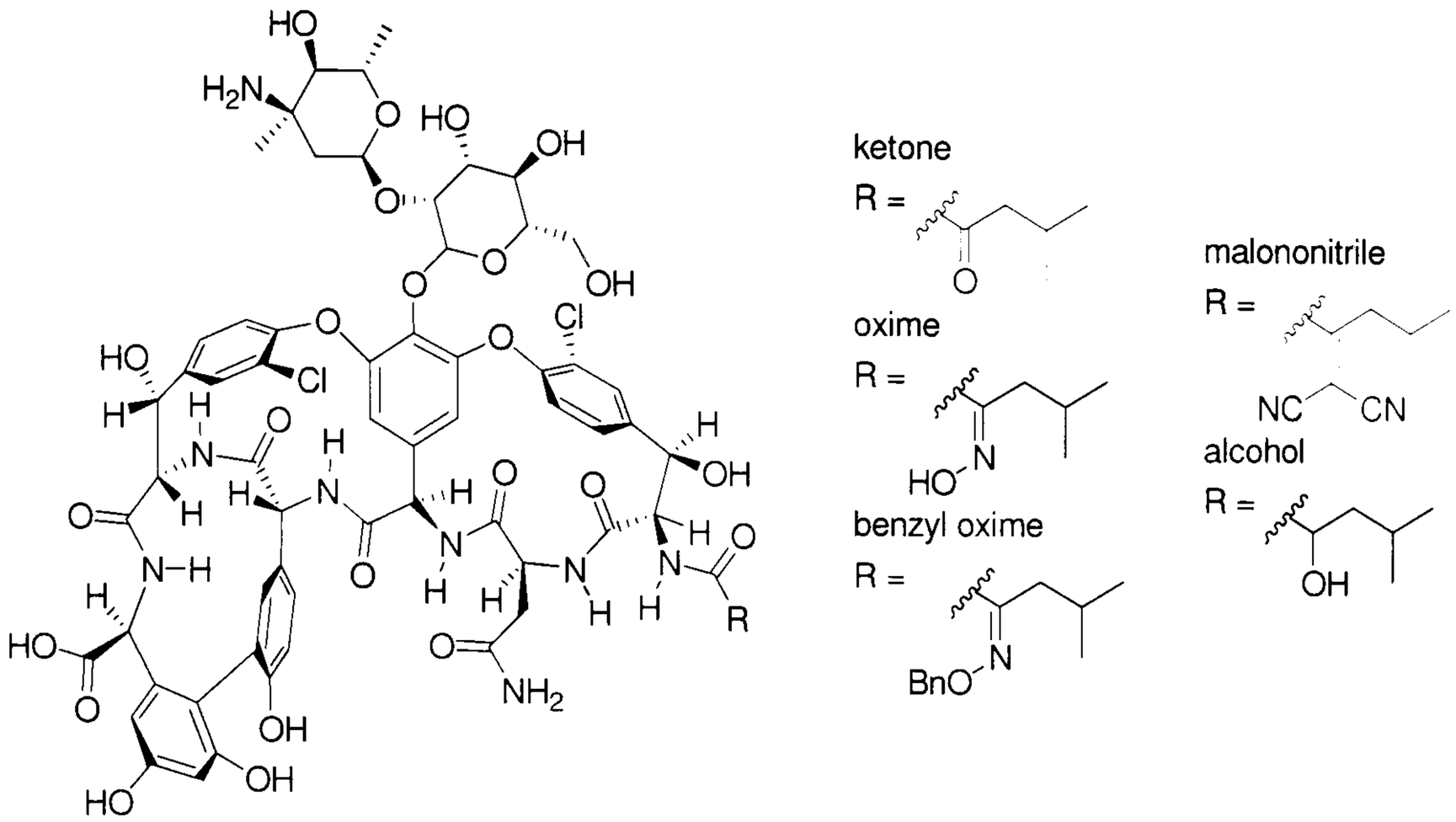

Figure 1.60. The compounds produced by Williams and co-workers.[107]

Compound	K_a (M^{-1}) Ac_2KAA
vancomycin	$8 \pm 2 \times 10^{5}$
N-desmethyl vancomycin	$1.7 \pm 0.7 \times 10^{6}$
ketone	$4.2 \pm 0.3 \times 10^{3}$
alcohol	$1.6 \pm 0.1 \times 10^{4}$
malonitrile	N/A
oxime	$1.0 \pm 0.6 \times 10^{4}$
benzyl oxime	$2.0 \pm 0.4 \times 10^{4}$

Table 1.14. Binding constant of vancomycin, *N*-desmethyl vancomycin and the compounds produced Williams and co-workers.[107]

Further work by Williams and co-workers[108] attempted to introduce a fourth amide into the binding pocket by acetylating *N*-demethylvancomycin and by replacing the *N*-methyl-D-leucine of vancomycin with *N*-acetyl-L-leucine, thus producing two *N*-acetyl-leucine derivatives, one D isomer and one L isomer. However, both of these showed reduced affinity to the tripeptide cell wall mimic. Again this is likely to be through loss of the Coulumbic interaction between the charged amine and the *C*-terminus of the tripeptide, since the acetamide will not protonate at physiological pH. Further analogues were created by producing the vancomycin ketone (Figure 1.60) and converting it to an acetylhydrazone, a tosyl-hydrazone and a semicarbazone (Figure 1.61). All three analogues showed reduced affinity to the tripeptide cell wall mimic. Again this can be explained by the introduction of a sp^2 centre replacing the amine of the leucine residue and forcing unfavourable conformational changes.

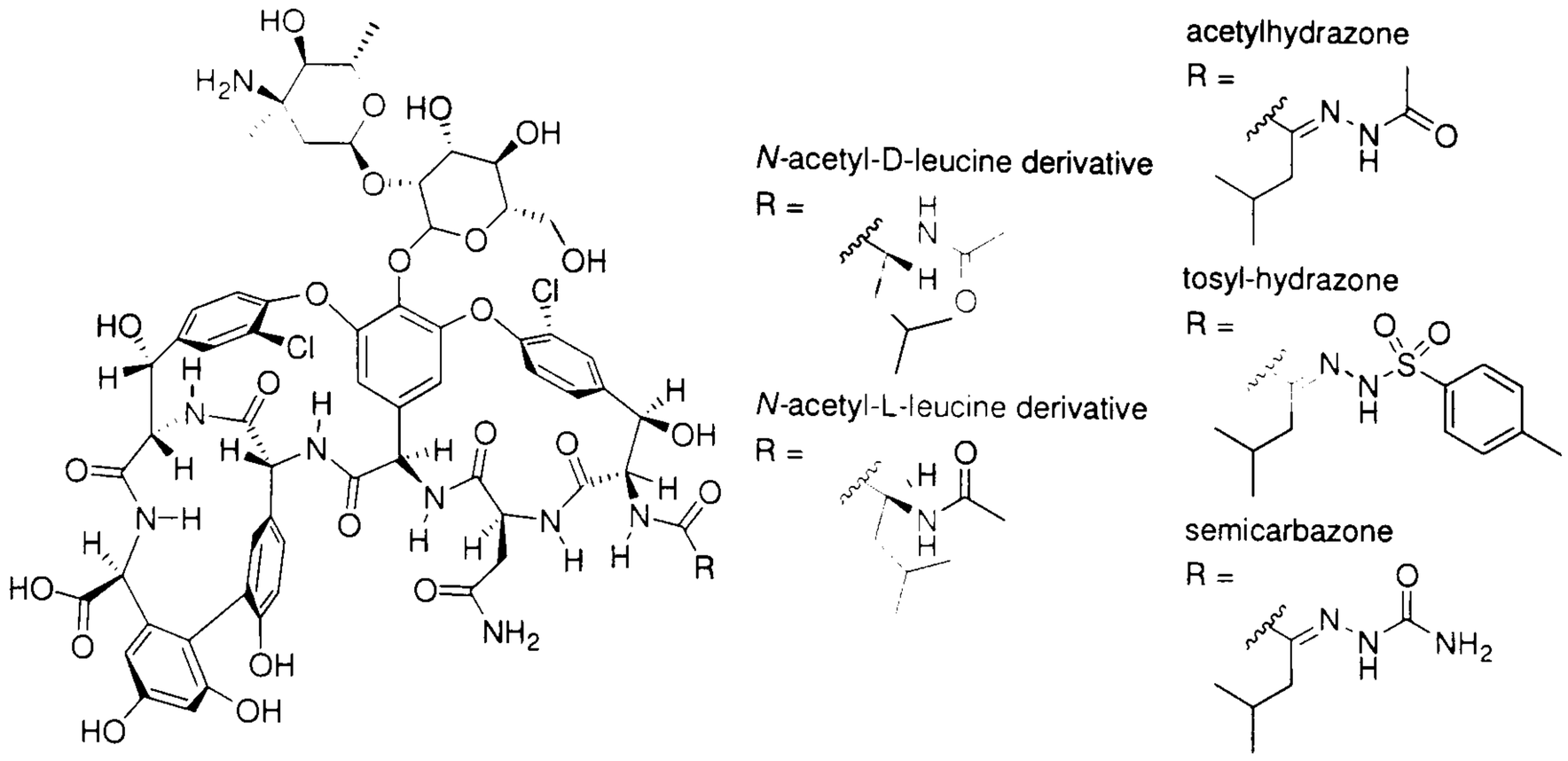

Figure 1.61. Further compounds produced by Williams and co-workers.[108]

Compound	K_a (M^{-1}) Ac_2KAA
vancomycin	8×10^5
N-desmethyl vancomycin	1.7×10^6
N-acetyl-L-leucine derivative	3.6×10^4
N-acetyl-D-leucine derivative	1.0×10^4
acetyl hydrazone	N/A
semicarbazone	N/A
tosyl hydrazone	2.0×10^4

Table 1.15. Binding constant of vancomycin, *N*-desmethyl vancomycin and the compounds produced Williams and co-workers.[108]

Nicolaou *et al.*[109] produced a series of analogues where vancomycin was alkylated on the vancosamine sugar with substituted benzyl groups, then the terminal *N*-methylleucine was removed and an amino acid added to both the *N*-terminus and the *C*-terminus. All of the resultant analogues showed lower antibacterial activity compared to vancomycin against the three susceptible bacteria tested, but two compounds showed higher antibacterial activity against all the resistant bacteria tested, as measured by MIC.

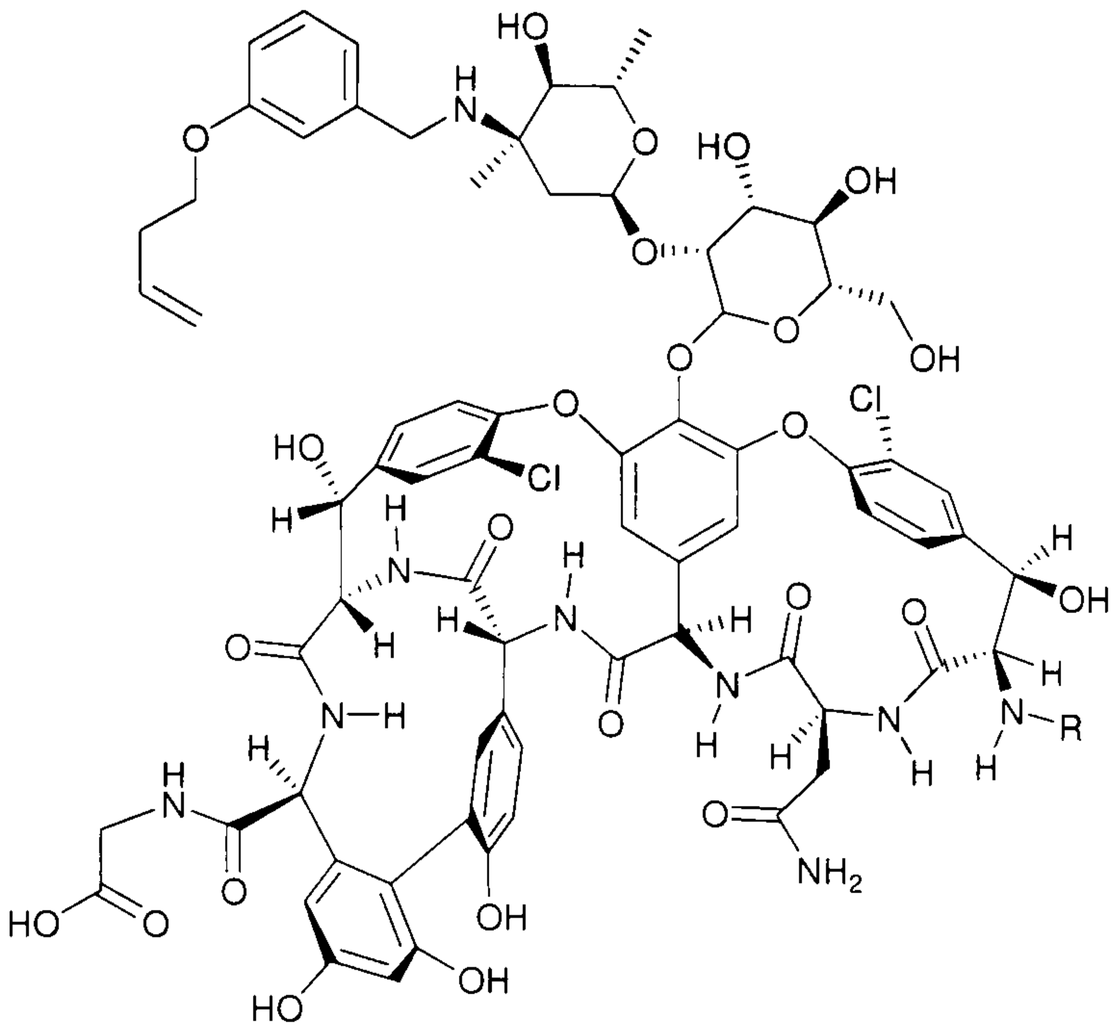

L-valine derivative (L-val)

R =

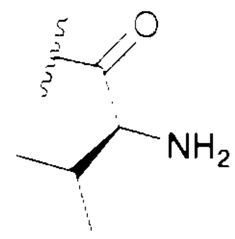

L-cyclohexylalanine derivative (L-cha)

R =

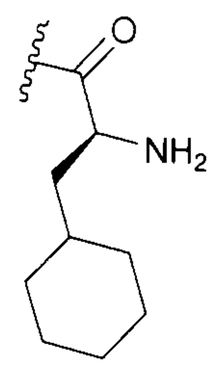

Figure 1.62. The two analogues active against resistant strains of bacteria produced by Nicolaou *et al.*[109]

Compound	MIC (μg/ml)							
	E. faecalis							
	VISA		vanc. sensitive	vancomycin resistant (Van A)				
	MU50	133	4002	1528	2689	2741	2781	2805
vancomycin	3.13	0.39	0.39	>100	50	>100	100	25
L-val	2	1	2	8	>16	2	16	8
L-cha	8	4	4	16	>16	16	16	16

Compound	MIC (μg/ml)						
	E. faecium						
	Van A	Van A & synercid (Sat G)			Van A & synercid (Sat A)		
	4001	1669	2671	2823	1803	1924	1944
vancomycin	>100	100	50	100	50	25	50
L-val	8	8	8	8	8	8	8
L-cha	16	16	16	8	16	8	8

Table 1.16. MIC data for vancomycin and the two analogues produced by Nicolaou *et al.*[109]

These results suggest that increasing the affinity to the tripeptide mimic of the cell wall by alterations to the *N*-terminus will be quite challenging. To produce a compound that shows not only increased binding to the cell wall mimic, but also improved biological activity against the whole organism observed in the MIC, would be a significant achievement. To extend the spectrum of action of vancomycin by restoring its activity against resistant strains would be an even greater challenge. However, it is believed that the use of the powerful computational tools available in Leeds should allow the design of an appropriate modification to the *N*-terminus in order to increase the number of

interactions between the tripeptide and the glycopeptide and thus increase the affinity and this is the basis of this project.

1.8 Project outline

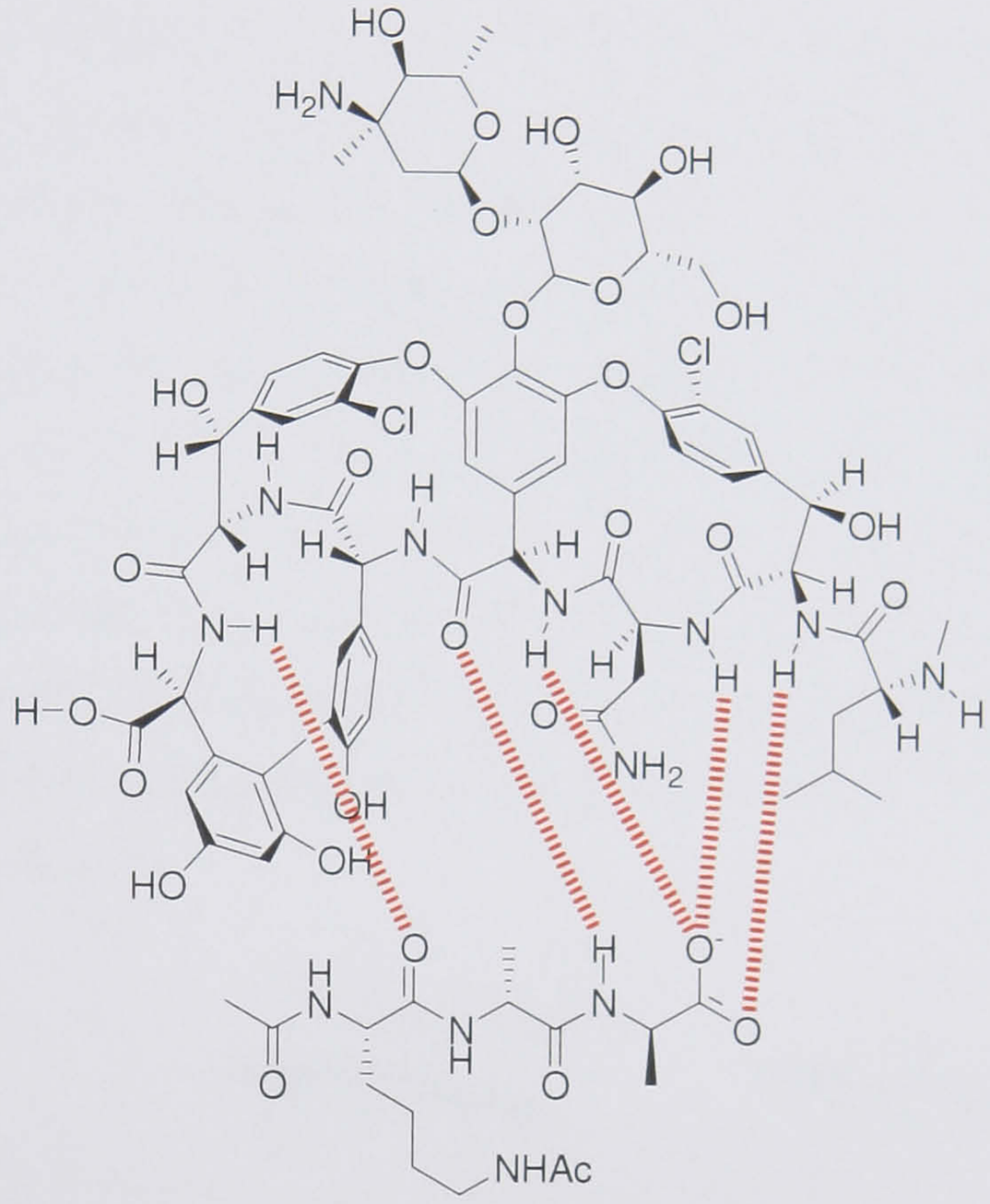

Figure 1.63. An exploded view of vancomycin binding a cell wall mimic.[107]

Figure 1.63 shows an exploded diagram of vancomycin bound to the tripeptide cell wall mimic, which is a tripeptide diacetyl-L-lys-D-ala-D-ala. As discussed earlier, vancomycin is bowl shaped and binds the tripeptide *via* a series of hydrogen bonds between the backbone amides of each moiety. Vancomycin attaches along the bottom of the tripeptide and wraps up along the sides. This leaves the top exposed to solvent and the available hydrogen bonding sites of this surface unutilised (Figure 1. 64).

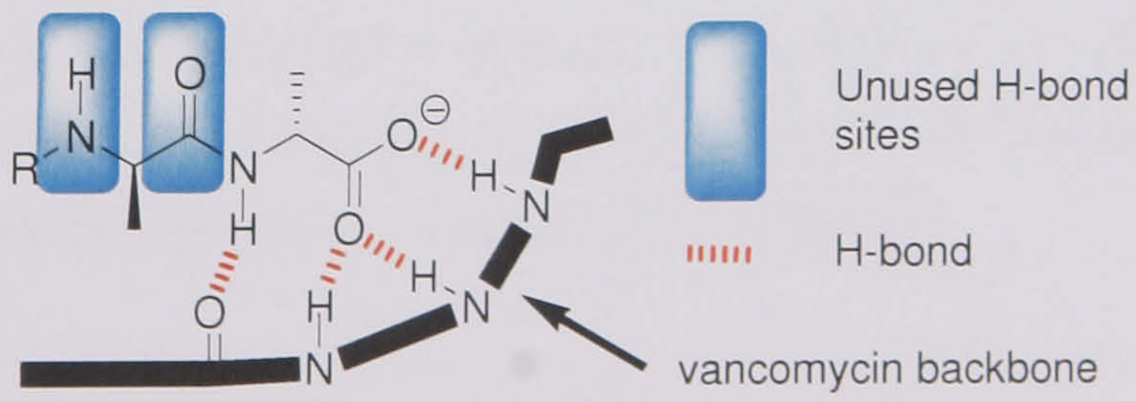

Figure 1.64. A schematic representation of vancomycin binding pocket.

The amino acid that completes the vancomycin heptapeptide is *N*-methyl D-leucine. The conformation this residue adopts is unfavourable for extension of the peptide, as shown by the compounds produced by Williams and co-workers.[108] There is also a further problem presented by this residue, the *N*-methyl substitutent means that the amide that results from acylation of this residue would have a methyl substitutent. The presence of the methyl on this resultant amide would prevent any interaction with the tripeptide, as it would have no hydrogens to hydrogen bond with and would no longer be charged at physiological pH. This makes this *N*-methyl D-leucine residue doubly unfavourable. However, it is possible to remove this terminal amino acid to give a hexapeptide, which terminates in a free amine eliminating this problem. This has been accomplished in the past by performing an Edman degradation, the conditions for which have been established by Booth *et al.*[110] It is envisaged that vancomycin hexapeptide could be alkylated on the newly freed amine in such a way that allows the formation of an amide that can offer a hydrogen bond to the carboxylic acid terminus of the tripeptide. If this hydrogen bond forms it should orientate the remainder of the modifying fragment along the top surface of the tripeptide and thus offer hydrogen bonds to the unsatisfied sites on that surface (Figure 1.65).

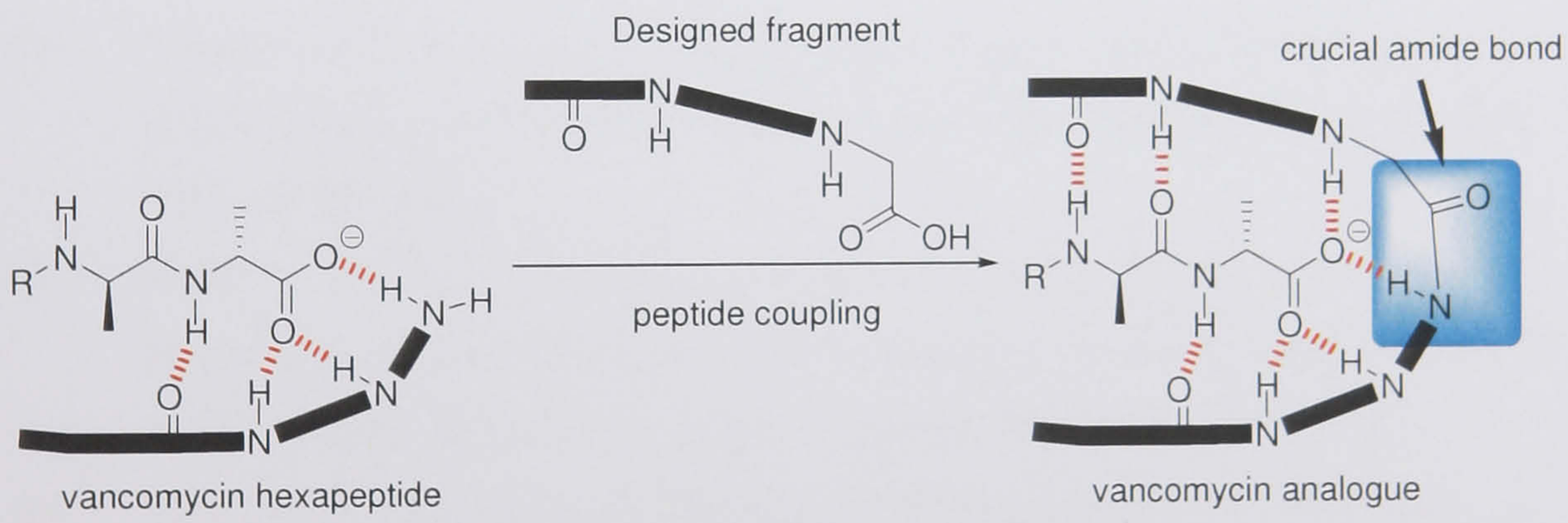

Figure 1.65. A schematic of project concept.

The increase in the number hydrogen bonds between the two molecules will increase the stability of the complex. This should not only increase the resulting compounds affinity to the tripeptide ligand and thus its effectiveness against the susceptible bacteria, but also should hopefully compensate for the effect of the replacement of the terminal D-alanine by either a lactate or a serine and thus reverse the resistance, making the new vancomycin analogue active against VRE or MRSA.

The modified vancomycin analogues will be designed using SPROUT. SPROUT is a *de-novo* design program that allows a user to take a 3D model of a structure and design a complimentary molecule that will offer binding interactions that satisfy the target. The best compounds that are designed will then be synthesised in the lab. In this sense 'best' includes both a consideration of what is most likely to improve the binding, but also whether it is possible to synthesise the compound. Therefore early in each SPROUT run, attempts will be made to prune out structures that are not going to be chemically stable, regardless of how highly they score in terms of binding affinity.

1.9 References

(1) Voet, D.; Voet, J. G. Prokaryotes. *Biochemistry*; 2nd ed.; John Wiley and Sons, Inc.: New York, 1995; pp 2-6.

(2) Prescott, L. M.; Harley, J. P.; Klein, D. A. DNA Replication. *Microbiology*; 4th ed.; The McGraw-Hill Companies, Inc., 1999; pp 216-221.

(3) Nicklin, N.; Graeme-Cook, K.; Paget, T.; Killington, R. A. DNA Replication. *Instant Notes in Microbiology*; BIOS Scientific Publishers Ltd: Oxford, 1999; pp 32-37.

(4) Voet, D.; Voet, J. G. Type II Topoisomerase Supercoil DNA at the Expense of ATP Hydrolysis. *Biochemistry*; 2nd ed.; John Wiley and Sons, Inc.: New York, 1995; pp 880-882.

(5) Fisher, L. M.; Pan, X.-S. Targeting of DNA Gyrase in Streptococcus Pneumoniae by Sparfloxcin: Selective Targeting of Gyrase or Topoisomerase IV by Quinolones. *Antimicrob. Agents Chemother.* **1997**, *41*, (2), 471-474.

(6) Osheroff, N.; Corbett, A. H.; Hong, D. Exploiting Mechanistic Differences between Drug Classes to Define Functional Drug Interaction Domains of Topoisomerase II. *J. Biol. Chem.* **1993**, *268*, (5), 14394-14398.

(7) Cozzarelli, N. R.; Zechiedrich, E. L.; Khodursky, A. B. Topoisomerase IV, not Gyrase, Decatenates Products of Site-specific Recombination in Escherichia Coli. *Genes Dev.* **1997**, 2580-2592.

(8) Voet, D.; Voet, J. G. Transcription. *Biochemistry*; 2nd ed.; John Wiley and Sons, Inc.: New York, 1995; pp 915-958.

(9) Nicklin, N.; Graeme-Cook, K.; Paget, T.; Killington, R. A. Transcription. *Instant Notes in Microbiology*; BIOS Scientific Publishers Ltd: Oxford, 1999; pp 40-45.

(10) Darst, S. A.; Campbell, E. A.; Korzheva, N.; Mustaev, A.; Murakami, K.; Nair, S.; Goldfarb, A. Structural Mechanism for Rifampicin Inhibition of Bacterial RNA Polymerase. *Cell* **2001**, *104*, 901-912.

(11) Chatterji, D.; Balakrishnan, V.; Varma, S. Piperine Augments Transcription Inhibitory Activity of Rimfampicin by Severalfold in Mycobacterium Smegmatis. *Curr. Sci.* **2001**, *80*, (10), 1302-1305.

(12) Prescott, L. M.; Harley, J. P.; Klein, D. A. Protein Synthesis. *Microbiology*; 4th ed.; The McGraw-Hill Companies, Inc., 1999; pp 226-233.

(13) Scholar, E. M.; Pratt, W. B. *The Antimicrobial Drugs*; 2nd ed.; Oxford University Press: Oxford, 2000.

(14) Kimball, J. W. *Biology*; 6th ed.; Wm. C. Brown Publishers: Dubuque, 1994.

(15) Luzzatto, L.; Apirion, D.; Schlessinger, D. Polyribosome Depletion and Blockage of the Ribosome Cycle by Streptomycin in *Escherichia coli*. *J. Mol. Biol.* **1969**, *42*, 315.

(16) Fu, W.; Retsema, J. Macrolides: structures and microbial targets. *Int. J. Antimicrob. Ag.* **2001**, *18*, S3-S10.

(17) Roberts, M.; Chopra, I. Tetracycline Antibiotics: Mode of Action, Applications, Molecular Biology and Epidemiology of Bacterial Resistance. *Microbiol. Mol. Biol. Rev.* **2001**, *65*, (2), 232-260.

(18) Appelbaum, P. C.; Ednie, L. M.; Rattan, A.; Jacobs, M. R. Antianaerobic Activity of RBX 7644 (Ranbezolid), a New Oxazolidinone, Compared with Those of Eight Other Agents. *Antimicrob. Agents Chemother.* **2003**, *47*, (3), 1143-1147.

(19) Appelbaum, P. C.; Bozdogan, B. Oxazolidinones: Activity, Mode of Action and Mechanism of Resistance. *Int. J. Antimicrob. Ag.* **2004**, *23*, 113-119.

(20) Prescott, L. M.; Harley, J. P.; Klein, D. A. Antibacterial Drugs. *Microbiology*; 4th ed.; The McGraw-Hill Companies, Inc., 1999; pp 684-690.

(21) Achari, A.; Somers, D. O.; Champness, J. N.; Bryant, P. K.; Rosemond, J. Crystal Structure of the Anti-Bacterial Sulfonamide Drug Target Dihydropteroate Synthase. *Nat. Struct. Biol.* **1997**, *4*, (6), 490-497.

(22) Chiras, D. *Human biology : health, homeostasis, and the environment*; 2nd ed.; West Publishing Company: Minneapolis, 1995.

(23) Bosscha, M. I.; van Dissel, J. T.; Kuijper, E. J.; Swart, W.; Jager, M. J. The Efficacy and Safety of Topical Polymyxin B, Neomycin and Gramicidin for

Treatment of Presumed Bacterial Corneal Ulceration. *Brit. J. Opthalmol.* **2004**, *88*, (1), 25-28.

(24) Langford, J. H.; Artemi , P.; Benrimoj, S. I. Topical Antimicrobial Prophylaxis in Minor Wounds. *Ann Pharmacother.* **1997**, *31*, (5), 559-563.

(25) Prescott, L. M.; Harley, J. P.; Klein, D. A. The Procaryotic Cell Wall. *Microbiology*; 4th ed.; The McGraw-Hill Companies, Inc., 1999; pp 51-58.

(26) Rogers, H. J.; Perkins, H. R.; Ward, J. B. *Microbial Cell Walls and Membranes*; 1st ed.; Chapman and Hall: London, 1980.

(27) Salton, M. R. J. The Bacterial Cell Envelope - A Historical Perspective. *Bacterial Cell Wall*; Elsevier: London, 1994; pp 1-22.

(28) van Heijenoort, J. Biosynthesis of the Bacterial Peptidoglycan Unit. *Bacterial Cell Wall*; Elsevier: London, 1994; pp 39-54.

(29) Prescott, L. M.; Harley, J. P.; Klein, D. A. Differential Staining. *Microbiology*; 4th ed.; The McGraw-Hill Companies, Inc., 1999; pp 25.

(30) Diversity and Taxonomy of Living Kingdoms, http://biology.unm.edu/ccouncil/Biology_124/Summaries/Kingdoms.html, accessed: March 2005 - July 2007.

(31) Hubbard, B. K.; Walsh, C. T. Vancomycin Assembley: Nature's Way. *Angew. Chem., Int. Ed.* **2003**, *42*, (7), 730-765.

(32) van Heijenoort, J. Recent Advances in the Formation of the Bacterial Peptidoglycan Monomer Unit. *Nat. Prod. Rep.* **2001**, *18*, (5), 503-519.

(33) Walsh, C. T. Enzymes in the D-Alanine Branch of Bacterial Cell Wall Peptidoglycan Assembley. *J. Biol. Chem.* **1989**, *264*, (5), 2393-2396.

(34) Bugg, T. D. H.; Walsh, C. T. Intracellular Steps of Bacterial Cell Wall Peptidoglycan Biosynthesis: Enzymology, Antibiotics and Antiiotic Resistance. *Nat. Prod. Rep.* **1992**, *9*, (3), 199-215.

(35) Mengin-Lecreulx, D.; van Heijenoort, J. Copurification of Glucosamine-1-Phosphate Acetyltransferase and *N*-Acetylglucosamine-1-Phosphate Uridyltransferase of Escherichia coli: Characterisation of glnU Gene Product as a Bifunctional Enzyme Catalysing Two Subsequent Steps in the Pathway for UDP-*N*-Acetylglucosamine Synthesis. *J. Bacteriol.* **1994**, *176*, (18), 5788-5795.

(36) Brown, E. D.; Gehrig, A. M.; Lees, W. J.; Mindiola, D. J.; Walsh, C. T. Acetyltransfer Preceeds Uridyltransfer in the Formation of UDP-*N*-Acetylglucosaminein Seperable Active Sites of the Bifunctional GlmU Protein of Escherichia coli. *Biochemistry* **1996**, *35*, 579-585.

(37) Schleifer, K. H.; Kandler, O. Peptidoglycan Types of Bacterial Cell Walls and their Taxonomic Implications. *Bacteriol. Rev.* **1972**, *36*, (4), 407-477.

(38) Ghuysen, J.-M.; Goffin, C. Multimodular Pencillin-Binding Proteins: An Enigmatic Family of Orthologs and Paralogs. *Microbiol. Mol. Biol. Rev.* **1998**, *62*, (4), 1079-1093.

(39) Ghuysen, J.-M. Biochemistry of the Penicilloyl Serine Transferases. *Bacterial Cell Wall*; Elsevier: London, 1994; pp 103-130.

(40) Matsuhashi, M. Utilization of Lipid-linked Precursors and the Formation of Peptidoglycan in the Process of Cell Growth and Division: Membrane Enzymes Involved in the Final Steps of Peptidoglycan Synthesis and the Mechanism of their Regulation. *Bacterial Cell Wall*; Elsevier: London, 1994; pp 55-72.

(41) Guilmi, A. M.; Dessen, A.; Dideberg, O.; Vernet, T. Bifunctional Penicillin-Binding Proteins: Focus on the Glycosyltransferase Domain and its specific Inhibitor Moenomycin. *Curr. Pharm. Biotechno.* **2002**, *3*, 63-75.

(42) Bouhss, A.; Mengin-Lecreulx, D.; Le Beller, D.; van Heijenoort, J. Topological analysis of the MraY protein catalysing the first membrane step of peptidoglycan synthesis. *Mol. Microbiol.* **1999**, *34*, (3), 576-585.

(43) Ha, S.; Chang, E.; Lo, M.; Men, H.; Park, P.; Ge, M.; Walker, S. The Kinetic Characterization of Escherichia coli MurG Using Synthetic Substrate Analogues. *J. Am. Chem. Soc.* **1999**, *121*, (37), 8415-8426.

(44) McCormick, M. H.; Starck, W. M.; Pittenger, G. E.; Pittenger, R. C.; McGuire, G. M. Vancomycin: a new antibiotic.; Antibiotica: New York, 1956; pp 606-611.

(45) Barna, J. C. J.; Williams, D. H. The Structure and Mode of Action of Glycopeptide Antibiotics of the Vancomycin Group. *Ann. Rev. Microbiol.* **1984**, *38*, 339-357.

(46) Nagarajan, R. Antibacterial Activities and Mode of Action of Vancomycin and Related Glycopeptides. *Antimicrob. Agents Chemother.* **1991**, *35*, (4), 605-609.

(47) Marshall, F. J. Structure Studies on Vancomycin. *J. Med. Chem.* **1965**, *8*, (1), 18-22.

(48) Harris, T. M.; Harris, C. M.; Kopecka, H. Vancomycin: Structure and Transformation to CDP-I. *J. Am. Chem. Soc.* **1983**, *105*, (23), 6915-6922.

(49) Harris, T. M.; Harris, C. M. Structure of Glycopeptide Antibiotic Vancomycin, Evidence for an Asparagine Residue in the Peptide. *J. Am. Chem. Soc.* **1982**, *104*, (15), 4293-4295.

(50) Smith, G. A.; Smith, K. A.; Williams, D. H. Structural Studies on Antibiotic Vancomycin - Evidence for Presence of Modified Phenylglycine and Beta-Hydroxytyrosine. *J. Chem. Soc., Perkin Trans. 1* **1975**, 2108-2115.

(51) Weringa, W. D.; Williams, D. H.; King, R. W.; Brown, J. P.; Feeney, J. Structure of an Amino-sugar from Antibiotic Vancomycin. *J. Chem. Soc., Perkin Trans. 1* **1972**, 443-446.

(52) Smith, G. A.; Williams, D. H.; Smith, K. A. Structural Studies on Antibiotic Vancomycin - Nature of Aromatic Rings. *J. Chem. Soc., Perkin Trans. 1* **1974**, 2369-2376.

(53) Johnson, A. W.; Smith, R. M.; Guthrie, R. D. Vancosamine - Structure and Configuration of a Novel Amino-sugar from Vancomycin. *J. Chem. Soc., Perkin Trans. 1* **1972**, 2153.

(54) Williams, D. H.; Kalman, J. R. Structural and Mode of Action Studies on the Antibiotic Vancomycin. Evidence from 270 MHz Proton Magnetic Resonance. *J. Am. Chem. Soc.* **1977**, *99*, (8), 2768-2774.

(55) Sheldrick, G. M.; Jones, P. G.; Kennard, O.; Williams, D. H.; Smith, G. A. Structure of Vancomycin and it's Complex with Aceyl-D-Alanyl-D-Alanine. *Nature (London)* **1978**, *271*, (5642), 223-225.

(56) Williamson, M. P.; Williams, D. H. Structural Revision of the Antibiotic Vancomycin. The use of Nuclear Overhauser Effect Difference Spectroscopy. *J. Am. Chem. Soc.* **1981**, *103*, (22), 6580-6585.

(57) Williams, D. H. Structural Studies on Some Antibiotics of the Vancomyin Group, and on the Antibiotic-Receptor Complexes, by ^{1}H NMR. *Acc. Chem. Res.* **1984**, *17*, 364-369.

(58) Harris, T. M.; Harris, C. M. Determination of the *N*-Terminal Residue of the Peptide in Ristocetin-A and Ristocetin-B by Reductive Isopropylation. *Tetrahedron Lett.* **1979**, *41*, 3905-3908.

(59) Harris, T. M.; Harris, C. M. Structure of Ristocetin A: Configurational Studies of the Peptide. *J. Am. Chem. Soc.* **1982**, *104*, (1), 363-365.

(60) Williams, D. H.; Rajananda, V.; Kalman, J. R. Structure and Mode of Action of the Antibiotic Ristocetin-A. *J. Chem. Soc., Perkin Trans. 1* **1979**, *3*, 787-792.

(61) Williams, D. H.; Rajananda, V.; Bojesen, G.; Williamson, M. P. Structure of the Antibiotic Ristocetin-A. *J. Chem. Soc., Chem. Commun.* **1979**, *20*, 906-908.

(62) Williams, D. H.; Kalman, J. R. NMR-Study of the Structure of the Antibiotic Ristocetin-A - Negative Nuclear Overhauser Effect in Structural Elucidation. *J. Am. Chem. Soc.* **1980**, *102*, (3), 897-905.

(63) Williamson, M. P.; Williams, D. H. A ^{13}C NMR-Study of the Carbohydrate Portion of Ristocetin-A. *Tetrahedron Lett.* **1980**, *21*, (43), 4187-4188.

(64) Williams, D. H.; Butcher, D. W. Binding Site of the Antibiotic Vancomycin for a Cell-Wall Peptide Analogue. *J. Am. Chem. Soc.* **1981**, *103*, (19), 5697-5700.

(65) Williams, D. H.; Williamson, M. P.; Butcher, D. W.; Hammond, S. J. Detailed Binding Sites of the Antibiotics Vancomycin and Ristocetin A: Determination of Intermolecular Distances in Antibiotic / Subtrate Complexes by Use of the Time-Dependent NOE. *J. Am. Chem. Soc.* **1983**, *105*, (5), 1332-1339.

(66) Williams, D. H.; Williamson, M. P.; Hammond, S. J. Interactions of Vancomycin and Ristocetin with Peptides as a Model for Protein Binding. *Tetrahedron* **1982**, *40*, (3), 569-577.

(67) Harris, C. M.; Kopecka, H.; Kannan, R.; Harris, T. M. The Role of the Chlorine Substituents in the Antibiotic Vancomycin: Preparation and Characterization of Mono- and Didechlorovancomycin. *J. Am. Chem. Soc.* **1985**, *107*, (23), 6652-6658.

(68) Kannan, R.; Harris, C. M.; Harris, T. M.; Waltho, J. P.; Skelton, N. J.; Williams, D. H. Function of the Amino Sugar and *N*-Terminal Amino Acid of the Antibiotic Vancomycin in its Complexation with Cell Wall Peptides. *J. Am. Chem. Soc.* **1988**, *110*, (9), 2946-2953.

(69) Nakamura, K.; Shigeru, N.; Yamamura, S. Interaction Between Bacterial Cell Wall Model and Aglucovancomycin or its Synthetic Analogues. *Tetrahedron Lett.* **1995**, *36*, (47), 8629-8632.

(70) Cristofaro, M. F.; Beauregard, D. A.; Yan, H.; Osborn, N. J.; Williams, D. H. Cooperativity Between Non-polar and Ionic Forces in the Binding of Bacterial Cell Wall Analogues by Vancomycin in Aqueous Solution. *J. Antibiot.* **1995**, *48*, (8), 805-810.

(71) Ge, M.; Chen, Z.; Onishi, H. R.; Kohler, J.; Silver, L. L.; Kerns, R.; Fukuzawa, S.; Thompson, C.; Kahne, D. Vancomycin deravatives that inhibit peptidoglycan biosynthesis without binding D-Ala-D-Ala. *Science* **1999**, *284*, 507-511.

(72) Chen, Z.; Eggert, U. S.; Dong, S. D.; Shaw, S. J.; Sun, B.; LaTour, J. V.; Kahne, D. Structural requirements for VanA activity of vancomycin analogues. *Tetrahedron* **2002**, *58*, 6585-6594.

(73) Leimkuhler, C.; Chen, L.; Barret, D.: Panzone, G.; Sun, B.; Falcone, B.; Oberthur, M.; Donadio, S.; Walker, S.; Kahne, D. Differential Inhibition of *Staphylococcus aureus* PBP2 by Glycopeptide Antibiotics. *J. Am. Chem. Soc.* **2005**, *127*, (10), 3250-3251.

(74) Roy, R. S.; Yang, P.; Kodali, S.; Xiong, Y.; Kim, R. M.; Griffin, P. R.; Onishi, H. R.; Kohler, J.; Silver, L. L.; Chapman, K. Direct Interaction of a Vancomycin Derivative with Bacterial Enzymes Involved in Cell Wall Biosynthesis. *Chem. Biol.* **2001**, *8*, 1095-1106.

(75) Try, A. C.; Sharman, G. J.; Dancer, R. J.; Bradsley, B.; Entress, R. M. H.; Williams, D. H. Use of Model Cell Membranes to Demonstrate Templated Binding of the Vancomycin Group Antibiotics. *J. Chem. Soc., Perkin Trans. 1* **1997**, *19*, 2911-2917.

(76) Waltho, J. P.; Williams, D. H. Aspects of molecular recognition: solvent exclusion and dimerization of the antibiotic ristocetin when bound to a model bacterial cell-wall precursor. *J. Am. Chem. Soc.* **1989**, *111*, (7), 2475-2480.

(77) Gerhard, U.; Mackay, J. P.; Maplestone, R. A.; Williams, D. H. The Role of the Sugar and Chlorine Substituents in the Dimerization of Vancomycin Antibiotics. *J. Am. Chem. Soc.* **1993**, *115*, (1), 232-237.

(78) Beauregard, D. A.; Williams, D. H.; Gwynn, M. N.; Knowles, D. J. Dimerization and Membrane Anchors in Extracellular Targeting of Vancomycin Group Antibiotics. *Antimicrob. Agents Chemother.* **1995**, *39*, (3), 781-785.

(79) Schäfer, M.; Schneider, T. R.; Sheldrick, G. M. Crystal structure of vancomycin. *Structure* **1996**, *4*, (12), 1509-1515.

(80) Loll, P. J.; Bevivino, A. E.; Korty, B. D.; Axlesen, P. H. Simultaneous Recognition of a Carboxylate-Containing Ligand and an Intramolecular Surrogate Ligand in the Crystal Structure of an Asymmetric Vancomycin Dimer. *J. Am. Chem. Soc.* **1997**, *119*, (7), 1516-1522.

(81) Kaplan, J.; Korty, B. D.; Axlesen, P. H.; Loll, P. J. The Role of Sugar Residues in Molecular Recognition by Vancomycin. *J. Med. Chem.* **2001**, *44*, (11), 1837-1840.

(82) Lehmann, C.; Bunkoczi, G.; Vertesy, L.; Sheldrick, G. M. Structures of Glycopeptides with Peptides that Model Bacterial Cell-Wall Precursors. *J. Mol. Biol.* **2002**, *318*, (3), 723-732.

(83) Shiozawa, H.; Zerella, R.; Bardsley, B.; Tuck, K. L.; Williams, D. H. Noncovalent Bond Lengths and Their Cooperative Shortening: Dimers of

Vancomycin Group Antibiotics in Crystals and in Solution. *Helv. Chim. Acta* **2003**, *86*, 1359-1370.

(84) Rao, J.; Whitesides, G. M. Tight Binding of a Dimeric Derivative of Vancomycin with Dimeric L-Lys-D-Ala-D-Ala. *J. Am. Chem. Soc.* **1997**, *119*, (43), 102810290.

(85) Staroske, T.; Williams, D. H. Synthesis of Covalent Head-to-Tail Dimers of Vancomycin. *Tetrahedron Lett.* **1998**, *39*, 4917-4920.

(86) Nicolaou, K. C.; Hughes, R.; Cho, S. Y.; Wissinger, N.; Labischinski, H.; Endermann, R. Synthesis and Biological Evaluation of Dimers with Potent Activity against Vancomycin -Resistant Bacteria: Target-Accelerated Combinatorial Synthesis. *Chem. Eur. J.* **2001**, *7*, (17), 3824-3843.

(87) Nicolaou, K. C.; Hughes, R.; Cho, S. Y.; Wissinger, N.; Smethurst, C.; Labischinski, H.; Endermann, R. Target-Accelerated Combinatorial Synthesis and Discovery of Highly Potent Antibiotics Effective Against Vancomycin-Resistant Bacteria. *Angew. Chem., Int. Ed.* **2000**, *39*, (21), 3823-3828.

(88) Kirst, H. A.; Thompson, D. G.; Nicas, T. I. Historical Yearly Usage of Vancomycin. *Antimicrob. Agents Chemother.* **1998**, *42*, (5), 1303-1304.

(89) Leclercq, R.; Derlot, E.; Duval, J.; Courvalin, P. Plasmid-Mediated Resistance to Vancomycin and Teicoplanin in *Enterococcus faecium*. *New Engl. J. Med.* **1988**, *319*, (3), 157-161.

(90) Bugg, T. D. H.; Wright, G. D.; Dutka-Malen, S.; Arthur, M.; Courvalin, P.; Walsh, C. T. Molecular Basis for Vancomycin Resistance in *Enterococcus faecium* BM4147: Biosynthesis of a Depsipeptide Peptidoglycan Precursor by Vancomycin Resistance Proteins VanH and VanA. *Biochemistry* **1991**, *30*, (43), 10408-10415.

(91) Walsh, C. T.; Fisher, S. L.; Park, I.-S.; Prahalad, M.; Wu, Z. Bacterial Resistance to Vancomycin: Five Genes and One Missing Hydrogen Bond Tell the Story. *Chem. Biol.* **1991**, *3*, (1), 21-28.

(92) Pootoolal, J.; Neu, J.; Wright, G. D. Glycopeptide Antibiotic Resistance. *Annu. Rev. Pharmacol. Toxicol.* **2002**, *42*, 381-408.

(93) Dong, S. D.; Oberthur, M.; Losey, H. C.; Anderson, J. W.; Eggert, U. S.; Peczuh, M. W.; Walsh, C. T.; Kahne, D. The Structural Basis for Induction of VanB Resistance. *J. Am. Chem. Soc.* **2002**, *124*, (31), 9064-9065.

(94) McCormick, M. H.; Crowley, B. M.; Boger, D. L. Partitioning the Loss in Vancomycin Binding Affinity for D-Ala-D-Lac into Lost H-Bond and Replusive Lone Pair Contributions. *J. Am. Chem. Soc.* **2003**, *125*, (31), 9314-9315.

(95) Park, I.-S.; Lin, C.-H.; Walsh, C. T. Bacterial Resistance to Vancomycin: Overproduction, Purification and Characterisation of VanC2 from Entrococcus casseliflavus as a D-Ala-D-Ser ligase. *Proc. Natl. Acad. Sci. U. S. A.* **1997**, *94*, 10040-10044.

(96) Glupczynski, Y.; Lagast, H.; Van Der Auwera, P.; Thys, J. P.; Crokaert, F.; Yourassowsky, E.; Meunier-Carpentier, F.; Klastersky, J.; Kains, J. P.; Serruys-Schoutens, E.; Legrand, J. C. Clinical Evaluation of Teicoplanin for Therapy of Severe Infections Caused by Gram-Positive Bacteria. *Antimicrob. Agents Chemother.* **1986**, *29*, (1), 52-57.

(97) Nicas, T. I.; Cole, C. T.; Preston, D. A.; Schabel, A. A.; Nagarajan, R. Activity of Glycopeptides against Vancomycin-resistant Gram-Positive Bacteria. *Antimicrob. Agents Chemother.* **1989**, *33*, (9), 1477-1481.

(98) Nagarajan, R.; Schabel, A. A.; Occolowitz, J. L.; Counter, F. T.; Ott, J. L.; Felty-Duckworth, A. M. Synthesis and Antibacterial evaluation of *N*-Alkyl Vancomycins. *J. Antibiot.* **1989**, *42*, 63-72.

(99) Nagarajan, R.; Schabel, A. A.; Occolowitz, J. L.; Counter, F. T.; Ott, J. L. Synthesis and Antibacterial Activity of *N*-Acyl Vancomycins. *J. Antibiot.* **1988**, *41*, 1430-1438.

(100) Allen, N. E.; LeTourneau, D. L.; Hobbs, J. N.; Thompson, R. C. Hexapeptide Derivatives of Glycopeptide Antibiotics: Tools for Mechanism of Action Studies. *Antimicrob. Agents Chemother.* **2002**, *46*, (8), 2344-2348.

(101) Allen, N. E.; Le Tourneau, D. L.; Hobbs Jr, J. N. The Role of Hydrophobic Side Chains as Determinants of Antibacterial Activity of Semisynthetic Glycopeptide Antibiotics. *J. Antibiot.* **1997**, *50*, (8), 677-684.

(102) Allen, N. E.; Le Tourneau, D. L.; Hobbs Jr, J. N. Molecular Interactions of a Semisynthetic Glycopeptide Antibiotic with D-Alanyl-D-Alanine and D-Alanyl-D-Lactate Residues. *Antimicrob. Agents Chemother.* **1997**, *41*, (1), 66-71.

(103) Mackay, J. P.; Gerhard, U.; Beauregard, D. A.; Maplestone, R. A.; Williams, D. H. Dissection of the Contributions toward Dimerization of Glycopeptide Antibiotics. *J. Am. Chem. Soc.* **1994**, *116*, (11), 4573-4580.

(104) Malabarba, A.; Nicas, T. I.; Thompson, R. C. Structural Modifications of Glycopeptide Antibiotics. *Med. Res. Rev.* **1997**, *17*, (1), 69-137.

(105) McAtee, J. J.; Castle, S. L.; Jin, Q.; Boger, D. L. Synthesis and Evaluation of Vancomycin and Vancomycin Aglycon Analogues that Bear Modifications in the Residue 3 Asparagine. *Bioorg. Med. Chem. Lett.* **2002**, *12*, 1319-1322.

(106) Crowley, B. M.; Boger, D. L. Total Synthesis and Evaluation of [Ψ[CH_2NH]Tpg^4] Vancomycin Agylcon: Reengineering Vancomycin for Dual D-Ala-D-Ala and D-Ala-D-Lac Binding. *J. Am. Chem. Soc.* **2006**, *128*, 2885-2892.

(107) Gale, T. F.; Gorlitzer, J.; O'Brien, S. W.; Williams, D. H. The Synthesis and Binding of N-Terminal Derivatives of Vancomycin to a Bacterial Cell Wall Analogue. *J. Chem. Soc., Perkin Trans. 1* **1999**, *16*, 2267-2270.

(108) Gorlitzer, J.; Gale, T. F.; Williams, D. H. Attempted Introduction of a Fourth Amide NH into the Carboxylate-binding Pocket of Glycopeptide Antibiotics. *J. Chem. Soc., Perkin Trans. 1* **1999**, 3253-3257.

(109) Nicolaou, K. C.; Cho, S. Y.; Hughes, R.; Winssinger, N.; Smethurst, C.; Labischinski, H.; Endermann, R. Solid- and Solution-Phase Synthesis of Vancomycin and Vancomycin Analogues with Activity against Vancomycin-Resistant Bacteria. *Chemistry- A European Journal* **2001**, *7*, (17), 3798-3823.

(110) Booth, P. M.; Stone, D. J. M.; Williams, D. H. The Edman Degration of Vancomycin: Preparation of Vancomycin Hexapeptide. *J. Chem. Soc., Chem. Commun.* **1987**, *22*, 1694-1695.

Chapter Two

Design Phase

2.1 Introduction

A significant part of this research was the design of the fragments intended to extend the hexapeptide core of vancomycin. This aspect of the work was novel as computer aided design had not been used in the design of complex semi-synthetic drugs. It was also an unusual application of the design software, SPROUT, as this program was developed by the ICAMS group at the University of Leeds to use the constraints of a cavity (active or allosteric site) within the structure of a target protein in order to help design strong binding inhibitors for that protein. Here, the problem is effectively reversed as vancomycin acts as a receptor for the peptides of the cell wall or the mimics of these peptides. This means that there were not the constraints normally available.

This section will explain SPROUT, the results achieved and how they were processed with MOLOC, a molecular modelling program.

2.2 SPROUT

SPROUT was created in the Institute for Computer Applications in Molecular Sciences (ICAMS), University of Leeds. The basic concept of the program is to design ligands by combining templates that represent small molecular fragments. These are usually constrained within a protein cavity, which provides electrostatic and steric control, preventing a combinatorial explosion. The program is composed of six modules that deal with different aspects of the structure generation process.

Five of the modules are regularly used and are discussed in detail below, most users do not often use the sixth module, which is the Template Library Manager (TLM) module. The TLM helps the user import new templates or edit existing templates and is not discussed here in detail.

SPROUT mainly uses PDB files, but MOL files can be used to import templates in the TLM module, and ligands or partial structures in the ELEFANT module. Neither hydrogens nor lone pairs of electrons are implicit in PDB files, so the program adds these. SPROUT represents both hydrogens and lone pairs as dummies. Dummy positions are calculated based on the existing atoms surrounding the atom to which the dummies are attached. Dummies are essentially vectors of a defined length, which have

assignable properties and represent the unsatisfied valancies of atoms in the existing structure. Dummies can have a combination of any of the following characteristics: they can be H-bond acceptors, donors, hydrophobic and/or joinable. Acceptor, donor or hydrophobic means the dummy would satisfy that type of site. joinable means that it can be used in forming new bonds during structure growth.

2.2.1 CANGAROO

CANGAROO stands for **C**left **AN**alysis by **G**eometry based **A**lgorithm **R**egardless **O**f the **O**rientation. This is the first of the five modules and is used to analyse a PDB file of the target structure. The target would normally be an enzyme complex and the tools within this module are used to identify an appropriate cavity for an inhibitor. Existing ligands and solvent molecules can be separated from the chains of a protein. Two files are created within this module: the cavity file, a PDB file that roughly defines the area of interest in the protein; and the receptor file, a PDB file that contains the residues that surround the cavity.

2.2.2 HIPPO

HIPPO stands for **H**ydrogen bonding **I**nteraction site **P**rediction as **P**ositions with **O**rientation. This module uses the two files created in CANGAROO to create target sites within the area of interest in a protein. The first stage is grid box generation, which takes the cavity file as a starting point and adds a user-defined margin (the grid box tolerance) to generate a box centred on the cavity and this defines the area of interest. The program ignores any part of the protein structure outside this grid box.

The program then uses the residue set defined within the receptor file to generate target sites. The residues are interpreted using a set of knowledge-based rules which firstly assigns dummies to satisfy the valency of all the atoms, and then examines the hetero-atoms that have dummies and generates target sites for each of these. The program attempts to match the sites into donor and acceptor pairs that satisfy the internal hydrogen bond interactions of the receptor and then it displays all the remaining unsatisfied sites for the user.

SPROUT can generate target sites for hydrogen-bond donor or acceptor sites, hydrophobic, covalent and metal ion sites. However, only acceptor and donor sites were used in this project and thus are discussed in detail below.

Acceptor sites are defined by locating electronegative hetero-atoms in the residue set the have unsatisfied donor dummies, then applying the set of knowledge-based rules that generate the site based on a series of tolerances around the perfect geometry for a hydrogen bond. The perfect geometry for a hydrogen bond would have the donor hetero-atom, the hydrogen, the lone pair and the acceptor hetero-atom all aligned. This means the angle between the donor, the hydrogen and the acceptor would be 180°. The hydrogen would be 1 Å from the donor and 1.85 Å from the acceptor. The perfect arrangement for a hydrogen bond very rarely occurs, so tolerances are added that favours the optimal placement of the acceptor atom to create the hydrogen bond. Adding a minimum and a maximum distance from the hydrogen, and allowing an angle tolerance from the line of the dummy creates the site. If an acceptor atom can be placed inside the red region it satisfies the site and can form a hydrogen bond to the donor, as show in Figure 2.1.

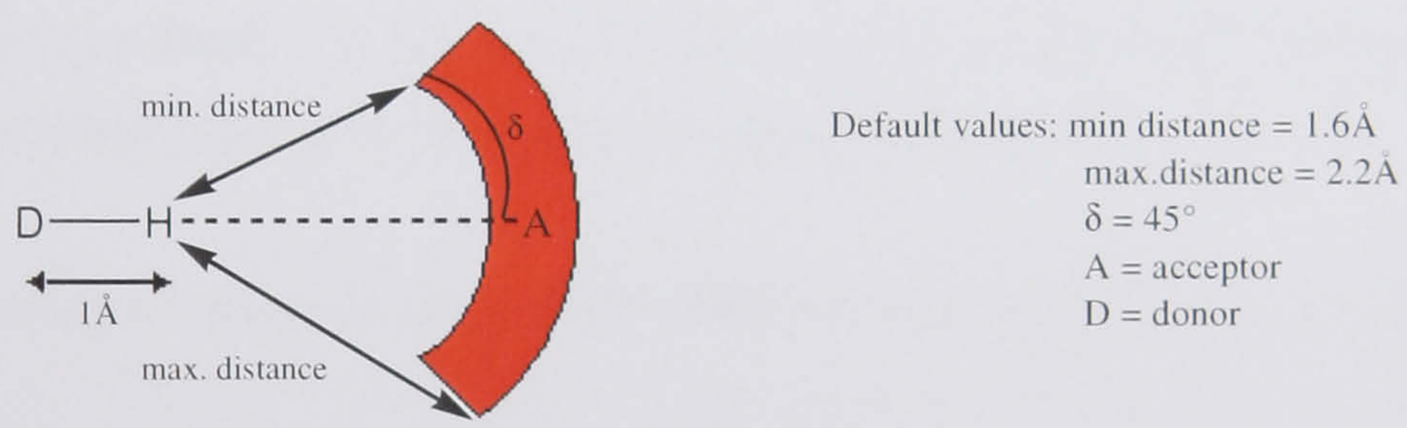

Figure 2.1. An acceptor site.

The user can alter the angle, δ, and the minimum and maximum distances, but the default values are defined based upon analysis of the Cambridge Crystallographic Database.

Donor sites are created in a similar fashion, again hetero-atoms that have an unsatisfied dummy are found, but this time the dummy must be an acceptor. The site is slightly more complex and has two regions, the first (white in Figure 2.2) is generated by taking the minimum and maximum distances and the angle tolerance, and the second (blue in Figure 2.2) is generated by adding 1 Å to the minimum and maximum distances, but uses the same angle tolerance. This generates two regions that are both part spheres a

smaller white, hydrogen atom region and a larger blue, donor atom region. If a donor atom can be placed in the blue region so that a dummy is in the white region, the site is satisfied and a hydrogen bond can be formed to the acceptor, as show in Figure 2.2.

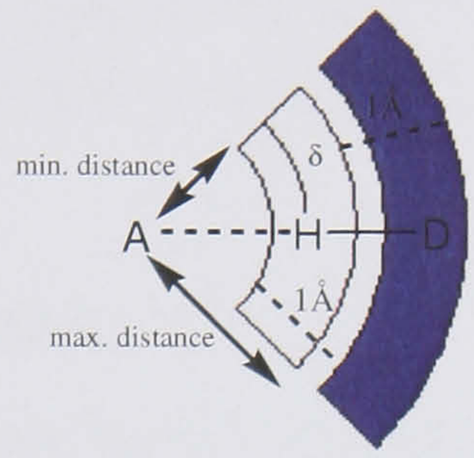

Default values: min. distance = 1.6Å
max. distance = 2.2Å
δ = 45°
A = acceptor
D = donor

Figure 2.2. A donor site.

The user can also alter the angle, δ, and the minimum and maximum distances for donor sites, but again the default values were set based on analysis of the Cambridge Crystallographic Database.

There are also sites called spheric sites that can be placed by the user. These are spheres that can be varied in size and can have defined types. The default spheric sites are generic and are satisfied by any atom. Donor, acceptor or hydrophobic spheric sites can only be satisfied if the corresponding atom type is docked to it.

The user selects a subset of targets in the HIPPO module that are taken on to the next module.

2.2.3 ELEFANT

ELEFANT stands for **ELE**ction of **F**unctional groups and **AN**choring them to **T**arget sites. In this module the user selects a site or a group of sites from the target set created in HIPPO and then templates, from the template list, are selected to dock to them. More than one template can be docked to each site or set of sites. When any template is selected the program docks it to the site in all the possible poses that satisfy the site type and the electrostatic and steric constraints around the site. Any undesirable poses can be deleted in this module. An example of an undesirable pose would be one that orientates all the joinable dummies away from the next docked template and would prevent that template being efficiently joined in the next module.

A set of templates that satisfies one site or one group of sites is called a tree, the whole set of trees is described as the forest. The poses of each template within the tree are described as nodes.

Once all the required sites have templates docked and the undesirable template poses removed, the forest is saved for use in the next module.

2.2.4 SPIDER

SPIDER stands for **S**tructure **P**roduction with **I**nteractive **DE**sign of **R**esults. This module generates whole structures that satisfy all the sites by joining the trees together. This is done with a repeated tree pair joining technique, where pairs of trees are selected and joined, then another pair is selected and joined, until all the trees are joined and there is only one tree that satisfies all the sites. The joining process begins by assigning a seed vertex, this is the atom within the node (docked template) of one tree which is closest to the node of the other tree in the pair. Each node in each tree is given a seed vertex and then the nodes are extended towards each other from the seed vertex with spacer templates that are selected by the user. The spacer templates can be added by a spiro, a fuse or a new bond join (Figure 2.3).

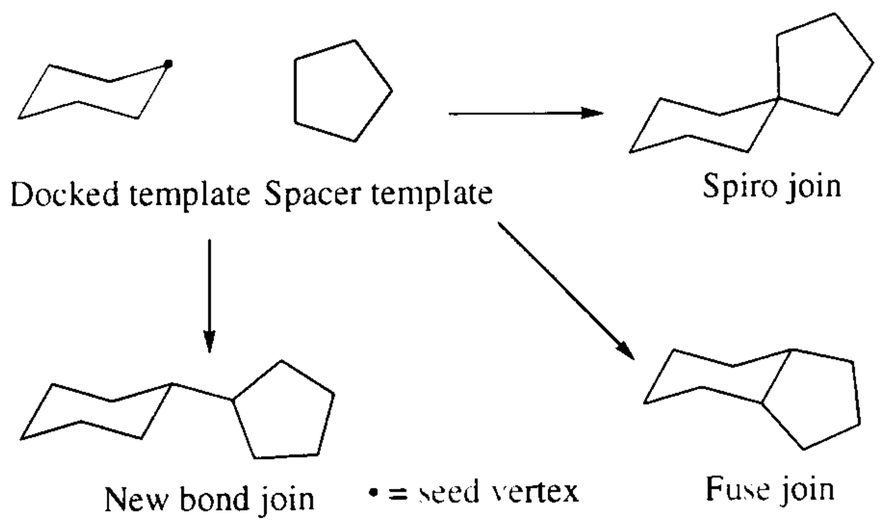

Figure 2.3. Spacer template addition.

During the extension process every spacer template is used to extend every node, so that all possible combinations are explored up to the point where the combinations are exhausted, the part-structures created span over half the distance between the two sites or the system runs out of memory.

When every node of both trees has been extended so that the halfway point between the two trees is reached, the program attempts to join the trees by overlapping fragments of

both part-structures (Figure 2.4). If they can be overlapped then the solutions are tested to ensure that they do not violate the boundary of the cavity or any of the user defined parameters. If they do not they are placed in the results tree, if they do they are discarded and then the search moves on to the next pair of extended nodes.

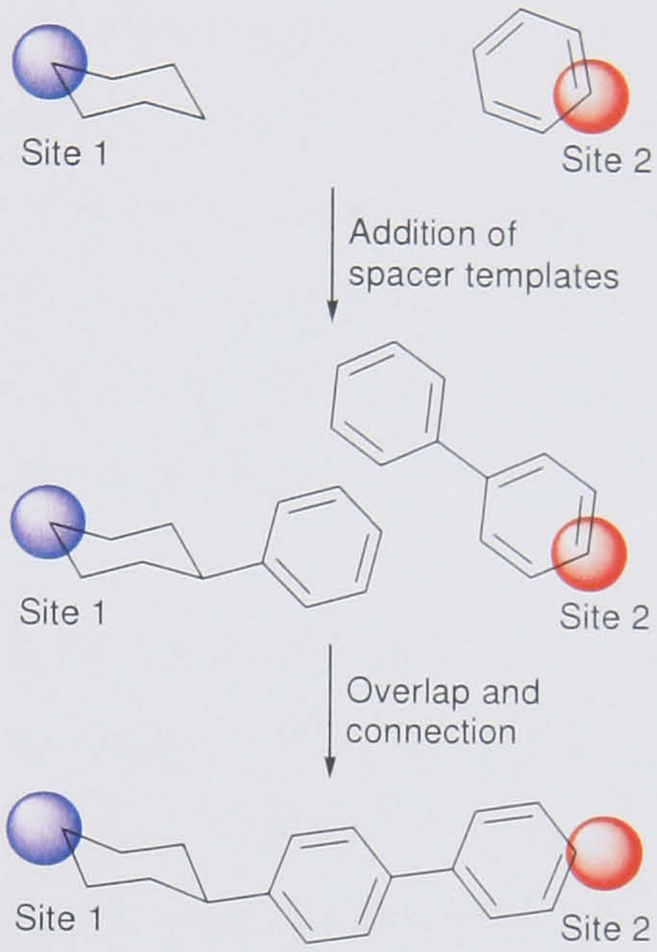

Figure 2.4. Extension and overlap during connection.

It is possible for the user to intervene after each tree pair is coupled and prune unfavourable nodes from the solution tree. This can be done manually, by deleting single nodes or it can be done using the automated tools of the next module. Alternatively, the program can be run continuously to automatically connect all available trees. It should be noted that although in most cases the user will connect all trees in SPIDER, this is not a requirement of the software and the user can stop after any number of tree pair connections and evaluate the results as complete structures.

2.2.5 ALLIGATOR

ALLIGATOR stands for **AL**gorithm for **LIGA**nd **T**esting and **O**rdering of **R**esults. This module is used to sort the structures produced and there are a number of tools available for this. Structure can be sorted on their physical properties, like 2D similarity, number of rotatable bonds, numbers of stereo-centres etc. There are also two scoring functions, one that estimates the affinity and the other that estimates the complexity. The affinity scoring function assesses the interaction between the structure and the target. This function takes into account hydrogen bonding, van der Waals, metal ion,

electrostatic and hydrophobic interactions, each factor is given a value that reflects its magnitude and is multiplied by a weighting factor. The values for each property are then added together and give an overall score, expressed as a pK_i value, which can be used to rank the structures created. The larger the negative number the higher the structure scores. The complexity function analyses just the structure and looks at the number of rotatable bonds, the number of stereo-centres, gauche interactions and the number of atoms. Again each factor is given a value that reflects its magnitude and is multiplied by a weighting factor. The values for each property are then added together and give an overall score that can be used to rank the structures created. The larger the positive number, the worse the structure is. Complexity is an undesirable property as it makes the structures less synthetically accessible.

There is a substructure search tool that can be used to find certain structural motifs, and this is often a useful way to prune partial-structures that are brought into ALLIGATOR part way through the joining phase in SPIDER. There are also a number of selection tools allowing the user to sort on a property then select structures that score either high or low in the given property.

There is a further tool in this module – hetero-substitution. This replaces generic atoms of the templates with specific hetero-atoms that satisfy the electrostatic constraints of the environment.

All these tools combine to help the user select structures with a high-predicted affinity and high synthetic tractability.

2.3 Results

SPROUT and MOLOC have been successfully used to create a number of analogues of vancomycin with predicted increased affinity for the tripeptide cell wall mimic.

2.3.1 SPROUT

Extensions of vancomycin hexapeptide have been designed using the crystal structure (PDB code 1FVM[1]) of the complex between vancomycin and a tripeptide cell wall mimic. This tripeptide is diacetyl-L-lys-D-ala-D-ala. The mimic approximates the intermediate that is bound by vancomycin in order to inhibit bacterial cell wall growth.

The crystal structure with resolution 1.8 Å was imported into SPROUT from the RCSB Protein Data Bank.[2] The tripeptide ligand was defined in CANGAROO as both the cavity and the receptor. This gave sites shown in Figure 2.5, when the sites were explored in HIPPO with the grid box tolerance set to 4.0.

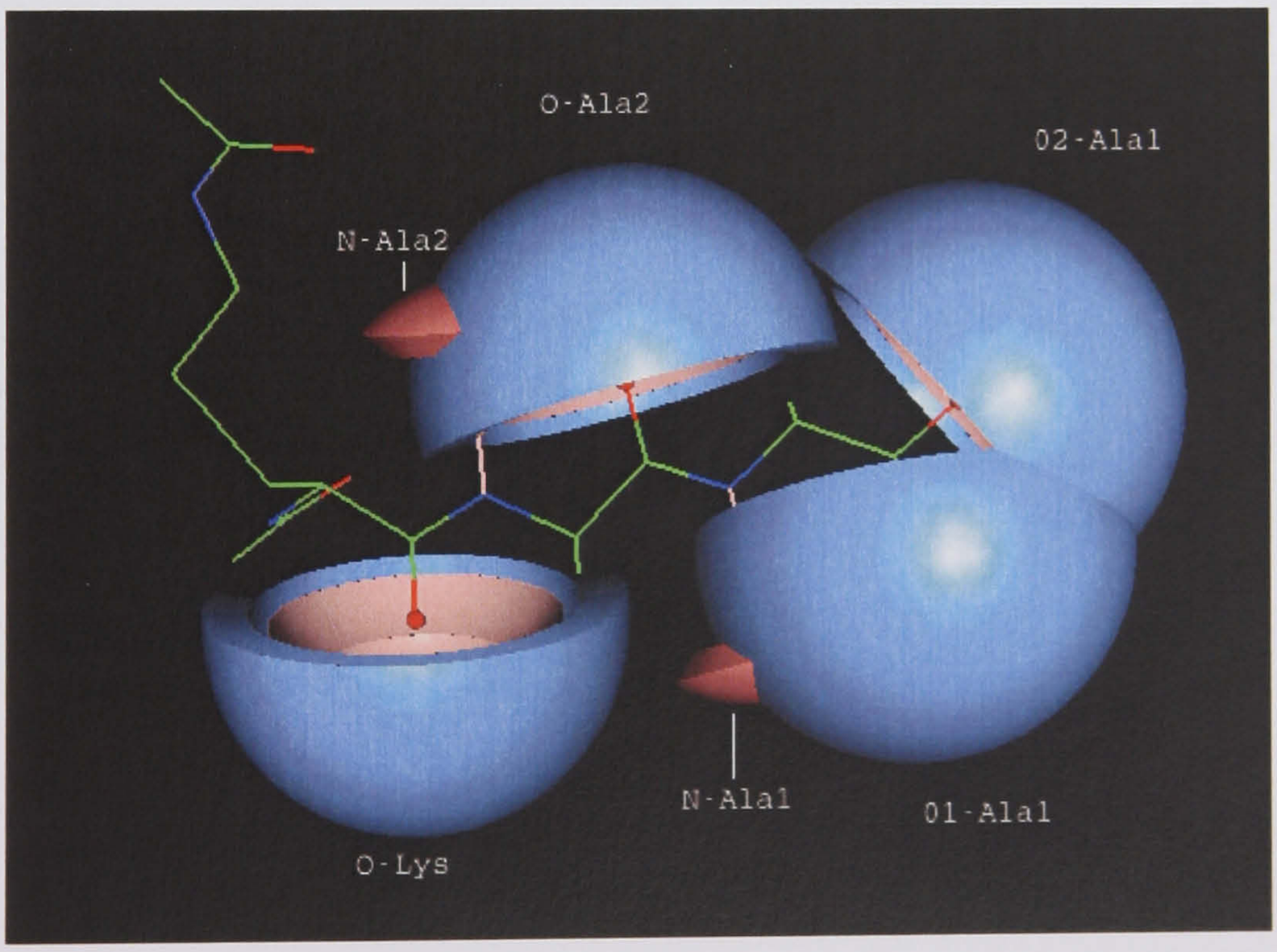

Figure 2.5. The tripeptide and its generated sites.

The sites generated from the two *N*-acyl residues were omitted for clarity and were not used in any of the SPROUT runs.

O-Lys, N-Ala1 and O1-Ala1 are all fully satisfied by vancomycin or its hexapeptide. O2-Ala1 is only partially satisfied, as only one of the two available hydrogen bonding lone pairs is used.

In all cases the extending fragments were joined to the vancomycin core by means of an amide bond. This amide was formed on the *N*-terminal amine of the last amino acid in the hexapeptide. Therefore three spheric sites were placed and an amide docked into them in order to represent this connection.

In the initial attempts to generate extending structures the three spheric sites for the amide and three unsatisfied sites along the top face of the tripeptide were selected, the sites were N-Ala2, O-Ala2, and O2-Ala1 (Figure 2.6).

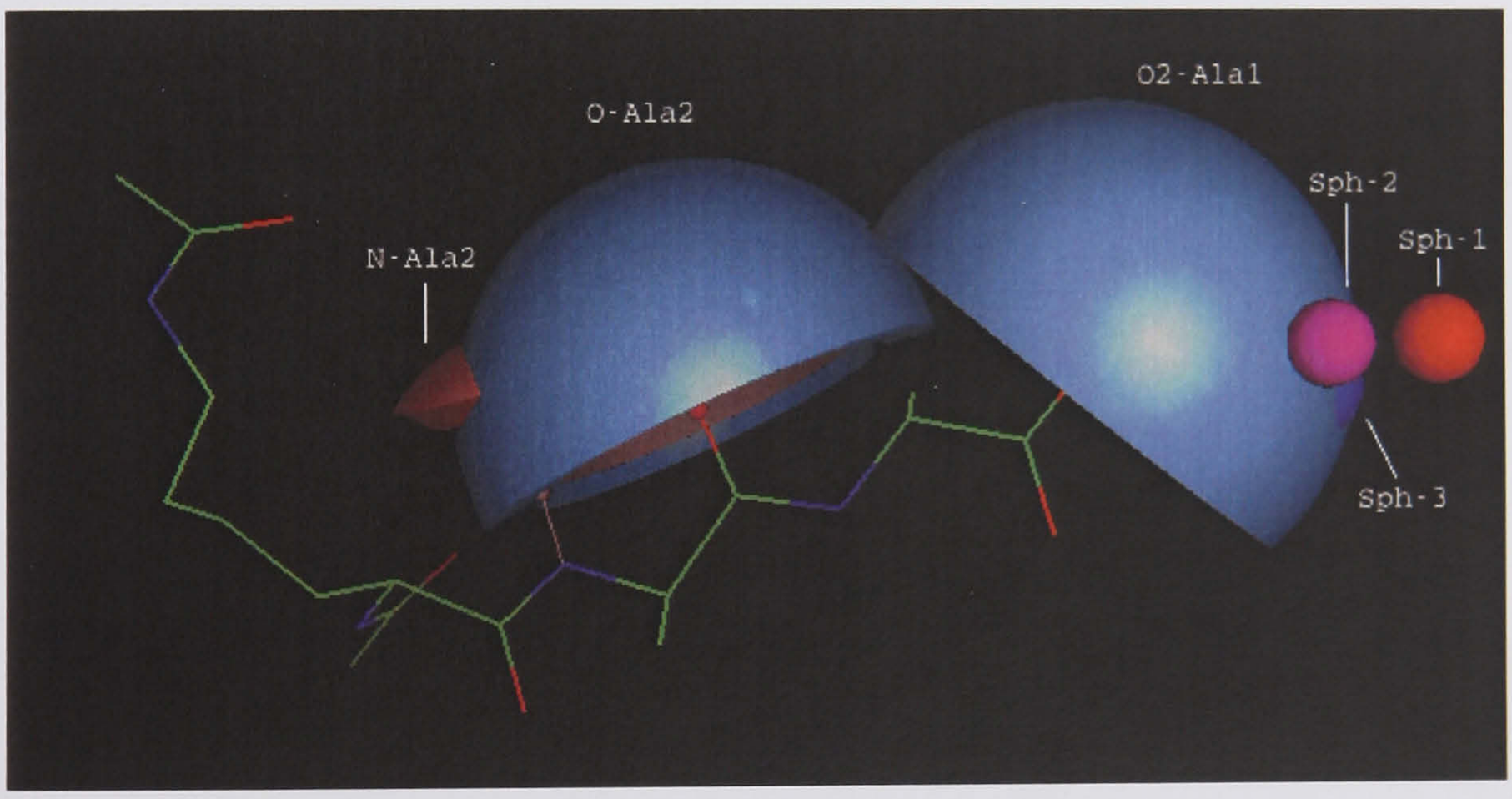

Figure 2.6. The tripeptide ligand, the generated H-bonding sites and three spheric sites for the connecting amide.

The following templates were docked to each site (Table 2.1).

Site(s)	Template(s)
Spheric 1, 2 and 3	Amide
O2-Ala1	Amide, piperazine, 6-membered aliphatic ring, 6-membered aromatic and 5-membered aromatic
O-Ala2	Amide, sp^3 amine, 6-membered aromatic and 5-membered aromatic
N-Ala2	Amide, carboxylic acid, sulphonamide and carbonyl

Table 2.1. Template selection in run 1.

Single sp^3 carbon, amide, 6-membered aromatic ring and 5-membered aromatic ring spacer templates were used during the connection phase in SPIDER. The lack of a steric constraint to minimise the combinatorial explosion, resulted in a large number of structures being generated. In fact, the number of results was large enough to cause SPROUT to crash. The structures created before the program crashed highlighted a further problem. The extending structures created were very close to the edge of sites O2-Ala1 and O-Ala2 and as a result would clash with the hexapeptide. Thus in order to add a steric constraint and provide a barrier to prevent the structures being created that would clash with the hexapeptide, a number of runs were performed where the tripeptide and parts of the hexapeptide were saved as a single PDB file and this was defined as both the cavity and the receptor. This did decrease the number of structures and prevented some of the clashes being present, but these combined structures were time consuming to create and did not remove all the undesirable results.

An alternate and more successful approach was to place a further spheric site (1 Å in diameter) within each of the donor sites (Figure 2.7) and dock the templates to both the donor and the spheric site at the same time as shown in Table 2.2 and 2.3.

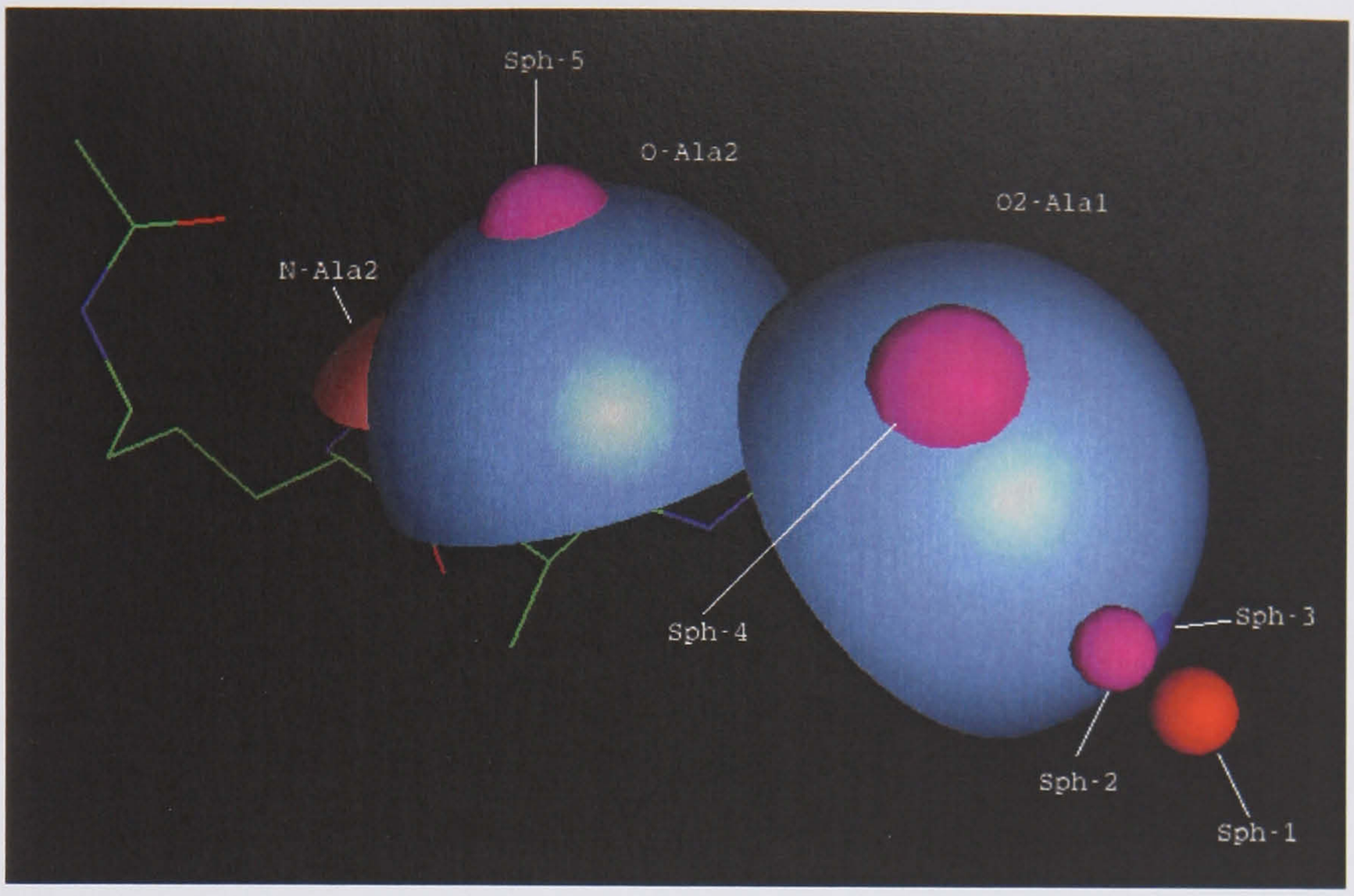

Figure 2.7. The tripeptide ligand, the generated H-bonding sites, the three spheric sites for the connecting amide and the two additional spheric sites.

One run was performed using spheric site 4 and the 6 original sites, with the templates in Table 2.2. The addition of spheric site 4 introduced a further steric constraint.

Site(s)	Template(s)
Spheric 1, 2 and 3	Amide
O2-Ala1 and spheric 4	Piperazine, 6-membered aromatic and 5-membered aromatic
O-Ala2	Amide, sp^3 amine, 6-membered aromatic and 5-membered aromatic
N-Ala2	Amide, carboxylic acid, sulphonamide and carbonyl

Table 2.2. Template selection in the run with the addition of spheric site 4.

Single sp^3 carbon, 6-membered aromatic and 5-membered aromatic ring spacer templates were used during the connection phase in SPIDER. This produced twenty extending structures after removal of chemically unstable or undesirable results. Of these, the eight highest scoring were taken on to combine in MOLOC.

A further run was performed using spheric site 4 and 5 with the 6 original sites and the templates shown in Table 2.3. This run has even greater steric constraint, as the addition of spheric site 5 provides further constraints to the growth of the structure.

Site(s)	Template(s)
Spheric 1, 2 and 3	Amide
O2-Ala1 and spheric 4	Piperazine, 6-membered aromatic and 5-membered aromatic
O-Ala2 and spheric 5	Amide, sp^3 amine, 6-membered aromatic and 5-membered aromatic
N-Ala2	Amide, carboxylic acid, sulphonamide and carbonyl

Table 2.3. Template selection in the run with both spheric site 4 and 5.

Single sp^3 carbon, 6-membered aromatic and 5-membered aromatic rings spacer templates were used during the connection phase in SPIDER. This produced eleven extending structures after removal of chemically unstable or undesirable results. Of these, the four highest scoring were taken on to combine in MOLOC.

2.3.2 MOLOC

The SPROUT runs had produced twelve structures that were to be combined with the hexapeptide to produce vancomycin analogues. During the editing process in MOLOC a number of additional structures were created by adding or removing spacer carbons from the original SPROUT structure and by variation of the placement of hetero-atoms. The extending fragments and the hexapeptide were combined by removing the amino group from the *N*-terminus of the hexapeptide. The hexapeptide and each extending fragment were then made single entries and then the bond that connects the extending fragment to the hexapeptide was added. When each analogue was complete they were minimised in MOLOC using the MAB force field, in the presence of the tripeptide in the conformation it adopted in the PDB 1FVM.[1]

This process created 18 analogues that were evaluated in MOLOC. For each of these five intermolecular energy interactions were recorded. These interactions were between the vancomycin analogue and the tripeptide chain after energy minimisation. They were hydrogen bond energy, repulsive and attractive van der Waals energies and repulsive and attractive columbic energies. From these five energies, the total energy of the intermolecular interactions was calculated, i.e. the sum of three attractive forces minus the sum of the two repulsive forces. A higher value for this total energy predicts a more stable complex between the analogue and the tripeptide. The five highest scoring complexes were taken back into SPROUT and scored and are shown on the following pages with their SPROUT scores; abbreviated structures are included for clarity. The complex of vancomycin and the tripeptide is included for comparison. The hydrogen bond network is shown in yellow for each complex.

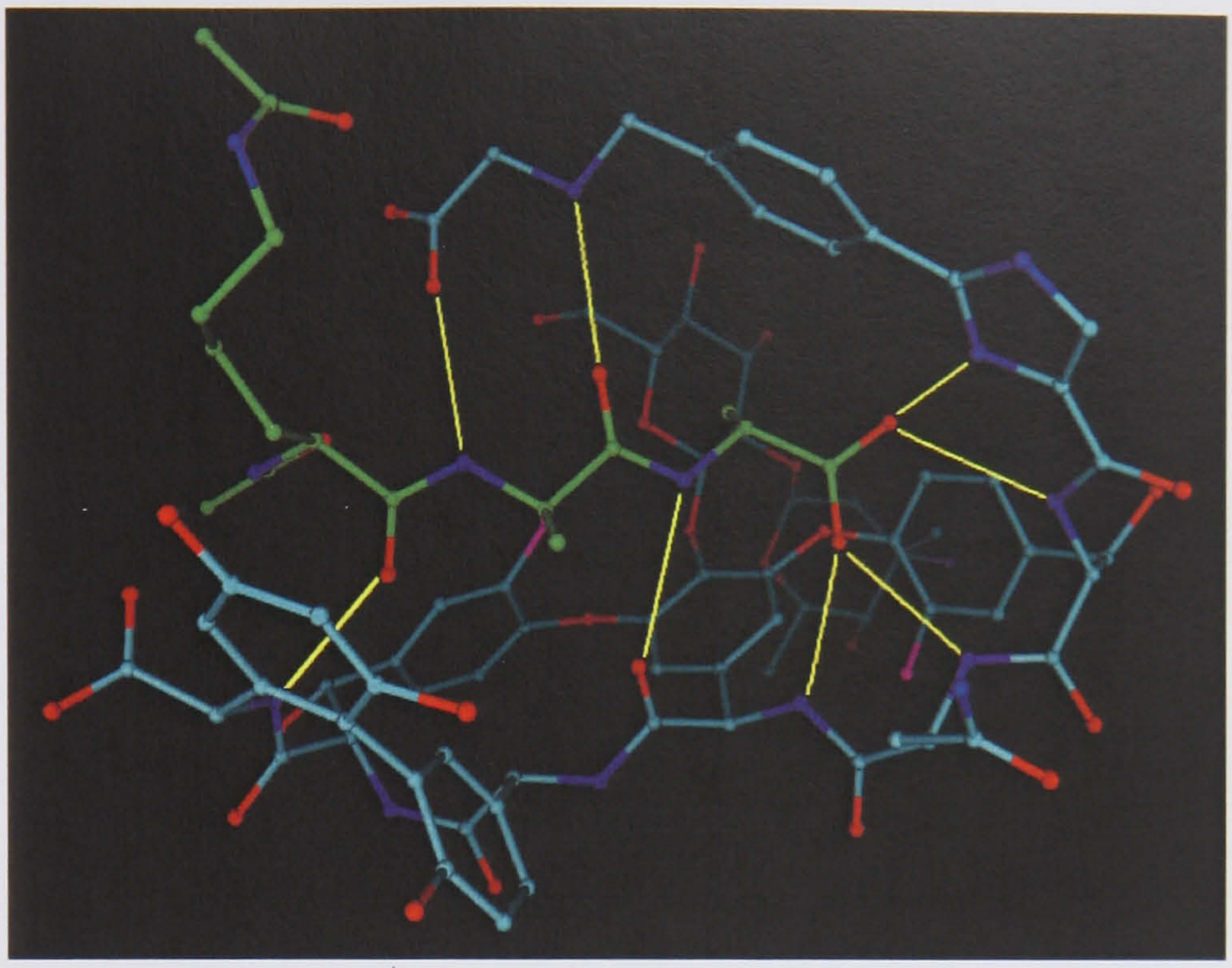

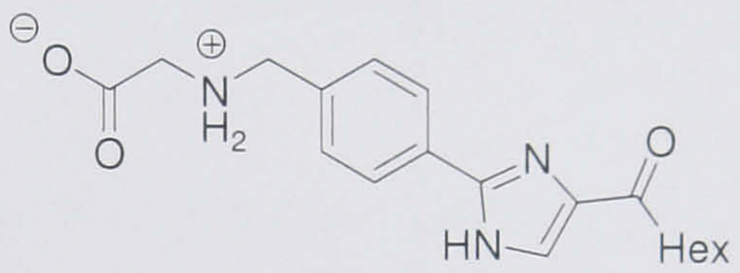

Figure 2.8. Compound 1, SPROUT score –9.25.

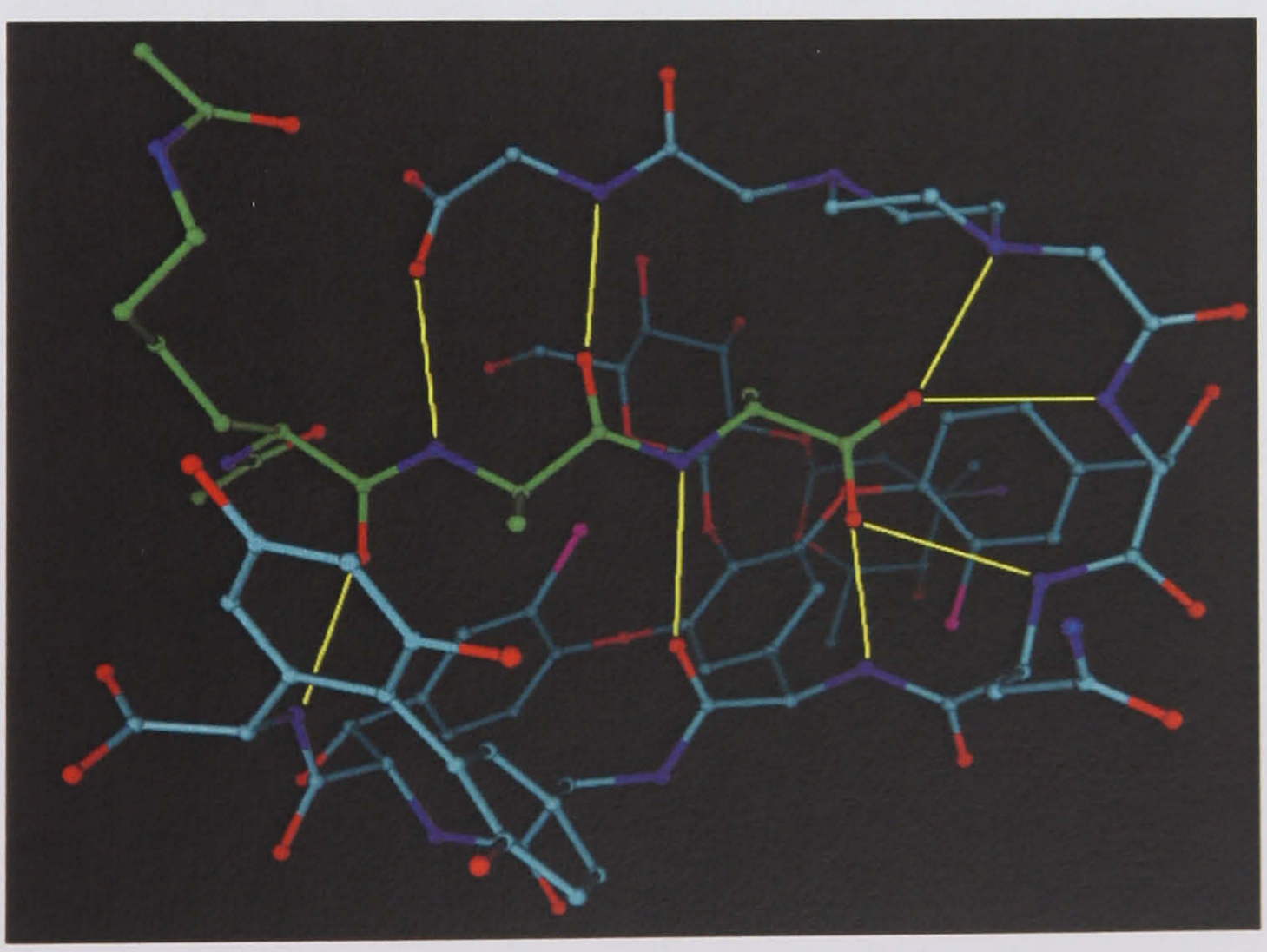

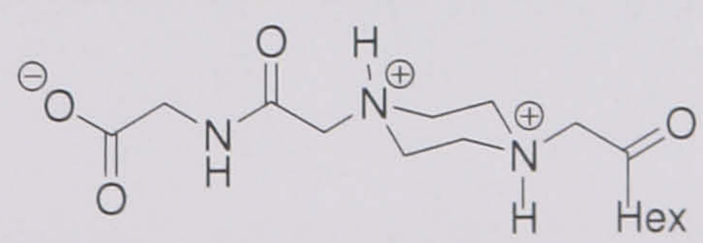

Figure 2.9. Compound 2, SPROUT score –9.10.

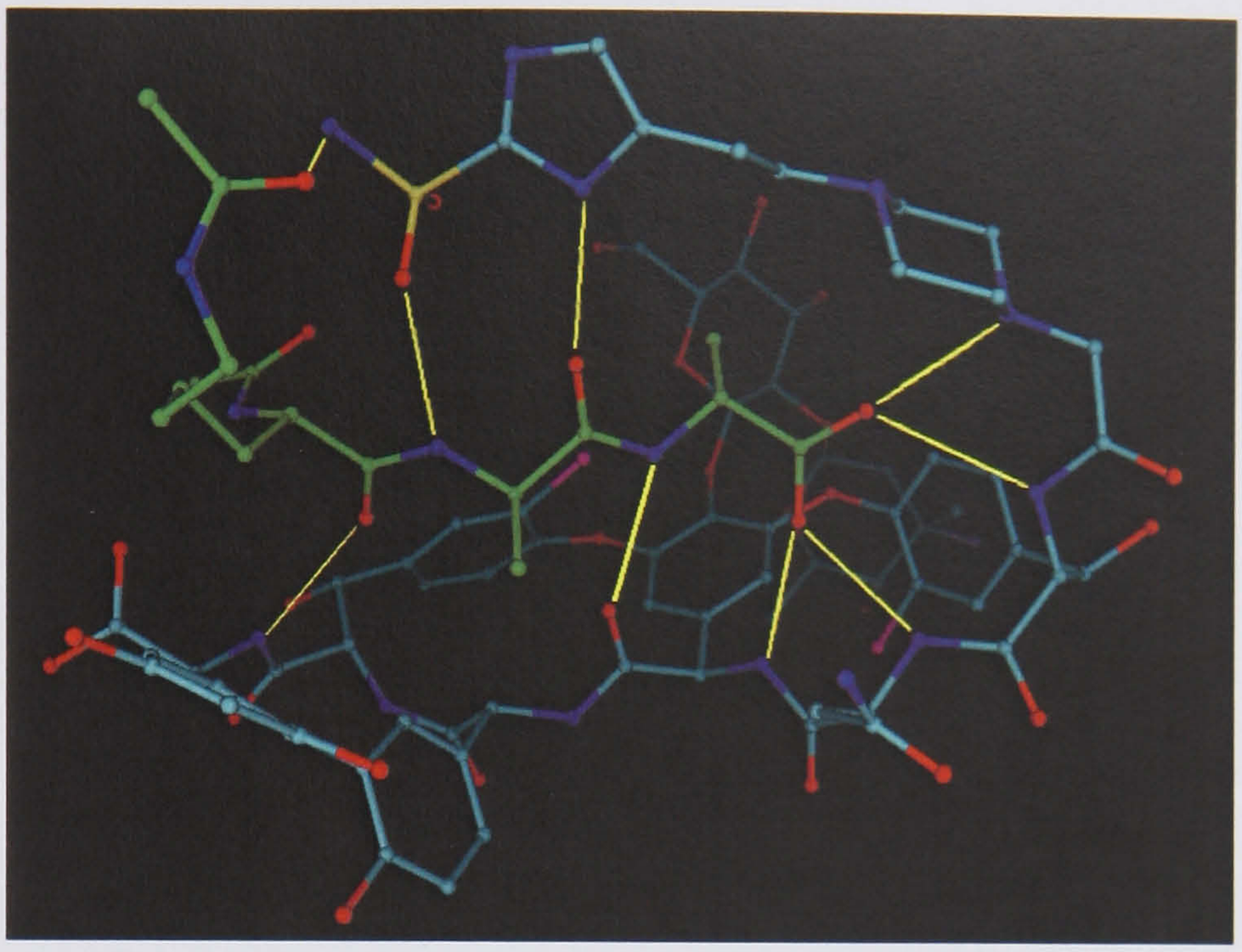

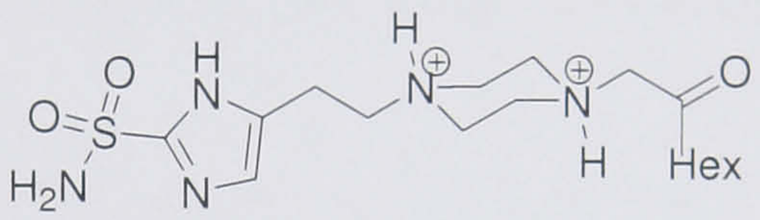

Figure 2.10. Compound 3, SPROUT score –8.93.

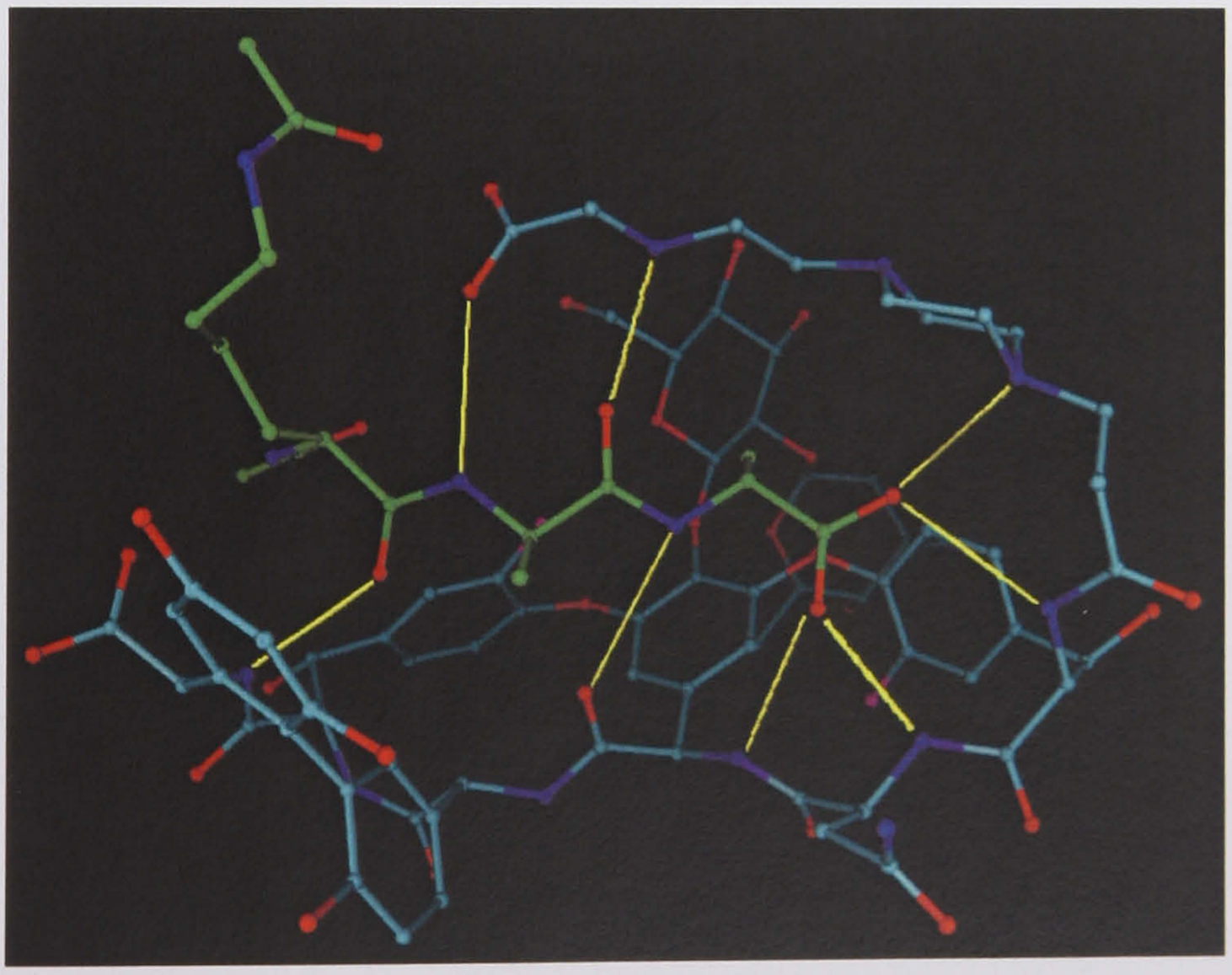

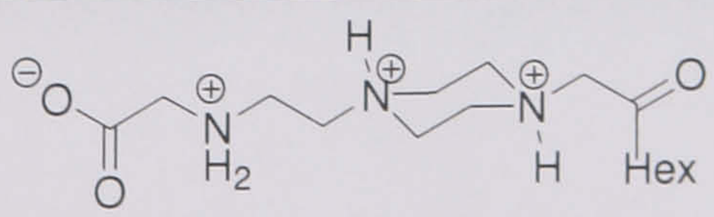

Figure 2.11. Compound 4, SPROUT score –8.31.

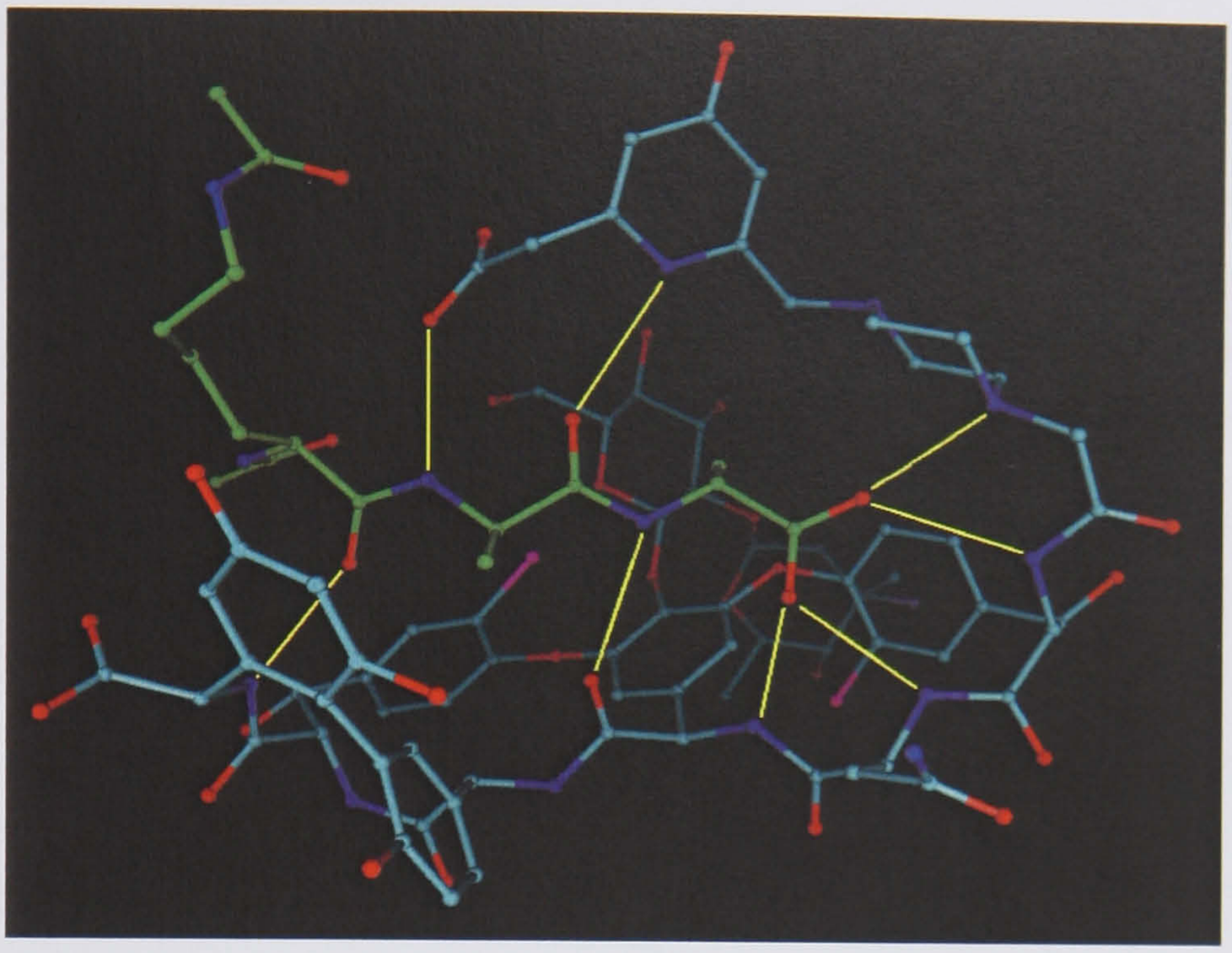

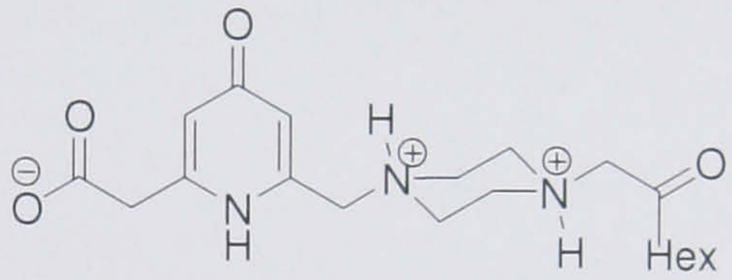

Figure 2.12. Compound 5, SPROUT score –8.20.

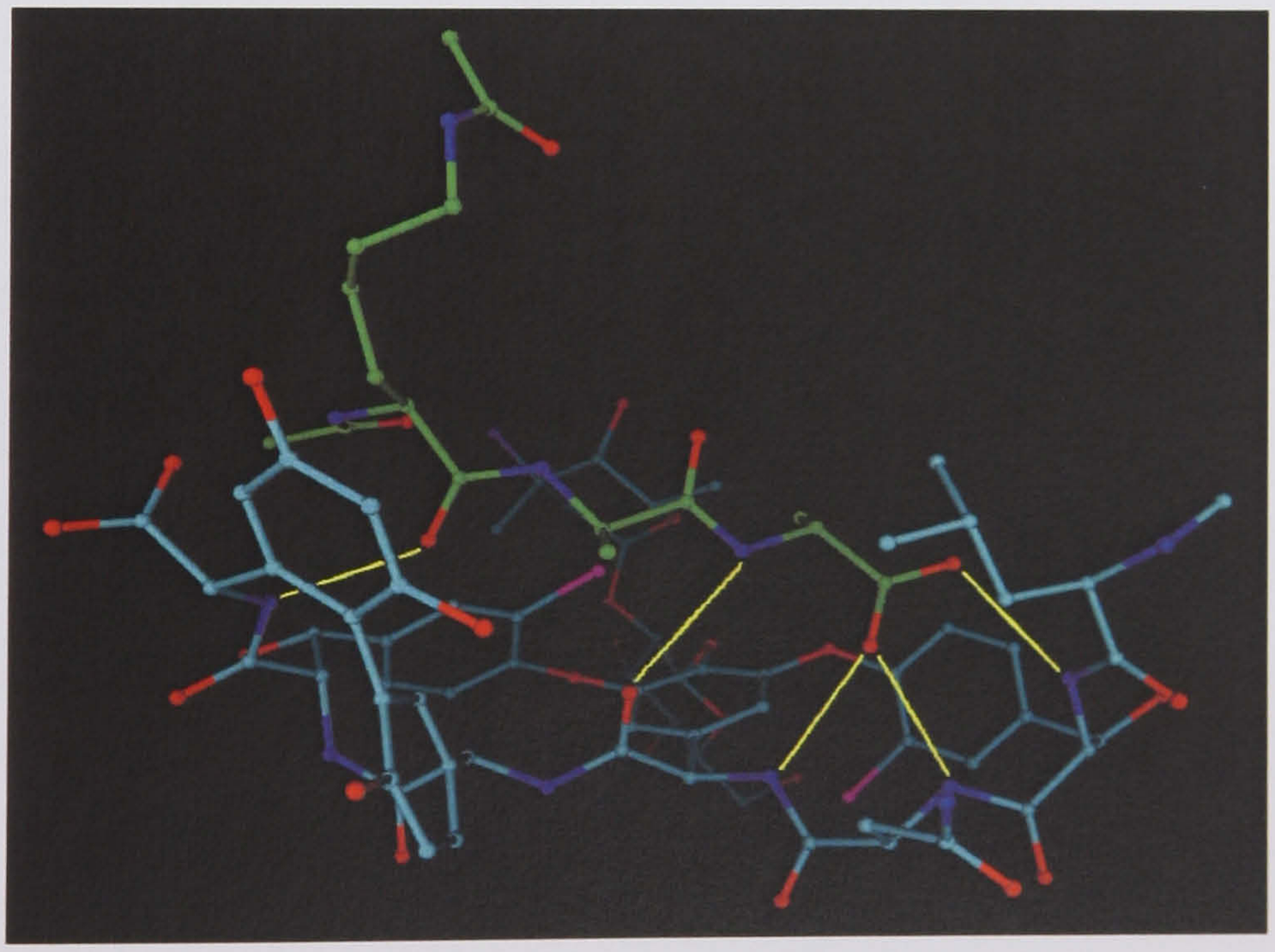

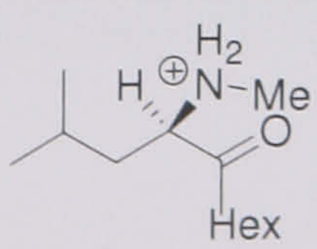

Figure 2.13. Vancomycin, SPROUT score –7.63.

2.3.3 Target selection

Examining the results showed that structures where a piperazine is docked to O2-Ala1 were high scoring. In ALLIGATOR there is a function called the vertex score table that breaks down the score and shows the contribution each atom of a structure makes to the total score. Analysis of this table for the piperazine methylene groups shows that they score well as hydrophobic atoms. This is because of a hydrophobic interaction with the methyl substitutent of alanine1. This interaction was highly desirable as it mimics the strong interaction between the *N*-methyl leucine side chain that is present in the tripeptide vancomycin complex. This resulted in the rejection of compound 1, as it did not contain a piperazine ring and the phenyl ring present formed only a weak interaction with the methyl of alanine1. Compound 2 was the next highest scoring compound and appeared to be synthetically amenable, it was predicted by SPROUT to have over an order of magnitude increase in affinity as compared to vancomycin and so was selected as the target compound.

2.4 Further designs

2.4.1 Amino acid variation

During the synthetic process that was underway to produce the initial target it became obvious that it should be relatively simple to produce further analogues of compound 2 by varying the terminal amino acid of the extending fragment. It was thought that inclusion of an amino acid with a lipophilic side chain would allow an extra hydrophobic interaction with the methyl substitutent of the second alanine in the tripeptide. The structure of compound 2 was therefore edited in MOLOC by adding a phenyl ring or a benzyl group. This created two new structures that were both minimised with the MAB force field in the presence of the tripeptide, with the conformation of the tripeptide fixed as it was in the PDB 1FVM.[1] The resulting structures were then imported into SPROUT to be scored. These are shown on the next page with their SPROUT scores, the abbreviated structure, and the hydrogen bond network displayed in yellow (Figures 2.14 and 2.15).

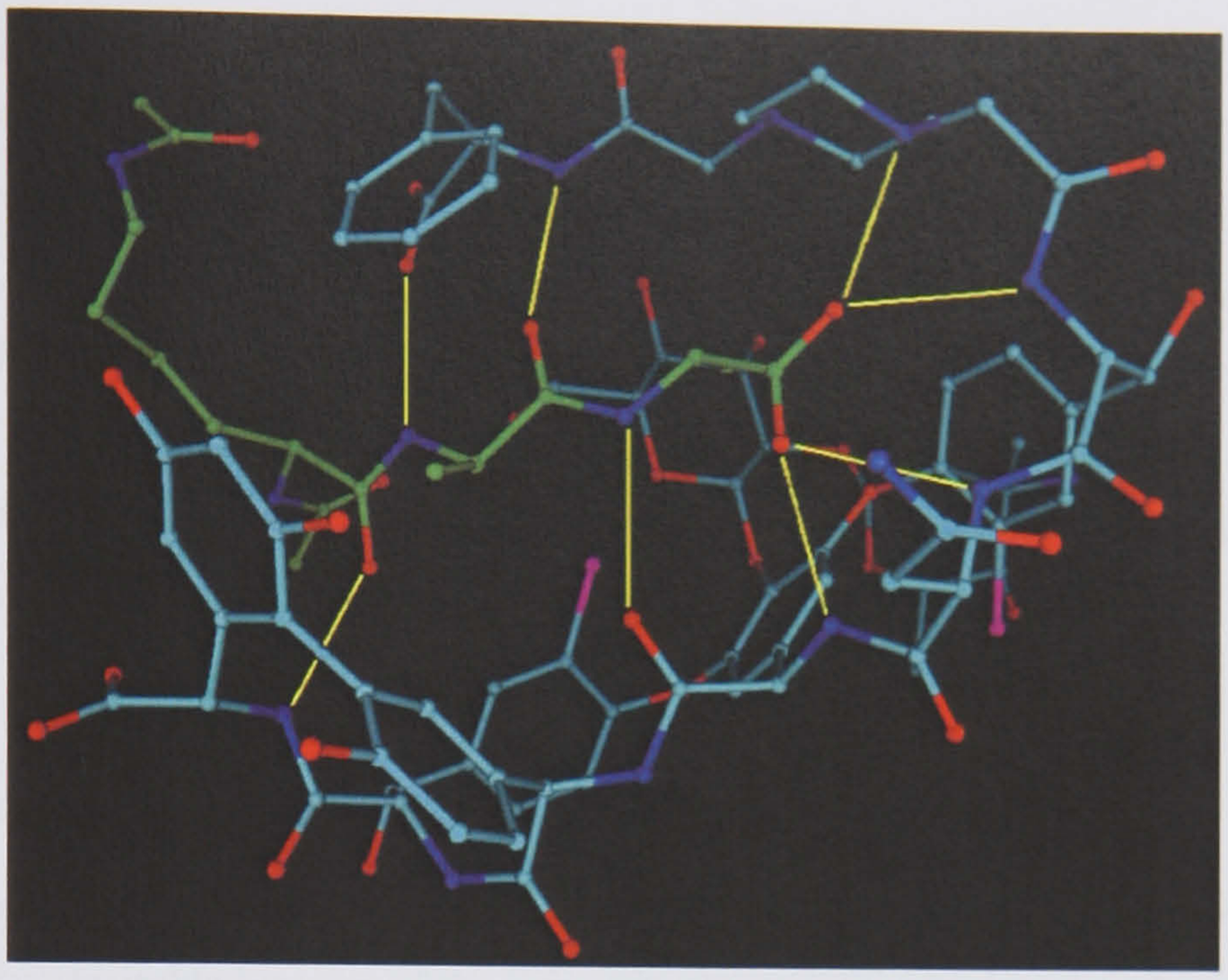

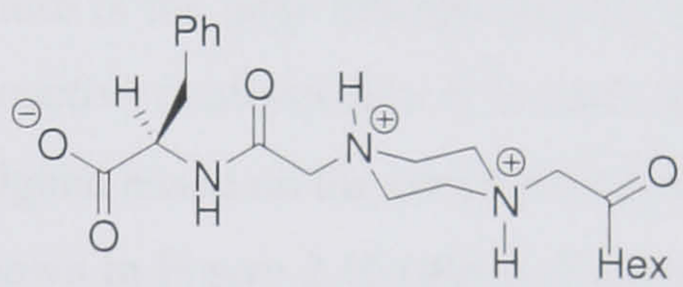

Figure 2.14. Compound 6, SPROUT score –9.38.

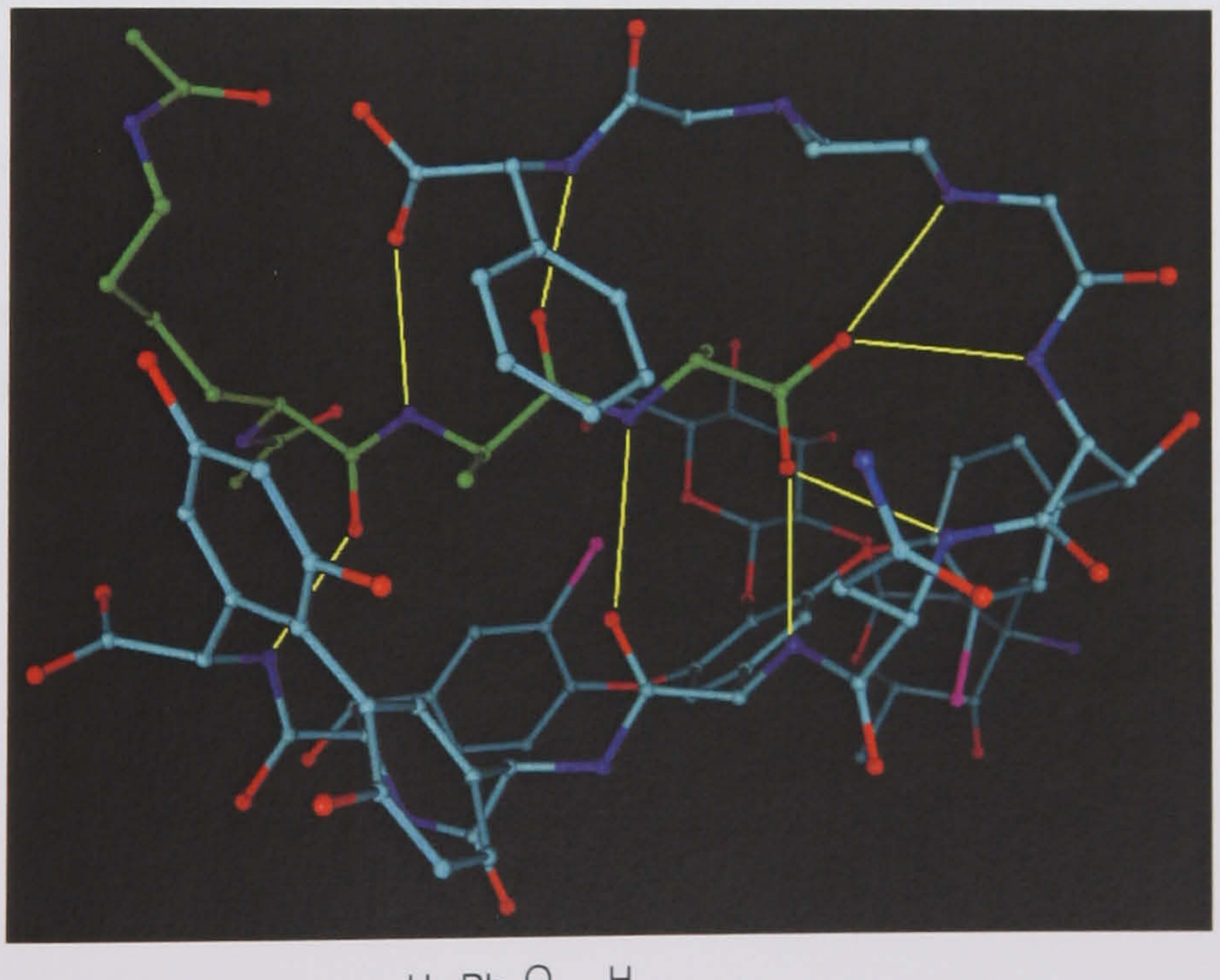

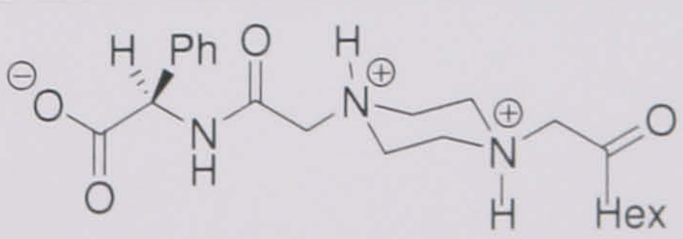

Figure 2.15. Compound 7, SPROUT score –8.14.

Both compound complexes have good predicted affinities, the compound 7 complex has over a 5-fold predicted increase in affinity and compound 6 complex has a predicted affinity nearly two orders of magnitude above that predicted for the vancomycin complex. Analysis of the vertex score table confirmed that the phenyl rings in both compounds had predicted hydrophobic interactions with the methyl group of the second alanine of the tripeptide. It was therefore decided to synthesise both of these compounds. Examining the structures shows that the amino acid must be the unnatural D-configuration.

2.4.2 A rigid analogue

The extending fragment for compound 2 has a large degree of conformational freedom and this is undesirable because of the large entropic penalty that results when the structure is fixed into its bioactive conformation as it binds the tripeptide. A rigidified structure was therefore designed based on the commercially available bicyclic compound theophylline, shown in Figure 2.16 (this is discussed in greater detail in Chapter 3, Section 1.10). This structure was designed by importing the structure of compound 2 into MOLOC and editing it to include theophylline in a pose which satisfied the same hydrogen bonding interactions as the original structure and then minimising the structure in the presence of the tripeptide. It was necessary to allow the side chain of the lysine group to be minimised as well, because of an unfavourable interaction between it and the theophylline ring. The resulting structure was imported into SPROUT and scored. The structure is shown in Figure 2.17 with its SPROUT score and an abbreviated structure, the hydrogen bonding network is shown in yellow.

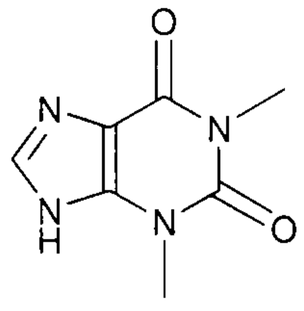

Figure 2.16. Theophylline.

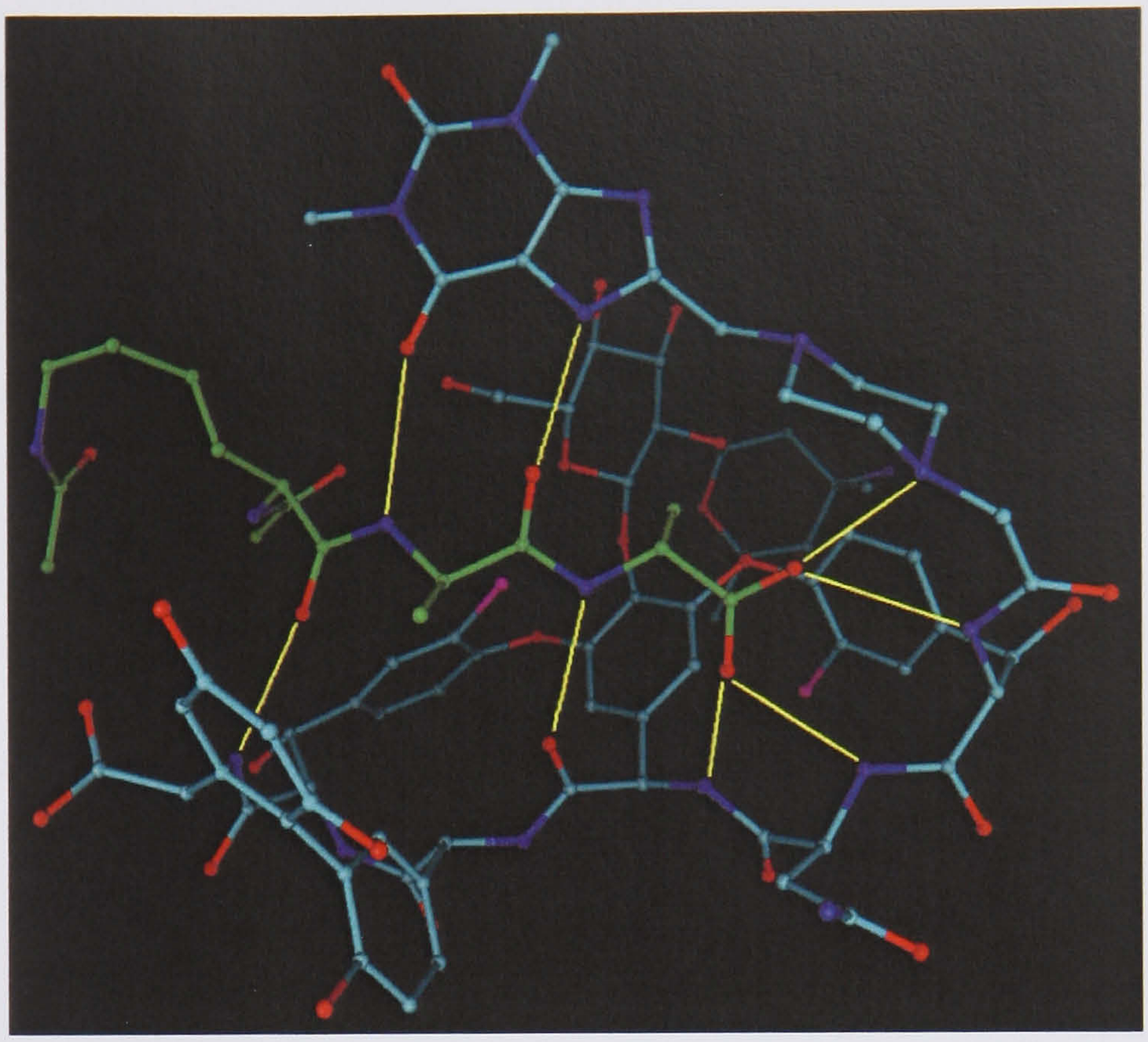

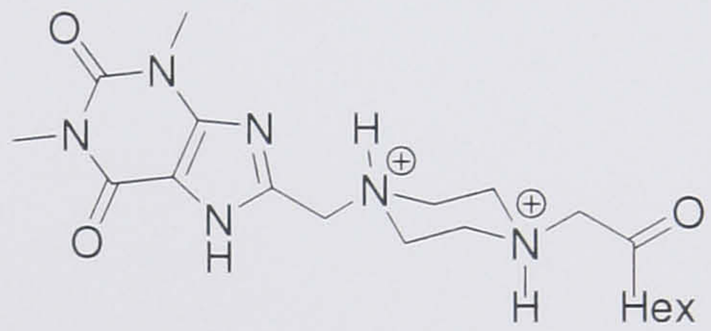

Figure 2.17. The rigid analogue, SPROUT score –8.14.

2.5 Conclusions on the design phase

The initial design phase was very successful producing five potential compounds with predicted affinity for the tripeptide higher than predicted for vancomycin. The selection of a target compound with synthetic accessibility was possible and the chosen structure stimulated a further design phase, which produced three further variations all with predicted increased affinity to the tripeptide.

This is the first instance of rational design of semi-synthetic natural product drugs of the vancomycin family.

2.6 References

(1) Nitanai, Y.; Kakoi, K.; Aoki, K., Complex of vancomycin with di-acetyl-lys-D-ala-D-ala, 2000, http://www.rcsb.org/pdb/explore.do?structureId=1FVM, accessed: September 2002.

(2) RCSB Protein Data Bank, http://www.rcsb.org/pdb/home/home.do, accessed: September 2002 to June 2007.

Chapter Three

Results and Discussion

3.1 Synthesis of piperazine extenders

3.1.1 Retrosynthesis of the piperazine extenders

Following the design phase and the adoption of the piperazine-based compounds as extensions of the vancomycin hexapeptide, it was necessary to analyse the compounds and produce a synthetic strategy. The first stage of this process was a retrosynthetic analysis, shown below in Figure 3.1.

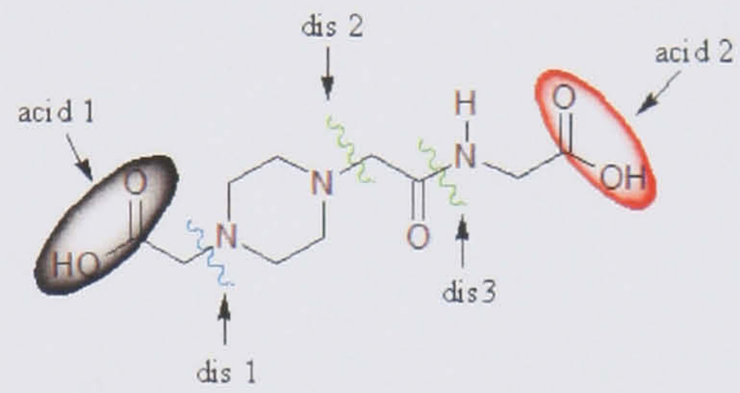

Figure 3.1. A retrosynthesis of the piperazine target.

It was necessary to be able to distinguish the two acid groups, as acid 1 will be coupled to vancomycin hexapeptide and the other will be left as the free acid. This requires the use of protecting group chemistry. Esters were the obvious choice as acid protecting agents and a number of strategies for the orthogonal protection of these acids are available.[1]

3.1.2 The designed fragment – first attempted synthesis

The designed fragment (1) was required as the mono-ester of acid 2.

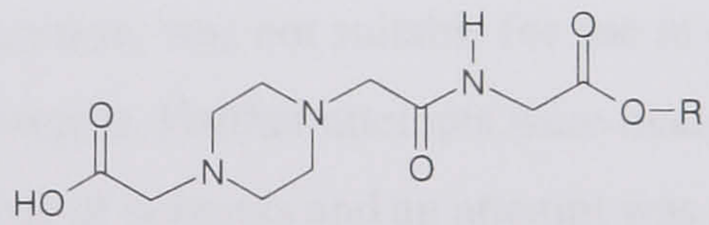

(1) - R = H
(2) - R = ^{t}Bu

The use of a commercially available mono-alkylated piperazine (3) as the starting material in this synthesis avoided the need for the disconnection at dis 1 (Figure 3.1). The necessity of cleaving the ethyl ester introduced by compound (3) under basic conditions led to the selection of an acid labile ester for acid 2. It was therefore decided to utilise a *tert*-butyl ester to protect acid 2. *tert*-Butyl esters should be cleavable with trifluoroacetic acid (TFA) after coupling to vancomycin; thus piperazine (2) became the initial target.

A possible retrosynthesis of (2) (Figure 3.1) is *via* disconnection at dis 3 to give *tert*-butyl glycine and the free acid, followed by disconnection at dis 2 to give α-chloroacetic acid and the commercially available mono-alkyl piperazine (3). A proposed forward synthesis is shown in Scheme 3.1.

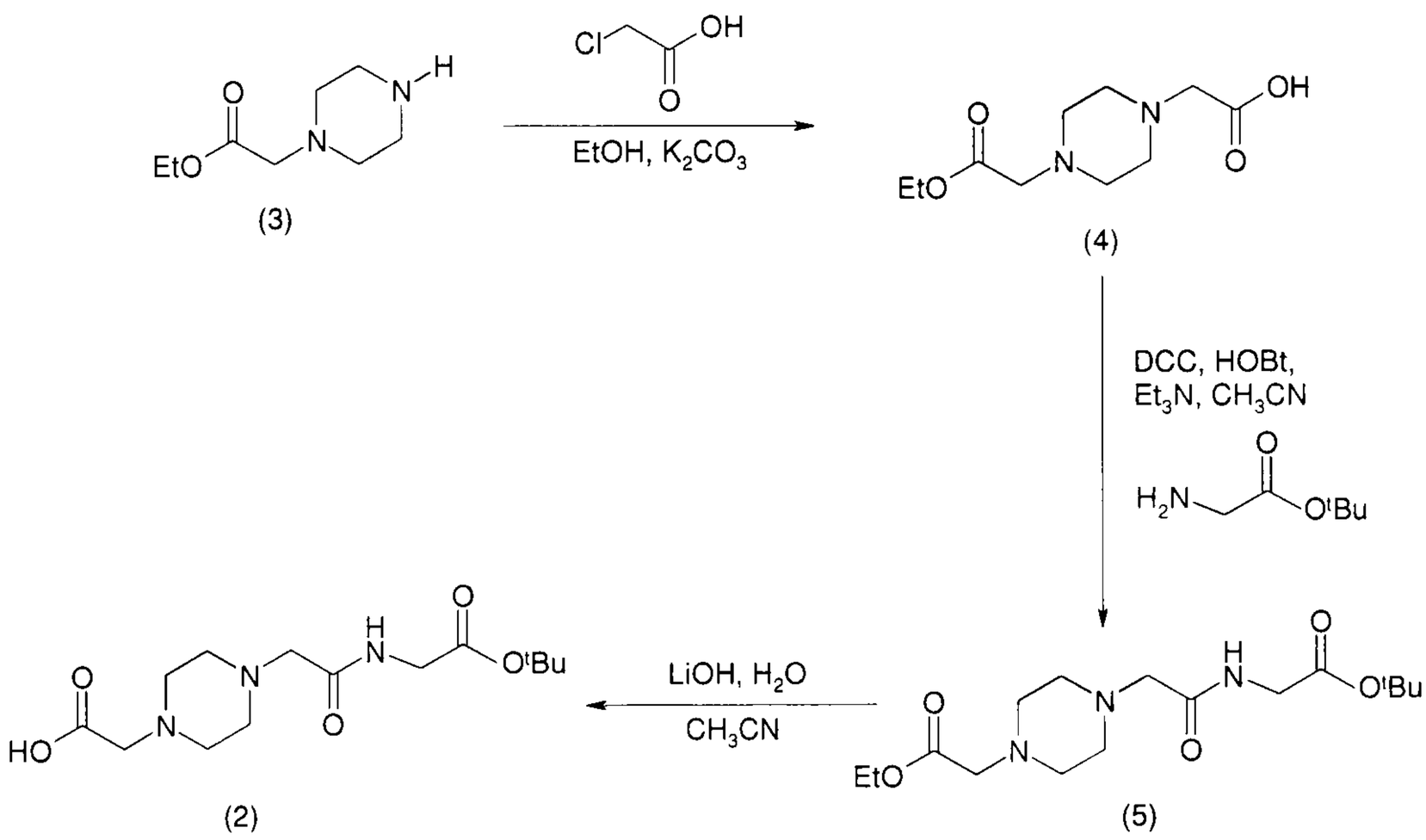

Scheme 3.1.

Alkylation of piperazine (3) with chloroacetic acid using the conditions of Witiak *et al.*[2] appeared to be efficient, judged using TLC analysis as the reaction progressed. TLC showed that the reaction had gone almost to completion, and starting material (3) had been consumed. However, the product was very difficult to isolate due to its high water solubility. Attempts to extract into different organic solvents from the aqueous reaction media were unsuccessful and the solvent system used for TLC analysis, although sufficient to monitor the reaction, was not suitable for use in column chromatography, due to the high methanol content. Further attempts were made to purify this compound by trituration using a number of solvents and an attempt was made at finding suitable conditions for the purification of this compound using HPLC, without success.

The difficulty in the isolation of this product appears to stem from its highly polar nature, as presumably it exists as a zwitter ion (6) in solution.

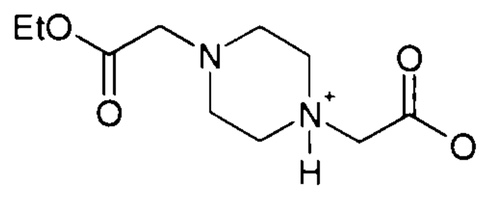

(6)

It was reasoned that an alternative method which would avoid the formation of product (6) by alkylation of piperazine (3) using an α-halo ester could be used to yield the fully protected piperazine di-ester (7). It was decided to use a tertiary butyl protecting group on the α-halo ester, as this would allow differentiation between the two ester groups, allowing them to be used selectively in different coupling steps (Scheme 3.2). It was reasoned that the *tert*-butyl moiety would be cleaved first and then taken without further purification to react with *tert*-butyl protected glycine. Then the ethyl ester could be cleaved and used to couple to vancomycin hexapeptide. After the coupling, the remaining *tert*-butyl ester could then be removed with TFA (Scheme 3.2).

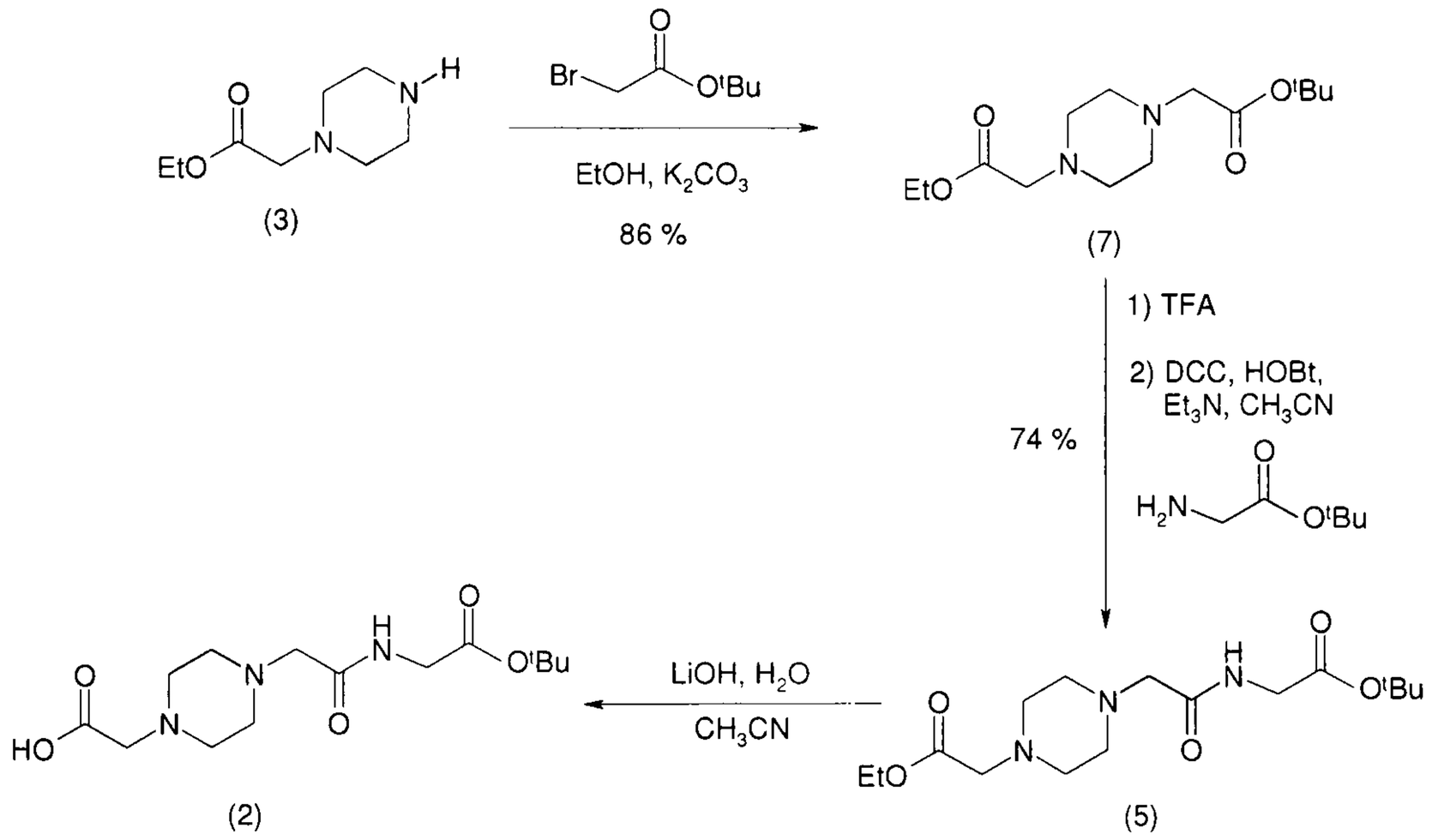

Scheme 3.2.

For the initial attempt to prepare (7), the reaction conditions described by Witiak[2] for the di-alkylation of piperazine-2,5-dicarboxylic acid with bromoacetic acid in aqueous potassium carbonate were used. However, it was found that *tert*-butyl bromoacetate was insoluble in the aqueous solution and addition of methanol was required in order to allow the bromoacetic ester to dissolve and the reaction to proceed.

Whilst facilitating the reaction, the addition of the methanol unfortunately also induced a trans-esterification of the desired ethyl ester into a methyl ester. This transformation was not complete and resulted in a mixture of ethyl and methyl esters. Therefore, in order to facilitate characterisation, this mixture was converted entirely into the methyl ester *via* treatment with an excess of basic methanol. This however, was a rather cumbersome process and the repeated handling steps greatly reduced the yield. Bearing

this in mind, a second attempt used ethanol as the reaction medium and yielded the ethyl ester (7) in 86 % yield.

Conversion of the di-ester (7) to intermediate (5) was performed by selective hydrolysis of the *tert*-butyl ester with TFA, followed by the direct coupling of the crude product to the *tert*-butyl ester of glycine using DCC and the conditions of Rees *et al.*[3] Purification using prep LCMS gave the desired compound in 74 % yield.

The key step in this synthesis was the cleavage of the ethyl ester of compound (5) to yield the acid required for coupling to vancomycin. In order to achieve this it was necessary to perform a basic hydrolysis[4] of the ethyl ester and it was hoped that the *tert*-butyl ester would be stable under these conditions.[1]

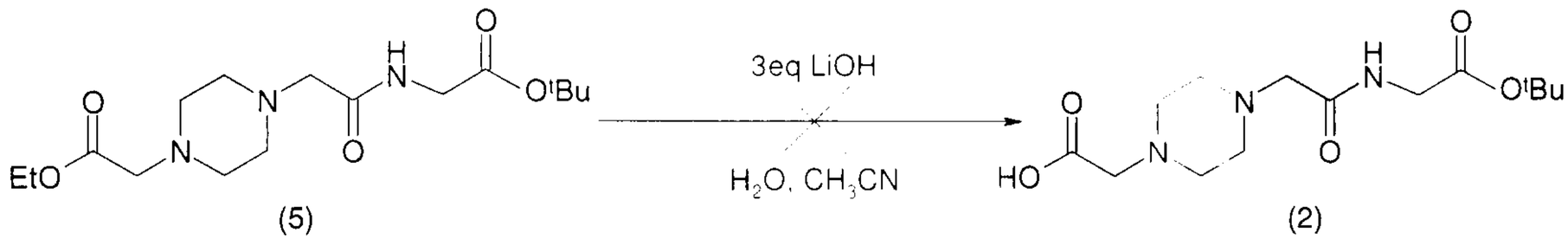

Scheme 3.3.

However, despite three attempts to prepare compound (2) *via* this method, only the di-acid, resulting from the cleavage of both esters, was produced in any significant quantities.

Cleavage to the di-acid was almost complete and essentially no desired mono-ester was observed. This seems to imply that hydrolysis of the *tert*-butyl ester was quite fast. This problem arose again in later experiments (Sections 3.1.3, 3.1.8 and 3.1.9), where di-ester (7) is cleaved using these conditions. Again *tert*-butyl ester cleavage competes with ethyl ester cleavage, but the predominant product is cleavage of the ethyl ester. The significant difference between the two experiments is that the reaction time is shorter (35 minutes as opposed to overnight). A further difference in the synthesis of the D-phenylglycine analogue was that the amount of LiOH used was reduced to 1.1 equivalents, further reducing this undesired cleavage. Had these alternative conditions been employed here more of product (2) may have been obtained.

However, it does appear that the *tert*-butyl ester in this compound is less stable to base than would be expected and less stable than di-ester (7). A possible explanation of this

is that the hydrolysis occurs in two steps; the first involves de-protonation of the amide NH by the basic nitrogen of the piperazine ring pushes electron density onto the oxygen of the amide. Then attack from the oxygen of the amide on the carbonyl of the *tert*-butyl ester displaces *tert*-butoxide forming a five membered ring. This ring is then hydrolysed by a hydroxide ion and produces the di-acid (Figure 3.2). This avoids direct attack on the sterically hindered *tert*-butyl ester, which would be a slow process, and thus could explain the higher rate of cleavage for the *tert*-butyl ester.

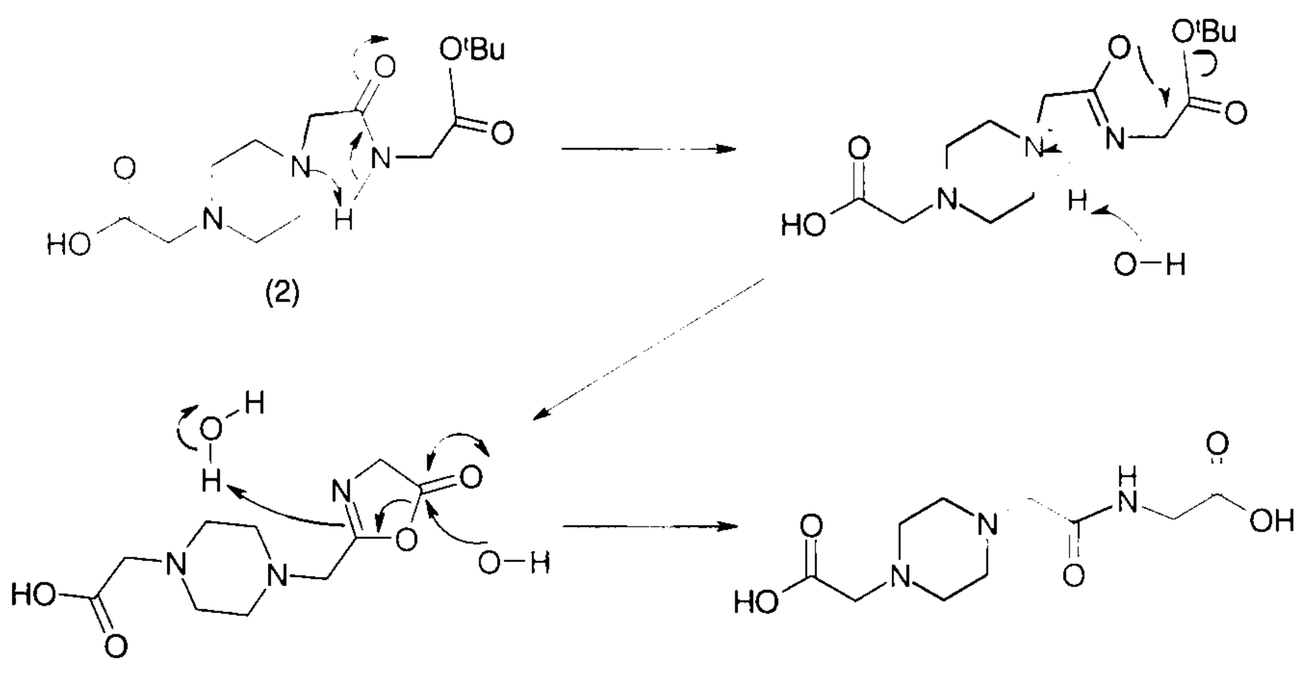

Figure 3.2. A proposed mechanism for the rapid hydrolysis of compound (2).

3.1.3 Piperazine fragments with alternative protecting groups

Following the failure to selectively cleave the ethyl group from ester (5) to yield the free acid (2) (Scheme 3.3), a new approach to the synthesis of acid (2) was necessary. The *tert*-butyl protecting group was still desired, as this is easily cleavable once coupled to vancomycin hexapeptide. Therefore, it was decided to replace the ethyl ester with an alternate ester. It was reasoned that the most acceptable replacements would be either a benzyl ester or a trimethylsilylethyl (TMSE) ester. These two alternatives offer synthetic benefits as they are both cleaved in neutral solution, therefore avoiding the basic conditions that were responsible for the cleavage of the *tert*-butyl group and the failure of the previous synthetic attempts.

The fact that the available starting material already contained an ethyl ester moiety necessitated a transesterification. With benzyl alcohol, this could be done directly, as using a large excess of this inexpensive material was acceptable. However, the TMSE protected alcohol was more expensive and the preferred route was *via* the free acid, as this allowed the formation of the desired ester using only a small excess of the alcohol.

The synthesis of both compounds could be achieved from a common intermediate (7), derived by the alkylation of the commercially available mono substituted piperazine (3), therefore the re-synthesis of intermediate (7) was necessary. This combined to give the synthetic plan shown in Scheme 3.4.

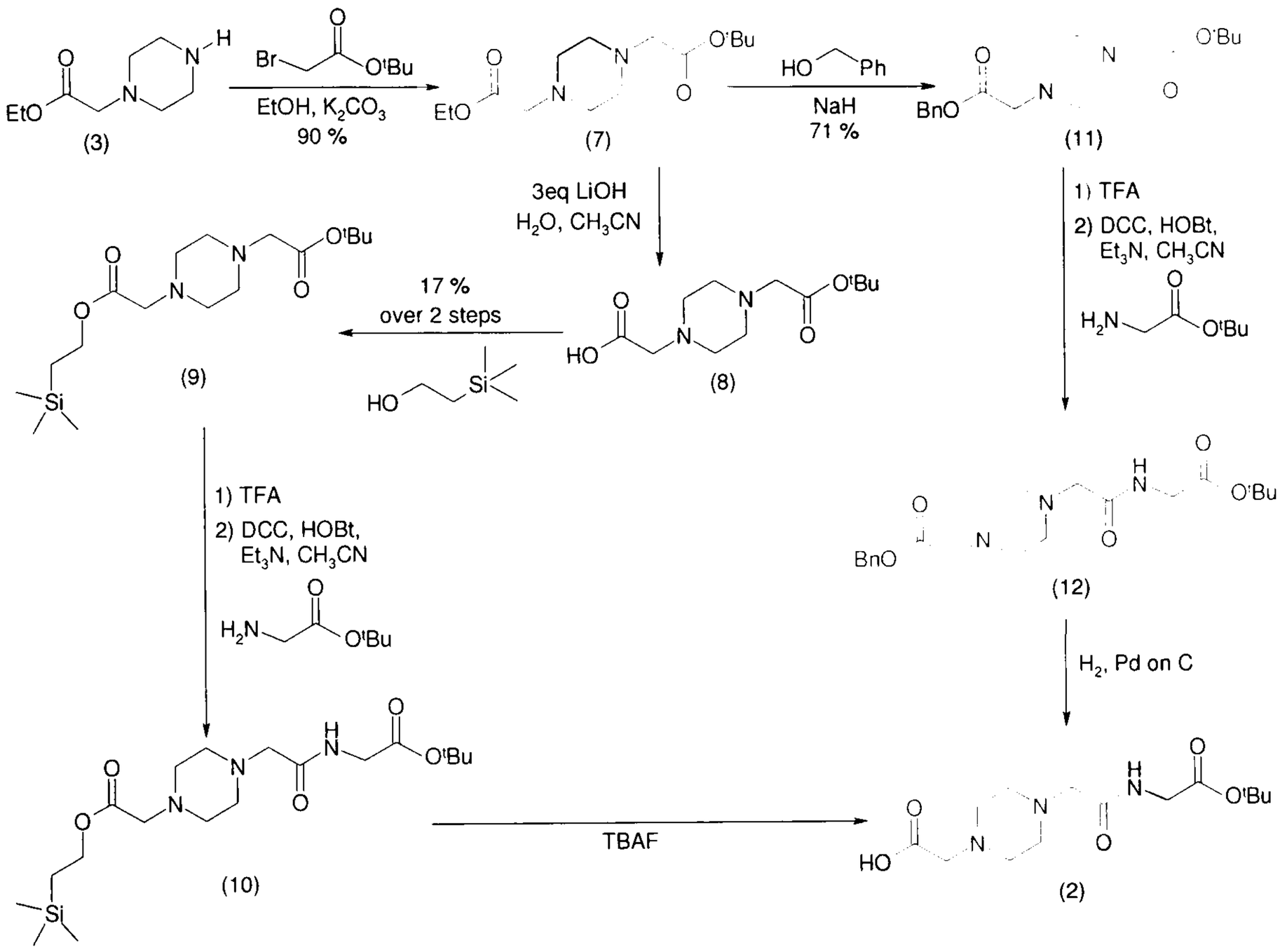

Scheme 3.4.

The re-synthesis of intermediate (7) was performed utilising the conditions developed previously. It was carried out on a large scale and resulted in 10 g of compound (7) (90 % yield) with good purity, providing a sufficient pool to allow for the examination of the subsequent reactions.

Due to the increasing reliance on *tert*-butyl glycine (14) in the synthesis of the piperazine extenders it was decided to synthesise a significant quantity from the inexpensive α-bromo intermediate (13), Scheme 3.5.

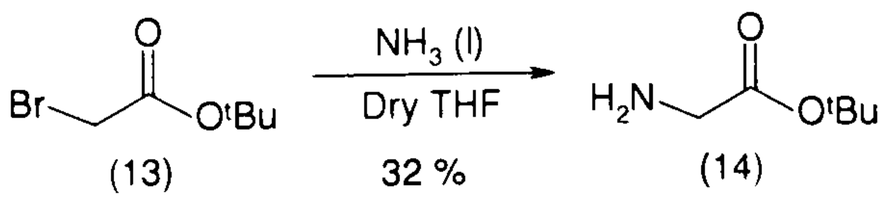

Scheme 3.5.

This was carried out on a large scale, but unfortunately amine (14) was obtained in only 32 % yield. The most likely explanation for this poor conversion is that the reaction was not cooled for long enough and the liquid ammonia evaporated prior to completion of the reaction.

The transesterification of ethyl ester (7) to benzyl ester (11) was accomplished *via* treatment of the ethyl ester with a four-fold excess of benzyl alcohol, which had been treated with a small quantity of sodium hydride. It was necessary to treat the mixture twice with the benzyl alcohol mixture. After reaction with the first quantity of benzyl alcohol the reaction mixture was evaporated, removing the ethanol produced in the reaction, before re-treating the solution with the second portion of benzyl alcohol, thus the reaction was forced forward (le Chatelier's principle[5]). This yielded the product (11) in 71 % yield, after purification using prep LCMS.

Two attempts were made to convert the ethyl ester (7) to the TMSE ester (9), detailed in Scheme 3.6. The first step of each of these was the conversion of the ethyl ester to the free acid (8), using a three-fold excess of LiOH in a base-catalysed hydrolysis. The free acid (8) was not isolated or characterised but its presence was indicated by the observation of a peak in the MS at 259 m/z, there was also a peak at 203 m/z this could be either the di-acid produced by cleavage of both esters or from fragmentation of the desired product (8). The initial attempt then utilised a coupling mediated with Mukaiyama's reagent, *N*-methyl, 2-chloropyridine.[6] This method proved inefficient, producing the product in only 17 % yield over two steps. A further problem with this reaction was the presence of excess LiOH (~2eq) carried through from the first step. This necessitated the use of 3.2 equivalents of the coupling agent, instead of the 1.2 eq. normally used for this type of esterification (Scheme 3.6). An interesting observation during this reaction was the TMSE di-ester was not seen, this suggests that the peak observed at 203 m/z in the MS is a fragment ion and the *tert*-butyl ester of di-ester (7, Scheme 3.6) is more stable than that of di-ester (5, Scheme 3.3).

The second attempt to convert ethyl ester (7) to the TMSE ester (9) overcame the problem of the excess LiOH by neutralising the solution with a small quantity of 3M HCl before concentrating under reduced pressure. Oxalyl chloride was then used to convert the free acid (8) to the corresponding acid chloride (15). The acid chloride was then reacted with TMSE alcohol in an attempt to yield the TMSE ester (9). This was not

successful however and it is likely that the acid chloride did not form. This could easily result if compound (8) was not sufficiently dry when it went into the reaction to form the acid chloride (15). (Scheme 3.6).

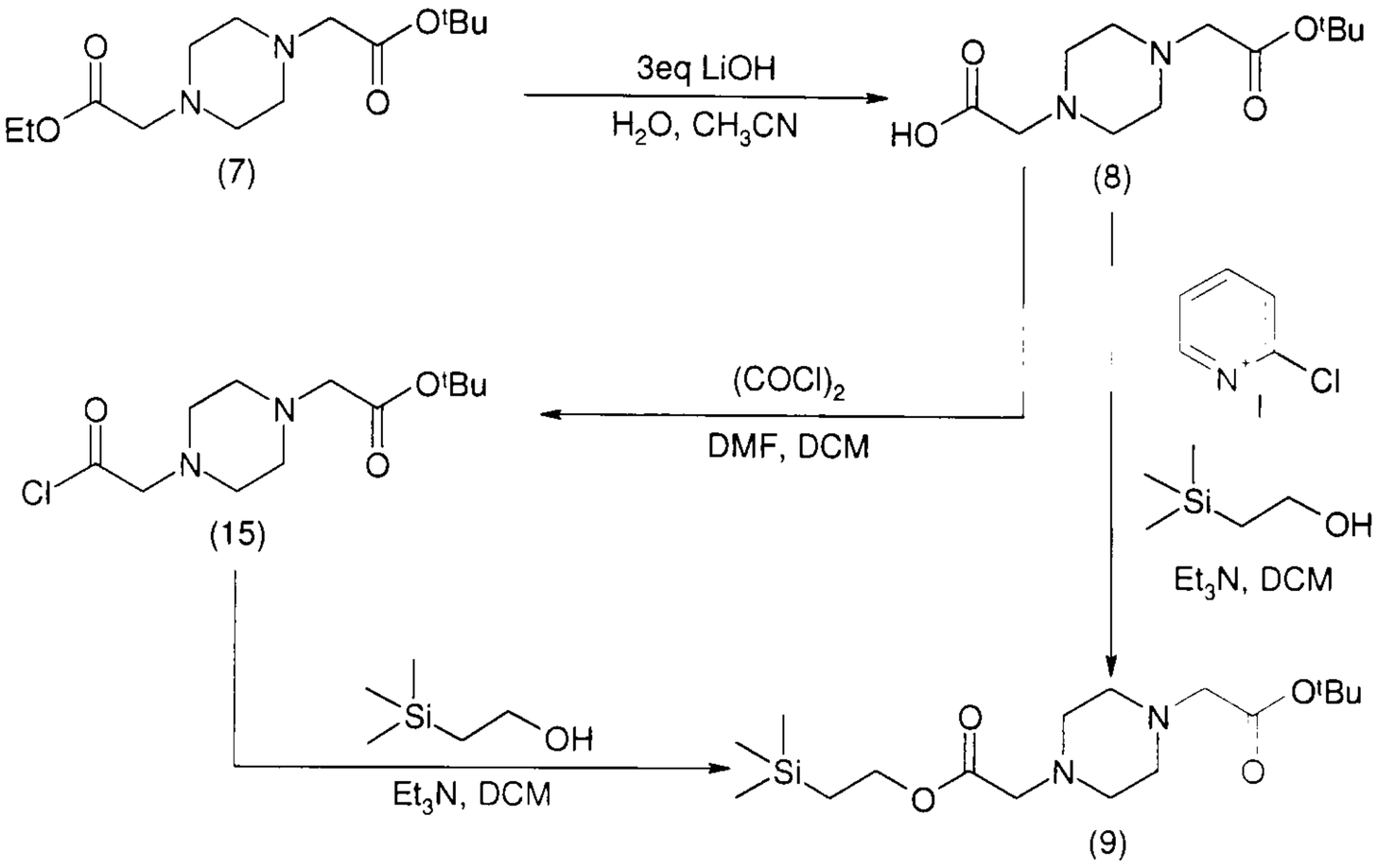

Scheme 3.6.

Other routes to this product were considered, but progress in other areas has made this route redundant and no further work was attempted.

3.1.4 Linear synthesis *via* the benzyl ester

Although both a benzyl ester and a trimethylsilylethyl (TMSE) ester were considered as alternative protecting groups for the acid unit that was eventually to be coupled to vancomycin, only the benzyl ester has been successfully formed. The TMSE ester proved difficult to synthesise, as discussed in Section 3.1.3, and it was therefore decided to concentrate on the benzyl ester. The benzyl group gives significant advantages; namely it introduces a good chromophore, imparts reasonable physical properties and is made with cheap starting materials. The water soluble coupling agent, 1-ethyl-3-(3-dimethylaminopropyl)-carbodiimide hydrochloride (EDC), was also used, as it was hoped that this would aid purification. These changes produced the new synthetic plan shown in Scheme 3.7.

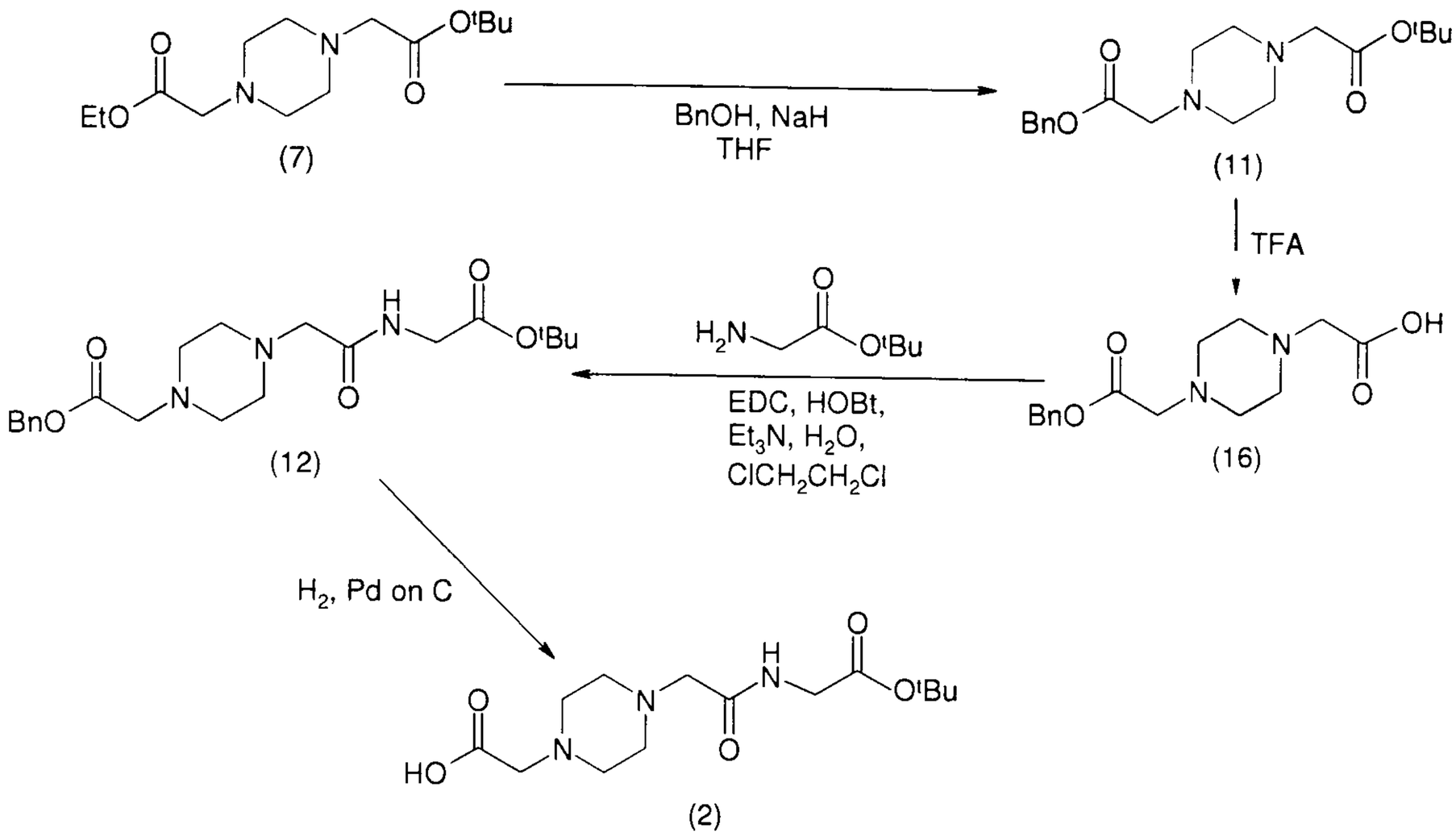

Scheme 3.7.

As discussed above in Section 3.1.3, the linear synthesis had progressed as far as the synthesis of the dialkyl piperazine (11). However, a further attempt at its synthesis was unsuccessful and mainly yielded the free acid (16), due to the premature hydrolysis of the *tert*-butyl ester of intermediate (11). The crude reaction mixture contained both the *tert*-butyl ester and the free acid, as indicated by LCMS, as well as significant amounts of other impurities. Due to the presence of the chromophore introduced by the benzyl ester, it was believed that separation using silica column chromatography would be feasible. This was attempted using a gradient elution of petrol and ethyl acetate. This was unsuccessful and resulted only in the isolation of benzyl alcohol and the dibenzyl ester, which resulted from the transesterification of both the ethyl and the *tert*-butyl esters of (7). The material remaining on the column was therefore removed using neat MeOH and the resultant solution was shown to contain the free acid (16) following LCMS analysis. The free acid was isolated in a 20 % yield using prep LCMS. It is unclear at which point the *tert*-butyl ester was cleaved as the acid is always present in the mass spectrum of these esters as a fragment ion, but due to the failure to isolate any *tert*-butyl ester (11) from the column it is evident that the silica induced at least partial hydrolysis. This partial hydrolysis may result from the acidic nature of silica gel, but is unusual as other *tert*-butyl esters have been purified on silica gel without cleavage.

The free acid (16) was then taken onto the peptide coupling with *tert*-butyl glycine to yield the extended precursor (12), (Scheme 3.7). The use of an alternative coupling

agent, 1-ethyl-3-(3-dimethylaminopropyl)-carbodiimide hydrochloride (EDC) was examined in this reaction. This was preferred to the normal coupling agent, dicyclohexyl carbodiimide, which produces a by-product, dicyclohexyl urea, which is very difficult to separate from the product. It was hoped that this would make the purification easier. A trial of this reaction using a small amount (50 mg) of the free acid (16), was attempted using the bi-phasic solution of dichloroethane (DCE) and H_2O, with HOBt, following the procedure of Nozaki and Muramatsu.[7,8] This produced 41.4 mg (60 %) of the desired compound (12), which was afforded in reasonable purity following a simple aqueous work-up. Repeating this experiment replacing the bi-phasic solvent with dry DMF, seemed to improve the yield, but this could not be confirmed as the product was impure (> 100 % yield). The samples from the reaction in the bi-phasic solution and the DMF reaction were combined for the next step and used without further purification.

The critical step in this sequence was again the selective de-protection of final piperazine di-ester to yield the target piperazine (2).

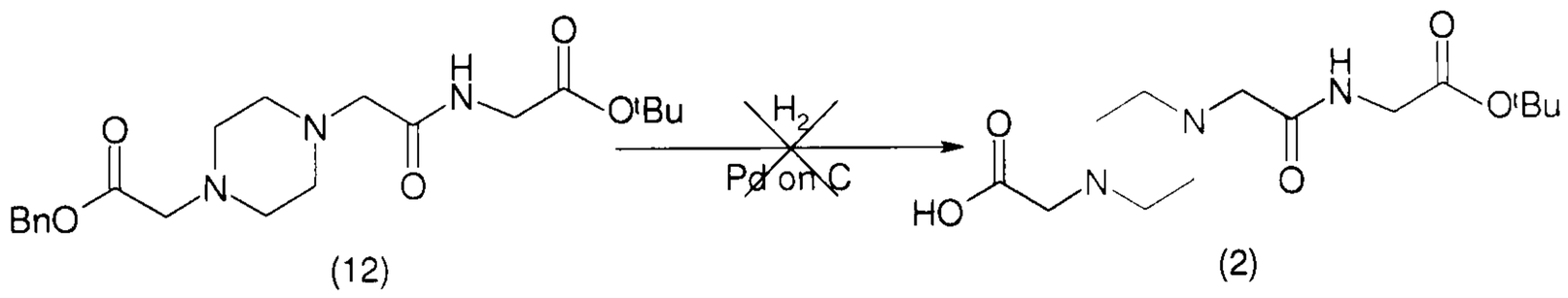

Scheme 3.8.

The cleavage of the benzyl ester was attempted using palladium on charcoal suspended in a stirred ethyl acetate solution of precursor (12), under an atmosphere of hydrogen (Scheme 3.8).[9] This was partially successful as it did result in the cleavage of some of the precursor, although this was not complete as shown by LCMS. It proved impossible to purify the sample by partitioning between a range of aqueous and organic solvents, again this stems from the highly polar nature of the compound, which presumably exists as the zwitter ion. There was insufficient material for purification using column chromatography, and there was no desire to use material this impure in a coupling with the valuable hexapeptide, so this reaction was terminated.

No further attempts at the linear synthesis were undertaken, as the alternative approaches have proved more successful.

3.1.5 Direct synthesis of piperazine (2) from the common intermediate

A report by Santilli *et al*,[10] describing the conversion of ethyl esters directly to amides offered an alternative approach to the synthesis of piperazine (2). This synthesis began with the common intermediate (7) and the cleavage of the *tert*-butyl protecting group using TFA, followed by the displacement of the ethyl ester with *tert*-butyl protected glycine in order to prepare compound (2) directly. The free acid intermediate (4) was not isolated or characterised, but was observed using MS analysis (Scheme 3.9).

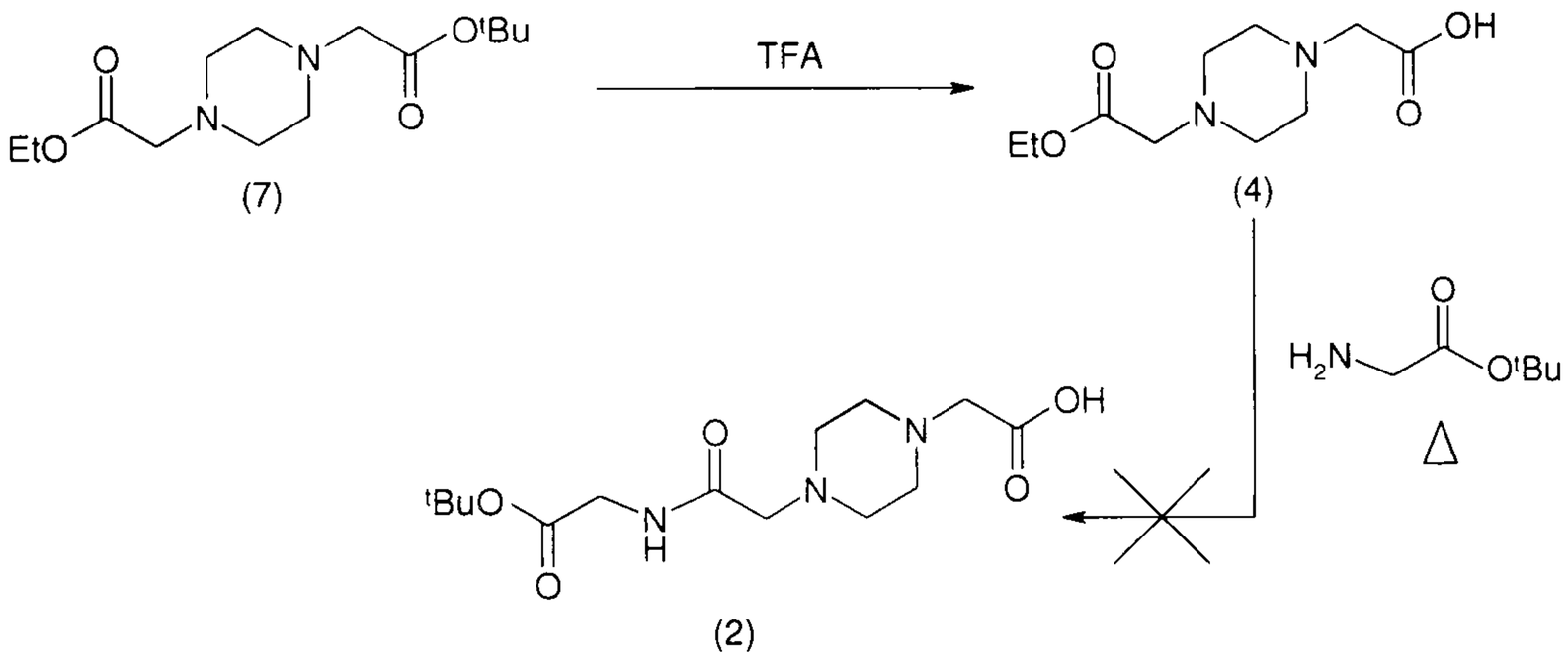

Scheme 3.9.

The *tert*-butyl group of piperazine (7) was removed because it would have been impossible to differentiate between the two *tert*-butyl groups of the potential product (17) if *tert*-butyl glycine had displaced the ethyl ester of compound (7).

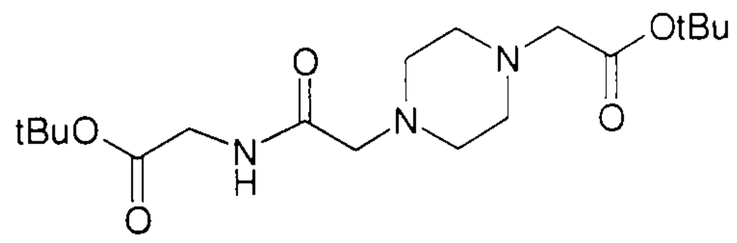

(17)

It was also believed that the *tert*-butyl ester of product (2) would be stable under these conditions as it would be too bulky to be displaced by an incoming amine. This was supported by the use of 4-amino-benzoic acid ethyl ester (18) in Santilli's paper,[10] where it appeared that the phenyl ring offered sufficient steric bulk to prevent the reaction of the adjacent ethyl ester.

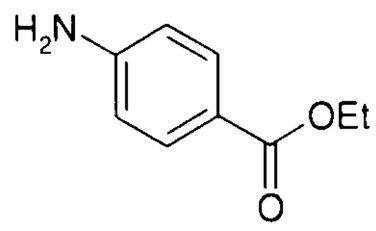

(18)

Although the paper reported good or reasonable yields in this type of reaction, using a diverse range of amines and examples that contained tertiary amine centres and amino acids, in our hands this reaction failed to produce any of compound (2), despite using a range of solvents, including ethanol, butanol and pyridine.[10]

It is believed that the failure of this reaction stems from the nature of the ethyl ester being converted, in all the examples in this paper the amines were reacted with ethyl cyanoacetate (19) and it is likely that this sort of activated ester is necessary for this reaction. It may even be the case that the reaction proceeds *via* an enone intermediate where one of the acidic α-hydrogens has been lost and the resultant anion displaces the alcohol from the ester to give the enone (20). This enone is then attacked by the amine to give the product (21), as shown in Figure 3.3.

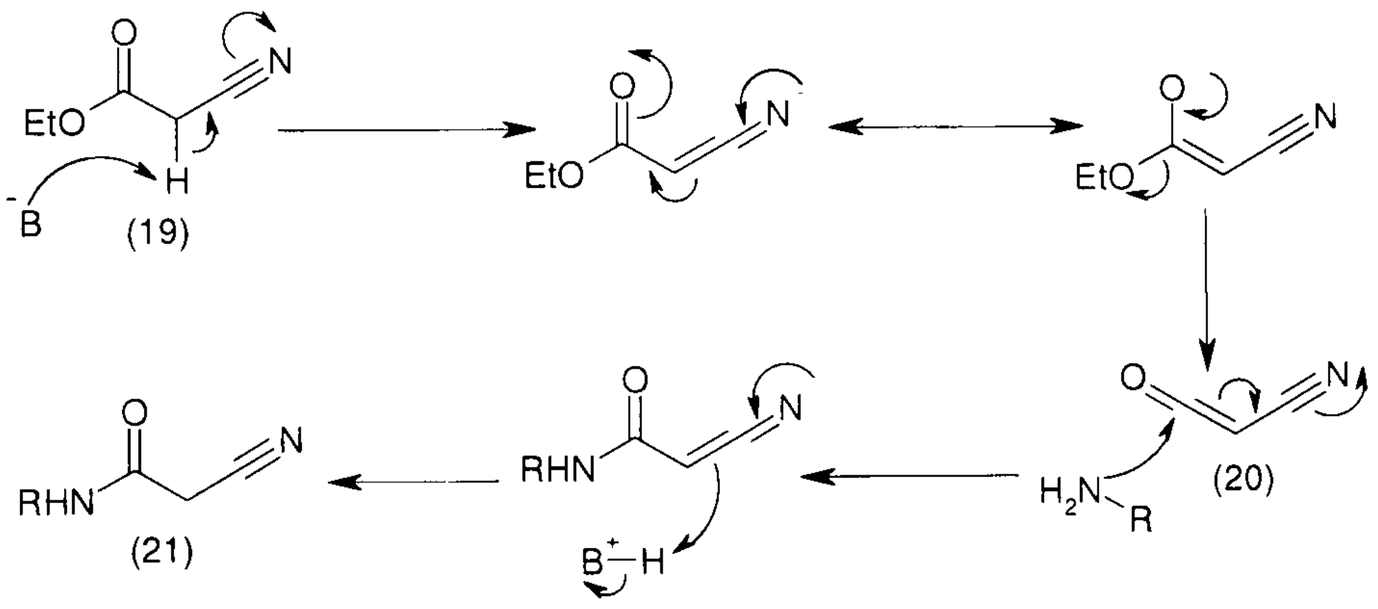

Figure 3.3. The suggested mechanism of direct conversion from Santilli *et al.*[10]

3.1.6 Convergent synthesis of piperazine (2)

Following the continued difficulty obtaining the desired compound (2), an alternative approach utilising a convergent synthesis was considered (Scheme 3.10).

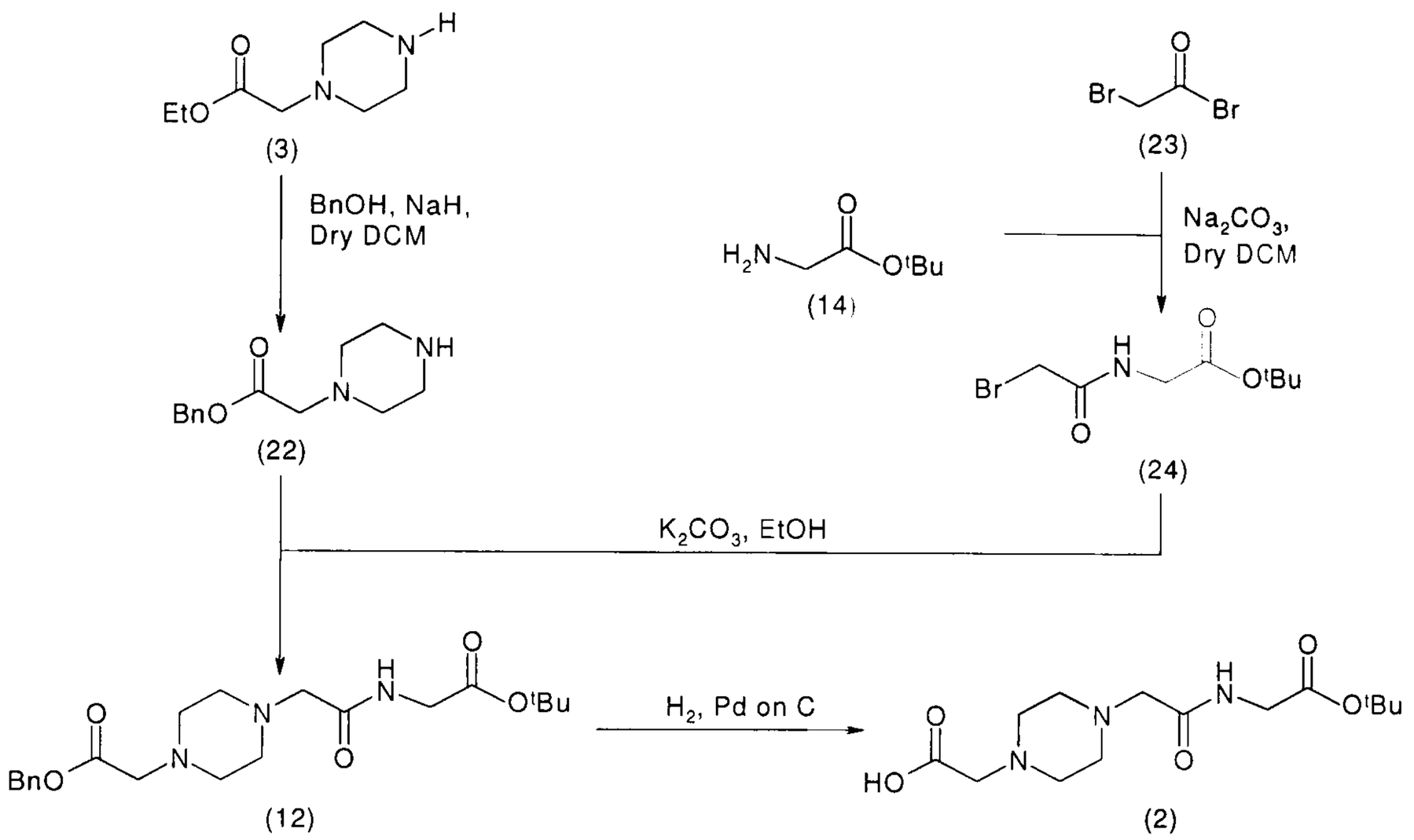

Scheme 3.10.

This synthesis has twin benefits. Firstly, convergent synthetic pathways are usually higher yielding than the corresponding linear routes and secondly, this route reduces the number of steps where it is necessary to handle compounds containing a piperazine ring. The high water solubility of these piperazine compounds means that their isolation is difficult and often necessitates the use of prep HPLC or prep LCMS purification. This tends to reduce the yields; therefore limiting the number of steps where this is necessary offers significant advantages.

It was reasoned that piperazine ethyl ester (3) could be converted into the desired benzyl ester (22) in a transesterification analogous to that used for the conversion of dialkylated piperazine (7) to piperazine (11), (Scheme 3.7). However this was unsuccessful and although some desired compound was obtained, it was insufficient for full characterisation.

An alternative approach to benzyl ester (22) was the direct synthesis from piperazine (25) and benzyl-α-bromoacetate, both of which are commercially available (Scheme 3.11).

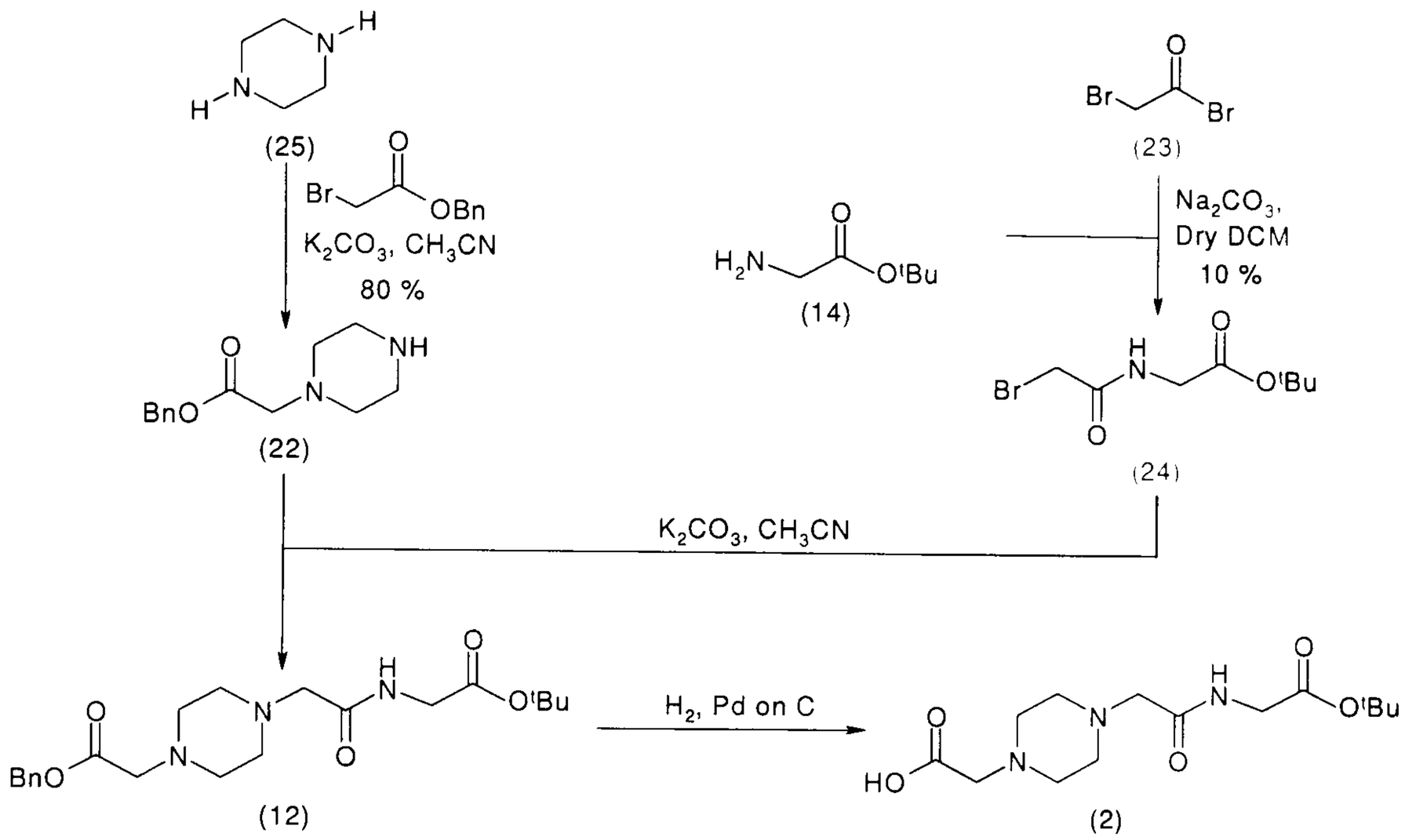

Scheme 3.11.

Three attempts have been made to produce the benzyl piperazine (22) using this direct method. The first used the conditions adapted from Witiak's paper[2] to synthesis piperazine (7), using ethanol as the solvent and potassium carbonate as base. This proved unsuccessful, as the ethanol transesterified the benzyl ester, giving ethyl ester (3) as the major product. However, Parker *et al.*[11] reported that nitrogen-containing macrocycles were alkylated using potassium carbonate in acetonitrile. Parker *et al.* also added sodium iodide to the reaction mixture, as this increases the reaction rate by halogen exchange to give the more reactive iodide as the alkylating agent, instead of the bromide. It was decided to omit the addition of the sodium iodide as only mono-alkylation was desired and a slower reaction rate would increase the chance of isolating this product. The reaction was therefore repeated using acetonitrile as the solvent. This produced the desired benzyl ester (22) with an impurity resulting from alkylation on both amines. Purification was attempted *via* silica column, but this proved inefficient with only a 37 % yield. The material isolated still had minor impurities, but was used as is in later synthesises. The major impurity in this reaction was the di-benzyl ester and it was believed that this was produced as the reaction mixture was too concentrated and possibly the addition of the benzyl-α-bromoacetate was also too rapid. Therefore in the third attempt to produce benzyl ester (22) both the solution of the piperazine (25) and

the solution of benzyl-α-bromoacetate were very dilute and the addition of the bromoacetate was very slow, drop-wise, over one hour. The product was again purified by column chromatography, but again failed to yield entirely pure material. This material had the free acid of (22), produced *via* loss of the benzyl group as a minor impurity. The material recovered represented an 80 % yield, though it was impure. No further attempts were made at purification of this product as the project finished before it was required for further syntheses.

Several attempts have been made towards the synthesis of compound (24), by reaction of α-bromoacetyl bromide (23) and *tert*-butyl glycine (14). Variations of the nature and the quantity of the base used in the reaction have produced a startling array of results. The initial conditions were from papers by Parker *et al.*[11] and White *et al.*[12] using sodium carbonate in DCM, Parker used these conditions to form the ethyl ester and White used them to form the methyl ester. The use of these conditions produced the desired compound, but this could not be purified despite the use of silica gel column chromatography. The column chromatography was ineffective due to the lack of a significant chromophore, which prevented monitoring by TLC.

This first attempt had used *tert*-butyl glycine ester that had been prepared previously and it was considered that some of the impurities present after the reaction might have come from this reactant. The reaction was repeated with commercially available *tert*-butyl glycine ester. This also yielded the desired product, but again in the presence of impurities. LCMS conditions were examined to purify this product, but none of the available methods offered sufficient separation.

In these reactions the carbonate does not dissolve in the organic solvent and it was therefore reasoned that the use of an organic base would create a homogeneous solution and might prevent the formation of these by-products. Triethylamine was selected as the organic base, because it had been used in the synthesise of methyl ester by O'Neil *et al.*[13] using THF as the solvent and by Marzilli *et al.*[14] to synthesise the ethyl ester using DCM as the solvent. It was decided to use DCM as the solvent and a four-fold excess of triethylamine (relative to the glycine), this produced compound (26), where triethylamine had displaced the α-bromine.

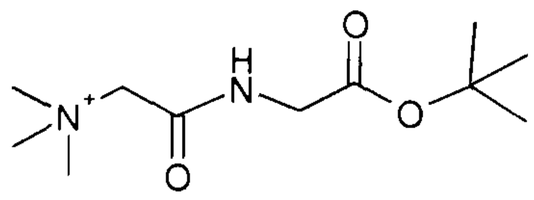

(26)

As the glycine is added as the HCl salt and the reaction should produce one equivalent of HBr, it was thought that the use of two equivalents of triethylamine would be sufficient, thus removing the excess triethylamine and reducing the displacement of the α-bromine. However, these conditions did not appear to produce any desired product as indicated by LCMS analysis. Further analysis using NMR (^{1}H and ^{13}C) showed that the desired compound may be present, but as a very minor component of the reaction mixture.

It was therefore decided that an alternative base was necessary and the next attempt at this reaction utilized diisopropylethylamine (Hunigs base). This is also an organic base and miscible with DCM, but is far less nucleophilic than triethylamine due to the steric hindrance of the two-isopropyl groups. Reaction with two equivalents of Hunigs base resulted in the formation of compounds (27) and (28). Acid (27) is the desired product that has lost the *tert*-butyl group and (28) is the result of *tert*-butyl glycine displacing both the acid bromide and the α-bromine (Figure 3.4).

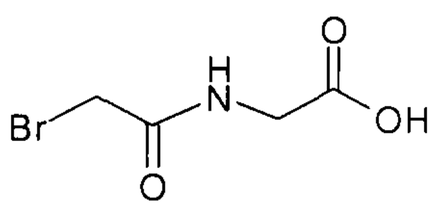

(27)

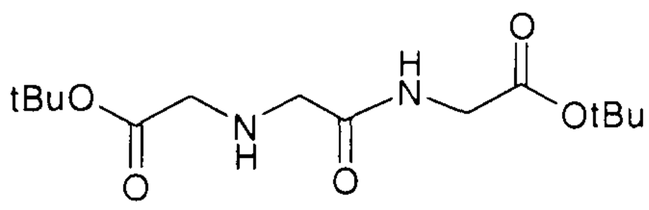

(28)

Figure 3.4. By-products (27) and (28).

Using three equivalents of Hunigs base the desired product was obtained, and a simple aqueous work up in diethyl ether removed all the impurities with the exception of a single compound. Analysis by MS showed that this compound has an m/z of 474, and fragment ions that indicate the sequential loss of three *tert*-butyl groups. This suggests that this compound has resulted from the addition of two molecules of the desired product with a third molecule of *tert*-butyl glycine ester to give (29).

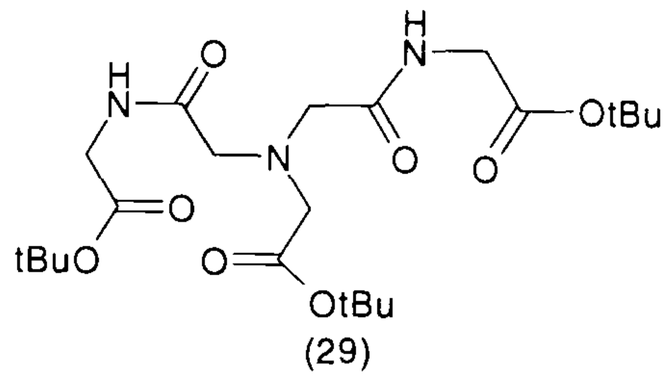

(29)

The sample containing compound (24) was purified using prep LCMS, to remove this final impurity (29). This was successful, but gave (24) in low yield (10 %). Due to the failure to produce the acylated amino acid derivative (24) in sufficient yield and purity, despite extensive alterations to the conditions, it was considered necessary to alter the reactants used. It was believed that changing from bromoacetyl bromide (23) to chloroacetyl chloride (30) would be advantageous, as the α-chlorine would be less reactive than the corresponding bromide and therefore less likely to participate in the detrimental side reactions.

3.1.7 Convergent approach with altered reagents

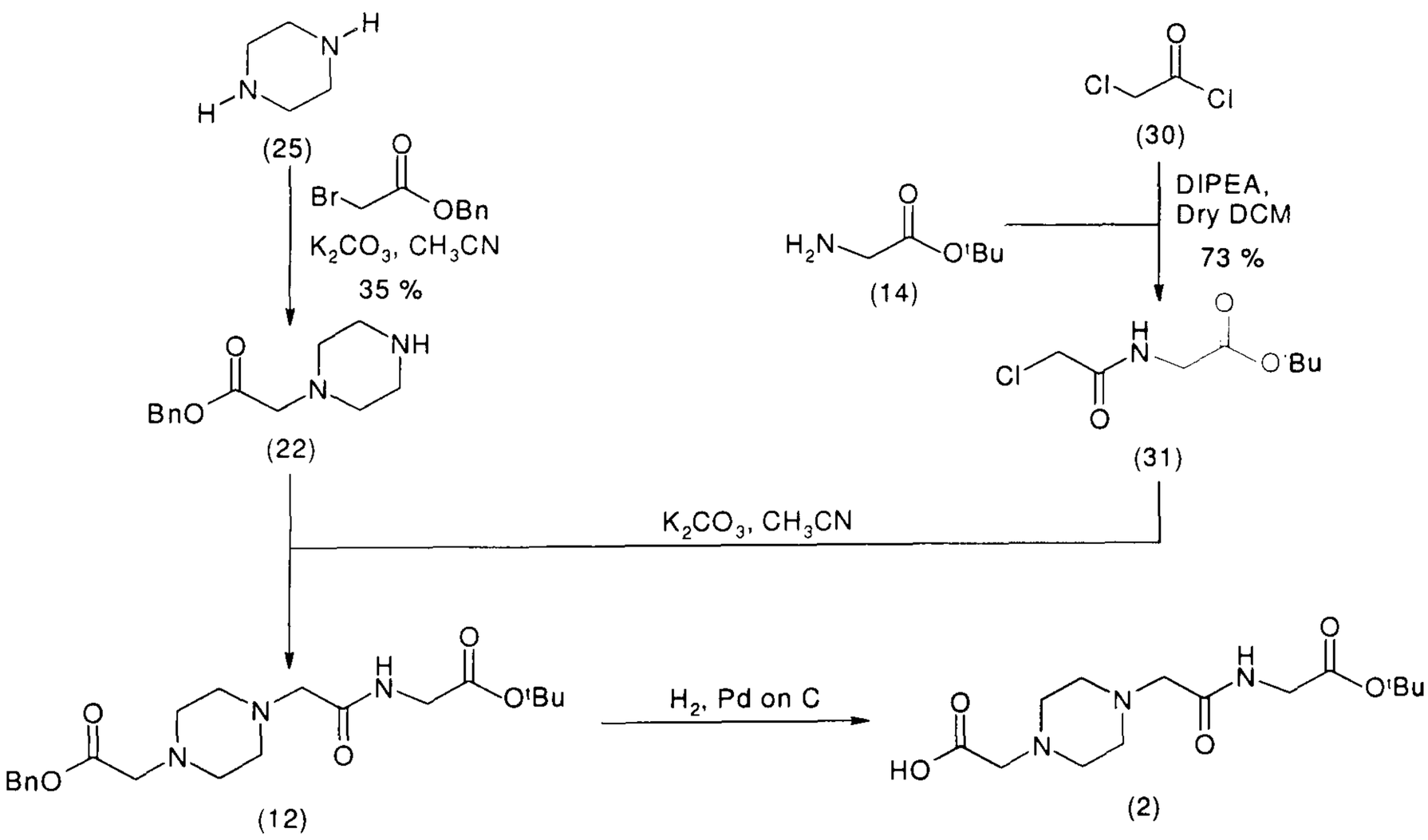

Scheme 3.12.

Switching to the less reactive chloroacetyl chloride (30) in this synthesis allowed the conversion of 1 g of *tert*-butyl glycine (14) to product (31) in a 73 % yield, after purification *via* silica gel column.

The addition of the α-chloro-compound (31) to the benzyl piperazine ester (22) was attempted using the conditions adapted from Witiak.[2] The reaction was followed by LCMS and appeared to yield product, but problems during the silica column chromatography of this compound resulted in failure to isolate the product. It was intended to repeat this synthesis and isolate the product correctly, but as other synthetic routes yielded product this has not been achieved.

3.1.8 Alternatively protected piperazine target – methyl esters

Due to the problematic nature of synthesising and selectively de-protecting piperazine (5) or piperazine (12) to yield piperazine (2), an alternative target was proposed. This target was the piperazine (32); it differs from (2) by utilising a methyl ester, whereas (2) had a *tert*-butyl ester. This removed the inherent instability of the *tert*-butyl ester, allowing a more facile selective deprotection. A large amount of compound (7) had already been prepared for the linear synthesis and was therefore available for this reaction.

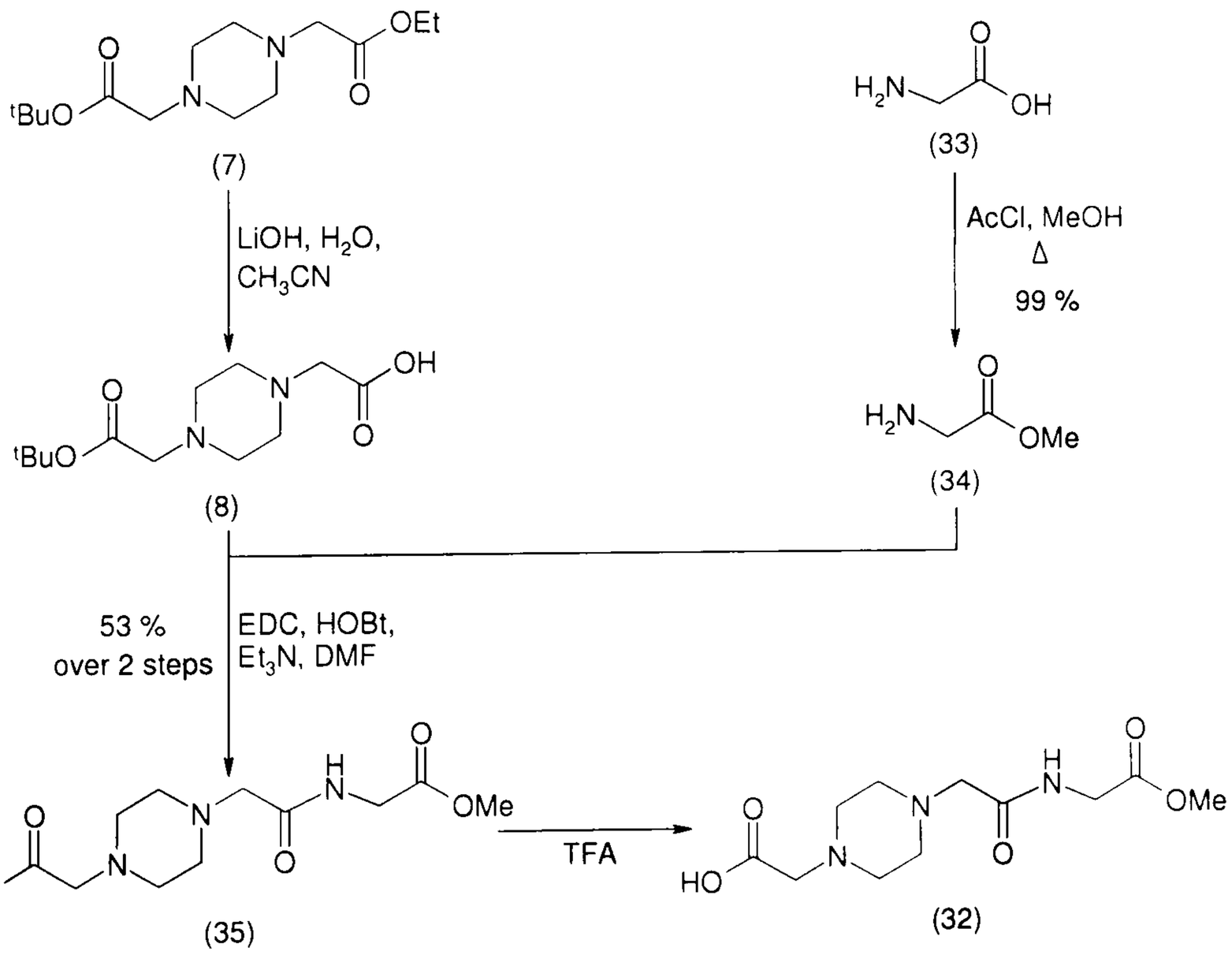

Scheme 3.13.

Scheme 3.13 shows the synthetic path to piperazine (32), however intermediate (8) was not isolated and was formed and used *in situ*. The synthesis was stopped at (35), as (32)

would be very difficult to purify and therefore would only be formed and used *in situ* when required.

Glycine (33) was converted to product (34) using conditions described by Hulme *et al.*[15] Hulme used these conditions to prepare *N,N,*O-tribenzyl serine methyl ester. These conditions gave product (35) as the hydrochloride salt without the need for purification in 99 % yield.

In each synthesis di-ester (7) was hydrolysed to piperazine (8) utilising aqueous lithium hydroxide to cleave the ethyl ester. The first attempt to convert (8) to (35) followed the reaction conditions of Nozaki and Muramatsu[7,8] for the peptide coupling, where they had used EDC in a bi-phasic solution of H_2O and dichloroethane (DCE) for coupling reactions. Although used earlier in Section 3.1.4 where it gave a good yield, in this example it was unsuccessful; yielding only 4.6 mg of product from 200 mg of starting material, a 2 % yield. It was believed that the use of a polar organic solvent that was miscible with water, instead of the DCE, would produce better results in the coupling step; therefore acetonitrile was used in this reaction. Upon attempting the reaction using acetonitrile the product was successfully formed. However, 1M Na_2CO_3 was used in the work-up and this cleaved the methyl ester. A further paper by Nozaki[16] using neat DMF as the solvent for EDC/HOBt coupling showed quantitive yields for the production of simple fully protected dipeptides. It was thus decided to use these conditions in a repeat of the coupling and the pH of the aqueous solvents used in the work-up was kept below pH 8. This produced the piperazine (35) in 53 % yield.

3.1.9 Variation of the amino acid

The nature of the synthetic route to the target piperazine methyl esters makes it easy to vary the amino acid used, it is simply a case of replacing the glycine with an alternative amino acid and repeating the synthesis laid out in Scheme 3.13. Examination of the SPROUT designed structure that results from the coupling of piperazine (32) to vancomycin hexapeptide, bound to the L-lys-D-ala-D-ala tripeptide, suggested that the use of D-amino acids with hydrophobic side chains would yield the best results. This is because the hydrophobic group would be positioned over the methyl group of the second D-alanine creating a strong lipophilic interaction (discussed in Chapter 2, Section 2.4.1). Two amino acids have been selected to produce these initial variations,

D-phenylalanine and D-phenylglycine. Both are commercially available and relatively inexpensive.

D-phenylalanine was not available as the methyl ester and was therefore purchased as the free acid, this necessitated the synthesis of D-phenylalanine methyl ester (37) and this was achieved using the method described by Hulme *et al.*[15]

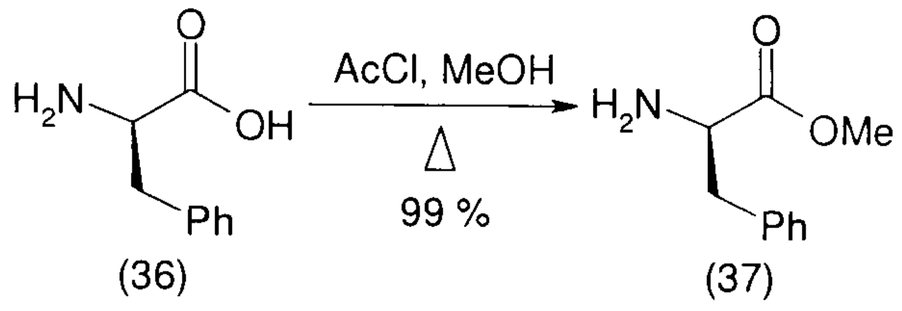

Scheme 3.14.

This reaction involved using three equivalents of acetyl chloride in an excess of methanol and heating at reflux for three hours. A reaction starting from 1.00 g of phenylalanine afforded 1.29 g of desired product (37), a 99 % yield (Scheme 3.14).

Piperazine (38) was formed using the approach established in the synthesis of (32), as shown in Scheme 3.13, which followed the work of Nozaki *et al.*[7,8,16] utilising EDC in a peptide coupling reaction.

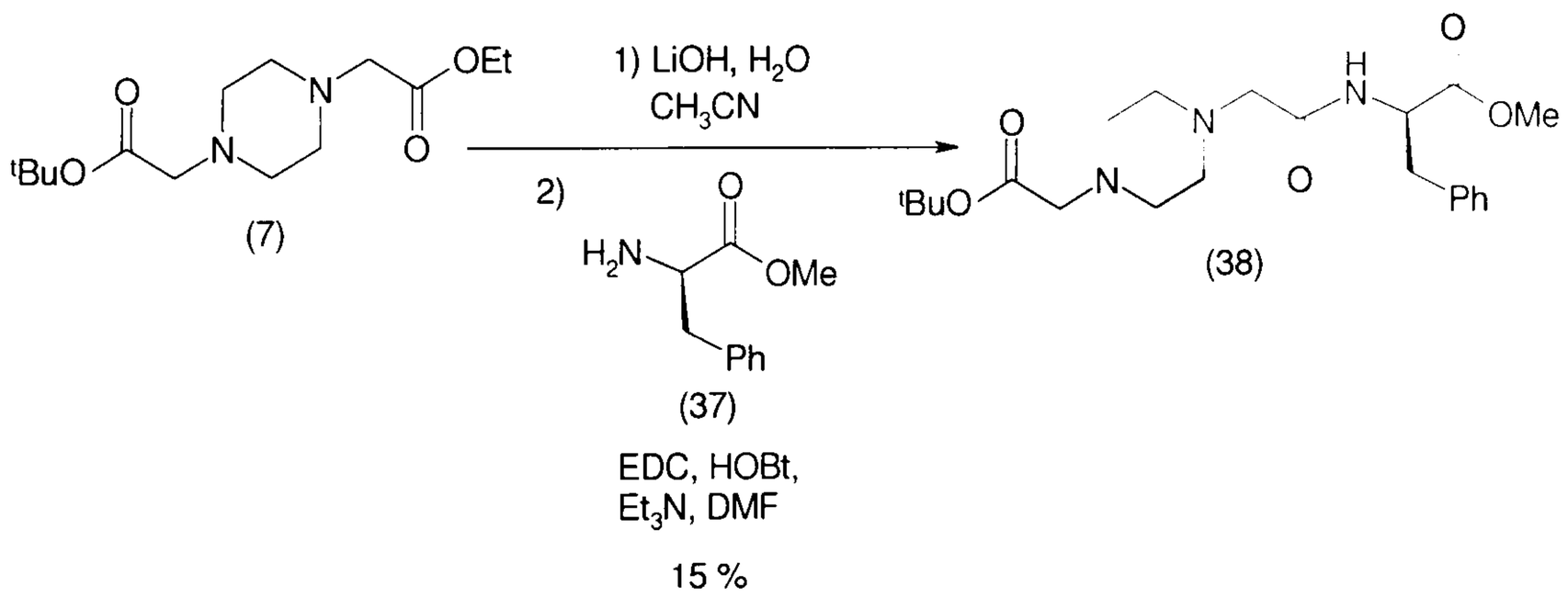

Scheme 3.15.

The product needed both a silica column and an alumina column to yield a sample that was pure as determined by NMR analysis. The reaction was attempted on 1.33 g of intermediate (7) and yielded 0.28 g (15 % yield) of piperazine (38) (Scheme 3.15).

Piperazine (40) was synthesised using the same approach, starting from the commercially available D-phenylglycine methyl ester (39), utilising EDC coupling of Nozaki *et al.*[7,8,16] (Scheme 3.16).

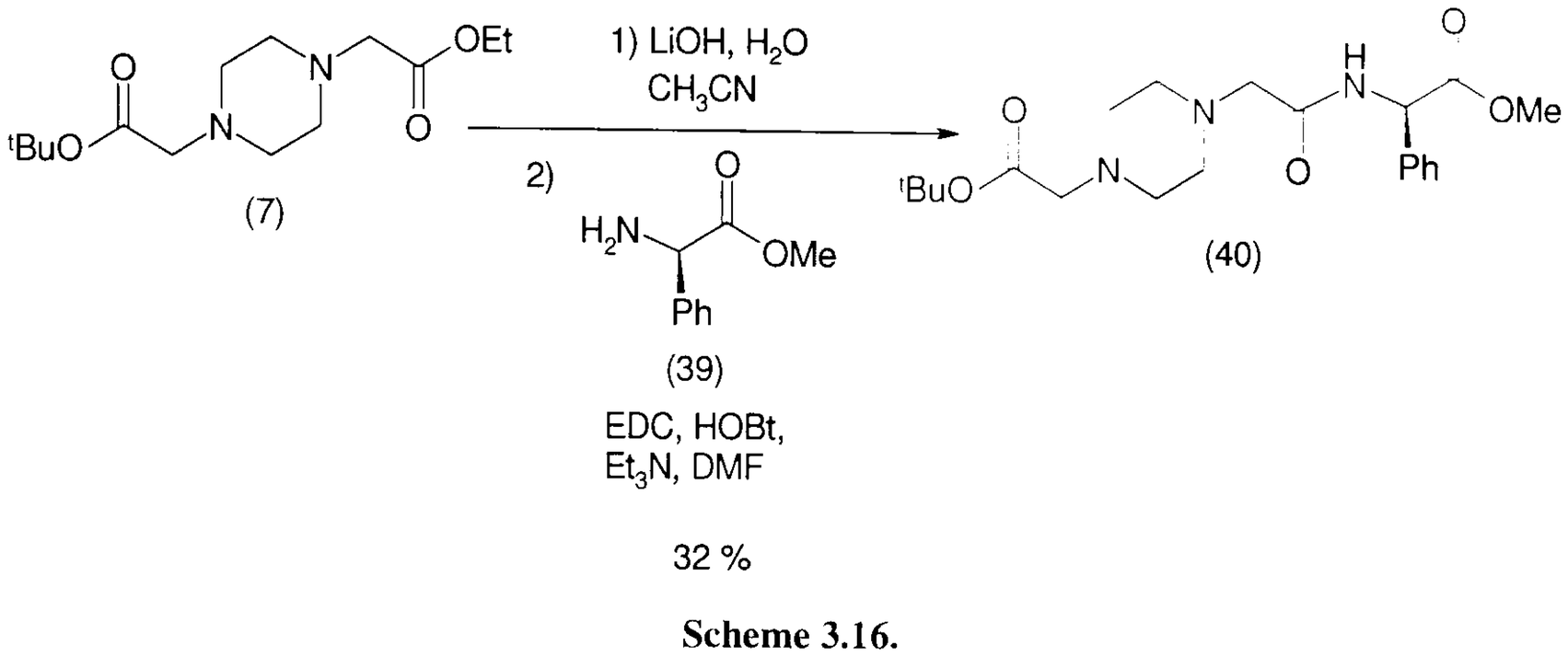

Scheme 3.16.

The product was obtained in good purity, as determined by NMR analysis, following purification by silica column chromatography. The reaction was attempted on 500 mg of intermediate (7) and yielded 224 mg of compound (40), as a glassy solid (32 % yield).

3.1.10 The rigid analogue

The principle of rigidifying a drug is not a new one and works on the simple premise that the more rotatable bonds a drug possesses the greater the entropic cost of binding. This entropic cost is incurred because binding can only happen in one conformation of the many possibilities available to the freely rotating molecule. Rigidifying the molecule removes some of the rotatable bonds; this reduces the number of possible conformations and lowers the entropic penalty of binding. This principle was therefore applied to the extended piperazine fragments and the obvious choice was to rigidify the terminal amino acid portion of structure (see A in Figure 3.5). This linear chain could be rigidified into two fused rings (B in Figure 3.5).

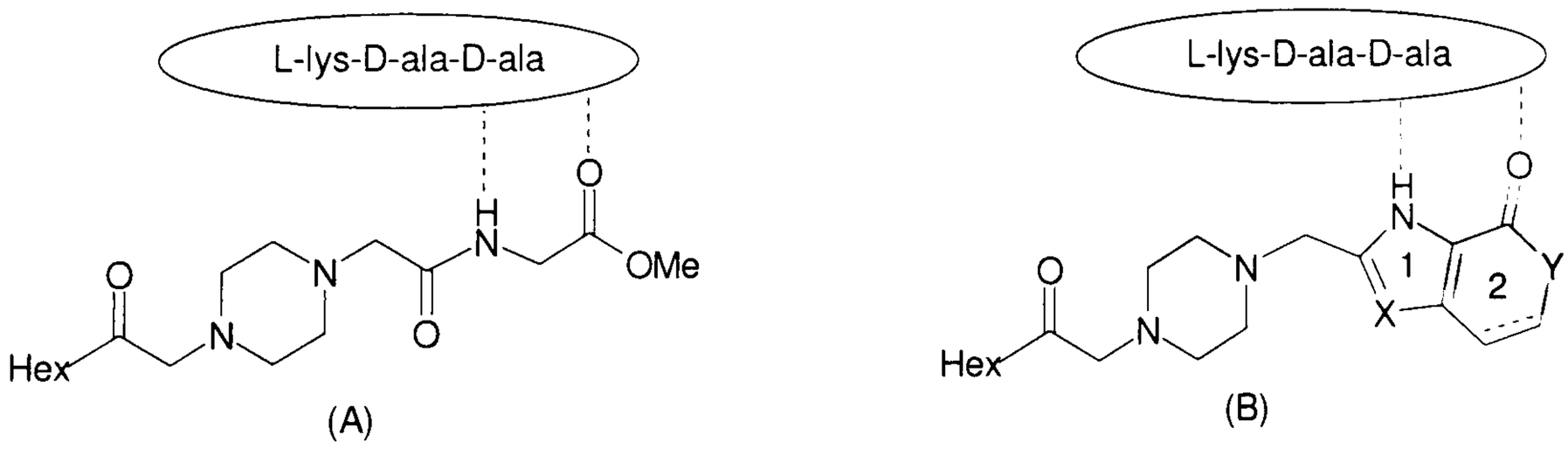

Figure 3.5. A representation of binding in A) the initial methyl ester design and B) the rigidified analogue.

It is necessary to retain the double bond in ring 1 of (B) so that the amine of that ring remains amide like, thus the X atom in ring 1 would ideally be a nitrogen atom, but could be carbon. In ring 2, the Y atom could be O, NH or even S, but Y being NH would make the carbonyl oxygen a better acceptor. Also in ring 2 the remainder of the ring could be saturated or aromatic. However, if ring 2 was aromatic it would ensure the entire structure was planar and this is preferable. In addition, structures that leave hydrophilic groups exposed to solvent would be more advantageous.

After a search of commercially available compounds had been undertaken, the best candidate for the rigid terminus was theophylline (41), a structure closely related to caffeine. It satisfied the needs for both rings and although ring 2 is not aromatic, it is planar and there are hydrophilic groups exposed to solvent.

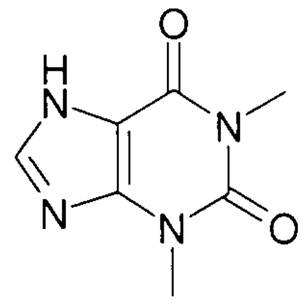

(41)

The synthetic pathway to convert theophylline (41) to a derivative containing a carboxylic acid (42) for coupling to vancomycin hexapeptide is set out below in Scheme 3.17.

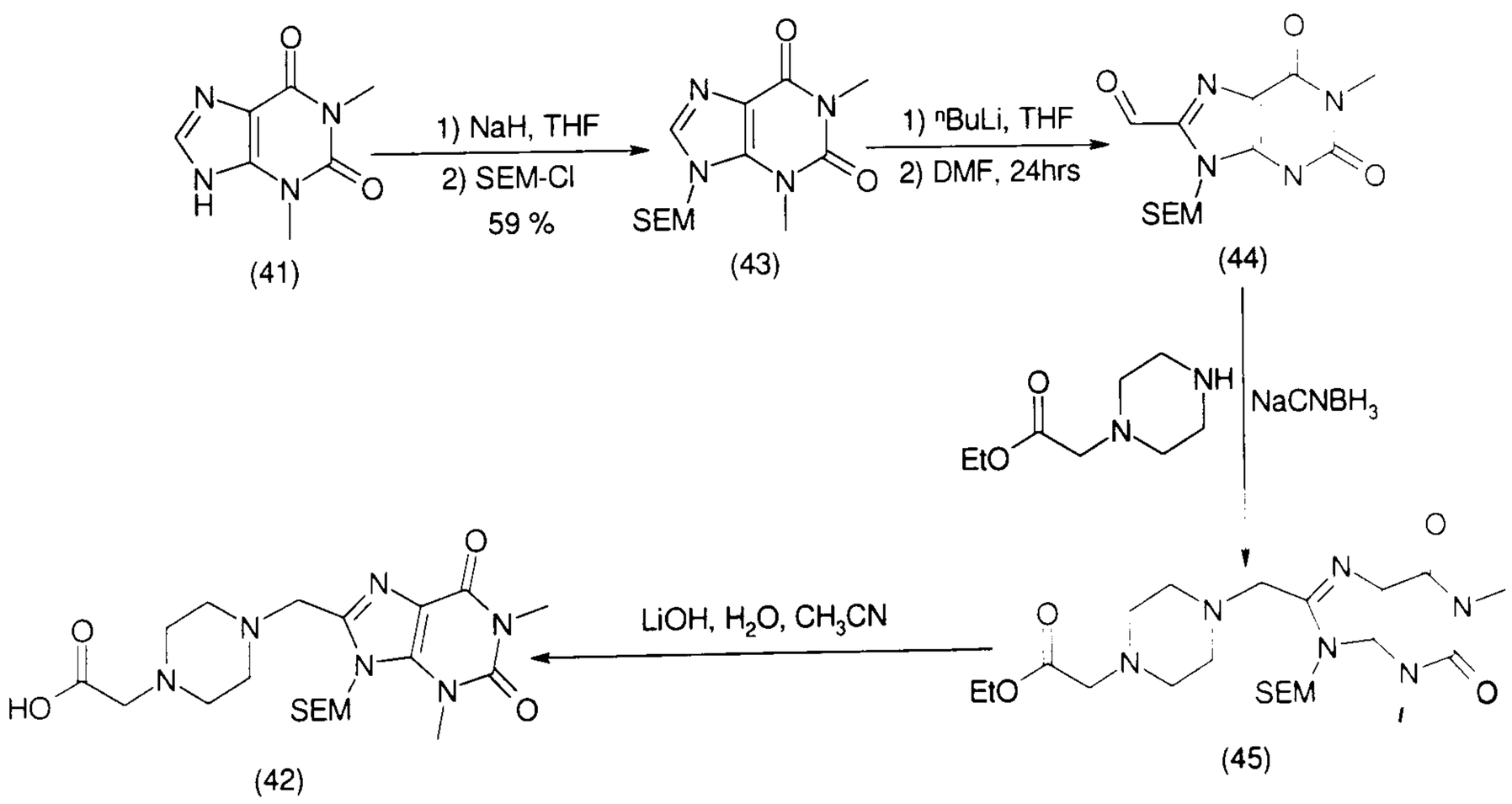

Scheme 3.17.

The first steps in this sequence are the protection of free NH using β-trimethylsilylethoxymethyl chloride (SEM-Cl) to give compound (43), followed by the introduction of a formyl group to give (44) by metalation and quenching with dimethyl formamide. Analoguous reactions have been performed on 4-isobutyl-imidazole as detailed by Lipshutz *et al.*[17] Compound (44) could then be reductively aminated with the commercially available piperazine ethyl ester to yield (45). Cleavage of the ethyl ester should furnish the free acid (42), which would allow coupling to vancomycin hexapeptide and then after the coupling treatment with tetrabutylaminium fluorate would remove the SEM protecting group.

SEM protection of theophylline was undertaken following the work of Lovely *et al.*[18] using sodium hydride to deprotonate theophylline (41) and then quenching with SEM-Cl to yield the protected theophylline (43). Purification by silica chromatography gave (46) as a yellow solid, 102 mg, 59 %.

The attempted formylation of the protected theophylline (43) *via* metalation and addition of DMF using the conditions of Brown[19] failed to yield the product. The most likely explanation of the failure of this reaction is that the reaction conditions were insufficiently anhydrous for the product to form and the metal species, if formed, was quenched back to the starting material.

There was insufficient starting material to repeat this reaction and an alternative route emerged before the re-synthesis of compound (43) could be completed.

3.1.11 An alternate approach to the rigid analogue.

Following failure of the formylation step, discussed above, renewed literature searching yielded a patent abstract, Danila *et al.*,[20] that indicted the direct alkylation of a piperazine with theophylline was possible using formaldehyde to form a iminium ion (Figure 3.6) that would undergo nucleophilic addition of the theophylline. Danila used this method to synthesise 8-[4-(phenyl-1-piperazinyl)methyl]theophylline.

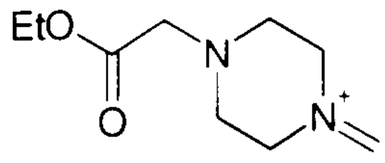

Figure 3.6. The iminium ion.

This method significantly shortened the synthetic route and led to the path set out in Scheme 3.18.

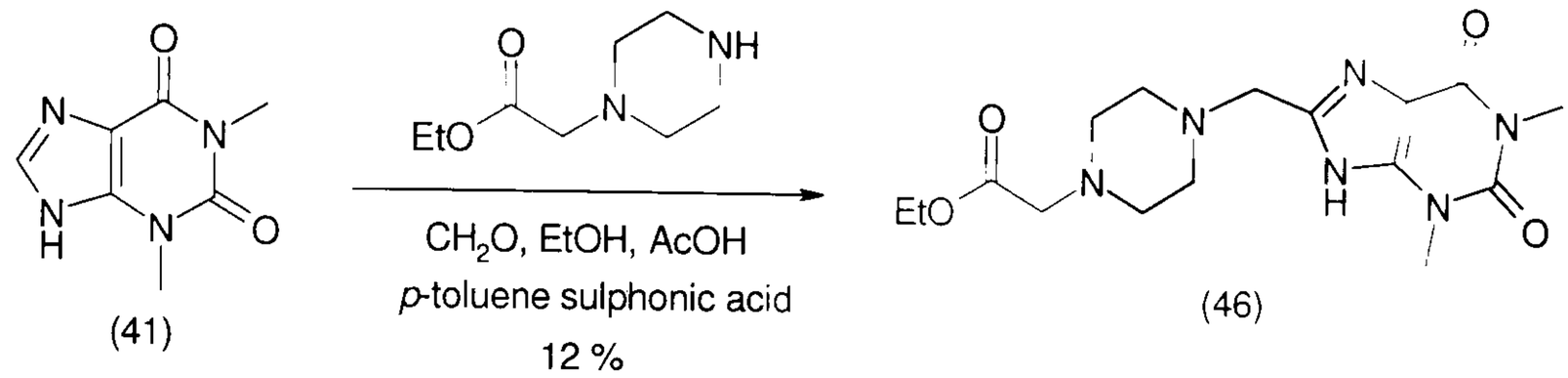

Scheme 3.18.

Three attempts were made at this synthesis using conditions adapted from the patent[19] and work by Joshi *et al.*[21] The first replicated the conditions of the patent abstract, utilising formaldehyde in an aqueous solution (37 % by volume) and had no acid for catalysis; this failed to yield product. The second attempt again used aqueous formaldehyde, but this time utilising acetic acid as a catalyst, this yielded product. However, after column chromatography and aqueous wash only 57 mg of product was recovered (6 %). The reaction was therefore repeated increasing the number of equivalents of formaldehyde and acid. This still did not result in full conversion therefore more acetic acid, *para*-toluene sulphonic acid and solid para-formaldehyde were added to the reaction mixture. This afforded the product as a solid in 12 % yield, after column chromatography and re-crystallisation from ethanol and hexane.

3.1.12 Conclusions and further work on piperazine synthesis

These piperazine based extending fragments have been difficult and time consuming to synthesise, but significant progress has been made reducing and in most cases removing the need for purification by HPLC or LCMS. Routes have been established to the methyl ester of the original target and two analogues of this compound. A novel rigidified extending structure was also successfully synthesised. The opportunity also exists to revisit the convergent synthesis of the free acid series and furnish at least one analogue there.

In both the convergent route to the free acid series and the route to the methyl esters the scope remains for the introduction of further analogues and the synthesis of either type of compound is limited only by the commercial availability of appropriately protected

amino acid esters, *tert*-butyl esters for the free acid series and methyl esters or unprotected amino acids for the methyl ester series.

The piperazines posed a difficult synthetic problem due to the considerable complications purifying and isolating these highly water soluble intermediates. It should also be noted that purification of piperazines with free carboxyl groups proved very difficult and should be avoided where possible. Despite these difficulties, large steps have been taken in developing methods and protection schemes and four variations of the original designed target have been achieved. This has fulfilled the second step in satisfying the aims of the project, as synthesising these extending fragments is the first step in synthesising the vancomycin analogues. Further more this work has developed the synthetic methods necessary and gained insights into the synthesis of these potentially problematic compounds, which now could be exploited if further work was continued in this area.

3.2 The synthesis of the hexapeptide skeletons

The main focus of this project was the synthesis of analogues of vancomycin, produced by acylating the vancomycin hexapeptide with fragments that had been designed *in silico*. As a result it is necessary for sufficient quantities of the hexapeptide to be available and this in turn necessitates the availability of a quick and high yielding method to produce this material. Such a method was not available at the beginning of this work, so it was necessary to develop suitable methodology as part of the project.

3.2.1 Edman degradation on vancomycin

The terminal amino acid residue of vancomycin is *N*-methyl leucine, which has been shown to adopt a conformation in which the terminal amine points away from the binding pocket. There is evidence for this in both the crystal structures reported by Williams[22] and Loll[23] and the PDB file (1FVM) used in the design phase. Williams *et al.*[24] also report this conformation in the solution phase and later confirmed it in a paper co-written with Harris.[25] The argument made for the adoption of this conformation is that this allows the leucine side chain to complete the carboxylate binding pocket, by providing a hydrophobic wall, whilst maintaining the salt bridge (a columbic or electrostatic interaction) between the *N*-Me and the carboxylate. A further consideration

is that if this residue was acylated it would become an amide and because the residue is *N*-methyl leucine, the nitrogen would be methylated and thus unable to form a hydrogen bond. It would also not be protonated under physiological conditions, and therefore could not form a salt bridge or a hydrogen bond, thus preventing it from satisfying the potential interactions with the carboxylate.

Therefore any functionality coupled to this amine would be missing crucial interactions with the peptide ligand and also would probably be oriented into solution and thus would have no effect on the binding to the tripeptide. It was therefore concluded that this terminal residue must be removed in order to produce stronger binding and hopefully more potent compounds.

The removal of the terminal amino acid can be achieved with an Edman degradation. This is a two-step reaction that initially involves alkylation of the terminal amine with an isothiocyanate to give a thiourea, followed by an acid catalysed cyclisation to cleave this alkylated residue from the remaining peptide chain and form a thiohydantoin derived from the terminal amino acid and the isothiocyanate used. This technique was developed by Pehr Edman[26,27] as a method for identifying amino acid sequences in protein and peptide chains.

When this technique is applied to vancomycin (47), using phenyl isothiocyanate (48), the thiourea (49) is produced. Treatment of this thiourea with TFA gives the hexapeptide (50) (33 % yield) and thiohydantoin (51), as described by Williams[28] and shown in Scheme 3.19.

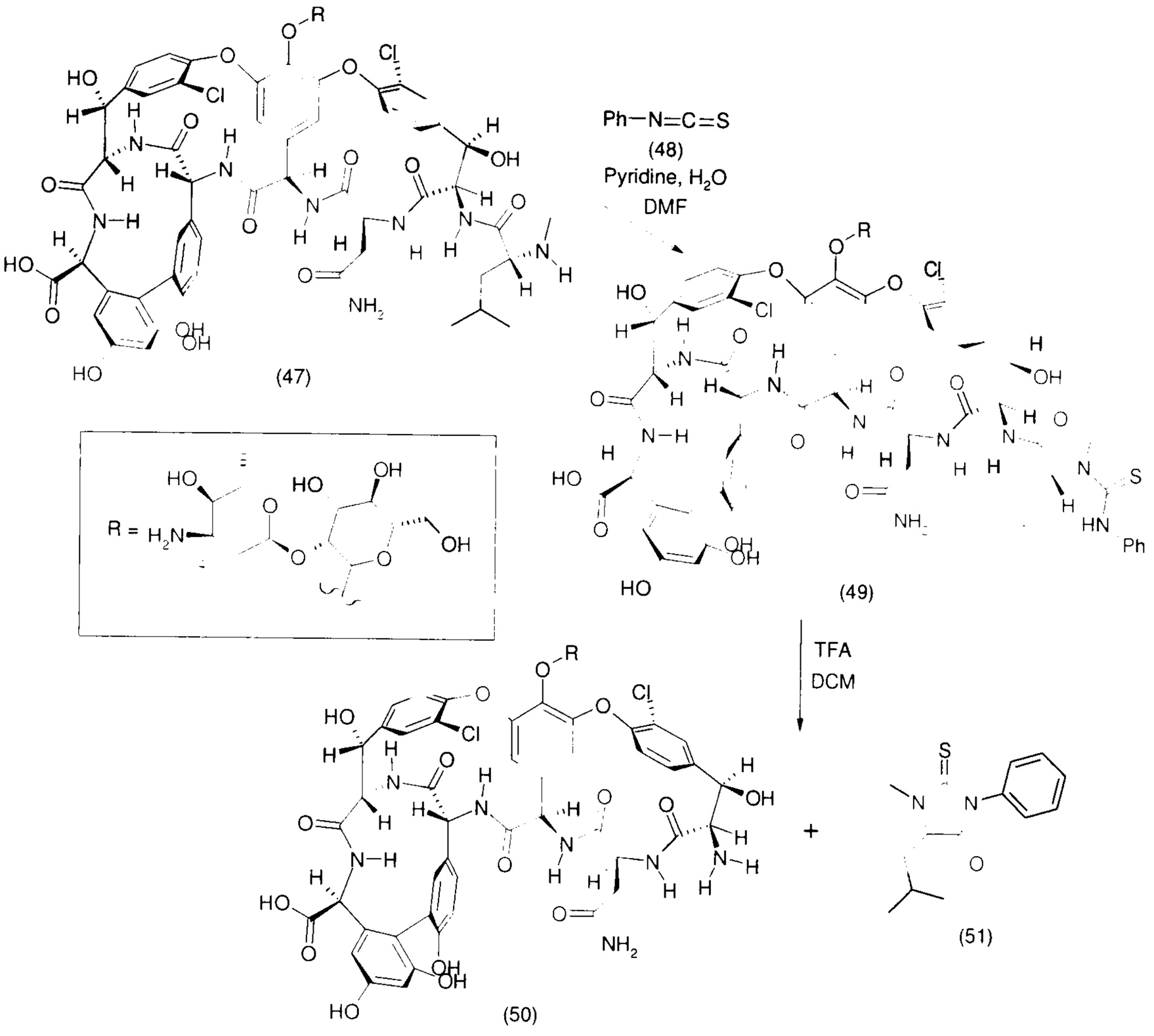

Scheme 3.19.

Initial examinations of the Edman degradation followed the procedure reported by William's.[28] Two attempts were made, each on 200 mg of vancomycin. The first exactly replicated the conditions used in the paper and gave only 13 mg of hexapeptide product, (7 % yield). However, unreacted vancomycin was detected in the HPLC trace during the purification of this product.

Therefore in the second attempt, the procedure was modified and the progress of the initial reaction with the isothiocyanate was followed by mass spectroscopy. Monitoring by MS indicated that the reaction required approximately 45 hrs until there was no trace of vancomycin. Also in the first attempt the recovery of the product after HPLC was accomplished using the Gene-vac, a heated vacuum centrifuge, which left a hard solid that was washed out of the vials, then re-dissolved in water and freeze-dried. In order to minimise the loss of material due to these various manipulations, which followed purification by HPLC, in the second attempt the fractions containing hexapeptide (53) were combined and concentrated on a rotary evaporator to afford a paste. Water was

then added and the solution was freeze-dried in the same flask. As a result of the reduction in the number of handling steps and ensuring that the reaction had gone to completion in the first step, the yield was significantly improved, resulting in 72 mg of product, (39 % yield) which is an improvement on the 33 % yield reported in the literature.

The literature was searched for alternative methods for the Edman degradation and a paper by Törnqvist *et al.*[29] was found that used 1M sodium carbonate to perform the cyclisation and cleavage stage of the degradation. Therefore an experiment was carried out to see if vancomycin could be converted to the hexapeptide (50), using the conditions of Williams to form the thiourea and aqueous base to induce the cyclisation. For this reaction 100 mg of vancomycin was converted to the thiourea and then 1M sodium carbonate was used to effect the cyclisation and cleavage. The yield for this reaction was disappointing however, furnishing only 27 mg, a 30 % yield. Attempts to improve this reaction by using two organic bases, DMAP and DBU, were unsuccessful. However, these reactions were also attempts to perform the transformation in a single step, in which the organic base was added to the reaction mixture after the first step and perhaps may have been more successful if the base had been added separately.

Further experimentation on the conditions of the first step were undertaken; two 100 mg reactions were compared, one with the standard conditions, using DMF, water and pyridine, and one in anhydrous DMF with pyridine. These gave interesting results as the anhydrous DMF reaction stopped at the thiourea, but the reaction using standard conditions resulted in all the thiourea formed being converted to hexapeptide, although this did require stirring for 7 days. Neither of the products was taken on further.

A similar reaction on 200 mg of vancomycin, using DMF, water and pyridine, gave 148 mg (83 % yield) of vancomycin hexapeptide, after HPLC purification, although this did require a total of 5 days for all the thiourea to be converted to hexapeptide.

Three further attempts have been made at producing vancomycin hexapeptide through this base catalysed process. Two of these were at 50 °C using aqueous base with conventional heating and one was at 65 °C using aqueous base again, but this time with microwave heating.

Both the reactions utilising aqueous base and conventional heating were unsuccessful. The first was purified by prep LCMS to yield the product in 28 % yield and the second was purified using prep HPLC and yielded the hexapeptide in 14 % yield.
The reaction attempted in the microwave was even less promising, and purification was abandoned because MS of the HPLC fractions indicated an unknown impurity that was inseparable by HPLC.

Following the failure of the degradations at elevated temperature to match the yield of hexapeptide achieved in the reaction at room temperature; other avenues for an improvement in this reaction were sought, because despite the significant improvement in yield, the room temperature aqueous base reaction was too slow to be synthetically useful. A paper written by researchers from Lilly,[30] utilised a similar degradation. However, the initial formation of the thiourea was done in the absence of DMF and the cyclisation and cleavage were carried out at reduced temperature.

The Lilly procedure also required two-stages. In the first stage vancomycin hydrochloride was treated with phenyl isothiocyanate in the presence of pyridine and water, and the crude thiourea (49) was recovered by evaporation. TFA in DCM was then used to induce the cleavage of the thiourea to yield the desired hexapeptide in 13 % yield, after HPLC purification and freeze-drying.

Although this did not improve the yield, a noteworthy observation from this experiment was that in the absence of DMF the initial reaction with phenyl isothiocyanate stopped at the thiourea without any further degradation to the hexapeptide as is observed in reactions where DMF is present. Perhaps for this reason it appears to produce fewer by-products from this initial stage of the reaction. Following this observation it was decided to produce a quantity of thiourea *via* this route and attempt to degrade it in a variety of different ways to optimise this part of the reaction.

3.2.2 Variation in the cyclisation and cleavage of the thiourea

Using the Lilly procedure,[30] 200 mg of vancomycin hydrochloride was treated with phenyl isothiocyanate; this yielded 203 mg (95 %) of the crude thiourea after isolation under reduced pressure. Following this, 10 mg portions of this were then taken and degraded in a variety of ways, as detailed in the tables below.

Variations of amount of TFA, all reactions are in DCM at room temperature.

Degradation	Eq. of Acid	Time (hrs)	Ratio [a] Hex : Thiourea	Purity [b]
1	2	3	22:78	High – 1450 m/z only impurity over 10 % intensity - unreacted vancomycin from thiourea formation
2	5	3	31:69	
3	10	3	35:65	

a – As judged by relative peak heights in MS of crude sample. b – As judged by MS of crude solid.

Table 3.1. Variations of amount of TFA in the Edman degradation of vancomycin.

Comparison of 5 or 10 equivalents of TFA or formic acid in DCM at 0°C.

Degradation	Acid	Eq. of Acid	Time (hrs)	Ratio [a] Hex : Thiourea	Purity [b]
4	TFA	5	24	48:52	OK – significant unknown impurity at 623.0 m/z.
5	TFA	10	24	78:22	
6	Formic	5	24	34:66	Poor – many impurities
7	Formic	10	24	23:77[c]	OK – unknowns at 435.4 and 519.0 m/z.

a – As judged by relative peak heights in MS of crude sample. b – As judged by MS of reaction mixture. c – DCM evaporated from reaction, therefore reaction did not get full 24 hr period, hence worse ratio then 5eq.

Table 3.2. Comparisons of TFA and formic acid in the Edman degradation of vancomycin.

Above reaction mixtures allowed to warm to 10 °C and stirring continued.

Degradation	Acid	Eq. of Acid	Time (hrs)	Ratio [a] Hex : Thiourea	Purity [b]
4	TFA	5	14	70:30	Good – minor impurities at 988.2 and 494.3 m/z.
5	TFA	10	14	92:8	
6	Formic	5	14	17:83	High – minor impurity at 394.4 m/z.
7	Formic	10	14	16:84	

a – As judged by relative peak heights in MS of crude sample. b – As judged by MS of crude solid.

Table 3.3. Comparisons of TFA and formic acid in the Edman degradation of vancomycin.

These results show that the initial conditions for the degradation using excess acid were unnecessary and that the excess acid results in elevated levels of impurity. The use of formic acid and low temperatures does not improve the synthesis; in fact, they are detrimental as they necessitate longer reaction times.

3.2.3 Edman degradation without HPLC purification

In an attempt to compare the effectiveness of TFA versus formic acid in the cleavage step, a further experiment was performed using 20 equivalents of each acid in separate 200 mg reactions. This reaction confirmed that TFA gives superior results in the cleavage step, but also introduced an interesting observation: whilst attempting to examine the TFA reaction by MS the sample prepared separated into two layers. The top layer was acetonitrile and the bottom layer water. These were decanted and the separate solutions analysed by MS; this indicated that the major product in the top layer was the thiohydantoin by-product and the bottom layer contained a reasonably clean sample of the hexapeptide. The reaction mixture was diluted with water and purified by washing it with acetonitrile to give a solid, which was predominantly the hexapeptide. However, MS of the crude solid showed that some thiohydantoin was still present, so this solid was suspended in acetonitrile with vigorous shaking, then collected by centrifugation. This yielded 182 mg of product, which suggests a yield of over 100 %! However, both HPLC and MS showed that the solid was largely hexapeptide (91 %, based on HPLC peak areas) and it was felt that this would be sufficiently pure for use in the coupling reactions without the need to resort to HPLC purification.

Further examination of the literature led to a paper by Nicolau,[31] which contained a purification of vancomycin analogues using methanol to dissolve the crude solid and Et_2O to precipitate it from solution and also indicates the use of acetone to precipitate vancomycin analogues from reaction mixtures. By combining this with the knowledge gained from the earlier attempts, a very successful preparation of the hexapeptide was possible. This entailed forming the thiourea by addition of phenyl isothiocyanate (51) in water and pyridine, without DMF. The reaction mixture was then evaporated to dryness and the cleavage performed using 20 equivalents of TFA in dry DCM. The DCM was evaporated to give the crude product, which was purified by repeated precipitation from methanol with acetone. This reaction has been carried out three times with 91, 87 and 95 % yields. This showed that it is both high yielding and easily repeatable. In addition, due to omission of the HPLC step, and a number of other time consuming steps, the whole sequence requires about a days work, as opposed to the earlier procedure that took around a week. HPLC analysis (see trace in Appendix A) indicates that the product is 90 % hexapeptide after purification in this fashion, which was deemed sufficient for use in the coupling reactions.

3.2.4 Aglucovancomycin

The preparation of aglucovancomycin (52) and aglucohexapeptide (53) were examined while optimisation of the Edman degradation of vancomycin was underway. The removal of the sugars from the peptide core was considered to be a useful option as they could potentially cause problems in the synthesis of new vancomycin analogues.

These potential problems stem from the presence of a free amine in the vancosamine sugar moiety; this amine introduced a synthetic challenge, because it necessitates distinguishing between two amine centres, the *N*-terminus and the sugar amine.

The first instance where this could have caused a problem was the Edman degradation, because the sugar amine (A in Figure 3.7) may have reacted with the phenyl isothiocyanate, instead of the *N*-methyl leucine terminus (B in Figure 3.7). Indeed, this side-product was observed in some of the attempted Edman degradations on vancomycin, but only in trace amounts. Considering the environments of these two amines this is not surprising, the *N*-terminal amine (B in Figure 3.7) is both electronically favoured, because it is a secondary amine, and it is sterically favoured because it is adjacent to a secondary carbon centre, whereas the primary amine of the sugar (A in Figure 3.7) is adjacent to a tertiary carbon centre.

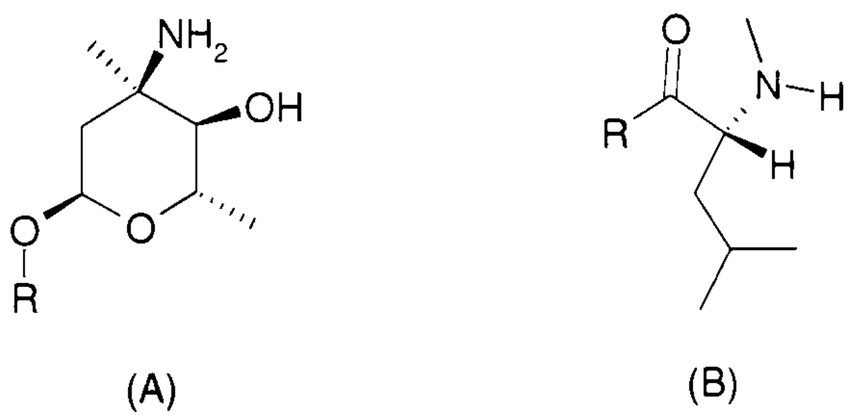

(A) (B)

Where R = The remainder of the vancomycin skeleton

Figure 3.7. Comparison of amine environments during phenyl isothiocyanate addition.

The second potential problem in the synthesis was the selective acylation of the *N*-terminus of the hexapeptide with piperazine extending groups. Here the outcome was a lot less clear because both amine centres are primary amines and both are in very sterically hindered environments. The sugar amine (A in Figure 3.8) is adjacent to a tertiary carbon centre and one bond away from a secondary carbon centre. The hexapeptide *N*-terminus (B in Figure 3.8) is adjacent to a secondary carbon centre, but is further hindered by being only one bond away from another secondary carbon centre.

In addition, the *N*-terminal amine (B in Figure 3.8) is within a macrocyclic ring, which places it in close proximity to an aromatic ring further hindering this centre. The experiments described in Section 3 of this Chapter, in which coupling of the extending fragments and vancomycin hexapeptide was attempted, showed that this was a real problem as in most of the reactions a side-product from double acylation (one at each amine) was observed.

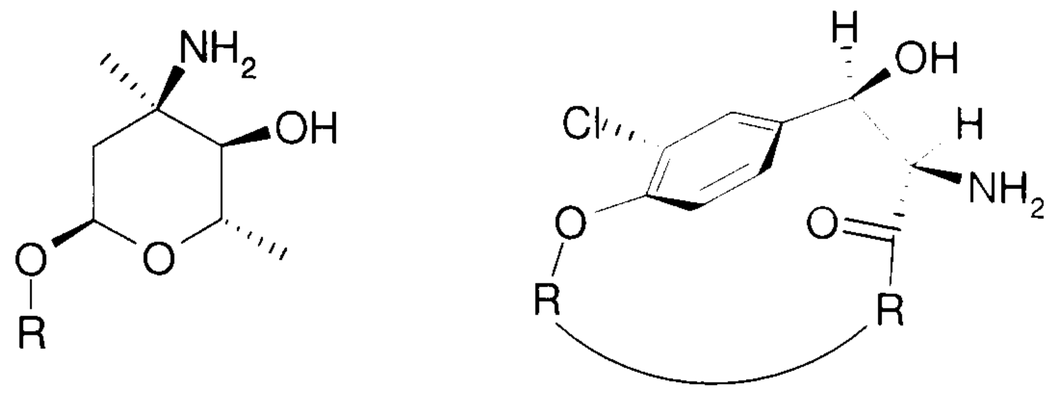

(A) (B)

Where R = The remainder of the vancomycin skeleton

Figure 3.8. Comparison of amine environments during coupling to the piperazine extender.

There were two further factors to consider; firstly, the removal of the sugar groups will greatly simplify NMR-based spectral analysis, and secondly, the removal of the sugars would remove a large number of hydrophilic groups that promote water solubility. Water solubility is a potent advantage for a drug and it is reflected by the lower affinity of the aglucovancomycin,[25] as compared to vancomycin, for all bacterial species. There is also evidence to suggest that the sugars are involved in the dimerization process and thus affect the binding to the cell wall, which further explains the loss of affinity in aglucovancomycin.[32]

Following consideration of these points it was decided to explore both conversion to aglucovancomycin and the further degradation to its hexapeptide. The first stage of this exploration was the synthesis of aglucovancomycin (Scheme 3.20).

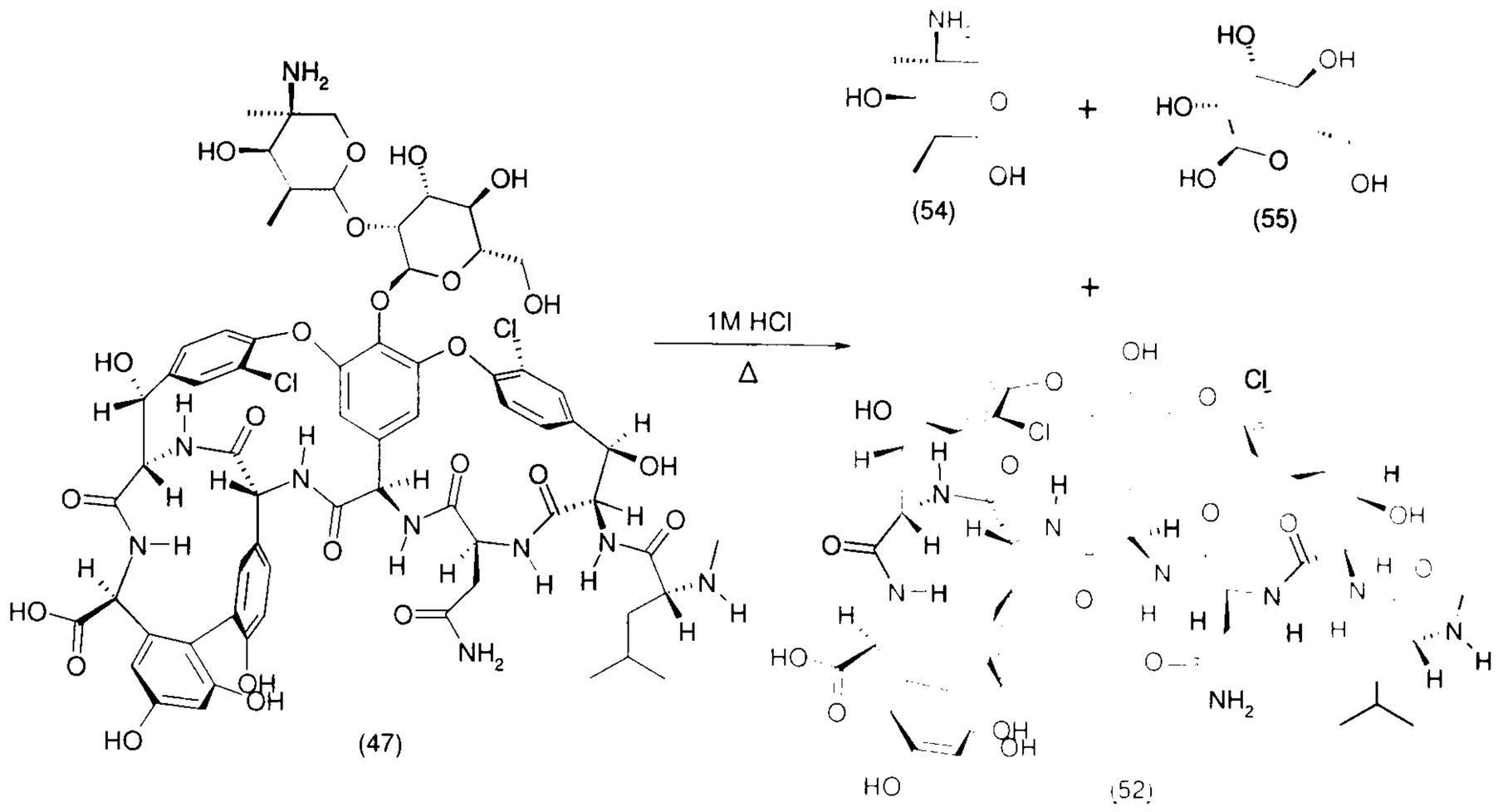

Scheme 3.20.

Aglucovancomycin (52) was prepared according to the literature method.[33] The reaction to remove the sugars is relatively simple and involves heating for two minutes in aqueous 1M HCl, followed by purification using reverse phase HPLC. The initial attempt used 300 mg of vancomycin (47) and yielded 30 mg of product (52), (13 % yield). A second attempt using 500 mg yielded 192.9 mg, (50 % yield). Improvements in the yield for the second attempt were gained using the experience from the Edman degradations, i.e. recovery of the product after HPLC by rotary evaporation and then freeze-drying. This reduces the handling steps, improving the yield.

The Edman degradation was attempted on aglucovancomycin (52) using the base catalysed cleavage of the thiourea (Scheme 3.21).

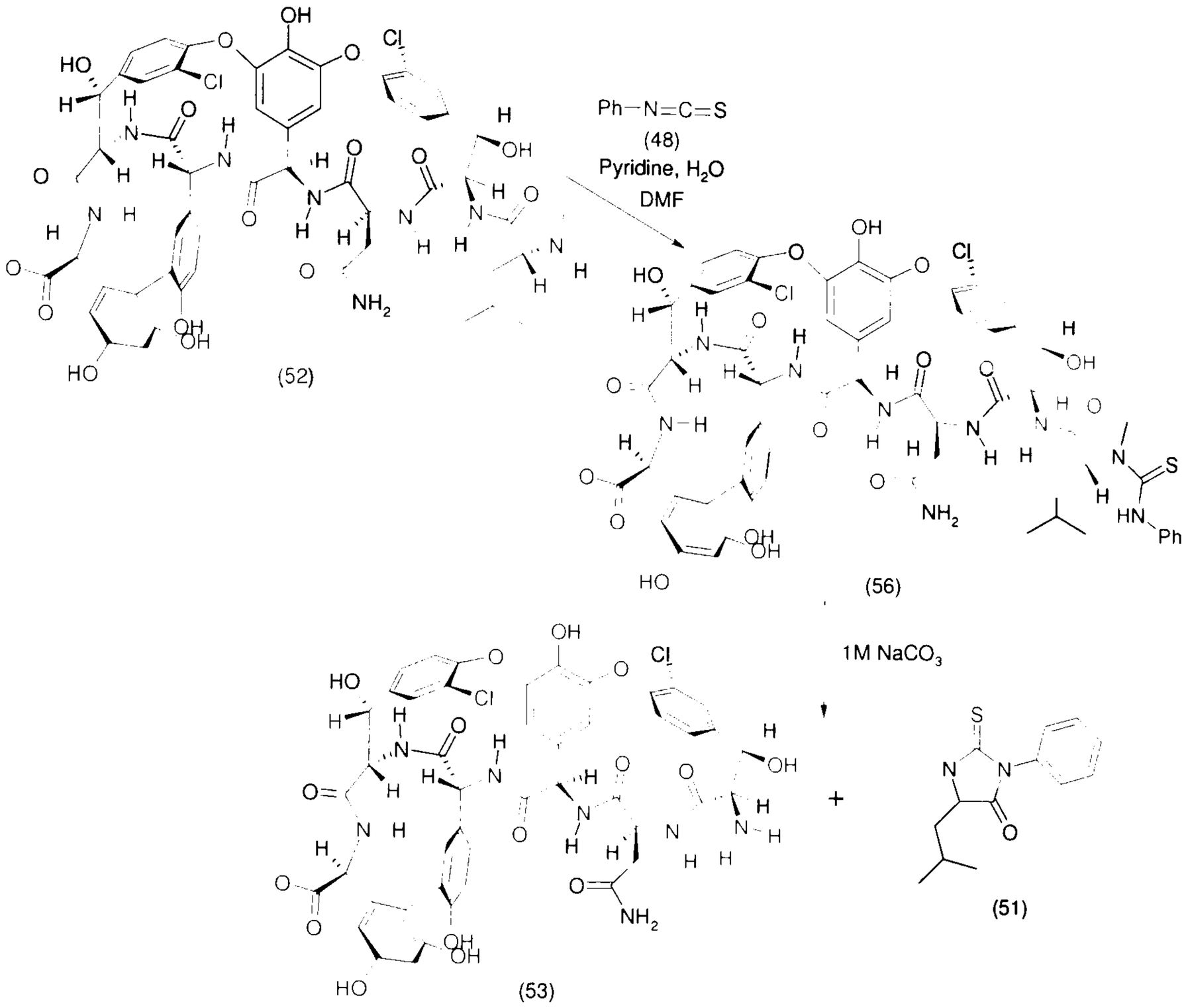

Scheme 3.21.

The initial reaction with phenyl isothiocyanate (48) produced the aglucothiourea (56) and the second stage produced the desired product (53), as observed in the crude MS. However the reaction was not left long enough and therefore the product was impure, containing aglucothiourea (56). The product was not purified, as conditions that would avoid HPLC were being sought.

3.2.5 Direct conversion to aglucohexapeptide

Research by Nagarajan,[34] at Lilly, showed that it was possible to cleave the sugars from vancomycin selectively using TFA. Below –10 °C the predominant product was loss of vancosamine (54), but above that temperature both sugars were lost. The observations in this work led to the idea that a combined reaction could be achieved. The combined synthesis would perform both the Edman degradation and the sugar cleavage in one pot, reducing the number of reactions needed to produce the product. Purification by

precipitation was also used, thus removing the need for HPLC purification in the synthesis of the aglucohexapeptide. This synthesis is set out in Scheme 3.22.

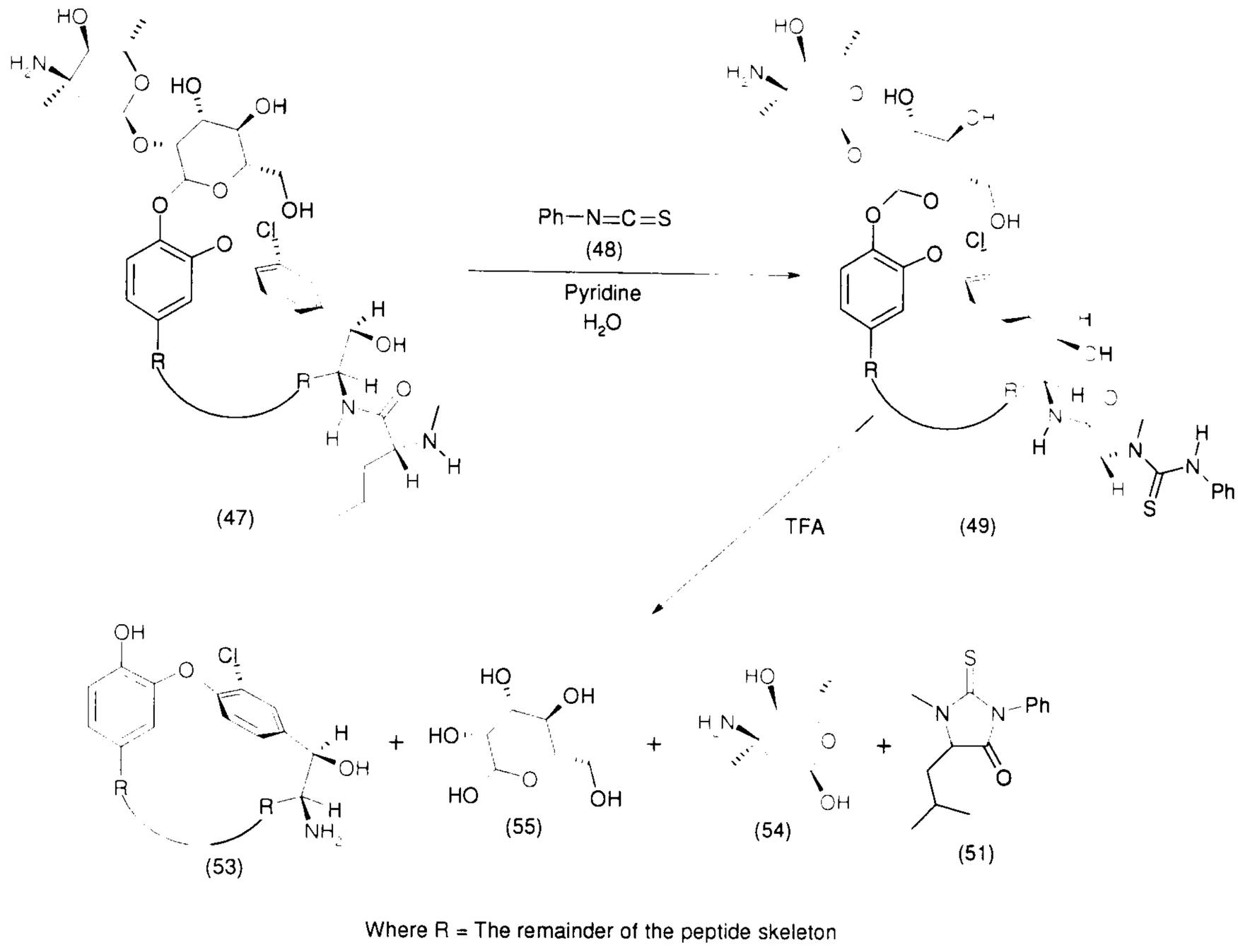

Scheme 3.22.

This reaction replicated the conditions used for the Edman degradation of vancomycin with the exception that neat TFA was used in the second step and the cyclisation/cleavage was stirred overnight. The neat TFA caused both the cyclisation/cleavage and hydrolysis of the sugars, producing the aglucohexapeptide (53), the thiohydantoin (51) and both sugars, glucose (55) and vancosamine (54). The reaction was carried out on a 250 mg scale and purification by repeated washing with acetonitrile produced 104 mg of product (53) (61 % yield).

3.2.6 Conclusions from the attempts to improve the Edman degradation

Significant progress has been made in the application of the Edman degradation to vancomycin since its initial use in this project. The development of the degradation catalysed by aqueous base increased the yield, but at the cost of increased reaction time. Thorough examination of the conditions in both steps of the reaction have led to a

method that is both fast and high yielding, but also does not need HPLC purification to furnish product in sufficient purity for use in the coupling reactions.

The techniques developed in the Edman degradation of vancomycin were then applied to the formation of the aglucohexapeptide. This allowed the development of a combined degradation and sugar cleavage, which produced the aglucohexapeptide from vancomycin without the need for HPLC.

These advances have allowed a sufficient quantity of hexapeptide skeletons to be made available to explore the key stage of this project, the coupling of the extending fragments synthesised in Section 3.1, to the hexapeptide skeletons synthesised in this section.

3.3 Coupling of vancomycin hexapeptide and the piperazine-based extender fragments

This section details the key step in the synthesis of the extended vancomycin analogues: the coupling reaction between the hexapeptide skeleton and the piperazine extenders. This was attempted with the hexapeptide that still carried the sugars, because if selectivity could be achieved in this acylation step, this would yield vancomycin analogues as opposed to analogues of aglucovancomycin. This was preferred as the sugars are involved in the binding event and have implications on the biological activity of the compound, as discussed in detail in Section 3.2.4.

3.3.1 Synthesis of the glycine containing analogue (58)

The first attempt at the synthesis of the vancomycin analogue (58) used 1-ethyl-3-(3-dimethylaminopropyl)-carbodiimide hydrochloride (EDC) and hydroxybenzatriazole (HOBt) as the coupling agents as detailed in Scheme 3.23. The choice of EDC and HOBt followed their successful use in the piperazine synthesis (Section 3.1) and the tripeptide synthesis (Section 3.4), where they replaced the use of dicyclohexyl carbodiimide (DCC) and HOBt, resulting in improved yields and eliminating the production of a troublesome by-product dicyclohexylurea (DCU); which proved difficult to remove from the products of the reactions.

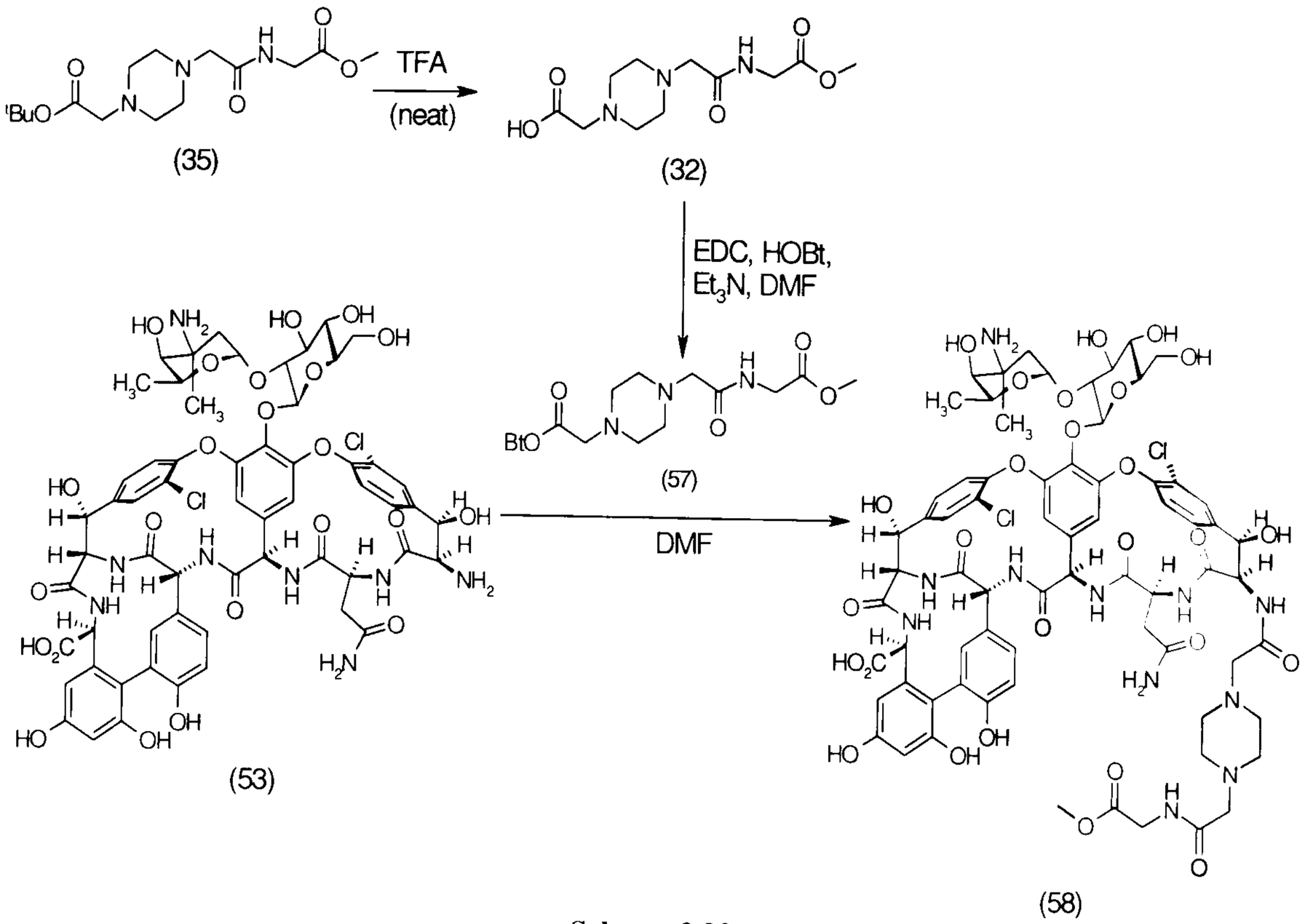

Scheme 3.23.

In the first step the *tert*-butyl ester (35) was cleaved in neat TFA yielding (32), as indicated by LCMS analysis of the reaction mixture. Product (32) was then isolated *via* evaporation and any excess TFA removed under high vacuum. The crude product of this reaction was then treated with EDC and HOBt to pre-form an activated benzatriazole ester (57). The pre-formed activated ester was then added to the hexapeptide (50). Treatment with 1.2 equivalents of the activated ester did not consume all the hexapeptide, so a further 0.6 equivalents were added. LCMS showed that addition of further quantities of the benzatriazole ester (57) did not drive the reaction to completion.

When samples of the reaction mixture were diluted with CH_3CN to prepare samples for LCMS a precipitate was observed; this re-dissolved with addition of water, thus allowing the LCMS to be recorded. Following this observation, a small quantity of the reaction mixture was diluted with CH_3CN and the resultant precipitate was collected *via* filtration under reduced pressure, to see if this offered a method of purification. LCMS analysis of the CH_3CN solution indicated that the reagents (EDC, HOBt and the piperazine extender) were present alongside only a trace of product. MS analysis of the solid showed the presence of the desired product, un-reacted hexapeptide and only traces of the other reagents.

This isolation procedure was therefore used on the remaining reaction mixture and the solid collected *via* filtration. This was followed by purification *via* LCMS, but this produced only 2 mg of the vancomycin analogue (58), a 3 % yield. MS analysis of the product showed that significantly the sugars of the acylated product were lost by fragmentation under the MS conditions. The fragmentation pattern (Figure 3.9) shows that alkylation must have occurred on the *N*-terminal amine of the hexapeptide as the peaks at 1432.9 m/z and 1270.9 m/z corresponded to (58) minus the vancosamine sugar and (58) minus both sugars (see Figure 3.9).

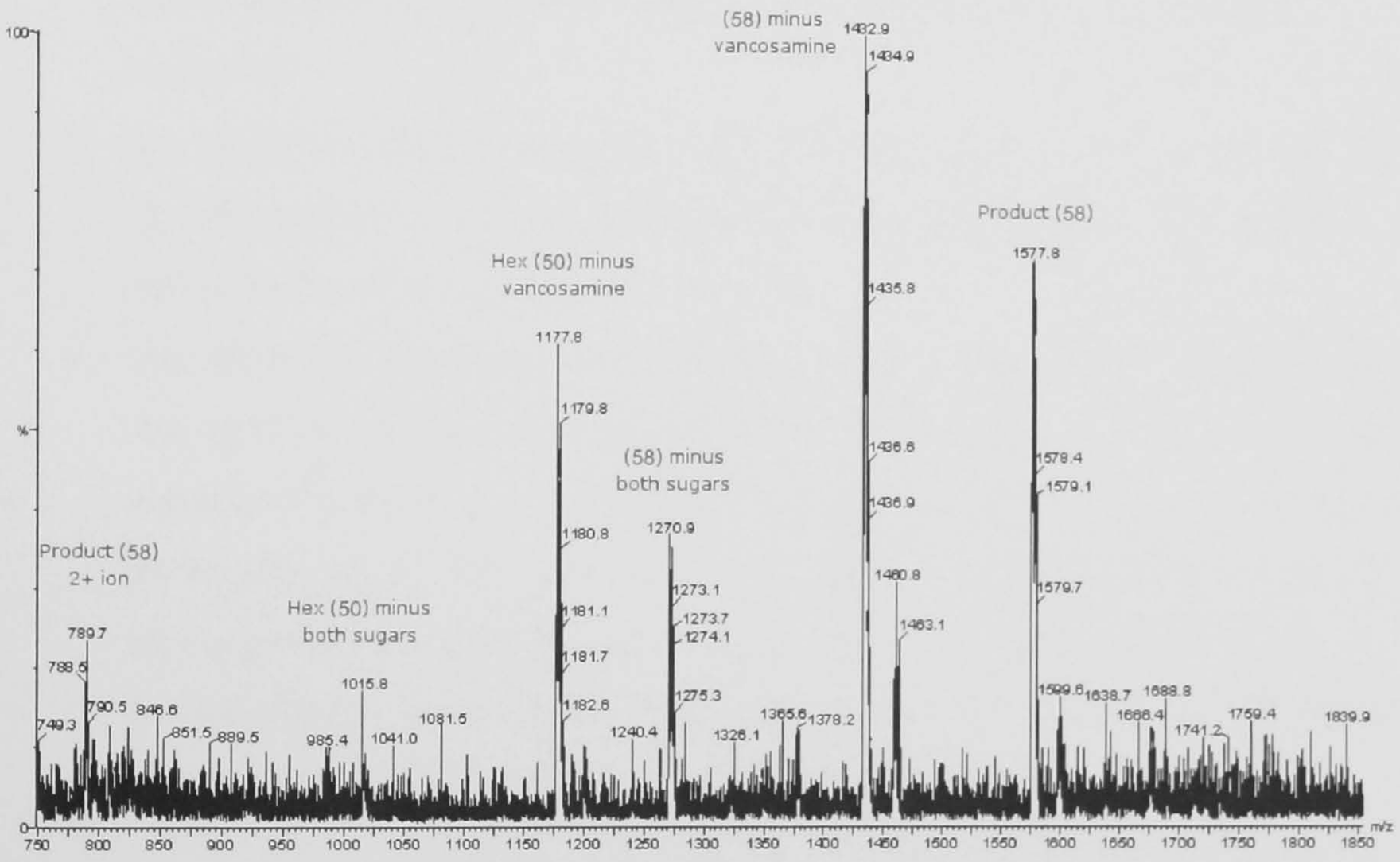

Figure 3.9. MS spectra of product (58).

This did not conclusively prove that acylation occurred at only the *N*-terminus though, as peaks at 1177.8 m/z and 1015.8 m/z could have been derived from hexapeptide that had been acylated on the amine of the vancosamine sugar and then fragmented. These fragments could also have resulted from fragmentation of the hexapeptide by MS; thus it is difficult to know if this is from fragmentation of hexapeptide acylated at the sugar amine, or from traces of unreacted hexapeptide in the product. There was little evidence of a peak at 1321 m/z, resulting from un-fragmented hexapeptide, so it seemed likely that these fragments were derived by acylation at the sugar amine. A comparison of the ratio of peak heights for the two types of fragment shows that the predominant product resulted from acylation on the *N*-terminal amine of the hexapeptide. Despite the poor yield, this was a significant result at this stage of the project and indicated that there was

a preference towards acylation at the *N*-terminus as was desired for the production of (58); and the hexapeptide with the sugars intact could be used in these coupling reactions instead of the aglucohexapeptide.

There still remained the problem of the very low yield to overcome. Some possible explanations for the poor yield were:

- Not all of the acid (32) was converted to the HOBt ester (57) and some still remained in the solution transferred to treat the hexapeptide. This may have had some effect on the coupling, but there was still EDC and HOBt in the mixture so this should have converted the acid to the activated ester as the ester was consumed.
- Not all the hexapeptide was consumed in this reaction, as some was evident in the MS analysis of the reaction mixture and the crude product; this maybe overcome by allowing longer reaction times.
- The attempt to purify the product *via* precipitation with CH_3CN, then filtration, may have introduced losses. Although the CH_3CN did not contain significant amounts of product, as indicated by LCMS, some material might have been lost on the filter paper. This precipitation technique is valuable though, as it allows the facile removal of HOBt, which has a very similar retention time to the desired product. To avoid the problems of potential loss *via* filtration it should be possible to recover the fine precipitate by centrifugation.

In order to address these problems the literature was searched to find alternative conditions for this coupling reaction. A paper by Nicolaou *et al.*[31] was discovered that detailed the production of vancomycin derivatives from the hexapeptide and used *O*-benzotriazol-1-yl-*N,N,N',N'*-tetramethyluronium hexafluorophosphate (HBTU) to add an amino acid to both the *C* and *N* terminus of the hexapeptide. This was substantially different from the attempted coupling reaction because the hexapeptide used in their study was alkylated on the sugar amine with substituted benzyl groups and the synthesis was carried out partially on solid-phase, but the conditions allowed them to produce 66 analogues of vancomycin. It was therefore decided that attempts should be made to utilise these conditions to see if they could be adapted to increase the yield in the coupling step required for the synthesis of (58).

This paper[31] also contained a purification technique similar to the CH_3CN method utilised above. It involved concentration of the reaction mixture and then re-dissolving the crude solid in MeOH and precipitating the glycopeptides by addition of Et_2O. This procedure had been used in the preparation of the hexapeptides, not in the coupling step, but was none the less of significant interest. These conditions utilising HBTU were incorporated into the synthesis of analogue (58), as shown in Scheme 3.24.

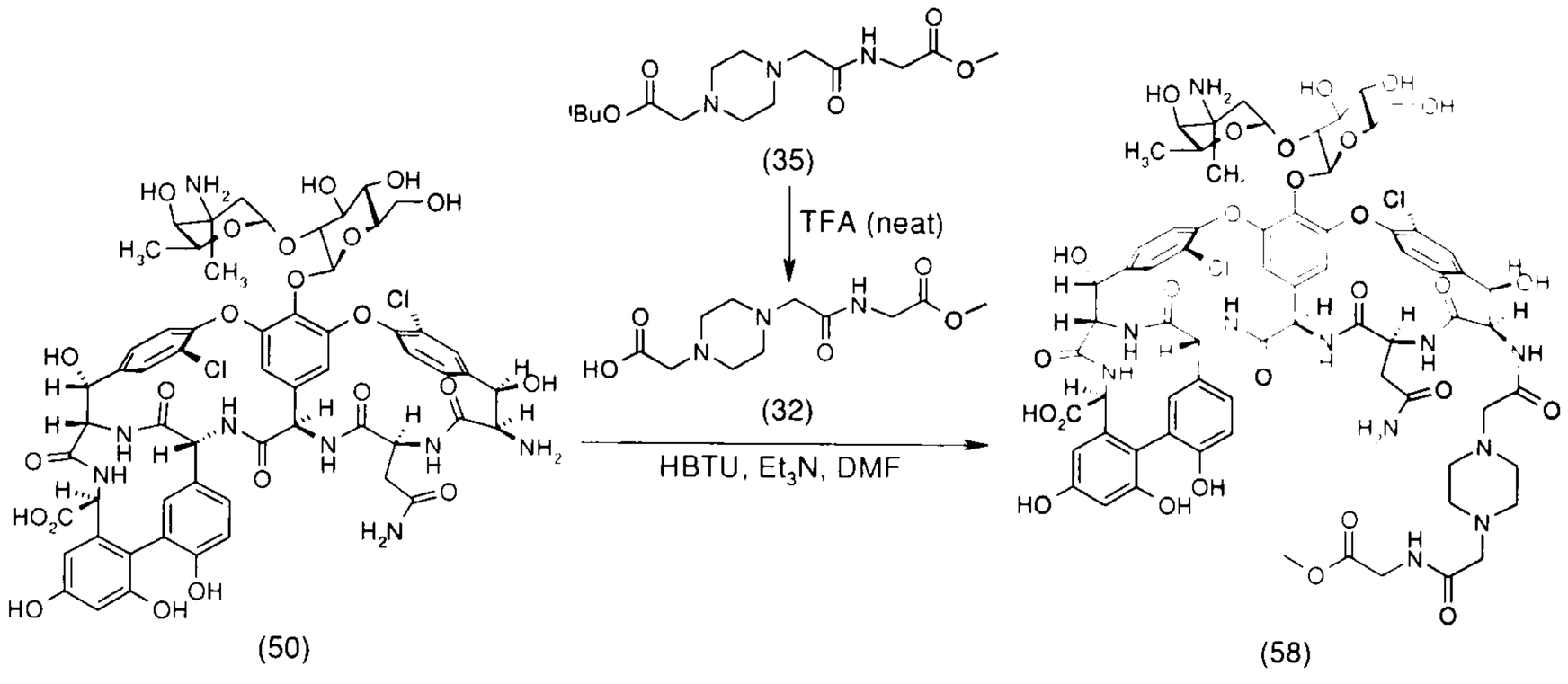

Scheme 3.24.

For this second attempt at the synthesis of (58), ester (35) was again hydrolysed to acid (32) in neat TFA, as confirmed by MS. The resultant residue was treated with HBTU in the presence of the hexapeptide. MS analysis of the reaction mixture revealed that this coupling again did not fully consume the starting materials despite stirring overnight. There was however a number of un-recognised impurities detected by this MS, so the reaction mixture was evaporated to a paste and then the glycopeptides were precipitated with MeOH/Et_2O, and then collected *via* centrifugation. The resultant solid contained desired product (58), hexapeptide (50) and traces of the other reagents as shown by LCMS. The MeOH/Et_2O solution was shown by LCMS analysis not to contain any glycopeptides. The mixture of compounds in the crude solid indicated by the LCMS was evident in the prep HPLC trace of the test injection as shown in Figure 3.10.

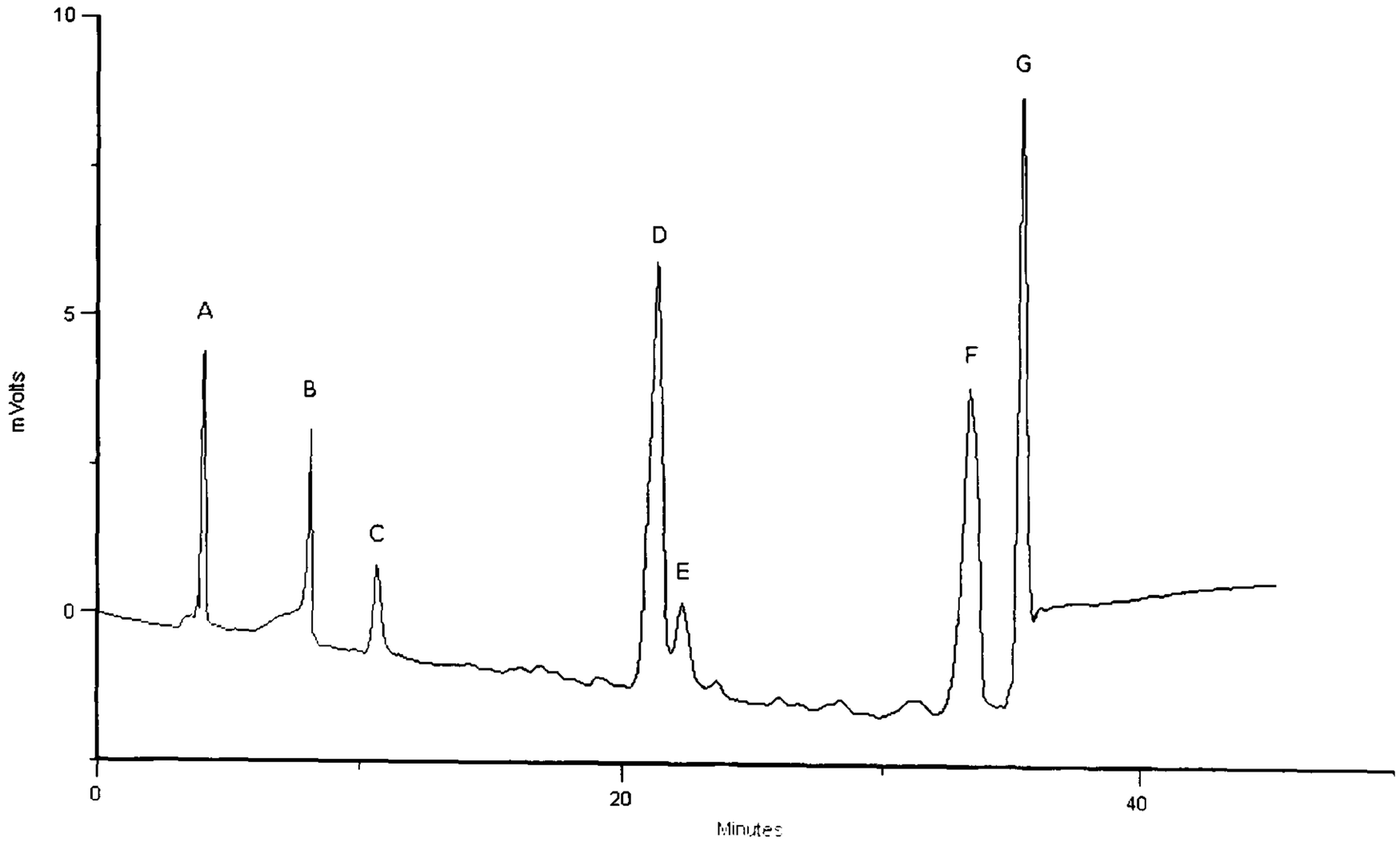

Figure 3.10. HPLC trace of the crude solid.

The three peaks A, B and D corresponded to the reagents and starting materials: HOBt, acid (32) and hexapeptide (50) respectively. C was not identifiable by MS and neither were F or G as the samples from this test injection were too weak to give a good MS spectrum. Peak E was interesting as its retention time was close to that of the hexapeptide and the observed parent ion (1348.9 m/z) in the MS of a sample from this peak was very close in weight to the hexapeptide, a difference of 26 mass units. Peak C was too weak to correspond to the desired product as the intensity of the peaks for the hexapeptide and its fragment ions were of almost equal intensity to the peaks of the product and its fragment ions in the MS of the crude solid. Therefore peaks D – G were collected by preparative HPLC using a C-18 reverse phase column and a gradient 0 –10 % acetonitrile over 30 minutes, followed by a 10 minute 98 % acetonitrile wash.

After prep HPLC, the fractions for each peak were combined and evaporated. MS and LCMS confirmed that the peak D sample was the hexapeptide and that the peak E sample showed the mass (1348.9 m/z) found during the test HPLC purification of the precipitated solid. It is surmised that this compound was produced *via* reaction of the hexapeptide with CO_2 present in the reaction mixture and the HBTU then causes a further reaction, which forms a carbonate between the *N*-terminal amine and the adjacent alcohol, this leads to the formation of compound (59) (Scheme 3.25, changes highlighted by the boxes).

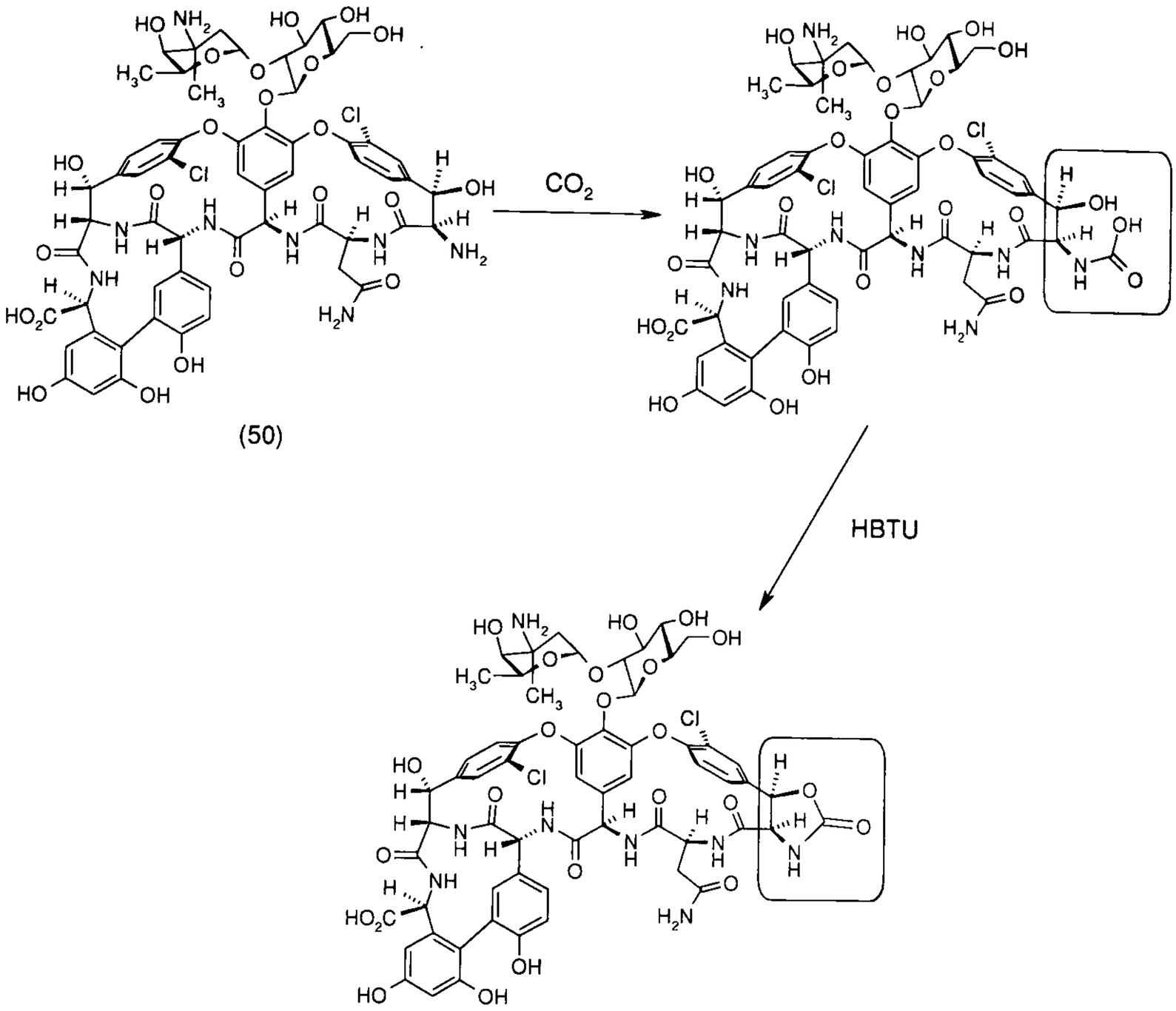

Scheme 3.25.

The sample obtained of peak F after preparative HPLC contained the desired product (58) as shown by MS and LCMS, but these techniques and further HPLC analysis showed that the product was impure. The sample from peak G also contained the desired product (58) and was significantly purer than peak F, as indicated by MS, LCMS and HPLC, but still was not entirely pure. The material recovered in the peak G fractions was freeze-dried and yielded 11.2 mg of compound that was predominantly product (58), (19 % yield). The presence of the desired compound in two separate peaks was an interesting observation. It is believed that this is an artefact of the rapidly changing gradient, which increases substantially from 10 % to 98 % CH_3CN over 2 minutes. It is likely that some material has moved with the solvent front as the eluent with higher CH_3CN content moved down the column, resulting in peak F; while the rest of the material has moved through the column normally, resulting in peak G. This provides an explanation of why neither sample of material is pure; therefore better column conditions were sought after the next reaction.

This last result still gave a low yield, but observation of the supposed compound (59) in the reaction mixture and the likelihood that it was derived from addition of CO_2 to the

hexapeptide offered a partial explanation for this low yield. It was decided to repeat the reaction under conditions that should eliminate the presence of CO_2; the steps necessary for this would also exclude water and oxygen rigorously from the reaction mixture and it was hoped these factors combined would increase the yield. To achieve this it was necessary to understand where H_2O or CO_2 could be entering the reaction, considering each of the reagents in turn:

- The DIPEA and DMF were both commercially obtained as anhydrous liquids in sure-seal bottles and kept under a positive pressure of nitrogen, it seems unlikely that the CO_2 came from these. However the DMF bottle was a few months old and therefore fresh dry DMF was sourced.
- The acid (32) was left under high vacuum for at least 12 hrs to remove any excess of TFA from the cleavage reaction; this therefore also seems an unlikely source for the CO_2 or H_2O.
- The HBTU was commercially obtained, but was not stored under N_2, so this is a possibility for the introduction of the CO_2. It was stored in a para-film sealed container at –18 °C and allowed to warm to room temperature before weighing, so was unlikely to contain any water.
- The hexapeptide was stored under N_2 at –18 °C after synthesis, but contains a number of nucleophilic groups that could trap CO_2, so it is also a potential source of CO_2.
- There is also the possibility that flushing the flask the N_2 is not sufficient to force all the atmospheric CO_2 or moisture from the reaction vessel.

These considerations combined to produce the following modifications to the reactions laid out in Scheme 3.24, thus giving the conditions for the third attempt at the synthesis of analogue (58). They were: TFA cleavage of ester (35); followed by storage overnight under high vacuum; then the solids, HBTU and the hexapeptide, were added to the residue of (32). These solids were than exposed to high vacuum for 10 minutes, then flushed with N_2, this was repeated twice and then the fresh DMF and DIPEA introduced without opening to the atmosphere, whilst maintaining the N_2 environment.

After 3 hours stirring under N_2, MS of the reaction mixture showed all of hexapeptide (50) had been consumed. The reaction mixture was diluted with CH_3CN to precipitate the glycopeptides, which were then collected by centrifugation. The crude solid (see Figure 3.11 for crude HPLC) was purified by HPLC. New conditions were established

as the earlier conditions resulted in the product being collected during the steep ramping of the acetonitrile concentration that precedes the wash and it was believed that this was the reason for the reduced purity of the product in the earlier purification attempt. The new conditions still used a C-18 reverse phase column, but the gradient was now 5 – 10 % over 10 minutes, followed by 10 – 15 % over twenty minutes and then the 98 % wash for 10 minutes.

Figure 3.11. HPLC trace of crude solid.

The material corresponding to the two major peaks, marked A and B, was collected. MS analysis of a sample of peak A from a test injection did not indicate any product (58). MS analysis of a sample of peak B indicated the desired product, compound (58) was present. The fractions from peak B were combined and freeze-dried and HPLC analysis indicated that it was a single compound, as only one peak was observed in the HPLC trace. The compound was returned in 29 % yield based on the amount of hexapeptide used.

MS analysis of the solid from peak B shows the desired product (58) at 1577.9 m/z as the singly charged ion and at 789.2 m/z as the doubly charged ion, (58) minus the vancosamine sugar at 1432.9 m/z and (58) minus both sugars at 1270.9 m/z. There was no indication of peaks at 1177.8 m/z and 1015.8 m/z that would result from

fragmentation of the compound acylated on the amine of the sugar, it therefore can be concluded that this is the desired compound (58), see Figure 3.12.

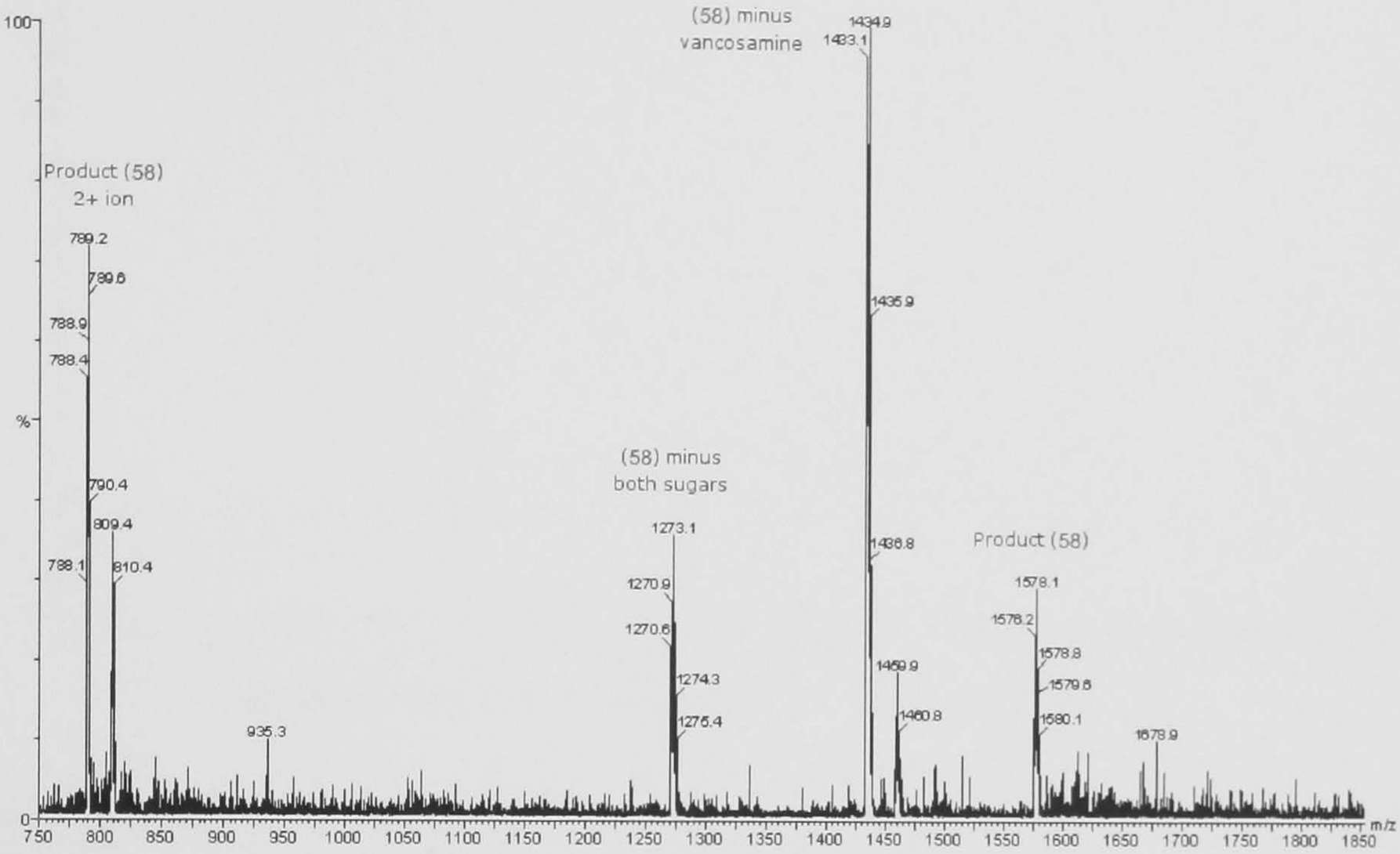

Figure 3.12. MS spectra for product (58) in peak B.

The hexapeptide used in the above reactions had been purified by prep HPLC after synthesis. As discussed previously, progress in the development of the Edman degradation reaction has yielded hexapeptide that has been purified by precipitation. It was decided to repeat the synthesis of (58) using hexapeptide prepared this way to ensure that it did not lower the yields in this reaction.

The reaction was repeated as above but the coupling reaction took ~ 26 hrs to consume all the hexapeptide. Purification was also as above and returned product (58) that was shown to have a minor impurity by HPLC analysis (see Figure 3.13). The material recovered represents a 22 % yield based on the amount of hexapeptide used, but is ~ 90 % pure. Further purification of this product was not attempted. MS fragmentation of the product again shows that synthesis of analogue (58) was achieved.

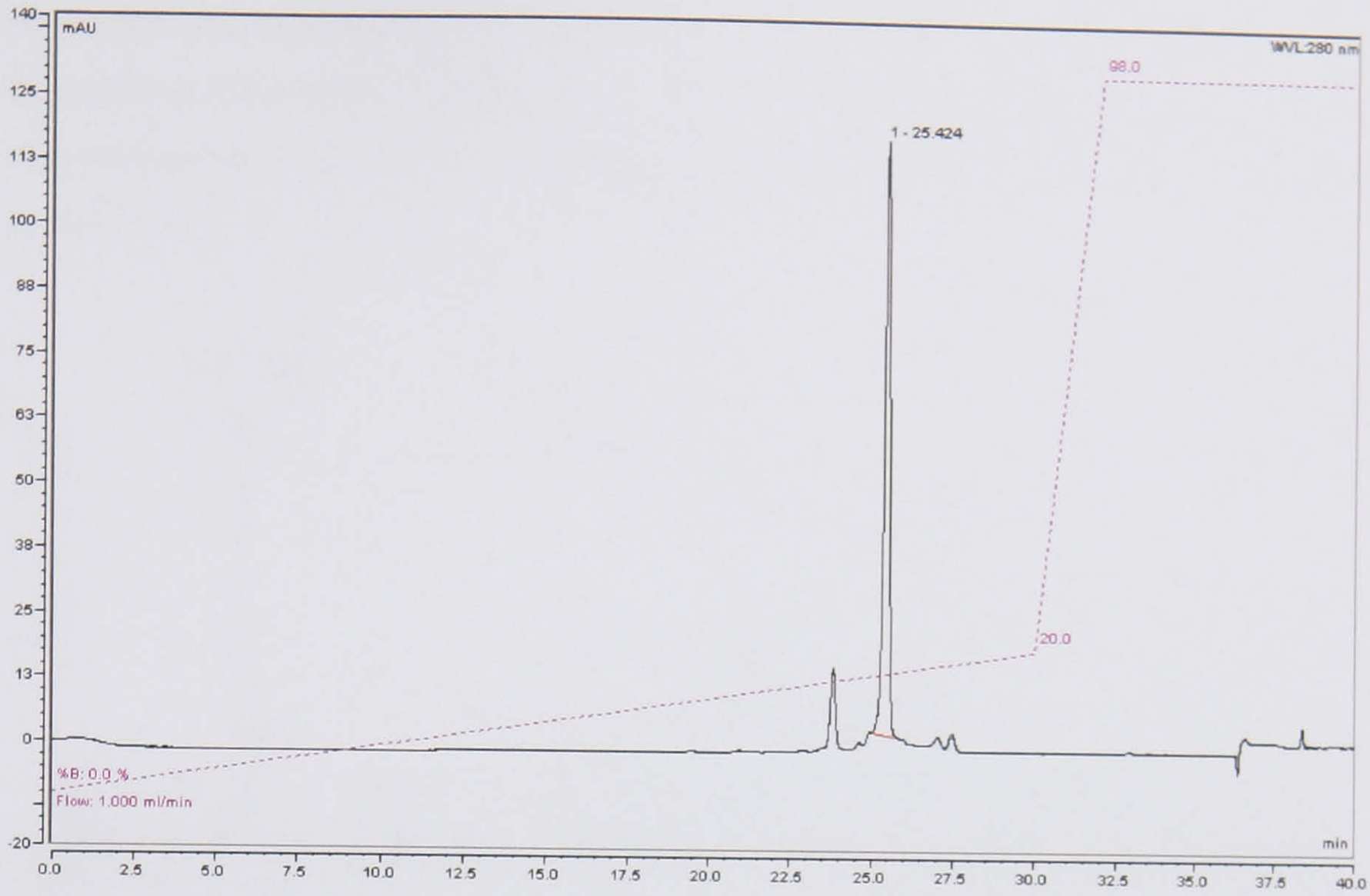

Figure 3.13. HPLC trace of compound (58) from the repeat reaction.

3.3.2 Synthesis of the D-phenylalanine containing analogue (61)

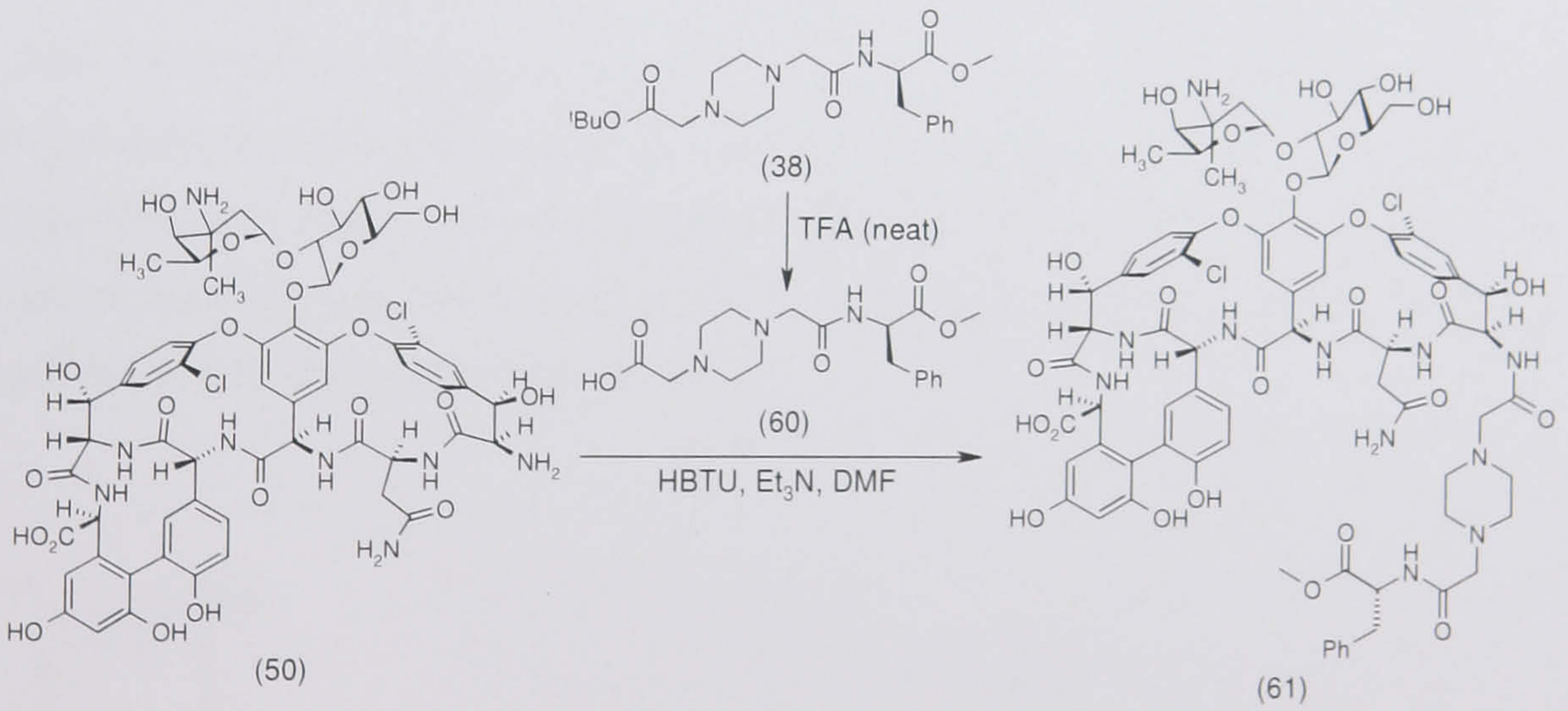

Scheme 3.26

TFA cleavage was carried on piperazine (38) to yield acid (60). This was coupled to hexapeptide purified by precipitation, as in the synthesis of analogue (58). However, acid (60) was treated for 15 minutes with the HBTU, DIPEA and DMF to pre-form the active ester, which was then transferred by cannular into the reaction vessel where the hexapeptide had been held under vacuum and then flushed with N_2 repeatedly to remove any CO_2. It was hoped that pre-forming the active ester would increase the

yield. The crude product was recovered by CH_3CN precipitation. MS (Figure 3.14) of this crude product shows a mixture of acid (60) as the M+H ion at 364.4 m/z, product (61) as the M+2H ion at 835.1 m/z and the doubly acylated by-product as the M+2H ion at 1007.5 m/z.

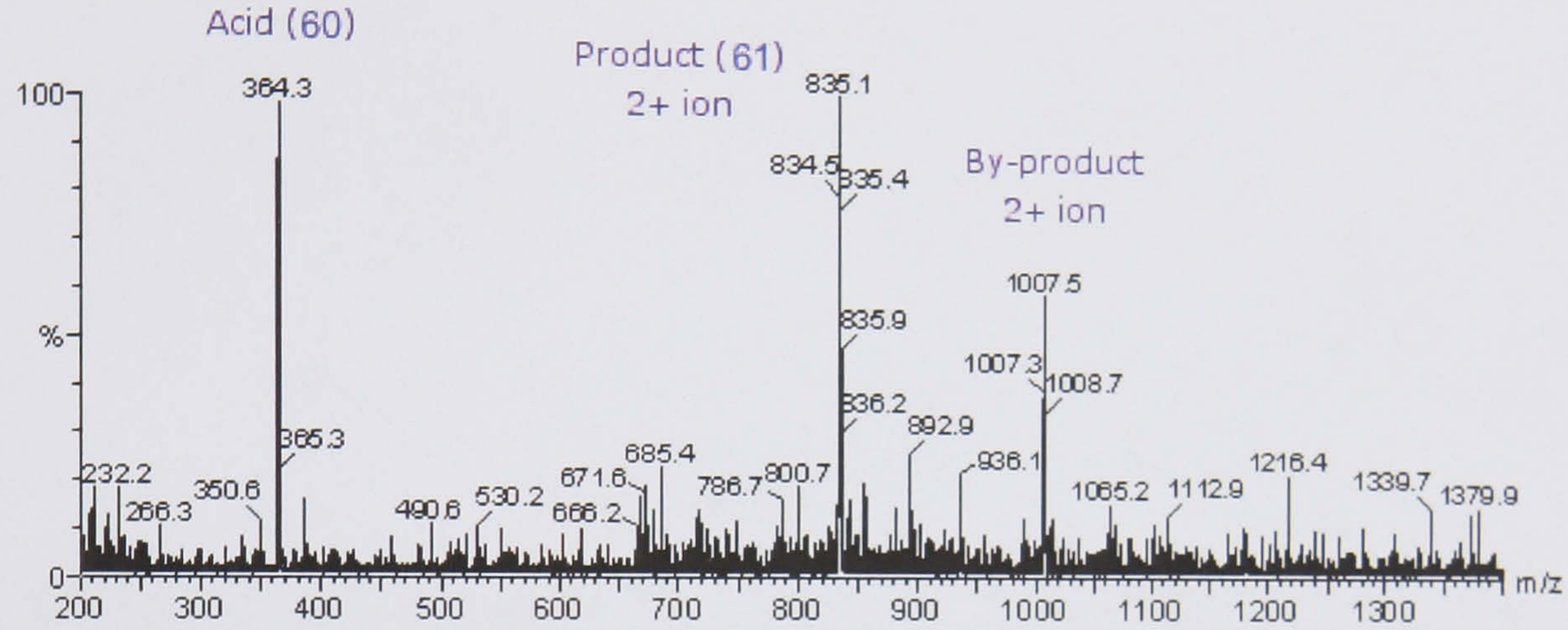

Figure 3.14. MS of the crude product in the synthesis of compound (61).

The ratio of product to the combined by-product peak heights is ~ 3:2. This crude material then underwent final purification *via* prep HPLC to give the desired product (61) in 22 % yield. Apparently, pre-forming the activated ester had no effect on the yield. The product purity was confirmed by HPLC analysis (single peak), and MS fragmentation (see Figure 3.15) shows that the terminal amine was acylated. Unusually this product preferred to exist as the doubly protonated 2+ ion under the MS conditions and the level of fragmentation is reduced. A six fold expansion of the area for the singly protonated ions does reveal their presence.

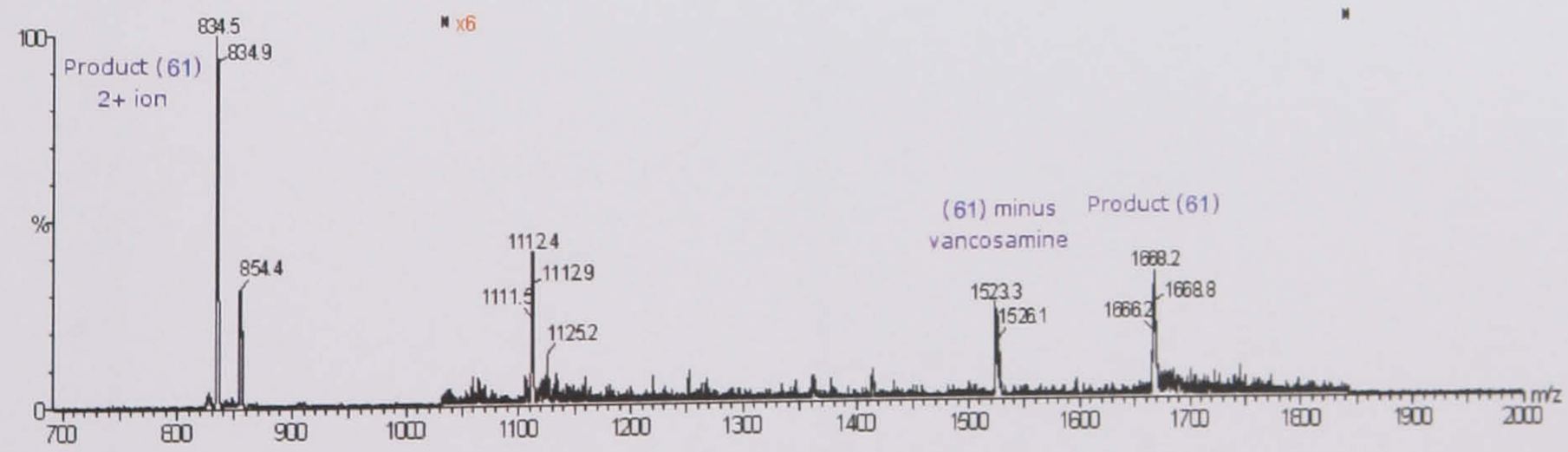

Figure 3.15. MS of the purified product in the synthesis of compound (61).

3.3.3 Synthesis of the D-phenylglycine containing analogue (63)

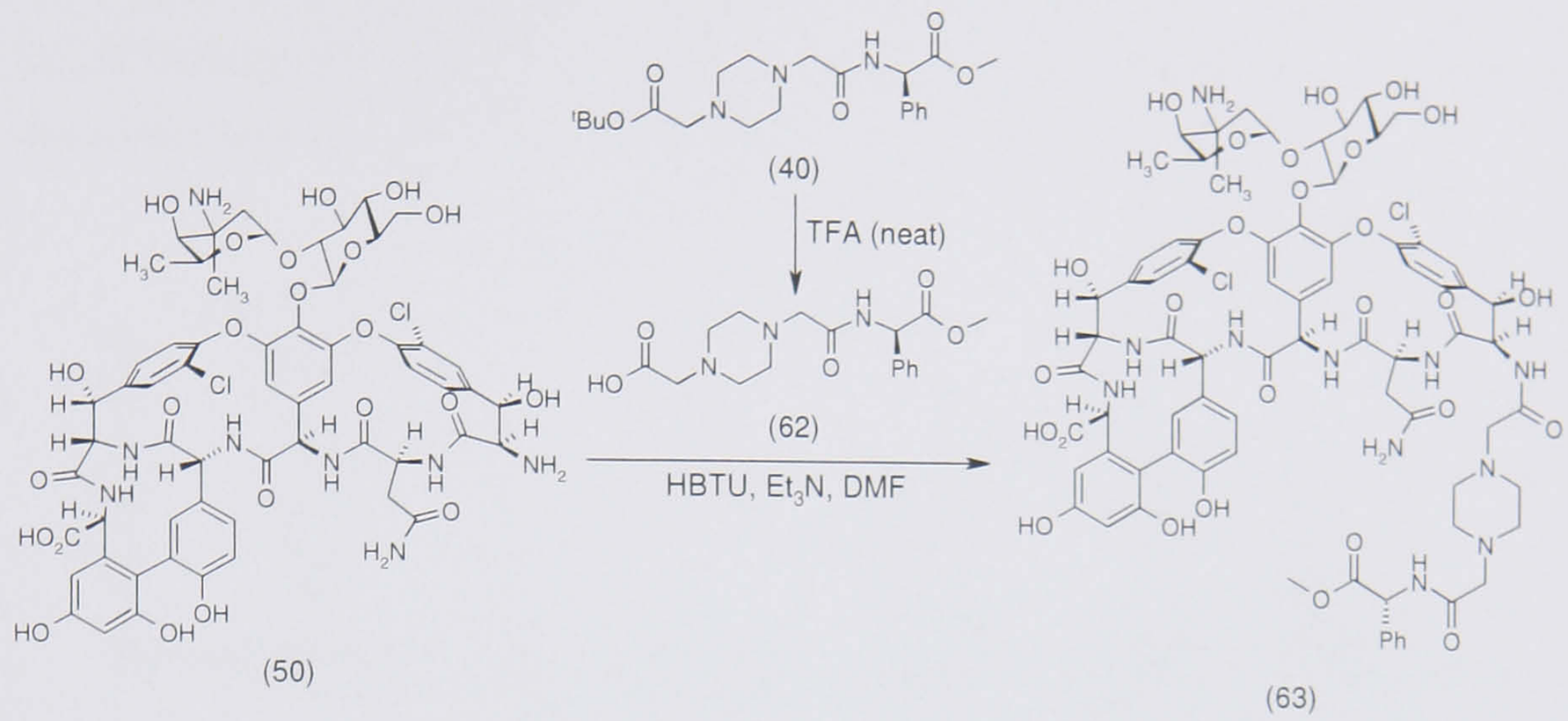

Scheme 3.27.

The reaction conditions developed for analogue (61) were repeated on piperazine (40), again using hexapeptide purified by precipitation. Only 1.5 equivalents of acid (62) and 1.4 equivalents of HBTU were used in contrast to the synthesis of (61) where 2 equivalents of acid (60) and 2 equivalents of HBTU were used. It was hoped that reducing the amount of acid and HBTU would reduce the production of the di-acylated by-product and thus increase the yield of the desired product (63). Double acylation was not observed and the product was therefore purified by CH_3CN precipitation and HPLC, to give product (63) in 28 % yield, based on the amount of hexapeptide used. HPLC analysis (Figure 3.16) showed that the material recovered was ~ 90 % pure with two minor impurities.

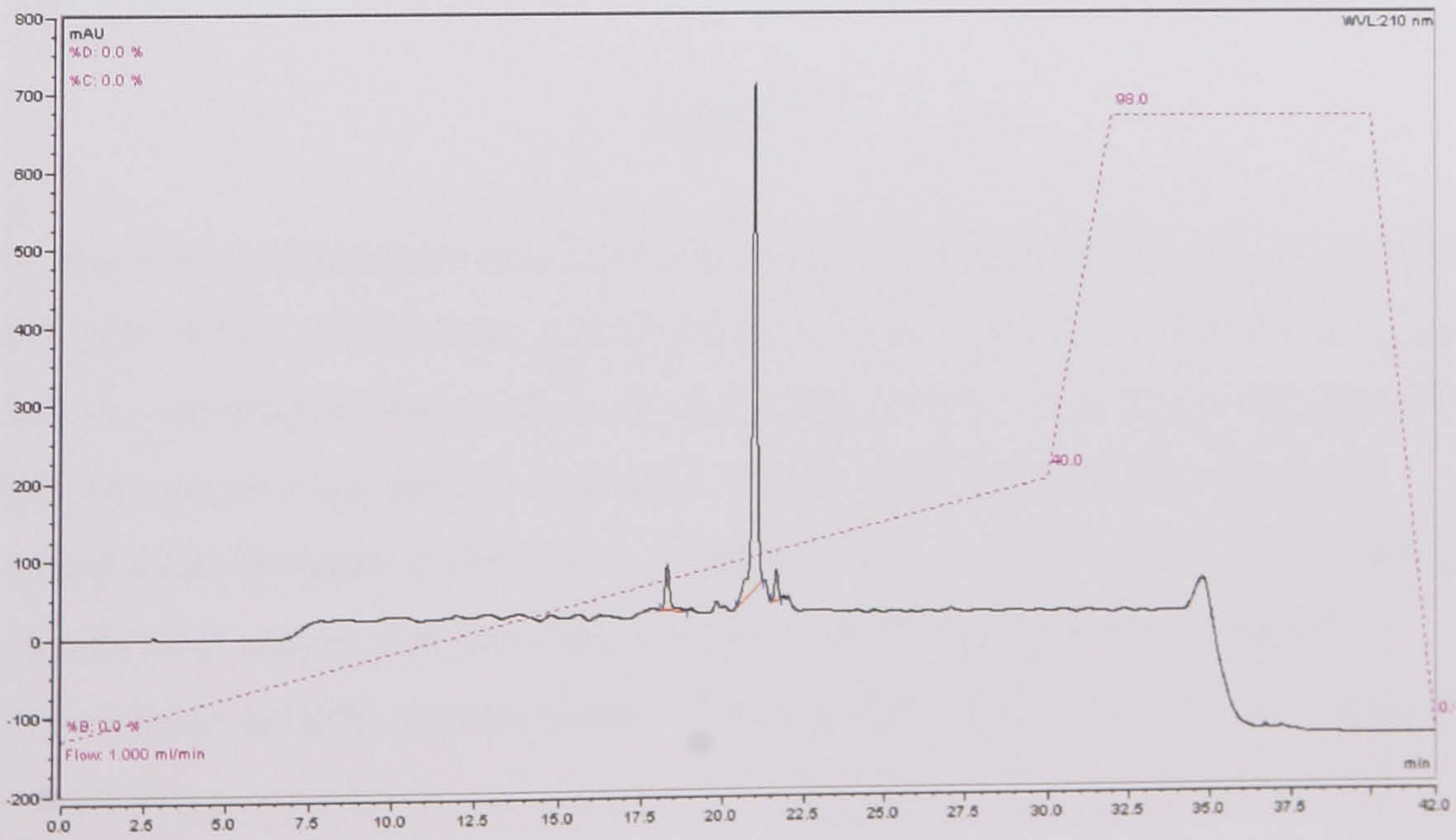

Figure 3.16. HPLC trace of product (63).

MS indicated product (63) at 1655.3 m/z as the M+H ion and at 827.2 m/z as the M+2H ion, (63) minus vancosamine at 1510.1 m/z and (63) minus both sugars at 1347.9 m/z, thus showing acylation occurred on the *N*-terminus (Figure 3.17).

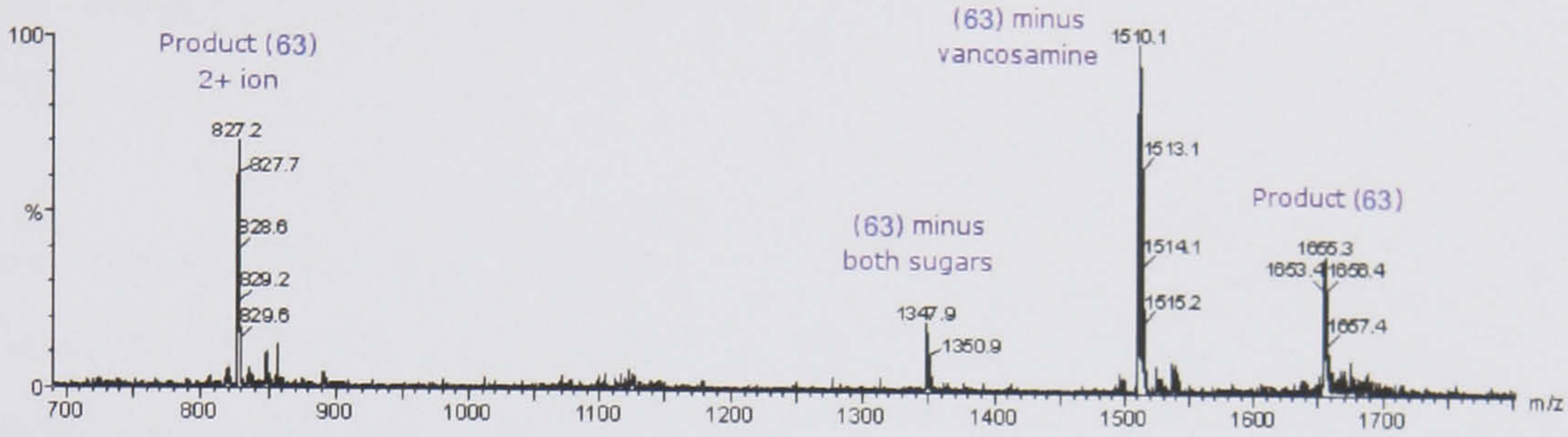

Figure 3.17. The MS spectra of the purified compound (63).

3.3.4 Attempted coupling of the rigid analogue

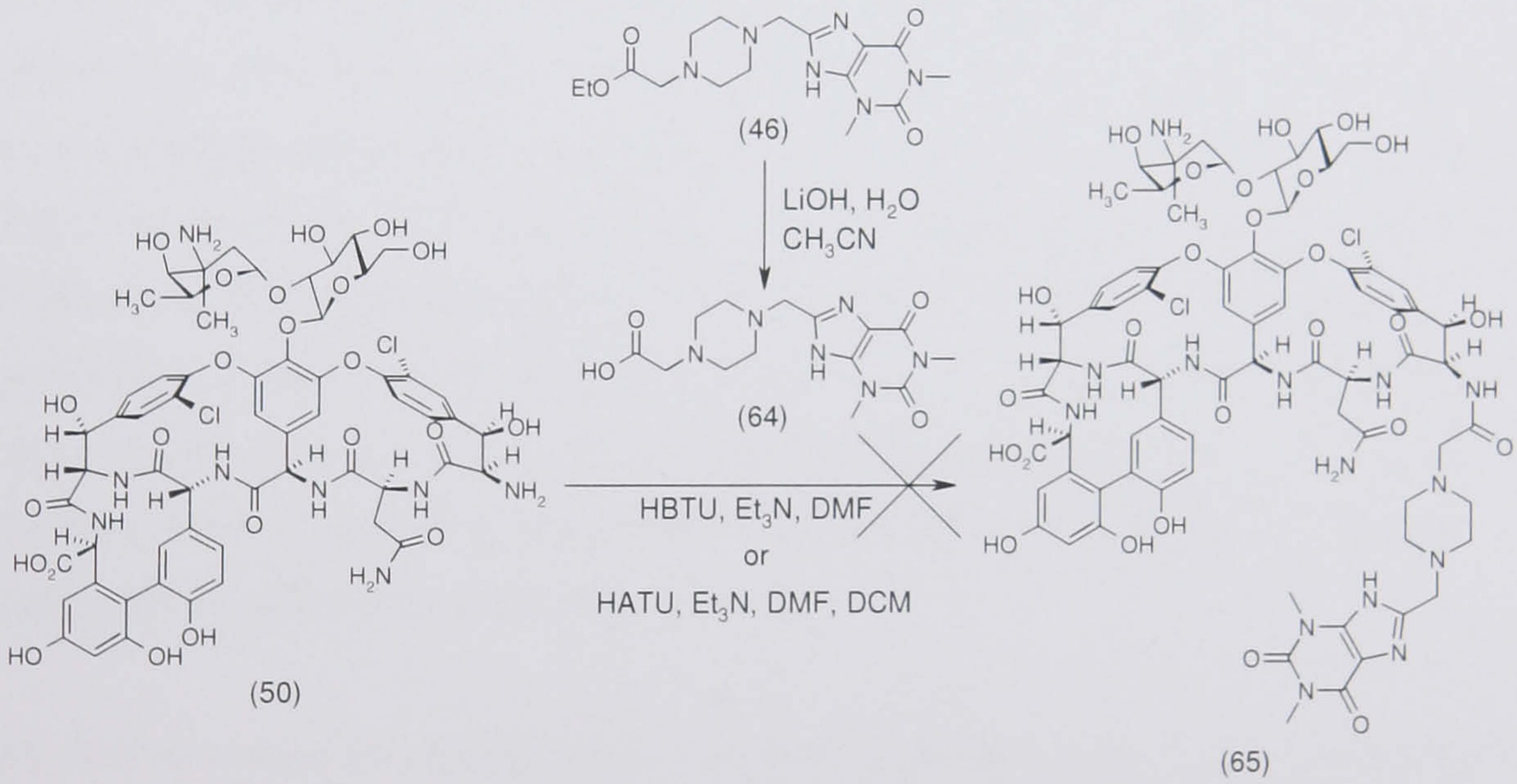

Scheme 3.28.

This reaction was attempted twice, in each case using lithium hydroxide to cleave the ethyl ester of (46), followed by neutralisation with conc. HCl and evaporation to yield acid (64). The first attempt used the one pot method used for the glycine analogue (58), where hexapeptide and HBTU were added to the residue from the first stage and evacuated and flushed with N_2, before addition of the solvents. However, only starting materials were observed in the reaction mixture. The acid of the rigid analogue was poorly soluble in DMF, and this seems to result in the failure to generate any product in this reaction.

The second attempt at the coupling used the method previously used for analogue (61). The ester was pre-formed but it was decided to attempt the reaction in DCM, in the hope that it would be a better solvent for the acid. It was also decided to change the coupling agent to HATU, which is more reactive than HBTU. However, HATU was poorly soluble in DCM, so DMF was added to this reaction in order to solubilise the HATU.

Again, only unreacted starting materials were observed and no product was formed. These experiments exhausted the supply of intermediate (46); therefore no further attempts were made at the synthesis of analogue (65).

3.3.5 Conclusions on coupling reactions

Selectivity for the *N*-terminus has been established and steps have been made to improve the low yielding nature of these reactions. Double acylation was observed in some couplings but conditions were modified to minimise formation of this by-product. These improvements in the methodology encorporated insights gained in the synthesis of the hexapeptide skeletons, and relied on observations during the reactions and purification to fine-tune this synthesis. Removal of CO_2 was proven to be of significant importance in these reactions and necessitates that the hexapeptide must be put under vacuum directly before the coupling and that atmospheric moisture and CO_2 must be rigorously excluded from the reaction vessel.

The failure to form the rigid analogue is particularly disappointing, because of the dual benefits this scaffold offered, namely lower entropic penalties on binding and the ability to offer hydrophilic groups to solvent. Though, this failure may be overcome if a suitable solvent could be found to sufficiently solubilise the hexapeptide, acid (64) and the coupling agent, and this would be a good starting point for any future investigations.

The results of the coupling reactions with the piperazine methyl esters were gratifying, as they have proved that coupling of the hexapeptide and these extenders can be achieved, thus validating the key step of the synthetic pathway, which completed the synthesis of three designed extensions of the vancomycin core. This is the first instance where a fragment designed to offer extra hydrogen bonding and lipophilic interactions

with the tripeptide target had been successfully synthesised, coupled to the hexapeptide core and purified, and is thus the first instance of the rational design of semi-synthetic analogues of a natural-product drug like vancomycin.

3.4 The tripeptide for binding studies

There have been a number of studies to elucidate and quantify the nature of the binding between vancomycin and either the bacterial cell wall or peptides that mimic it. A range of peptides have been used and indeed there is a degree of diversity in the natural terminus of the cell wall peptide, as mentioned in the introduction (Chapter 1, Section 1.4). However, the crystal structure (PDB code 1FVM)[35] used for the design stage contained diacetyl-L-lys-D-ala-D-ala (Ac_2KAA, 66) as the cell wall mimic.

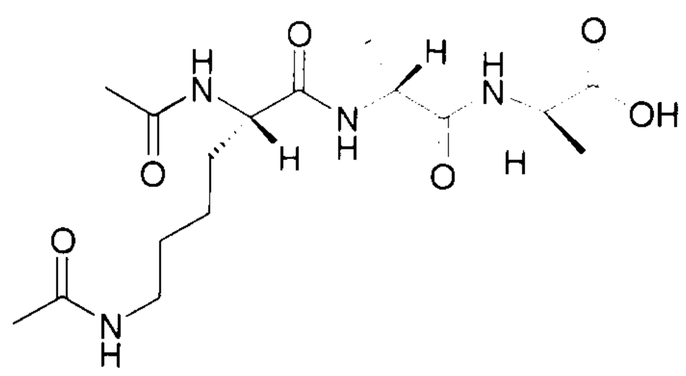

(66)

This was considered a close mimic of the natural substrate, because although the cell wall building blocks, lipid I and II, contain a pentapeptide; only the three terminal residues are involved in the formation of the hydrogen bond network with vancomycin. It was therefore decided to use Ac_2KAA in our binding studies, thus it became necessary to synthesise this compound. It was hoped that an increase in the binding affinity to Ac_2KAA could be achieved in the initial stage of this investigation, but it was a further aim that the modified vancomycin analogues produced would also have an increased affinity to the variants of this compound that mimic the terminus of the peptides used by resistant bacteria. As discussed in Chapter 1, there are two different alterations to the *C*-terminal amino acid that confer resistance. Replacement of the terminal D-alanine with D-serine, which is less frequently observed, and replacement with D-lactate, which is the most common form of resistance. To mimic these replacements the sequences needed would be: diacetyl-L-lys-D-ala-D-ser (Ac_2KAS, 67) and diacetyl-L-lys-D-ala-D-lactate (Ac_2KAlac, 68). The differences from Ac_2KAA are circled in the diagram.

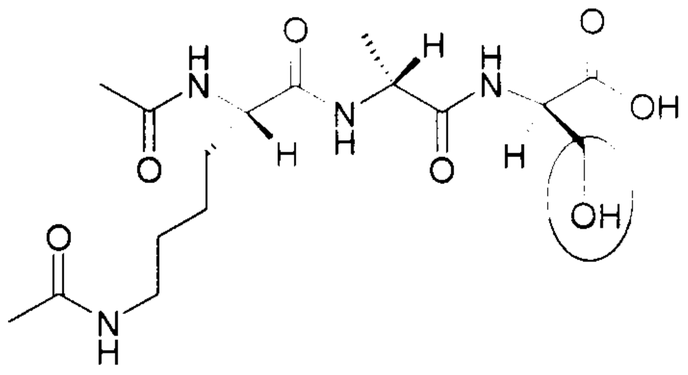

(67)

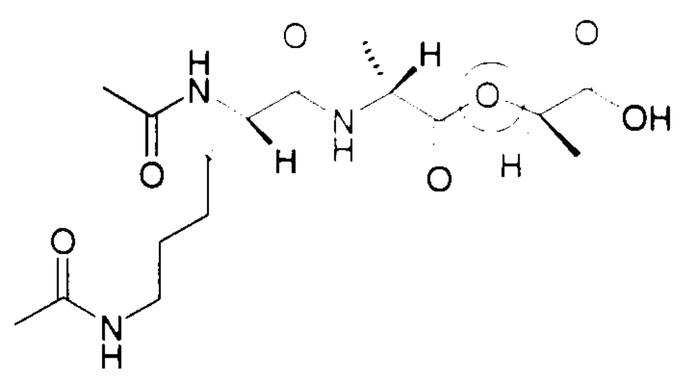

(68)

Neito and Perkins[36] reported the synthesis of Ac_2KAA. However, they performed the synthesis from the *C*- to the *N*-terminus, and this was considered to be undesirable for this case, as a separate synthesis would have to be undertaken to furnish each of the desired analogues (67 – 68). A more efficient synthesis of all three peptides would be achieved if the synthesis began at the *N*-terminus.

The use of *tert*-butoxycarbonyl (BOC) protecting groups to protect both nitrogens of the lysine amino acid was considered desirable because they are known to be stable in the conditions used for the peptide coupling reactions and are frequently used within this context. Thay have a further advantage that they are also lipophilic and it was believed that this would aid purification of these compounds. The acid groups were protected as methyl esters because conditions were known for the formation of these esters. Also, work by Horton,[4] from this research group, had developed conditions for the cleavage of methyl esters in high yield. This led to a synthetic sequence which would begin with the protection of both nitrogens of lysine with BOC groups and then the sequential coupling of D-alanine methyl ester, methyl ester cleavage with lithium hydroxide, followed by a further coupling of the methyl ester of D-alanine, D-serine or D-lactate, depending on the analogue required. After the final coupling the BOC groups could be cleaved, the amino groups acetylated and the terminal methyl ester cleaved to give the free acids (67 – 68). This route is outlined in Scheme 3.29.

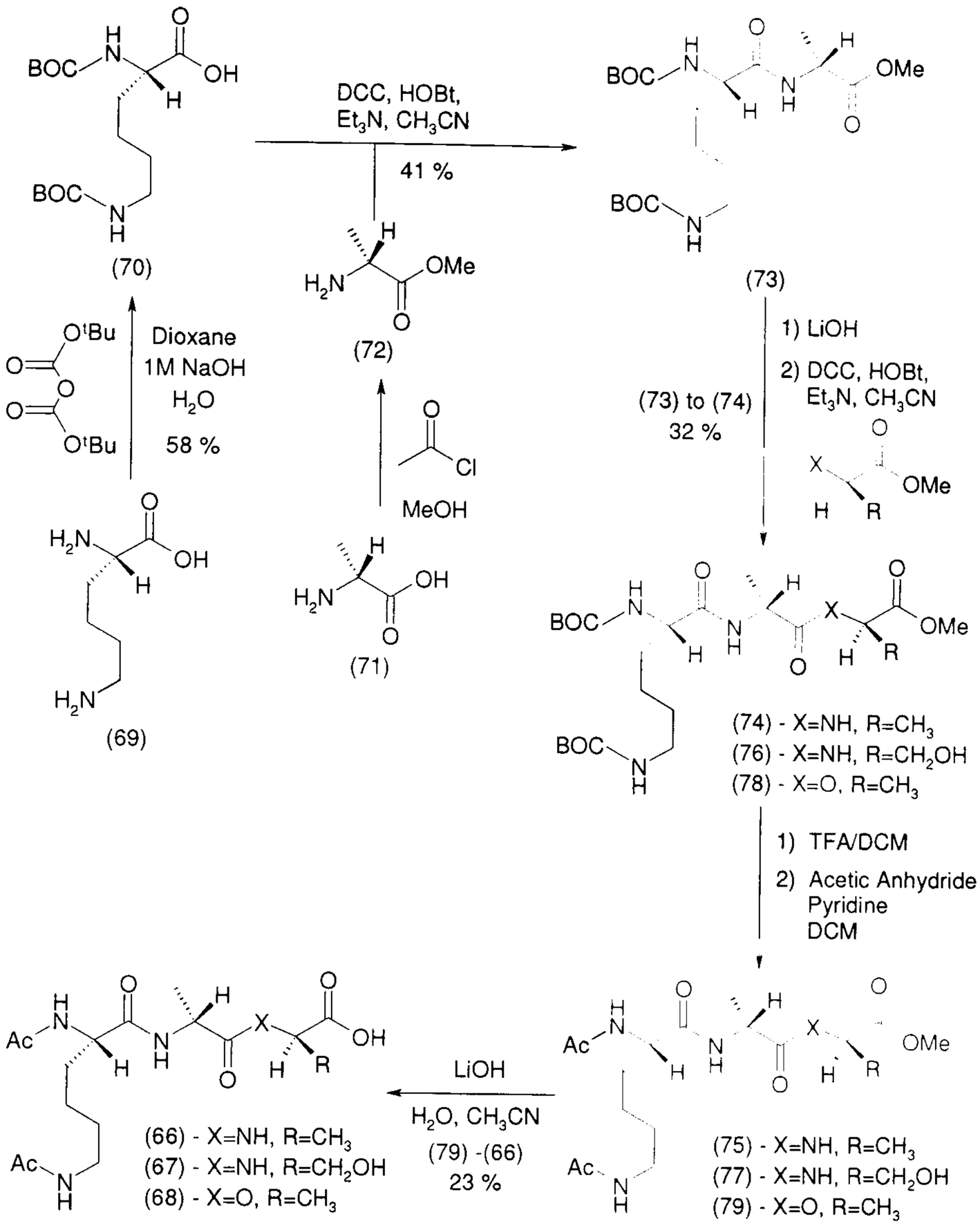

Scheme 3.29.

3.4.1 Tripeptide synthesis

Due to the fact that this synthetic path was untested it was considered logical to test it on a small scale and furnish compound (66) and then repeat the synthesis on a larger scale to furnish a sufficient quantity of intermediate (73) to yield the required analogues (66 – 68).

The first stage of this process was the protection of the main amino acid building blocks, L-lysine (69) and D-alanine (71). L-lysine was obtained as the free amino acid and BOC protected with BOC anhydride using the conditions of Tsuchida *et al.*[37] This reaction was relatively inefficient; the first attempt gave the BOC protected compound (70) in a 28 % yield. Repeating the reaction gave (71) in a 58 % yield, which was acceptable but still low for such a trivial protection step.

D-alanine was also acquired as the free amino acid and was reacted with methanol in the presence of acetyl chloride, following the conditions of Hulme,[15] as used in Section 3.1. This again proceeded smoothly yielding (72) as the HCl salt. As a large quantity of this intermediate was required, this reaction was performed twice on 2.5g of D-alanine. From one reaction 2.6 g of the methyl ester (72) was isolated (65 %) and 3.9 g for the other (94 %).

Dicyclohexyl carbodiimide (DCC) was used to couple (70) and (72) in the presence of hydroxybenzatriazole (HOBt) and triethylamine using the conditions of Rees *et al.*[3] This reaction proceeded smoothly and afforded the desired product, intermediate (73) in 82 % yield after filtration to remove the solid dicyclohexylurea (DCU) by-product and an aqueous work-up. This reaction was repeated but purification was achieved by column chromatography on silica gel. The yield was lower (41 %), but the product was purer, as trace amounts of DCU were observed when the product purified by aqueous work-up was used in subsequent reactions, whereas this was not observed in the product purified by silica column.

The protected dipeptide (73) was partially deprotected by hydrolysis of the methyl ester using lithium hydroxide.[4] A trial of this reaction on 100 mg of the material purified by aqueous work-up yielded 87 mg (90 %), which was clean except for DCU remaining from the previous reaction as a minor impurity. Repetition on a large scale with the remaining 840 mg of material from the reaction purified by aqueous wash produced 768 mg of the free acid (95 %), again with DCU as an impurity and a trace of HOBt. The HOBt signal was weaker, so this was probably present in the small-scale reaction but just not observed. The product from the large-scale reaction was taken on without further purification and coupled to D-alanine methyl ester (72) to yield the protected tripeptide (74). This coupling again used DCC, HOBt and triethylamine. However, purification required an aqueous work-up and two subsequent purifications by silica gel column chromatography to yield material of sufficient purity. As a result of this involved purification the yield for this reaction was low, only 27 %.

Repeating the ester cleavage on dipeptide (73) that had been purified by column chromatography was very successful. The hydrolysis progressed smoothly; consuming all the starting material and partitioning the product between base and EtOAc, and then acidifying the base and extraction with DCM gave the desired free acid in 97 % yield

and good purity. Taking this material and performing the DCC, HOBt and triethylamine mediated coupling to (72), yielded (74). Purification by aqueous work-up and preparative LCMS gave the desired compound in high purity with 32 % yield.

In the first attempt to convert (74) to (66), the conversion to the acyl-protected tripeptide (75) was performed as a separate step, followed by the methyl ester cleavage. To convert (74) to (75) the two amino groups of the lysine from compound (74) were deprotected using a solution of 25 % TFA in DCM under the conditions of Fairlie *et al.*[38] No attempt was made to purify at this stage and the material was simply concentrated under vacuum and then any remaining TFA removed under high vacuum. This was taken on and treated with DMAP, Hunigs base and acetic anhydride in THF. The reaction mixture was concentrated and it was hoped that the di-acylated tripeptide (75) could be isolated by aqueous work up. However, this was unsuccessful and it was necessary to concentrate the aqueous layers in order to recover the product. This crude mixture was taken on without further purification. The MS and LCMS data suggested that the methyl ester had partially hydrolysed. This was not viewed as a significant problem as the next step involved the hydrolysis of this ester.

The attempted cleavage of the methyl ester using the conditions that had been established earlier yielded only a small amount of acid (66). The presence of a large amount of impurities within the crude sample of the precursor (75) may account for this low yield. After LCMS purification, only 16 mg of compound (66) was recovered and this was still slightly impure. Based on the 100 mg of (74) used in these reactions this is only a 22 % yield.

It was decided that the remaining material would converted from the BOC protected tripeptide ester (74) to the *N*-acyl tripeptide with a free acid (66) without any purification. To this end, the diisopropylethylamine in the acylation step was replaced with triethylamine, this meant that it could be more easily removed by concentration *in vacuo*. It was hoped that this would reduce the number of impurities carried through the reactions and improve the yield.

Ester (74) was treated with 25 % TFA in DCM and after 3.5 hrs analysis using LCMS indicated that there was still some mono-BOC compound present. The compound was therefore treated with neat TFA overnight. Despite a significant reduction in this

impurity, some still remained even with these forcing conditions. The material was therefore taken on with this minor impurity. The acylation proceeded smoothly and took only 2 hrs. The mixture was then hydrolysed using LiOH in H_2O and CH_3CN, then purified using LCMS to give 30 mg of the desired product (66), a 23 % yield.

3.4.2 The repeat synthesis of tripeptide

The above route did not furnish sufficient quantities of Ac_2KAA (72) and none of the key intermediate (73) remained, which would allow the production of Ac_2KAlac or Ac_2KAS. There were three significant problems that caused this: the Boc protection of lysine from the free amino acid was low yielding, only 58 %; the peptide couplings were low yielding (41 and 32 %) and conversion to the di-acylated, free acid (66) was low yielding (23 %). It was necessary to solve these problems in order to progress with this synthesis, dealing with each of them in turn produced the following suggestions:

- Only small amounts of starting material were observed in the crude reaction mixture of the BOC protection. Therefore the product was probably being lost to side-reactions or during the purification steps. As the free acid on lysine was a likely cause of any side-reactions and also made purification more difficult, it was thought that protection of this group prior to the BOC protection would increase the yield for this step. As the formation of methyl esters was quick and high yielding and their hydrolysis seemed equally efficient in the earlier synthesis, this seemed the most appropriate strategy.
- The low yield of the peptide couplings was a significant problem and also the prevalence of a persistent impurity, dicyclohexyl urea, from the coupling agent suggested a solution to this problem. This was the use of an alternate coupling agent 1-ethyl-3-(3-dimethylaminopropyl)-carbodiimide hydrochloride (EDC). EDC is water soluble, as is the urea by-product produced by using it in these coupling reactions, and it was hoped that this would both increase the yield of the reaction and allow easier purification.
- The conversion from (74) to (66) utilised three reactions that were all individually high yielding and should produce the minimum of by-products and thus simplify purification. There was a minor problem in the TFA hydrolysis of the BOC carbamates, but this could be overcome by using fresh TFA. This problem was insufficient to explain the low yield though: this suggested that there were problems with the purification, as no problems were observed in the

two other reactions. This led to two possible causes; impurities in the starting materials or reagents being carried through the reaction and losses due to poor purification techniques. Eliminating any sources of impurities would make purification simpler, improving yields. There were also problems injecting the crude product dissolved in neat MeOH during the LCMS purification, which may have introduced losses and could be avoided.

With these changes it was hoped that sufficient quantities of the tripeptide (66) could be achieved to cover all of our testing needs and also leave sufficient quantities of intermediate (73) to synthesize both Ac_2KAlac and Ac_2KAS if needed. The synthesis is set out in Scheme 3.30.

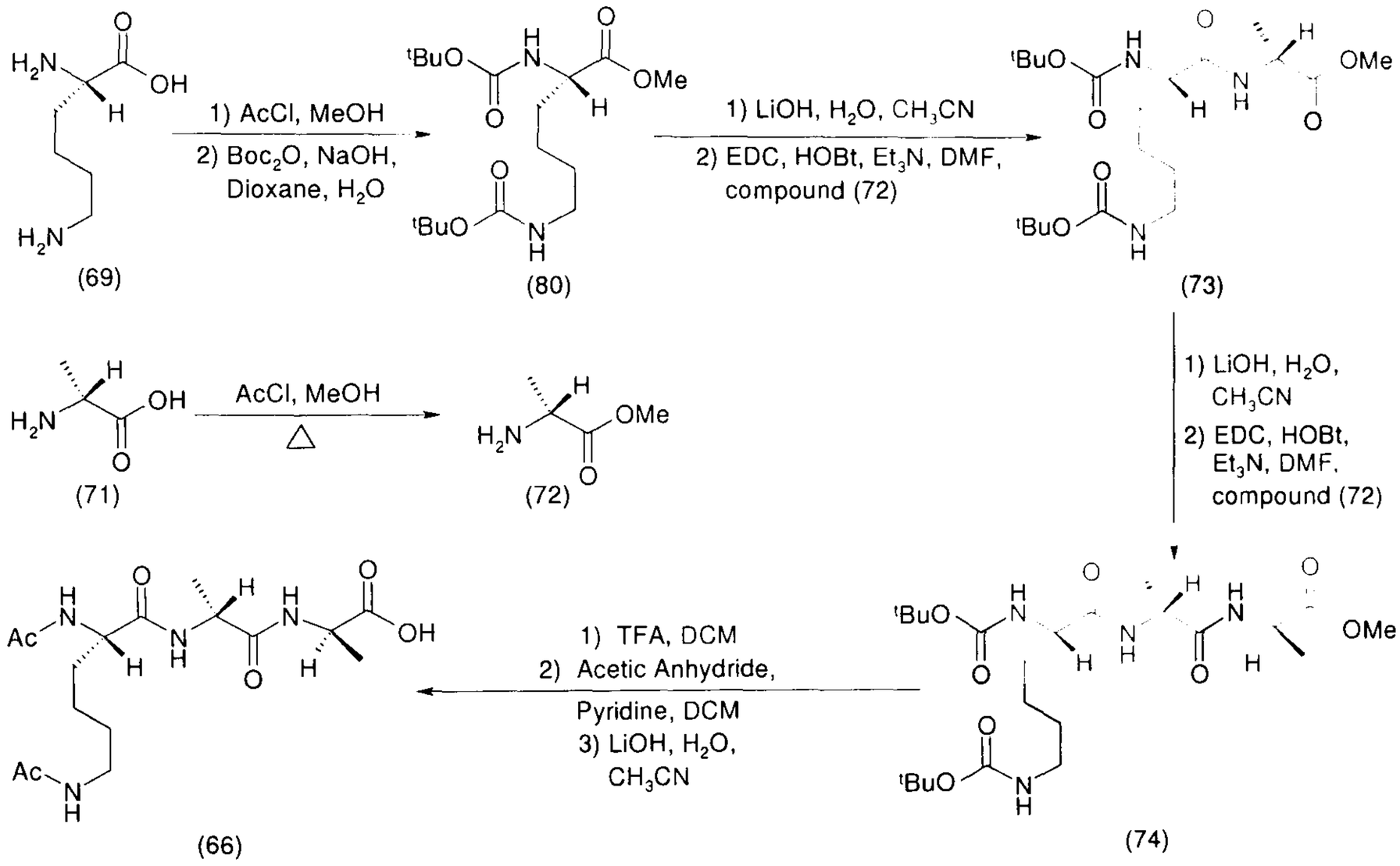

Scheme 3.30.

Sufficient quantities of (72) remained from the earlier synthesis, so it was not necessary to synthesis this again. This synthesis therefore began with the production of lysine methyl ester, this utilised the same methods used to produce glycine, D-alanine and phenylalanine methyl ester.[15] It was performed on 5.0 g of lysine hydrochloride and produced 6.4 g of lysine methyl ester dihydrochloride, a quantitive conversion.

The lysine methyl ester was protected by treatment with three equivalents of BOC anhydride in the presence of sodium hydroxide to afford amino acid (80). This used 6.1 g of the methyl ester and yielded 6.0 g of di-BOC lysine methyl ester (80), as a

white solid after purification by column chromatography, a yield of 64 %. This is only a marginal increase in yield for this BOC protection, but the product achieved is significantly purer than the BOC-protected free acid in the first synthesis and passed microanalysis.

Hydrolysis of (80) using lithium hydroxide proceeded smoothly, showing complete conversion to product after 90 min, as indicated by LCMS analysis. The free acid was then coupled to D-alanine methyl ester (72) using water-soluble carbodiimide (EDC) and HOBt in DMF.[7,8,16] This produced 6.3 g of product (73) as a white solid, following aqueous work-up, a 90 % yield. This was pure enough to pass microanalysis without any further purification.

Only 4.0 g of the material produced was taken on to produce the di-BOC tripeptide (74). The first step was again hydrolysis with lithium hydroxide, this reaction was successful and MS analysis showed only product after 1 hr. The yield of the subsequent peptide coupling reaction was low, only 1.59 g (34 %) of (74) was isolated after the aqueous work-up. The low yield was the result of failing to neutralise the reaction mixture before the solvent was removed under vacuum in the lithium hydroxide cleavage. This meant that the excess lithium hydroxide was carried into the coupling reaction and appears to have reacted with the coupling agent and resulted in a poor conversion in the peptide coupling. Analysis of the aqueous waste by MS found the acid present as both the sodium and lithium salts. The solutions were acidified and extracted and thus 2.12 g of the acid were recovered; this is the equivalent of 2.19 g of methyl ester (73). Taking this recovered starting material into account the yield is 75 %.

Conversion of the di-BOC methyl ester (74) to the di-acylated free acid (66) was performed in three stages. In the first stage the BOC protecting groups were removed using neat TFA, the reaction was complete after 80 minutes, as indicated by MS. The TFA was removed under vacuum and any excess removed by leaving the sample under high vacuum. The residue from this reaction was then used directly in the second stage, where acetic anhydride, DMAP and triethylamine were used to acylate the free amines of the tripeptide. An aqueous wash was attempted to purify the crude product, however it appears that the saturated sodium hydrogen carbonate, used in the work-up, was sufficiently basic enough to induce partial hydrolysis of the methyl ester. It was possible to isolate both the acid and the remaining methyl ester from the aqueous solvents and

proceed with the reaction. Despite attempts to purify this product by aqueous extraction, column chromatography and re-crystallisation a sample which would pass microanalysis could not be achieved. Conditions were therefore sought that would allow purification by prep LCMS and during this process it was observed that compound with the correct mass for the di-acyl free acid (66) was present in three of the peaks in the total ion count trace. This is presumably caused by the presence of diastereoisomers resulting from the base-induced epimerisation at one or more of the chiral centres in the tripeptide; purification was therefore stopped at this point.

3.4.3 The tripeptide synthesis *via* solid-phase

Following the problems with the above synthesis and its failure to yield the tripeptide needed for the testing phase of this project, it was decided to synthesise the tripeptide on solid-phase. The synthesis was carried out *via* standard Fmoc chemistry as described in the Novabiochem catalogue[39] and began with Fmoc D-alanine already attached to a Wang resin. The Fmoc deprotection was achieved with 20 % piperidine in DMF and the peptide couplings used HATU. Conversion from the di-Fmoc protected tripeptide to the di-acyl tripeptide was performed on the resin, using piperidine deprotection followed by capping with acetic anhydride in the presence of pyridine. The final cleavage was carried out using freshly distilled TFA. This differed from standard cleavage conditions as no scavengers were employed. None of the side-chains required protecting groups and therefore no by-products from protecting group cleavage were present to be scavenged, thus the scavengers were unnecessary.

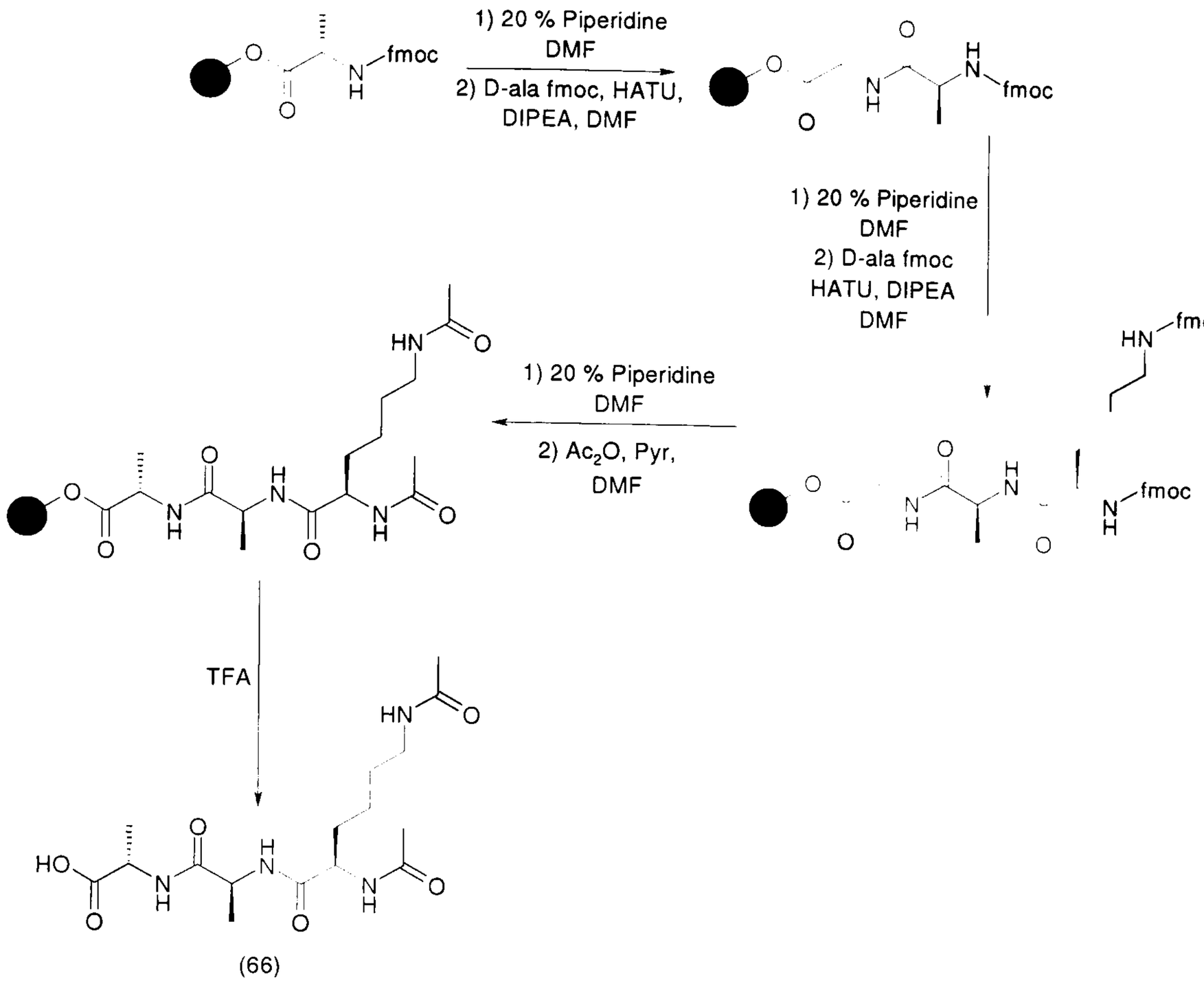

Scheme 3.31.

The synthesis was performed on 500 mg of pre-loaded resin (0.8 mmol/g loading) and was monitored by both Kaiser test and a test cleavage of small samples from the resin for LCMS analysis, by both measures the synthetic scheme appeared successful. A small-scale cleavage on 117 mg of resin yielded 31 mg of tripeptide (66) as a glassy solid. Repeating this step on the bulk of the compound yielded a further 98 mg. However, LCMS analysis of these samples showed the presence of a peak at 387 m/z, which corresponds to the methyl ester. This was present in both samples but was stronger in the large scale cleavage. The ^{1}H NMR spectra did not agree with the LCMS analysis; as the methyl ester was not observed in the small sample, but was present as a minor impurity in the large sample. HPLC analysis showed two major components in each sample, the samples were therefore combined and purified by preparative HPLC, and then the resulting product fractions were freeze-dried, yielding 31 mg, 21 %. The presence of the methyl ester impurity is not understood at this point, but it is possibly derived by inadvertent acid catalysed esterification, where residual TFA from the cleavage step catalyses a reaction with the methanol that was added to the sample to prepare aliquots for analysis.

3.4.4 Conclusions on the tripeptide synthesis

The failure of the designed route to produce the desired compound was a significant setback, particularly after the efforts to improve the synthesis had been so successful. Use of the methyl ester of lysine increased the yield and improved the purity of the product and replacing DDC with EDC gave both better yields and eased the purification.

It is believed that the racemisation of the chiral centres was the result of the use of an excess of lithium hydroxide in the cleavage of the methyl esters. Three equivalents were used, as this was a procedure that had been successfully employed within the group before. However the earlier use did not highlight this problem. One equivalent should be sufficient to cleave the methyl esters and this might limit any racemisation, or the use of methyl esters could be revised and an alternative acid protecting group used; benzyl esters maybe a good choice as they would offer a chromophore that would aid purification on silica column.

The solid-phase synthesis has provided sufficient material to test the analogues against Ac_2KAA (66); unfortunately neither Ac_2KAS (67) nor Ac_2KAlac (68) have been synthesised.

3.5 Testing

There are a great many ways to establish the association constants for the analogues produced during this project; UV difference spectroscopy, nanoelectrospray ionisation – mass spectrometry (nano ESI-MS), measurement of shifting signals in ^1H NMR on complex formation and surface plasmon resonance (SPR) are examples of the numerous techniques available. There are also biological methods to asses if the analogues have increased affinity to the complete peptide wall, minimum inhibitory concentration measurements for example, although most of the biological methods are not direct measures of affinity as they are dependant upon other factors like adsorption, solubility and lack of resistance in the target organism.

3.5.1 Nanoelectrospray ionisation – mass spectrometry (nano ESI-MS)

3.5.1.1 The precedent

Jørgensen, Roepstorff and Heck[40] established nano ESI-MS as a technique to directly quantify the binding interactions of glycopeptides and cell wall precursors without the need to use titration curves. The first step in establishing this technique was to prove the solution phase stereospecificity for sequences terminating in D-ala-D-ala is preserved when the ionisation under nanoflow conditions occurs. They did this by analysing the region for the doubly charged complex of the MS produced by injecting an equimolar mixture of diacetyl-L-lys-D-ala-D-ala; diacetyl-L-lys-L-ala-L-ala d_6 and vancomycin in ammonium acetate buffer. The complex for the D-isomer was observed but the L-isomer was not, which is consistent with the results determined in solution.[36]

The presence of the deuterium label enables the two complexes to be distinguished, as complexes of the same molecular weight are indistinguishable by this technique. To ensure that the deuterium label did not have an effect on the complex formation they performed another experiment with equimolar amounts of acetyl-D-ala-D-ala-D-ala; acetyl-D-ala-D-ala-D-ala d_3 and vancomycin and found that there was no difference in the abundance of the deuterated and non- deuterated complexes.

They then went on to derive the association constants of vancomycin and ristocetin with five cell wall peptide analogues at three different concentrations. They found that the constants obtained at each concentration were in agreement with each other and with the published results of Neito *et al.*[41] obtained using different techniques. Thus showing that this technique is a valid way to directly quantify the solution binding properties of glycopeptides of the vancomycin family.

Heck and van de Kerk-van Hoof[42] used nano ESI-MS to calculate the association constants of α- and β- avoparcin and interestingly in this paper they also quote the ESI MS derived constant of vancomycin and compare it to the literature values; the ESI MS derived constant is 7.3×10^5 and the literature values quoted are 1.5×10^6 from Neito and Perkins,[36] 4.1×10^5 from Allen *et al.*[43] and 3.0×10^5 from Popieniek and Pratt.[44]

Numerous other papers have been produced that have used nano ESI-MS to analyse complexes of many variants of the cell wall mimicking peptide,[45–48] including a water

soluble variant of lipid II[49] and a range of glycopeptides. In addition, the process of dimerisation in glycopeptide binding has been investigated with this technique.[50]

3.5.1.2 The theory

The calculation of ligand binding affinity by nano ESI-MS involves measuring the ions produced by the free glycopeptide and its non-covalent complexes with the peptide ligand. The method relies on the assumption that the ion abundance is equivalent to the solution concentration, when applied to vancomycin this assumption means that the technique relies on vancomycin (1447 Da) ionising to the same degree as the non-covalent complex (~ 1700-1900 Da, dependant on peptide ligand). It also assumes that complex formation does not significantly alter the physcio-chemical properties like hydrophobicity and polarity that are also important in ionisation.[48] However, the work of Heck *et al.*[40] substantiated this assumption by deriving association constants that were comparable to those present in the literature obtained by other means, but they also showed that the conditions for ionisation must be sufficient to de-solvate the species as they are introduced to the machine and ionise them without destroying the complex and that the stability of the complex was dependant on pH, so the solutions must therefore be buffered.

3.5.1.3 The testing in practice

The nano ESI-MS testing was performed in the laboratory of Dr Alison Ashcroft, Astbury Centre for Structural Molecular Biology, Department of Biochemistry and Microbiology, University of Leeds.

The technique used in this project was based on that of Jørgensen, Roepstorff and Heck,[40] but this work simplified the process by considering equimolar mixtures of each glycopeptide and the Ac_2KAA tripeptide separately, as opposed to using three different cell wall mimics as they did. The three analogues, vancomycin and the hexapeptide were each separately prepared in equimolar mixtures with Ac_2KAA. Vancomycin and the hexapeptide were run as controls to validate the results achieved.

Each of the glycopeptides was run three times using equimolar (200 μM) mixtures of Ac_2KAA and the glycopeptide, results were recorded over 50 scans, the scans were

summed and the profile data was centred by mass. Both 1+ and 2+ ions were observed. Figure 3.18 shows a typical MS trace achieved.

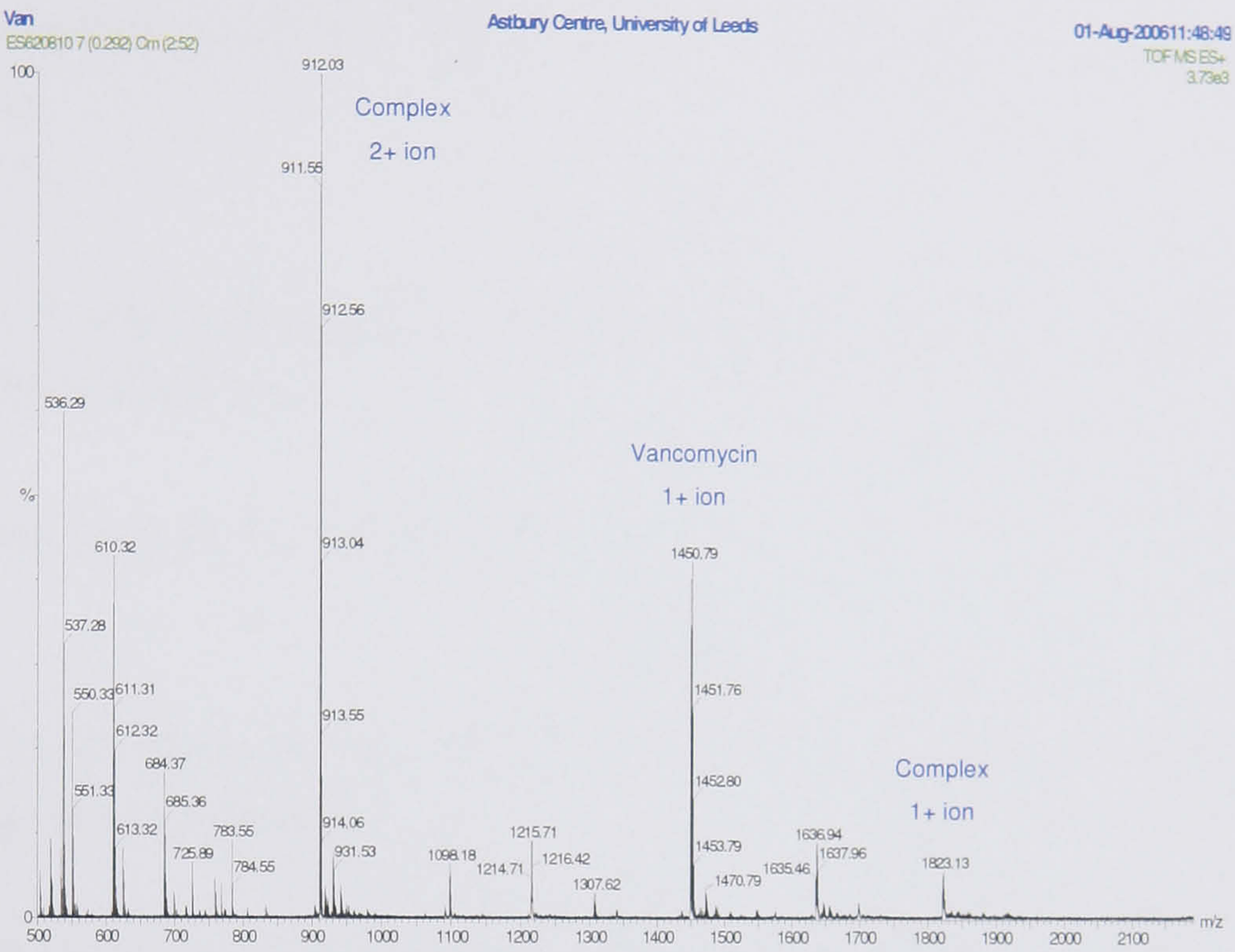

Figure 3.18. MS trace achieved with a 1:1 ration of vancomycin and Ac_2KAA.

The MassLynx software was used to convert the total ion counts spectra to a list of mass versus peak area, and for each injection the abundance of each type of ion was calculated by summing the peak area for all the mass centred peaks from each ion type, then the ions (e.g. 1+ and 2+) for the complex were added together and all the ions for the free glycopeptide were added together.

This gave two abundances one for the complex (c) and one for the free glycopeptide (fg), adding these together gives the total response for all the glycopeptide injected (tg). As the initial solution injected was prepared by mixing equal volumes of two 200 μM solution we know that the initial concentration of the glycopeptide in the solution must have been 100 μM. The concentration of complex [c] can be calculated in μM by:

$$[c] = \frac{c}{tg/100}$$

To get the concentration of the complex in M, the equation would be:

$$[c] = \frac{c/1000000}{tg/100}$$

Which can be simplified to:

$$[c] = \frac{c/10000}{tg}$$

The corresponding equation to obtain the molar concentration of the free glycopeptide would be:

$$[fg] = \frac{fg/10000}{tg}$$

Where c = complex abundance, fg = free glycopeptide abundance and tg = total glycopeptide abundance.

The equation to calculate the association constant is:

$$K_a = \frac{[c]}{[fg] \times [ft]}$$

Where [c] = complex concentration, [fg] = free glycopeptide concentration and [ft] = free tripeptide concentration.

We have two of the three values needed to calculate the association constant, the remaining missing value [ft] can not be calculated directly in this experiment, as the tripeptide is much smaller and has completely different physico-chemical properties to the free glycopeptide and the complex, and would therefore ionise differently, but it can be easily inferred.

The complex is a one to one complex, one glycopeptide and one tripeptide, the mixture is an equimolar combination of tripeptide and glycopeptide. Therefore for every glycopeptide molecule in the complex, there is one tripeptide molecule in the complex; but also for every free glycopeptide molecule, there is a free tripeptide. So, [fg] = [ft] and the equation to calculate the association constant can thus be simplified to:

$$K_a = \frac{[c]}{[fg]^2}$$

This was used to calculate the values in Table 3.4 below, which shows the association constant obtained for each injection, the average association constant for the three injections and the ratio of the association constant for each glycopeptide compared to vancomycin. The analogues are identified by the terminal amino acid of the extending fragment.

Glycopeptide	K_a (M^{-1}) from injection:			Average K_a (M^{-1})	Ratio to vancomycin
	1	2	3		
Hexapeptide (50)	1.07E+03	1.02E+03	8.00E+02	9.63E+02	0.016
Vancomycin (47)	7.31E+04	6.25E+04	5.10E+04	6.22E+04	1
Glycine Analogue (58)	1.07E+05	8.98E+04	8.54E+04	9.41E+04	1.512
Phenylglycine Analogue (63)	9.24E+04	8.01E+04	8.11E+04	8.45E+04	1.359
Phenylalanine Analogue (61)	1.74E+05	1.59E+05	1.63E+05	1.65E+05	2.658

Table 3.4. K_a data generated from nano ESI-MS runs.

The association constant obtained for vancomycin (6.22×10^4) is lower than the 7.3×10^5 reported by Jørgensen, Roepstorff and Heck[40] and is outside the literature range of 3.0×10^5 to 1.5×10^6. However, the relationship between the values obtained for the hexapeptide and vancomycin confirm the technique is able to measure the relative affinity, as it is known that removing the terminal *N*-methyl-D-leucine residue destroys the binding pocket and results in loss of antibacterial activity.[34] Removal of this residue results in a 65-fold reduction in the observed binding affinity. This dramatic reduction in affinity were also observed in other glycopeptides by Allen *et al.*[30] They found that converting LY264826 to its hexapeptide LY312607 produced a 115-fold reduction in binding affinity and converting LY307599 to it's hexapeptide LY314015 produced a 590-fold reduction in binding affinity, as measured by affinity capillary electrophoresis.[30]

The observation of increased association constants for every analogue, as compared to vancomycin under the same conditions, was a important accomplishment for this project. In particular the observation of greater than two-fold increase for the D-phenylalanine analogue was especially gratifying. These values are not necessarily the absolute values for the association constants of these glycopeptides, as the orders of magnitude are significantly different from the range previously quoted for vancomycin. The extending fragments are fulfilling their purpose and offer extra contacts to the tripeptide, increasing the affinity for the peptide sufficiently not only to compensate for the loss of the contribution from the *N*-methyl-D-leucine residue, but to exceed it and increase the affinity for the tripeptide as was designed.

3.5.2 Minimum inhibitory concentration (MIC)

MIC measurements were performed on the hexapeptide, vancomycin and three analogues by Dr. Julieanne Bostock in the Institute for Molecular and Cellular Biology, Department of Biochemistry and Microbiology, University of Leeds. These were performed as a standard two-fold dilution series. The MIC determined is the lowest concentration required to inhibit bacterial growth. Growth was monitored by measurement of the optical density readings at 600nm, while the culture was incubated at 37 °C for 16 hrs. MIC were determined against *E. coli* 1441; an *E. coli* mutant, SM1411, in which the drug efflux pump present in the outer membrane is disabled; and *S. aureus* 8325-4 as shown in Table 3.5.

Compound	*E. coli* 1441 (μg/ml)	SM1411 (μg/ml)	*S. aureus* 8325-4 (μg/ml)
Hexapeptide (50)	>512	>512	>512
Vancomycin (47)	1	1	1
Glycine Analogue (58)	>512	>512	256
Phenylglycine Analogue (63)	>512	>512	64
Phenylalanine Analogue (61)	>512	>512	128

Table 3.5. MIC data for vancomycin, vancomycin hexapeptide and analogues.

This showed that the hexapeptide was inactive as was expected, vancomycin was active against all strains and the analogues were only active against the Gram-positive *S. aureus*. This was unusual, as vancomycin should not inhibit the growth of Gram-negative bacteria, as it should not pass through the outer membrane of the bacteria. This suggested that the vancomycin sample was contaminated with a broad spectrum bactericidal agent and thus prompted the examination of the sample of vancomycin used in the MIC. The supply of vancomycin used was rated at > 95 % purity by the supplier, but HPLC analysis (Appendix B) shows that the sample is far more impure than that (< 75 %, as indicated by HPLC peak area). A sample of this has been purified by HPLC, but unfortunately it was not possible to repeat this testing before the submission of this document.

Nicolaou[31] reports the MIC of vancomycin against a different strain of *S. aureus*, 4002, as 0.39 μg/ml and Kahne[51] reports MIC's against three further strains of *S. aureus*; MB2985 as 0.5 μg/ml, CL3033 as 1 μg/ml and COL as 1 μg/ml. So it appears that the

anomalous activity of vancomycin in this assay only extends to it inhibiting growth in Gram-negative bacteria and the MIC value against *S. aureus* is of an appropriate magnitude.

It was disappointing that the MIC values for the analogues were lower than that expected for vancomycin and the increase in affinity demonstrated in the nano ESI-MS study did not translate into biological activity.

It was also unfortunate that there was not the opportunity to test the analogues against *S. aureus* strains resistant to vancomycin before the submission of this document.

3.5.3 Conclusion on testing

It was gratifying to achieve increased affinity as measured in the nano ESI-MS, as this was the aim of the project. It was disappointing, but not entirely unexpected, that this did not translate into increased biological activity as measured by the MIC assay. The lack of an increase in biological activity was considered possible because biological activity is dependant upon more than just the affinity for the target. There are factors which affect the biological activity of glycopeptides such as the dimerization, which is important in their mode of action, and also subtle changes in the charge density around the molecule can play significant roles in determining the conformation of the compound. An example of this is the potential interactions between the positively charged piperazine ring and amino group of the sugar, this could introduce a repulsive interaction that changes the conformation of the sugar and which could have an implication for both the binding of the tripeptide and on the dimerization of the compound, and thus affect the biological activity.

However, both the MIC and the nano ESI-MS show that the extending groups must be forming contacts to the peptide targets, as in both instances the analogues have better results than the hexapeptide and this validates the modelling results further, ruling out one possible result which could have the extending fragment adopting a conformation which rotated it away from the peptide and into solution and would have thus given the analogues an affinity for the tripeptide around the same magnitude as that observed for the hexapeptide.

3.6 Conclusions and future work

The project succeeded in its initial aims to design, synthesise and test analogues of vancomycin in order to produce increased affinity for the tripeptide mimic diacetyl-L-lys-D-ala-D-ala. This is the first example of rational drug design being applied to a complex natural product drug, like vancomycin, in order to produce semi-synthetic derivatives with increased affinity for their targets.

This work sets out a synthetic route to a series of analogues, which could be easily exploited to create further analogues. It also offers the possibility of furnishing the rigidified analogue with further synthetic efforts. Further exploration of the convergent synthesis towards the piperazines protected with benzyl and *tert*-butyl ester groups offers a route into a further series of analogues, which terminate in the free acid.

It would also be interesting to test the analogues produced and any further analogues created against mimics of the resistant cell walls and in whole cell assays against bacterial strains resistant to vancomycin.

3.7 References

(1) Kocienski, P. J. *Protecting Groups*; Georg Thieme Verlag: New York, 1994; 259.

(2) Witiak, D. T.; Nair, R. V.; Schmid, F. A. Synthesis and Antimetastatic Properties of Stereoisomeric Tricyclic Bis(dioxopiperazines) in the Lewis Lung Carcinoma Model. *J. Med. Chem.* **1985**, *28*, (9), 1228-1234.

(3) Booij, L. H. D. J.; van der Broek, L. A. G. M.; Caulfield, W.; Dommerholt-Caris, B. M. G.; Clark, J. K.; van Egmond, J.; McGuire, R.; Muir, A. W.; Ottenheijm, H. C. J.; Rees, D. C. Non-depolarizing Neuromuscular Blocking Activity of Bisquaternary Amino Di- and Tripeptide Derivatives. *J. Med. Chem.* **2000**, *43*, (25), 4822-4833.

(4) Horton, J. The Design and Synthesis of New and Selective Inhibitors of Bacterial MurD. In *Department of Chemistry*; University of Leeds: Leeds, 2003; pp 175.

(5) Jones Jr, M. *Organic Chemistry*; W W Norton & Company: New York, 1997; pp 305-306.

(6) Mukaiyama, T.; Usui, M.; Schimada, E. A Convenient Method for the Synthesis of Carboxylic Esters. *Chem. Lett.* **1975**, *4*, (10), 1045-1048.

(7) Nozaki, S.; Kimura, A.; Muramatsu, I. Rapid Peptide Synthesis in Liquid Phase. Preparation of Angiotensin II as an Example. *Chem. Lett.* **1977**, 1057-1058.

(8) Nozaki, S.; Muramatsu, I. Rapid Peptide Synthesis in Liquid Phase. Preparation of Angiotensin II and Delta-sleep-inducing Peptide by the "Hold-in-Solution" Method. *Bull. Chem. Soc. Jpn.* **1982**, *55*, 2165-2168.

(9) Miyashita, K.; Iwaki, H.; Tai, K.; Murafuji, H.; Sasaki, N.; Imanishi, T. Regio- and stereoselective α-alkylation of *N*-terminalamino acid residue of peptides using a pyidoxal model compound with a chiral ansa-structure. *Tetrahedron* **2001**, *57*, 5773-5780.

(10) Osdene, T. S.; Santilli, A. A.; McCardle, L. E.; Rosenthale, M. E. Pteridinecarboxamide Diuretics. II. Reaction of 4,6-Diamino-5-nitropyrimidines with *N*-Substituted Cyanoacetamides. *J. Med. Chem.* **1967**, *10*, 165-171.

(11) Kataky, R.; Parker, D.; Teasdale, A.; Hutchinson, J. P.; Buschmann, H.-J. Binding Properties of Amide and Amide-Ester *N*-Functionalised Polyaza Macrocycles. *J. Chem. Soc., Perkin Trans. 2* **1992**, 1347-1351.

(12) White, B. D.; Mallen, J.; Arnold, K. A.; Fronczek, F. R.; Gandour, R. D.; Gehrig, L. M. B.; Gokel, G. W. Peptide Side-Arm Derivatives of Lariat Ethers and Bibracchial Lariat Ethers: Syntheses, Cation Binding Properties, and Solid State Structural Data. *J. Org. Chem.* **1989**, *54*, 937-947.

(13) O'Neil, I. A.; Potter, A. J.; Southern, J. M.; Steiner, A.; Barkley, J. V. Conformationally defined piperazine bis(*N*-oxides) bearing amino acid derived side chains. *J. Chem. Soc., Chem. Commun.* **1998**, 2511-2512.

(14) Lipowska, M.; Hansen, L.; Xu, X.; Marzilli, P. A.; Taylor, A. J.; Marzilli, L. G. New N_3S Donor Ligand Small Peptide Analogues of the *N*-Mercaptoacetyl-glycylglycylglycine Ligand in the Clinically Used Tc-99m Renal Imaging Agent: Evidence for Unusual Amide Oxygen Coordination by Two New Ligands. *Inorg. Chem.* **2002**, *41*, (11), 3032-3041.

(15) Hulme, A. N.; Curley, K. S. Approaches to the synthesis of (2R,3S)-2-hydroxymethylpyrrolidin-3-ol (CYB-3) and its C(3) epimer: a cautionary tale. *J. Chem. Soc., Perkin Trans. 1* **2002**, *8*, 1083-1091.

(16) Nozaki, S. Efficient Amounts of Additives for Peptide Coupling Mediated by a Water-soluble Carbodiimide in Aqueous Media. *Chem. Lett.* **1997**, 1-2.

(17) Lipshutz, B. H.; Vaccaro, W.; Huff, B. Protection of Imidazoles as their β–Trimethylsilylethoxymethyl (SEM) Derivatives. *Tetrahedron Lett.* **1986**, *27*, (35), 4095-4098.

(18) He, Y.; Chen, Y.; Du, H.; Schmid, L. A.; Lovely, C. J. A convenient synthesis of 1,4-disubstituted imiazoles. *Tetrahedron Lett.* **2004**, *45*, 5529-5532.

(19) Skorey, K. I.; Somayaji, V.; Brown, R. S. Direct O-Acylation of Small Molecules Containing CO_2^- --- HN <-- HO Units by a Distorted Amide: Enhancement of Amide Basicity by a Pendant Carboxylate in a Serine Protease Mimic. *J. Am. Chem. Soc.* **1989**, *111*, (4), 1445-1452.

(20) Danila, G.; Cojocaru, Z.; Nechifor, M.; Dorneanu, V. 8-[4-(Phenyl-1-piperazinyl)methyl]theophylline: Romania, 1986, RO 88944.

(21) Joshi, S.; Khosla, N.; Khare, D.; Sharda, R. Synthesis and *in vitro* study of novel Mannich bases as antibacterial agents. *Bioorg. Med. Chem. Lett.* **2005**, *15*, 221-226.

(22) Williams, D. H.; Butcher, D. W. Binding Site of the Antibiotic Vancomycin for a Cell-Wall Peptide Analogue. *J. Am. Chem. Soc.* **1981**, *103*, (19), 5697-5700.

(23) Loll, P. J.; Bevivino, A. E.; Korty, B. D.; Axelson, P. H. Simultaneous Recognition of a Carboxylate-Containing Ligand and an Intramolecular Surrogate Ligand in the Crystal Structure of an Asymmetric Vancomycin Dimer. *J. Am. Chem. Soc.* **1997**, *119*, (7), 1516-1522.

(24) Williamson, M. P.; Williams, D. H.; Hammond, S. J. Interactions of Vancomycin and Ristocetin with Peptides as a Model for Protein Binding. *Tetrahedron* **1984**, *40*, (3), 569-577.

(25) Kannan, R.; Harris, C. M.; Harris, T. M.; Waltho, J. P.; Skelton, N. J.; Williams, D. H. Function of the Amino Sugar and N - Terminal Amino acid of the AntibioticVancomycin in its Complexation with Cell Wall Peptides. *J. Am. Chem. Soc.* **1988**, *110*, 2946-2953.

(26) Edman, P. Method for Determination of the Amino Acid Sequence in Peptides. *Acta Chem. Scand.* **1950**, *4*, 283-293.

(27) Edman, P. Preparation of Phenyl Thiohydantoins from Some Natural Amino Acid. *Acta Chem. Scand.* **1950**, *4*, 277-283.

(28) Booth, P. M.; Williams, D. H. Preparation and Conformational Analysis of Vancomycin Hexapeptide and Aglucovancomycin Hexapeptide. *J. Chem. Soc., Perkin Trans. 1* **1989**, *12*, 2335-2339.

(29) Rydberg, P.; Lüning, B.; Wachtmeister, C. A.; Eriksson, L.; Törnqvist, M. Applicability of a Modified Edman Procedure for Measurement of Protein Adducts: Mechanisms of Formation and Degradation of Phenylthiohydantoins. *Chem. Res. Toxicol.* **2002**, *15*, (4), 570-581.

(30) Allen, N. E.; LeTourneau, D. L.; Hobbs, J. N.; Thompson, R. C. Hexapeptide Derivatives of Glycopeptide Antibiotics: Tools for Mechanism of Action Studies. *Antimicrob. Agents Chemother.* **2002**, *46*, (8), 2344-2348.

(31) Nicolaou, K. C.; Cho, S. Y.; Hughes, R.; Winssinger, N.; Smethurst, C.; Labischinski, H.; Endermann, R. Solid- and Solution-Phase Synthesis of Vancomycin and Vancomycin Analogues with Activity against Vancomycin-Resistant Bacteria. *Chem. Eur. J.* **2001**, *7*, (17), 3798-3823.

(32) Gerhard, U.; Mackay, J. P.; Maplestone, R. A.; Williams, D. H. The Role of the Sugar and Chlorine Substituents in the Dimerization of Vancomycin Antibiotics. *J. Am. Chem. Soc.* **1993**, *115*, (1), 232-237.

(33) Marshall, F. J. Structure Studies on Vancomycin. *J. Med. Chem.* **1965**, *8*, (1), 18-22.

(34) Nagarajan, R.; Schabel, A. A. Selective Cleavage of Vancosamine, Glucose and *N*-Methyl-leucine from Vancomycin and Related Antibiotics. *J. Chem. Soc., Chem. Commun.* **1988**, (19), 1306-1307.

(35) Nitanai, Y.; Kakoi, K.; Aoki, K., Complex of vancomycin with di-acetyl-lys-D-ala-D-ala, 2000, http://www.rcsb.org/pdb/explore.do?structureId=1FVM, accessed: September 2002.

(36) Nieto, M.; Perkins, H. R. Modification of the Acyl-D-alanyl-D-alanine Terminus Affecting Complex-Formation with Vancomycin. *Biochem. J.* **1971**, *123*, 789-803.

(37) Takeoka, S.; Mori, K.; Ohkawa, H.; Sou, K.; Tsuchida, E. Synthesis and Assembly of Poly(ethylene glycol)-Lipids with Mono-, Di-, and Tetraacyl Chains and a Poly(ethylene glycol) Chain of Various Molecular Weights. *J. Am. Chem. Soc.* **2000**, *122*, (33), 7927-7935.

(38) Abbenante, G.; March, D. R.; Bergman, D. A.; Hunt, P. A.; Garnham, B.; Dancer, R. J.; Martin, J. L.; Fairlie, D. P. Regioselective Structural and Functional Mimicry of Peptides. Design of Hydrolytically-Stable Cyclic Peptidomimetic Inhibitors of HIV-1 Protease. *J. Am. Chem. Soc.* **1995**, *117*, (41), 10220 - 10226.

(39) Novobiochem Synthesis Notes. *The Fine Art of Solid-Phase Synthesis*, 2002/3 catalog.

(40) Jørgensen, T. J. D.; Roepstorff, P.; Heck , A. J. R. Direct Determination of Solution Binding Constants for Noncovalent Complexes between Bacterial Cell Wall Peptide Analogues and Vancomycin Group Antibiotics by Electrospray Ionization Mass Spectrometry. *Anal. Chem.* **1998**, *70*, (20), 4427-4432.

(41) Nieto, M.; Perkins, H. R. The Specificity of Combination between Ristocetins and Peptides Related to Bacterial Cell Wall Mucopeptide Precursors. *Biochem. J.* **1971**, *124*, 845-852.

(42) van de Kerk-van Hoof, A.; Heck , A. J. R. Interactions of α- and β- avoparcin with bacterial cell-wall receptor-mimicking peptides studied by electrospray ionization mass spectroscopy. *J. Antimicrob. Chemother.* **1999**, *44*, 593-599.

(43) Allen, N. E.; LeTourneau, D. L.; Hobbs, J. N. Molecular interactions of a semisynthetic glycopeptide antibiotic with D-alanyl-D-alanine and D-alanyl-D-lactate residues. *Antimicrob. Agents Chemother.* **1997**, *41*, 66-71.

(44) Popieniek, P. H.; Pratt, R. F. Rates of specific peptide binding to the glycopeptide antibiotics vancomycin, ristocetin and avoparcin. *J. Am. Chem. Soc.* **1988**, *110*, 1285-1286.

(45) Jørgensen, T. J. D.; Staroske, T.; Roepstorff, P.; Williams, D. H.; Heck , A. J. R. Subtle differences in molecular recognition between modified glycopeptide antibiotics and bacterial receptor peptides identified by electrospray ionization mass spectrometry. *J. Chem. Soc., Perkin Trans. 2* **1999**, 9, 1859-1863.

(46) Bonnici, P. J.; Damen, M.; Waterval, J. C. P.; Heck , A. J. R. Formation and Efficacy of Vancomycin Group Glycopeptide Antibiotic Stereoisomers Studied by Capillary Electrophoresis and Bioaffinity Mass Spectrometry. *Anal. Biochem.* **2001**, *290*, 292-301.

(47) Vollmerhaus, P. J.; Tempels, F. W. A.; Kettenes-van der Bosch, J. J.; Heck , A. J. R. Molecular interactions of glycopeptide antibiotics investigated by affinity capillary electrophoresis and bioaffinity electrospray ionisation-mass spectrometry. *Electrophoresis (Weinheim, Fed. Repub. Ger.)* **2002**, *23*, 868-879.

(48) Heck , A. J. R.; Jørgensen, T. J. D. Vancomycin in vacuo. *International Journal of Mass Spectrometry* **2004**, *236*, 11-23.

(49) Vollmerhaus, P. J.; Breukink, E.; Heck , A. J. R. Getting Closer to the Real Bacterial Cell Wall Target: Biomolecular Interactions of Water-Soluble Lipid II with Glycopeptide Antibiotics. *Chem. Eur. J.* **2003**, 9, (7), 1556-1564.

(50) Staroske, T.; O'Brien, D. P.; Jørgensen, T. J. D.; Roepstorff, P.; Williams, D. H.; Heck , A. J. R. The Formation of Heterodimers by Vancomycin Group Antibiotics. *Chem. Eur. J.* **2000**, *6*, (3), 504-509.

(51) Ge, M.; Chen, Z.; Onishi, H. R.; Kohler, J.; Silver, L. L.; Kerns, R.; Fukuzawa, S.; Thompson, C.; Kahne, D. Vancomycin Deravatives That Inhibit Peptidoglycan Biosynthesis Without Binding D-Ala-D-Ala. *Science* **1999**, *284*, 507-511.

Chapter Four

Experimental

4.1 General procedures and instrumentation

Proton nuclear magnetic resonance spectra were recorded at 300 MHz on a Bruker DPX300 spectrometer, or at 500 MHz on a Bruker Avance 500 machine. Chemical shifts are expressed in parts per million (ppm) downfield of tetramethylsilane (singlet at 0 ppm, TMS) for samples in $CDCl_3$. Carbon 13 spectra were recorded at either 75 MHz or 125 MHz on the above spectrometers, respectively. Chemical shifts are expressed in parts per million, referenced to the central peak of the triplet of $CDCl_3$ (77.0ppm).

For ^{1}H NMR or ^{13}C NMR samples ran in alternative solvents the chemical shifts were calibrated such that the residual solvent peak matched published values. All coupling constants are quoted in Hertz (Hz). Multiplicities are as follows: s-singlet, d-doublet, t-triplet, q-quartet, quin-quintet, sept-septet, m-multiplet, obs-obscured. DEPT and 2-dimensional COSY and HMQC spectra were used to assist in the assignment of complex spectra. Where extensive overlapping of signals in 1-dimensional proton spectra was observed, multiplicities and coupling constants could not be resolved.

Electrospray (ES) spectra were recorded on a Micromass LCT K111 spectrometer, a Waters ZMD spectrometer or a Bruker MicrOTOF spectrometer. Molecular ions are reported as mass with percentage abundance quoted in brackets.

Optical rotations were recorded on an Optical Activity AA-1000 polarimeter and are quoted in units of 10^{-1} deg cm^2 g^{-1} as a solution in $CHCl_3$ or MeOH with the concentration quoted in brackets (g/100 ml).

Elemental analysis was carried out by the Microanalysis laboratory, School of Chemistry, University of Leeds, using a Carlo Erba Elemental Analyser MOD 1106.

Thin layer chromatography (TLC) was carried out using pre-coated glass-backed silica gel 60 F_{254} (Merck) plates, which were visualised using ultraviolet light and permanganate. Silica gel used for column chromatography was Merck flash silica 60. 37-70 μm particle size.

Analytical HPLC was carried out with CH_3CN in water on a Dionex/Gynkotek system equipped with 250 x 4.6 mm analytical columns using full-spectrum UV detection.

Preparative HPLC was carried out with CH_3CN and water on a Gilson preparatory system equipped with 250 x 21.2 mm preparatory columns using single-wavelength UV detection.

LCMS was carried out on a Waters Micromass ZQ equipped with a XTerra MS C18 5 μm 4.6 x 50 mm analytical column and a XTerra Prep MS C18 5 μm 19 x 50 mm preparatory column. Both methods use gradient elutions of water with 0.1 % formic acid and CH_3CN with 0.1 % formic acid. The gradients are shown in Table 4.1.

Time (minutes)	Method 1 (% CH_3CN)	Method 2 (% CH_3CN)
0-3.5	0	0
3.5-7.5	0 to 50	0 to 30
7.5-8	50 to 95	30 to 95
8-11	95	95
11-12	95 to 20	95 to 20
12-14	20	20

Table 4.1. LCMS methods.

Petrol refers to light petroleum (b. p. 40-60) and ether refers to diethyl ether. EtOAc and petrol were distilled before use. DCM was distilled over calcium hydride, THF was distilled over sodium and benzophenone, and MeOH was distilled from methoxide generated from a mixture of magnesium and iodine in MeOH before use. All other reagents were used as received.

Solvents were removed at reduced pressure using a Buchi rotary evaporator connected to a rotary oil pump, and followed by drying under high vacuum at 0.5 mmHg.

In all cases, except those using aqueous conditions, reactions were carried out under a positive pressure of dry, oxygen free nitrogen and glassware was oven dried before use.

4.2 Computational design

The computational designs in Section 2.3.1 were produced with version 3.4 of SPROUT on a Silicon Graphics machine, running a Unix operating system. The starting fragments and connecting fragments and results are described in Section 2.3.1. The structural variations (with altered amino acids, Section 2.4.1, and the rigidified structure, Section 2.4.2) were produced by editing structures in MOLOC. All the structures were re-scored using version 6.1 of SPROUT running on a Linux PC. The score data in all the figures in Sections 2.3.1, 2.4.1 and 2.4.2 come from SPROUT version 6.1.

4.3 Synthesis of extending fragments

4.3.1 The first synthesis of piperazine (2)

(4-*tert*-Butoxycarbonylmethyl-piperazin-1-yl)-acetic acid ethyl ester (7)

Conditions adapted from Witiak.[1]

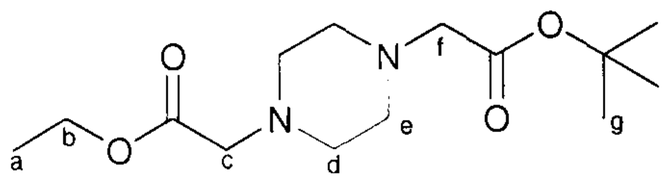

(7)

Piperazin-1-yl-acetic acid ethyl ester (3), (1.00 g, 5.81 mmol) and K_2CO_3 (2.01 g, 14.52 mmol, 2.5 eq) were dissolved in EtOH (25 ml). *tert*-Butyl bromoacetate (1.29 ml, 8.71 mmol, 1.5 eq) was then added and the reaction mixture was left stirring at room temperature for 50 hrs. The reaction mixture was concentrated *in vacuo*, then the residue dissolved in water (30 ml) and extracted with EtOAc (3 × 30 ml). The organic phases were then combined, dried with $MgSO_4$, filtered and then concentrated *in vacuo* to yield the title compound as an orange gum (1.42 g, 4.97 mmol, 86 %); δ_H ($CDCl_3$, 300 MHz) 4.18 (2H, q, J = 7.1, H_b), 3.21 (2H, s, $H_{c/f}$), 3.11 (2H, s, $H_{c/f}$), 2.65 (8H, bs, H_{d+e}), 1.46 (9H, s, H_g), 1.27 (3H, t, J = 7.1, H_a); δ_C ($CDCl_3$, 75 MHz) 170.7 (C), 169.9 (C), 81.5 (C), 61.0 (CH_2), 60.3 (CH_2), 59.9 (CH_2), 53.3 (CH_2), 53.2 (CH_2), 28.4 (CH_3), 14.6 (CH_3).

Data consistent with sample made in Section 4.2.2.

{4-[(*tert*-Butoxycarbonylmethyl-carbamoyl)-methyl]-piperazin-1-yl}-acetic acid ethyl ester (5)

Conditions adapted from Rees.[2]

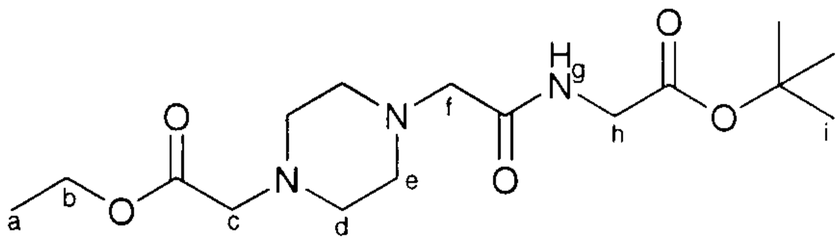

(5)

Piperazine (7) (0.92 g, 3.21 mmol) was dissolved in TFA (20 ml) and stirred for 4.5 hrs, before being concentrated *in vacuo*. Any excess TFA was then removed by exposure to high vacuum for 12 hrs. HOBt (0.43 g, 3.21 mmol, 1 eq), DCC (0.66 g, 3.21 mmol, 1 eq) and Et_3N (0.49 ml, 3.53 mmol, 1.1 eq) were added to the resultant residue, which was then dissolved in anhydrous DCM (30 ml) and stirred for 15 minutes. *tert*-Butyl glycine (0.54 g, 3.21 mmol, 1 eq) was then added and stirring maintained for ~ 95 hrs. The reaction mixture was then placed in the freezer overnight to precipitate the DCU by-product. The by-product was removed *via* filtration under reduced pressure and the filtrate was concentrated *in vacuo*. The resultant residue was then dissolved in 1M $NaHCO_3$ (40 ml) and extracted with EtOAc (3 × 30 ml); the organic layers were combined, dried with $MgSO_4$, filtered and evaporated to dryness. Final purification used preparative LCMS (method 1) and afforded the title compound as a brown oil (0.31 g, 0.901 mmol, 28%); δ_H ($CDCl_3$, 300 MHz) 7.59 (1H, bs, H_g), 4.19 (2H, q, J = 7.1, H_b), 3.97 (2H, d, J = 5.6, H_h), 3.25 (2H, s, $H_{c/f}$), 3.07 (2H, s, $H_{c/f}$), 2.67 (8H, bs, H_{d+e}), 1.47 (9H, s, H_i), 1.28 (3H, t, J = 7.1, H_a); δ_C ($CDCl_3$, 75 MHz) 170.8 (C), 170.6 (C), 169.3 (C), 82.6 (C), 61.6 (CH_2), 61.1 (CH_2), 59.6 (CH_2), 53.6 (CH_2), 53.3 (CH_2), 41.8 (CH_2), 28.5 (CH_3), 14.7 (CH_3); LCMS (method 1) *m/z* 344.3, retention time 6.31 minutes.

4.3.2 Synthesis of piperazine (2) *via* alternative protecting groups

(4-*tert*-Butoxycarbonylmethyl-piperazin-1-yl)-acetic acid ethyl ester (7)

Conditions adapted from Witiak.[1]

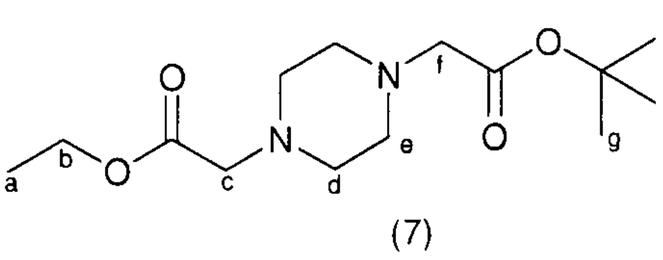

(7)

Piperazin-1-yl-acetic acid ethyl ester (3), (6.73 g, 39.1 mmol) and K_2CO_3 (13.51 g, 97.8 mmol, 2.5 eq) were dissolved in EtOH (100 ml). *tert*-Butyl bromoacetate (8.66 ml, 58.7 mmol, 1.5 eq) was then added dropwise over 15 minutes, after which the solution was stirred at room temperature for 24 hrs. The reaction mixture was filtered to remove the solid by-products and concentrated *in vacuo* to yield the title compound as an orange gum (10.10 g, 35.3 mmol, 90 %); δ_H ($CDCl_3$, 300 MHz) 4.18 (2H, q, J = 7.1, H_b), 3.21 (2H, s, $H_{c/f}$), 3.11 (2H, s, $H_{c/f}$), 2.65 (8H, bs, H_{d+e}), 1.46 (9H, s, H_g), 1.27 (3H,

t, J = 7.1, H_a); δ_C ($CDCl_3$, 75 MHz) 170.5 (C), 169.8 (C), 81.3 (C), 60.9 (CH_2), 60.2 (CH_2), 59.8 (CH_2), 53.2 (CH_2), 53.0 (CH_2), 28.4 (CH_3), 14.5 (CH_3); m/z (ES) 287.4 ($M+H^+$, 100 %), 573.6 ($2M+H^+$, 85 %); (Found: M^+, 287.1955. $C_{14}H_{27}N_2O_4$ requires M, 287.1965).

Amino-acetic acid tert-butyl ester (14)

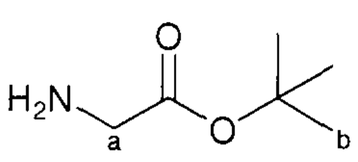

(14)

An excess of ammonia (70 ml) was condensed into a reaction vessel cooled at – 40 °C and then diluted with THF (40 ml). *tert*-Butyl bromoacetate (19.82 g, 102.0 mmol) was then added to this solution over 15 minutes; the resulting solution was then stirred for two hours at – 40 °C. The reaction mixture was then allowed to warm to room temperature whilst stirring for a further 14 hours. The solids were filtered off and the solution evaporated to dryness. This yielded the title compound as a pale yellow oil (4.22 g, 32.2 mmol, 32 %); δ_H ($CDCl_3$, 300 MHz) 3.36 (2H, s, H_a), 2.45 (2H, bs, NH_2), 1.48 (9H, s, H_b); δ_C ($CDCl_3$, 75 MHz) 171.4 (C), 81.6 (C), 51.2 (CH_2), 28.4 (CH_3).

^{1}H NMR is consistent with that reported by Lugtenburg *et al.*[3]

(4-*tert*-Butoxycarbonylmethyl-piperazin-1-yl)-acetic acid benzyl ester (11)

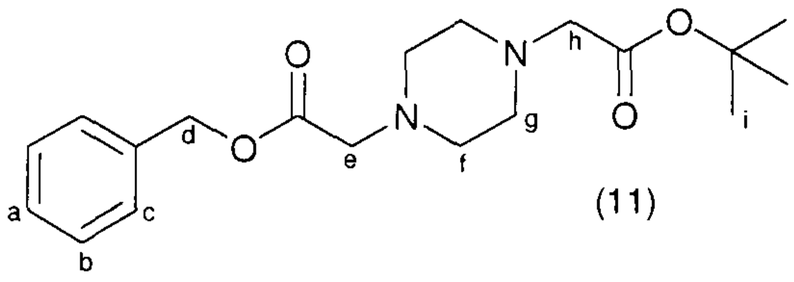

(11)

Piperazine (7) (0.50 g, 1.75 mmol) was dissolved in dry THF (10 ml), then benzyl alcohol (0.72 ml, 6.99 mmol, 4 eq) and NaH (60 % in mineral oil, 20 mg) were added to the stirred solution. The reaction was stirred at room temperature for 4.5 days, at which point MS indicated un-reacted piperazine (7) was still present. The reaction mixture was therefore concentrated under reduced pressure and then re-treated with benzyl alcohol (0.72 ml, 6.99 mmol, 4 eq) and NaH (60 % in mineral oil, 20 mg) in dry THF (10 ml). After a further 24 hrs stirring at room temperature the reaction had gone to completion as judged by MS, and the reaction mixture was concentrated *in vacuo*. The resultant solid was then dissolved in EtOAc (30 ml) and extracted with 0.25 M HCl solution (2 × 50 ml). The aqueous layers were then combined and basified (pH 8-9) with solid Na_2CO_3, before being extracted with DCM (3 × 50 ml). The organic layers were combined, dried with $MgSO_4$, concentrated *in vacuo* and then purified by preparative LCMS (method 2) to yield the title compound as a pale yellow oil, (0.431 g, 1.24 mmol, 71 %); δ_H ($CDCl_3$, 300 MHz) 7.33-7.20 (5H, m, H_{a-c}), 5.16 (2H, s, H_d), 3.27 (2H, s, $H_{e/h}$), 3.17 (2H, s, $H_{e/h}$), 2.67 (8H, bs, H_{f+g}), 1.46 (9H, s, H_i); δ_C ($CDCl_3$, 75 MHz) 170.4

(C), 129.0 (CH), 128.8 (CH), 81.9 (C), 66.8 (CH_2), 60.2 (CH_2), 59.7 (CH_2), 53.1 (CH_2), 28.5 (CH_3).

(4-*tert*-Butoxycarbonylmethyl-piperazin-1-yl)-acetic acid 2-trimethylsilanyl-ethyl ester

Conditions adapted from Horton[4] and Mukaiyama.[5]

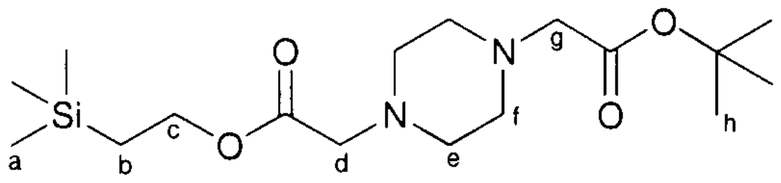

(9)

Piperazine (7) (0.20 g, 0.70 mmol) was dissolved in CH_3CN (2.5 ml) and a solution of lithium hydroxide (88 mg, 2.10 mmol, 3 eq) in water (2.5 ml) was added. The solution was stirred for 40 minutes and then evaporated to dryness. The residue was dissolved in anhydrous DCM (10 ml) and Et_3N (0.21 ml, 0.16 mmol, 2.2 eq), 2-trimethylsilanyl-ethanol (83 mg, 0.70 mmol, 1 eq) and 2-chloro-1-methyl-pyridinium iodide (0.21 g, 0.84 mmol, 1.2 eq) were added and the solution was stirred at room temperature. After ~80 hrs stirring starting material still remained, as indicated by MS. A further portion of 2-chloro-1-methyl-pyridinium iodide (0.357 g, 1.40 mmol) was added and the stirring continued for a further 72 hrs. The reaction mixture was diluted with DCM (40 ml) and then washed with water (4 × 50 ml), the aqueous layers were combined and extracted with DCM (50 ml), the organics were combined, dried with $MgSO_4$, filtered and evaporated to dryness. This gave the title compound as a brown gum (0.043 g, 0.35 mmol, 17 %) δ_H ($CDCl_3$, 300 MHz) 4.18 (2H, m, H_c), 3.15 (2H, s, $H_{d/g}$), 3.09 (2H, s, $H_{d/g}$), 2.63 (8H, bs, H_{e+f}), 1.42 (9H, s, H_h), 0.97 (2H, m H_b), 0.00 (9H, s, H_a); *m/z* (ES) 359.4 ($M+H^+$, 100 %), 314.5 ($M-{}^tBu+H^+$, 15 %).

4.3.3 Piperazine (2) *via* the benzyl ester

(4-Benzyloxycarbonylmethyl-piperazin-1-yl)-acetic acid (16)

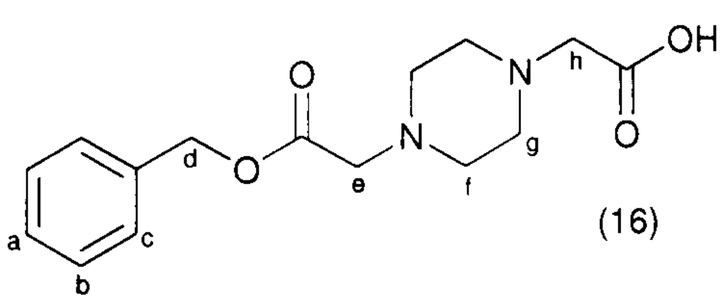

(16)

Piperazine (7) (0.50 g, 1.75 mmol) was dissolved in dry THF (10 ml), then benzyl alcohol (0.72 ml, 6.99 mmol, 4 eq) and NaH (60 % in mineral oil, 20 mg) were added to the stirred solution. The solution was stirred at room temperature for 40 hrs. LCMS analysis of the reaction mixture indicated that the reaction had still not gone to completion. The reaction mixture was therefore concentrated under reduced pressure and then re-treated with benzyl alcohol (0.72 ml, 6.99 mmol, 4 eq) and NaH (60 % in mineral oil, 20 mg) in dry THF (10 ml). After a further 40 hrs stirring at room temperature the reaction mixture was

concentrated *in vacuo*. Purification by column chromatography, using a gradient elution beginning with 2:1 petrol to EtOAc moving to neat EtOAc, removed two fast eluting impurities. The remaining material was removed from the column by washing with neat MeOH and the purified by LCMS (method 1). This afforded the title compound as an orange/brown solid (0.103 g, 20 %): δ_H ($CDCl_3$, 300 MHz) 7.40-7.29 (5H, m, H_{a-c}), 5.15 (2H, s, H_d), 3.52 (2H, bs, H_h), 3.45 (4H, bs, H_g), 3.33 (2H, bs, H_e), 2.89 (4H, bs, H_f); δ_C ($CDCl_3$, 75 MHz) 170.1 (C), 169.5 (C), 135.8 (C), 129.0 (CH), 128.9 (CH), 128.8 (CH), 67.0 (CH_2), 59.3 (CH_2), 58.7 (CH_2), 52.7 (CH_2), 50.5 (CH_2); *m/z* (ES) 293.3 ($M+H^+$, 100 %), 201.0 ($M-{}^tBu+H^+$, 75 %); (Found: M^+, 293.1501. $C_{15}H_{20}N_2O_4$ requires *M*, 293.1516).

4-[(*tert*-Butoxycarbonylmethyl-carbamoyl)-methyl]-piperazin-1-yl}-acetic acid benzyl ester (12)

Conditions adapted from Nozaki *et al.*[6,7]

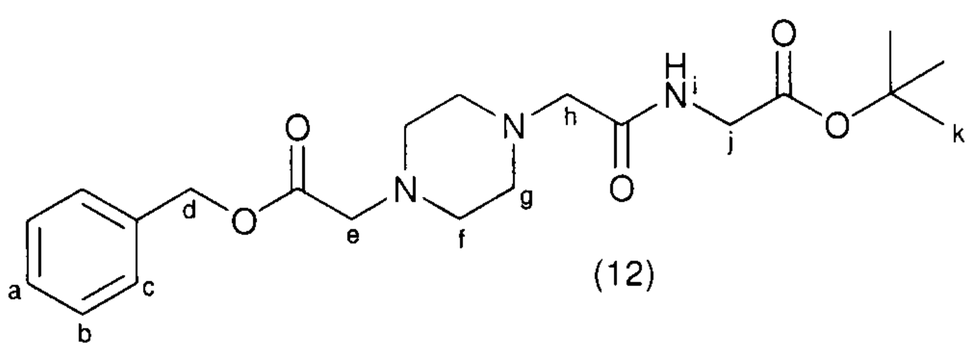

(12)

Piperazine (16) (50 mg, 0.17 mmol), glycine *tert*-butyl ester hydrochloride (29 mg, 0.17 mmol, 1 eq), Et_3N (0.024 ml, 0.17 mmol, 1 eq) and HOBt (23 mg, 0.17 mmol, 1 eq) were dissolved in 1,2-dichloroethane (10 ml). EDC (33 mg, 0.17 mmol, 1 eq) and water (4 ml) were then added and the biphasic mixture was stirred for 2.5 hrs at room temperature. The mixture was concentrated *in vacuo* and partitioned between ether (3 × 20 ml) and 0.5 M Na_2CO_3 solution (20 ml). The combined organics were dried with $MgSO_4$ and concentrated to give the title compound as a yellow oil (41 mg, 0.11 mmol, 60 %): δ_H ($CDCl_3$, 300 MHz) 7.62-7.58 (1H, m, H_i), 7.45-7.31 (5H, m, H_{a-c}), 5.20 (2H, s, H_d), 3.99 (2H, d, J = 5.6, H_j), 3.32 (2H, s, H_e), 3.09 (2H, s, H_h), 2.68 (8H, bs, H_{f+g}), 1.48 (9H, s, H_k); δ_C ($CDCl_3$, 75 MHz) 169.4 (C), 169.0 (C), 167.9 (C), 134.7 (C), 127.6 (CH), 127.4 (CH), 81.1 (C), 65.4 (CH_2), 60.3 (CH_2), 58.1 (CH_2), 52.3 (CH_2), 51.9 (CH_2), 40.4 (CH_2), 27.1 (CH_3); LCMS (method 1) *m/z* 406.2, retention time 7.30 minutes; *m/z* (ES) 833.4 (M_2+Na^+, 14 %), 811.5 (M_2+H^+, 56 %), 406.2 ($M+H^+$, 100 %); (Found: M^+, 406.2336. $C_{21}H_{32}N_3O_5$ requires *M*, 406.2336).

4.3.4 Convergent synthesis of piperazine (2)

Piperazin-1-yl-acetic acid benzyl ester (22)

Conditions adapted from Parker.[8]

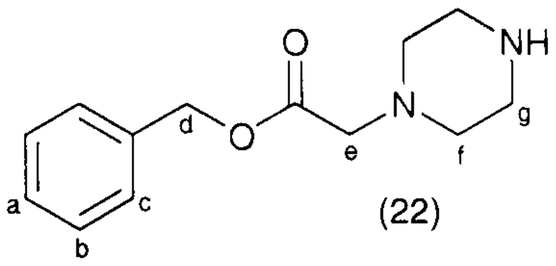

(22)

Anhydrous piperazine (0.50 g, 4.37 mmol, 2 eq) and K_2CO_3 (0.75 g, 5.46 mmol, 2.5 eq) were stirred in dry CH_3CN (20 ml) at room temperature. Benzyl bromoacetate (0.35 ml, 2.18 mmol) was added slowly over ten minutes, stirring was maintained for a further 3 hrs and then the reaction mixture was concentrated under reduced pressure. LCMS (method 1) showed the desired product (retention time: 6.13 mins; mass found: 235.3 *m/z*) and the dialkylated by-product (retention time: 7.52 mins; mass found: 383.1 *m/z*). The crude product was purified *via* silica gel chromatography (gradient elution, 10 – 50 % MeOH in $CHCl_3$). This gave the title compound as pale yellow solid (0.19 g, 0.81 mmol, 37 %): δ_H ($CDCl_3$, 300 MHz) 7.45-7.31 (5H, m, H_{a-c}), 5.20 (2H, s, H_d), 3.29 (2H, s, H_e), 2.98 (4H, t, J = 4.9, $H_{f/g}$), 2.60 (4H, t, J = 4.9, $H_{f/g}$); δ_C ($CDCl_3$, 75 MHz) 170.6 (C), 136.1 (C), 129.0 (CH), 127.8 (CH), 127.8 (CH), 66.8 (CH_2), 60.3 (CH_2), 54.4 (CH_2), 46.2 (CH_2); LCMS (method 1) *m/z* 235.3, retention time 6.17 minutes; *m/z* (ES) 235.1 ($M+H^+$, 100 %); (Found: M^+, 235.1432. $C_{13}H_{19}N_2O_2$ requires *M*, 235.1441).

(2-Chloro-acetylamino)-acetic acid tert-butyl ester (31)

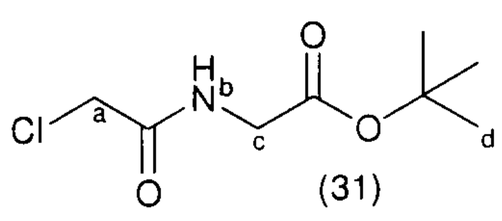

(31)

tert-Butyl glycine hydrochloride (1.00 g, 5.97 mmol) and DIPEA (3.12 ml, 17.91 mmol, 3 eq) were dissolved in dry DCM (5 ml) and stirred at room temperature. A solution of chloroacetylchloride (0.48 ml, 5.97 mmol, 1 eq) in DCM (10 ml) was added slowly to the reaction mixture over approximately 1 hr, whilst stirring was maintained. The colourless solution turned amber on addition of the chloroacetylchloride and darkened to brown/black by the time the addition was complete. The reaction mixture was stirred for a further 14 hr at room temperature and then evaporated to dryness. The crude solid was partitioned between EtOAc (200 ml) and water (300 ml). The aqueous layer was then extracted with a further portion of EtOAc (200 ml). The organics were then combined, dried with $MgSO_4$, filtered and evaporated. The resultant oily solid was purified *via* silica gel chromatography using a 15 % ether in $CHCl_3$ as the eluent, which afforded the title compound as a yellow crystalline solid (0.90 g, 4.34 mmol, 73 %): (Found: C, 46.4; H, 6.65; N, 6.5; Cl, 17.2; $C_8H_{14}ClNO_3$ requires: C, 46.3; H, 6.80; N, 6.8; Cl, 17.1 %); δ_H ($CDCl_3$, 300 MHz) 7.02 (1H, m, H_b), 4.02 (2H, s, H_a), 3.91 (2H, d,

J = 5.1, H_c), 1.50 (9H, s, H_d); δ_C ($CDCl_3$, 75 MHz) 168.7 (C), 166.4 (C), 83.2 (C), 42.8 (CH_2), 42.6 (CH_2), 28.4 (CH_3); LCMS (method 1) *m/z* 208.4, retention time 8.06 minutes; *m/z* (ES) (Found: M^+, 152.0110. $C_4H_7NO_3Cl$ requires *M*, 152.0114).

4.3.5 Piperazine methyl esters

2-Amino-propionic acid methyl ester hydrochloride (34)[9]

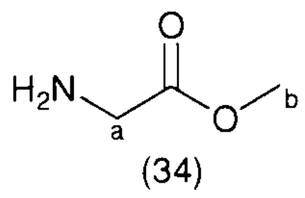

(34)

Acetyl chloride (7.10 ml, 100 mmol, 3 eq) was added dropwise to stirred dry MeOH (40 ml) at 0 °C and stirring maintained for 15 minutes after completion of the addition. Glycine (2.50 g, 33 mmol) was then added in small portions with vigorous stirring. This solution was refluxed for 3 hrs. The reaction mixture was then concentrated under vacuum and afforded the title compound as a white powdery solid (4.15 g, 33 mmol, 99 %); (Found: C, 28.5; H, 6.30; N, 11.0; Cl, 28.1; $C_3H_8ClNO_2$ requires: C, 28.7; H, 6.42; N, 11.2; Cl, 28.2 %); δ_H (D_2O, 300 MHz) 3.89 (2H, s, H_a), 3.79 (3H, s, H_b); δ_C (D_2O, 75 MHz) 169.1 (C), 53.7 (CH_3), 40.4 (CH_2).

^{1}H NMR is consistent with that reported by Caballero *et al.*[10] and Stammer *et al.*[11]

{4-[(Methoxycarbonylmethyl-carbamoyl)-methyl]-piperazin-1-yl}-acetic acid tert-butyl ester (35)

Conditions adapted from Horton[4] and Nozaki.[12]

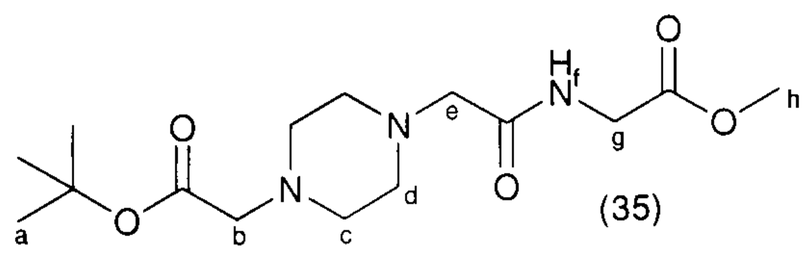

(35)

Piperazine (7) (0.50 g, 1.75 mmol) was dissolved in CH_3CN (5 ml) and a solution of lithium hydroxide monohydrate (0.22 g, 5.25 mmol, 3 eq) in water (5 ml) was added and the resultant solution was strired at room temperature for 45 min and then concentrated under reduced pressure. Glycine methyl ester hydrochloride (34) (0.33 g, 2.63 mmol, 1.5 eq), Et_3N (0.37 ml, 2.63 mmol, 1.5 eq), HOBt (0.36 g, 2.63 mmol, 1.5 eq) and EDC (0.50 g, 2.63 mmol, 1.5 eq) were added to this residue, which was then dissolved in anhydrous DMF (25 ml). The mixture was stirred for 44 hrs at room temperature and then diluted with water (100 ml). The solution was saturated with solid NaCl, then made basic (pH 7.5 – 8) with saturated $NaHCO_3$ solution. This was then extracted with ether (5 × 100 ml). The organics were then combined, dried ($MgSO_4$), filtered and concentrated *in vacuo*. This afforded the title compound as an orange/brown oil (0.30 g, 0.91 mmol, 53 %); δ_H ($CDCl_3$, 300 MHz) 7.67 (1H, m, H_f), 4.11 (2H, d, J = 5.1, H_g), 3.80 (3H, s, H_h), 3.17 (2H, s, H_b), 3.10

(2H, s, H_e), 2.69 (8H, bs, H_{c+d}), 1.51 (9H, s, H_a); δ_C ($CDCl_3$, 75 MHz) 171.1 (C), 170.9 (C), 169.9. (C), 81.7 (C), 61.6 (CH_2), 60.1 (CH_2), 53.7 (CH_2), 53.2 (CH_2), 52.8 (CH_3), 41.0 (CH_2), 28.5 (CH_3); LCMS (method 1) *m/z* 330.3, retention time 5.91 minutes; *m/z* (ES) (Found: M^+, 330.2036. $C_{15}H_{28}N_3O_5$ requires *M*, 330.2029).

2-Amino-3-phenyl-propionic acid methyl ester hydrochloride (37)[9]

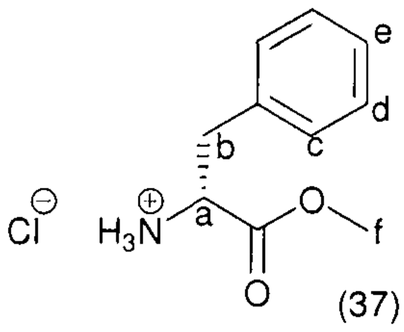

(37)

Acetyl chloride (1.29 ml, 18.0 mmol, 3 eq) was added dropwise to dry MeOH (15 ml) at 0 °C and stirring maintained for 10 minutes after completion of the addition. D-Phenylalanine (1.00 g, 6.1 mmol) was then added in small portions with vigorous stirring. This solution was refluxed for 3 hrs. The reaction mixture was then concentrated under vacuum to afford the title compound as a white powdery solid (1.29 g, 5.99 mmol, 99 %); mp 157-159 °C (lit.[13] 159-161 °C); $[\alpha]_D^{27}$ –25.6 (*c* 1.00 in MeOH); (lit.[13] –16.5 in MeOH); δ_H (D_2O, 300 MHz) 7.43-7.26 (3H, m, H_{d+e}), 7.25 (2H, d, J = 6.7, H_c), 4.39 (1H, dd, J = 7.6, 5.8, H_a), 3.80 (3H, s, H_f), 3.30 (1H, dd, J = 14.5, 5.8, H_b), 3.18 (1H, dd, J = 14.5, 7.6, $H_{b'}$); δ_C (D_2O, 75 MHz) 170.4 (C), 134.1 (C), 129.8 (CH), 129.7 (CH), 128.5 (CH), 54.5 (CH), 54.0 (CH_3), 36.0 (CH_2); δ_H (DMSO, 300 MHz) 8.85 (3H, s, NH_3), 7.40-7.16 (5H, m, H_{c-e}), 4.27-4.15 (1H, m, H_a), 3.64 (3H, s, H_f), 3.31-3.18 (1H, m, H_b), 3.10 (1H, dd, J = 14.5, 7.6, $H_{b'}$).

^{1}H NMR in DMSO is consistent with that reported by Gardossi *et al.*[14]

2-[2-(4-*tert*-Butoxycarbonylmethyl-piperazin-1-yl)-acetylamino]-3-phenyl-propionic acid methyl ester (38)

Conditions adapted from Horton[4] and Nozaki.[12]

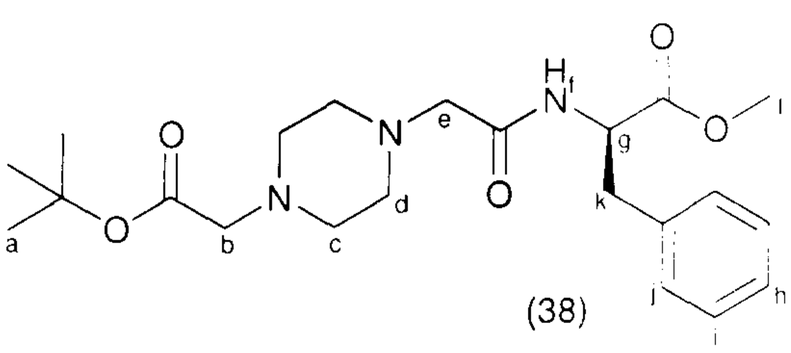

(38)

Piperazine (7) (1.33 g, 4.64 mmol) was dissolved in CH_3CN (2.5 ml) and a solution of lithium hydroxide monohydrate (0.58 g, 13.92 mmol, 3 eq) in water (2.5 ml) was added. The resultant solution was stirred at room temperature for 1 hr and then concentrated under reduced pressure. 2-Phenylalanine methyl ester hydrochloride (37) (1.00 g, 4.64 mmol, 1 eq), Et_3N (0.97 ml, 6.96 mmol, 1.5 eq), HOBt (0.75 g, 5.57 mmol, 1.1 eq) and EDC (0.98 g, 5.10 mmol, 1.1 eq) were added to the residue and then dissolved in anhydrous DMF (9.5 ml). The mixture was stirred for 25 hrs at room temperature, at which point LCMS indicated the starting material had been consummed. The reaction mixture was evaporated to dryness and the

product purified by silica gel column, eluting with neat EtOAc. LCMS indicated minor impurities and the crude material was therefore columned on alumina using 30 % petrol in EtOAc as the eluent. This afforded the title compound as a brown oil (0.28 g, 0.66 mmol, 15 %); $[\alpha]_D^{27}$ –16.4 (*c* 1.00 in $CHCl_3$); δ_H ($CDCl_3$, 300 MHz) 7.55 (1H, d, *J* = 8.1, H_f), 7.35-7.19 (3H, m, H_{h+i}), 7.12 (2H, d, *J* = 6.4, H_j), 4.89 (1H, ddd, *J* = 8.1, 6.9, 5.5, H_g), 4.75 (3H, s, H_l), 3.19 (1H, dd, *J* = 14.1, 5.5, H_k), 3.10 (1H, dd, *J* = 14.1, 6.9, $H_{k'}$), 3.08 (2H, s, H_b), 3.01 (2H, d, *J* = 16.4, H_e), 2.93 (2H, d, *J* = 16.4, $H_{e'}$), 2.60-2.39 (8H, m, H_{c+d}), 1.47 (9H, s, H_a) δ_C ($CDCl_3$, 75 MHz) 172.5 (C), 170.5 (C), 169.9 (C), 136.3 (C), 129.6 (CH), 129.1 (CH), 127.6 (CH), 81.6 (C), 61.5 (CH_2), 60.2 (CH_2), 53.5 (CH_2), 53.3 (CH_2), 52.8 (CH), 52.7 (CH_3), 38.1 (CH_2), 28.5 (CH_3); *m/z* (ES) 420.1 ($M+H^+$, 100 %), 442.2 ($M+Na^+$, 72 %), 420.1 ($M-{}^tBu+H^+$, 51 %); (Found M^+, 420.2467. $C_{22}H_{34}N_3O_5$ requires *M*, 420.2498).

[2-(4-*tert*-Butoxycarbonylmethyl-piperazin-1-yl)-acetylamino]-phenyl-acetic acid methyl ester (40)

Conditions adapted from Horton[4] and Nozaki.[12]

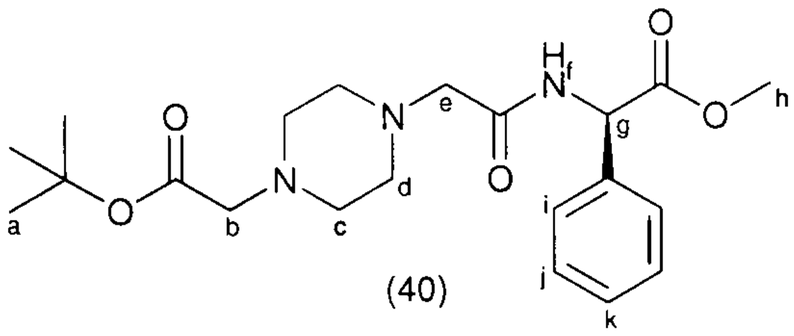

(40)

Piperazine (7) (500 mg, 1.75 mmol) was dissolved in CH_3CN (2 ml) and a solution of lithium hydroxide monohydrate (81 mg, 13.92 mmol, 1.1 eq) in water (2 ml) was added. The resultant solution was strired at room temperature for 35 minutes and then concentrated under reduced pressure. D-Phenylglycine methyl ester hydrochloride (529 mg, 2.62 mmol, 1.5 eq), Et_3N (1.22 ml, 6.99 mmol, 4 eq), HOBt (283 mg, 2.10 mmol, 1.2 eq) and EDC (402 mg, 2.10 mmol, 1.2 eq) were added and then the reactants were dissolved in anhydrous DMF (9 ml). The mixture was stirred for 12 hrs at room temperature, at which point MS indicated the starting material had been consummed. The reaction mixture was concentrated to a paste and then dissolved in $CHCl_3$ (50 ml) and then washed with 1M HCl (2 × 25 ml), saturated aqueous $NaHCO_3$ (2 × 25 ml) and water (2 × 25 ml). The aqueous layers were combined, made basic (pH ~9.5) and extracted with ether (5 × 50 ml). The organics, both ether and $CHCl_3$, were combined, dried with $MgSO_4$, filtered and evaporated to a yellow paste. The crude product was then purified by silica gel column with 1 % EtOH in EtOAc as the eluent, this afforded the title compound as an amber oil (0.224 g, 5.42 mmol, 32 %); $[\alpha]_D^{27}$ –58.4 (*c* 1.00 in $CHCl_3$); δ_H ($CDCl_3$, 300 MHz) 8.10 (1H, d, *J* = 8.0, H_f), 7.40-7.29 (5H, m, H_{i-k}), 7.25 (2H, d, *J* = 8.0, H_g), 3.73 (3H, s, H_h), 3.14 (2H, s,

H_b), 3.05 (2H, s, H_e), 2.73-2.49 (8H, m, H_{c+d}), 1.47 (9H, s, H_a): δ_C ($CDCl_3$, 75 MHz) 171.8 (C), 170.3 (C), 169.9 (C), 137.0 (C), 129.5 (CH), 129.0 (CH), 127.6 (CH), 81.6 (C), 61.6 (CH_2), 60.2 (CH_2), 56.2 (CH), 53.7 (CH_2), 53.3 (CH_2), 53.2 (CH_3), 28.6 (CH_3); *m/z* (ES) 406.0 ($M+H^+$, 100 %), 349.9 ($M-{}^tBu+H^+$, 28 %); (Found M^+, 406.2322. $C_{21}H_{32}N_3O_5$ requires *M*, 406.2336.

4.3.6 The rigid analogue synthesis

1,3-Dimethyl-9-(2-trimethylsilanyl-ethoxymethyl)-3,9-dihydro-purine-2,6-dione (43)

Condition adapted from Lovely *et al.*[15]

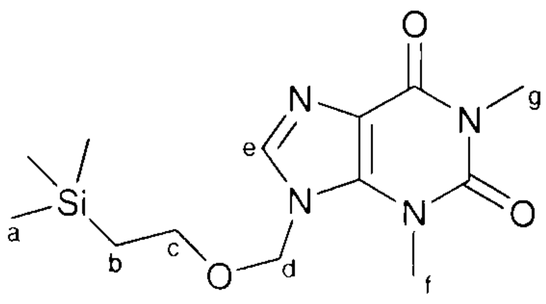

(43)

Theophylline (100 mg, 0.56 mmol) was dissolved in THF (5 ml) and the suspension was stirred and cooled to 0 °C. NaH (60 % in mineral oil, 24 mg, 0.61 mmol, 1.1 eq) was added in three portions and then the solution was allowed to stir for 90 minutes as it warmed to room temperature. The mixture was again cooled to 0 °C and (2-chloromethoxy-ethyl)-trimethyl-silane (97.9 µl, 0.56 mmol, 1 eq) was added drop wise over 5 minutes, stirring was maintained and the mixture was allowed to warm to room temperature. After 15 hrs, MS indicated the starting materials had been consumed and the reaction mixture was quenched by addition of water (2 ml) and then concentrated under vacuum. The residue was dissolved in DCM (30 ml) and washed with water (2 × 20 ml) and brine (2 × 20 ml) and then dried with $MgSO_4$, filtered and evaporated to dryness. The crude product was then purified *via* silica column using neat EtOAc as the eluent. This yielded the title compound as a yellow solid (0.102 g, 0.33 mmol, 59 %); (Found: C, 50.3; H, 7.25; N, 17.9; $C_{13}H_{22}N_4O_3Si$ requires: C, 50.3; H, 7.14; N, 18.1 %) δ_H ($CDCl_3$, 300 MHz) 7.76 (1H, s, H_e), 5.72 (2H, s, H_d), 3.66 (2H, m, H_c), 3.63 (3H, s, H_f), 3.44 (3H, s, H_g), 0.96 (2H, m, H_b), 0.00 (9H, s, H_a); δ_C ($CDCl_3$, 75 MHz) 156.6 (C), 153.1 (C), 150.3 (C), 142.9 (CH), 108.3 (C), 76.6 (CH_2), 68.6 (CH_2), 31.3 (CH_3), 29.5 (CH_3), 19.2 (CH_2), 0.00 (CH_3); LCMS (method 1) *m/z* 311.1, retention time 8.32 minutes.

[4-(1,3-Dimethyl-2,6-dioxo-2,3,6,9-tetrahydro-1H-purin-8-ylmethyl)-piperazin-1-yl]-acetic acid ethyl ester (46)

Condition adapted from Danila.[16]

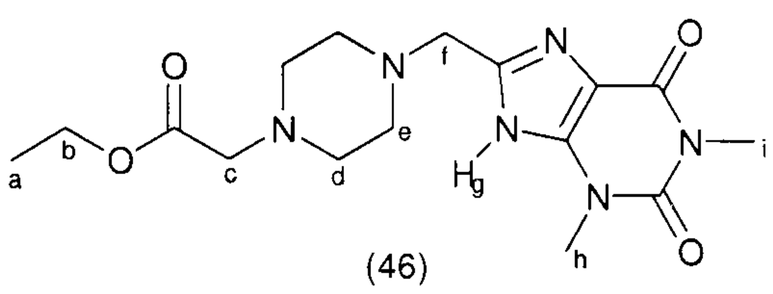

(46)

Theophylline (0.50 g, 2.78 mmol), piperazin-1-yl-acetic acid ethyl ester (3) (0.48 g, 2.78 mmol, 1 eq), formaldehyde (37 % in H_2O, 0.68 ml, 8.33 mmol, 3 eq) and acetic acid (32 µl, 0.56 mmol, 20 mol %) were dissolved in EtOH (10 ml) and heated to reflux. After 24 hrs LCMS indicated starting materials were still present, a further portion of acetic acid (32 µl, 0.56 mmol, 20 mol %) was added. TLC indicated theophylline was still present after a further 2 hrs, therefore solid *para*-formaldehyde (0.25 g, 8.33 mmol, 3 eq) and *p*-toluene sulphonic acid (5 mg, cat.) were added. MS after a further 24 hrs stirring indicated no theophylline, the reaction mixture was concentrated under vacuum and the crude product was separated by silica gel column using 20 % EtOH in EtOAc as the eluent. The final impurities were removed by re-crystallisation from EtOH and hexane to yield the title compound as an off-white solid (123 mg, 0.34 mmol, 12 %); (Found: C, 52.7; H, 6.65; N, 23.1; $C_{16}H_{24}N_6O_4$ requires: C, 52.7; H, 6.64; N, 23.1 %); δ_H ($CDCl_3$, 300 MHz) 4.19 (2H, q, J = 7.1, H_b), 3.77 (2H, s, H_f), 3.62 (3H, s, H_h), 3.45 (3H, s, H_i), 3.23 (2H, s, H_c), 2.66 (8H, bs, H_{d+e}), 1.27 (3H, d, J = 7.1, H_a); δ_C ($CDCl_3$, 75 MHz) 170.6 (C), 154.5 (C), 152.0 (C), 151.9 (C), 149.6 (C), 107.2 (C), 61.1 (CH_2), 59.6 (CH_2), 56.0 (CH_2), 53.5 (CH_2), 53.1 (CH_2), 30.6 (CH_3), 28.8 (CH_3), 14.7 (CH_3); *m/z* (ES) 365.2 ($M+H^+$, 100 %).

4.4 Synthesis of hexapeptide skeletons

The hexapeptide skeletons are significantly more complex than the earlier compounds and therefore have been named with an alternative system according to the conventions of Williams and co-workers.[17,18]

4.4.1 Vancomycin hexapeptide (47) synthesis

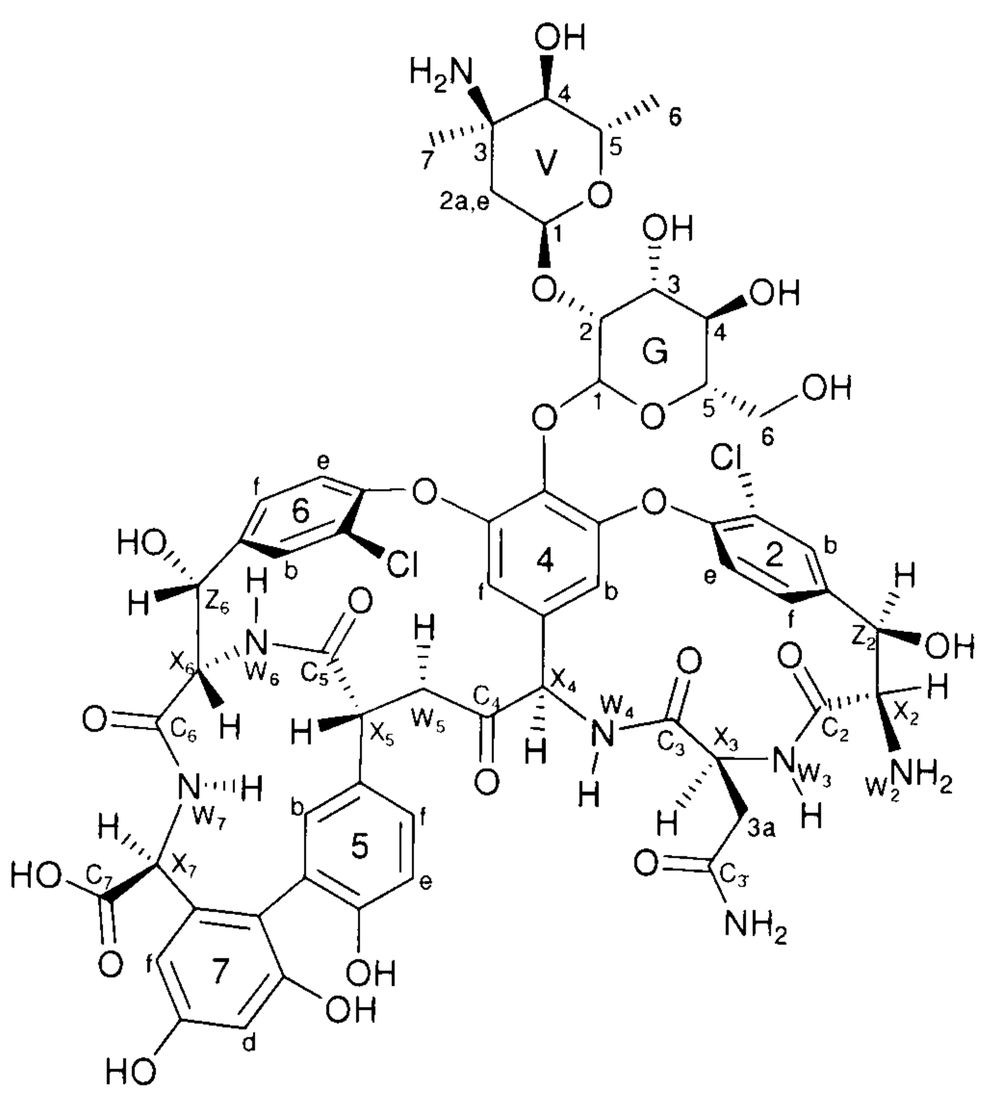

By the method of Booth and Williams.[17]: Phenyl isothiocyanate (18 µl, 148 µmol, 1.1 eq) in DMF (200 µl) was added to a solution of vancomycin hydrochloride (200 mg, 134 µmol) in pyridine (0.4 ml) and water (0.4 ml). The mixture was then stirred at room temperature. After 45 hrs MS showed the vancomycin had been consumed and indicated the presence of the mass ion, 1584 *m/z*, which corresponds to the thiourea. The solution was therefore evaporated to a paste without heating, water (2 ml) added and the mixture lyophilised. The resultant pale brown powder was dissolved in DCM (2 ml) and TFA (2 ml, excess) added. This solution was stirred for two minutes, and then evaporated to dryness without heating. The resulting solid was then dissolved in MeOH and purified using HPLC, on a discovery C-18 reverse phase column, with a gradient elution of 0 to 10 % CH_3CN in water with a 0.1 % TFA modifier. The resulting fractions containing vancomycin hexapeptide dissolved in dilute aqueous CH_3CN were then combined and concentrated *in vacuo* to yield a thick paste. This was then dissolved in water and lyophilised to afford the title compound as a colourless solid (72 mg, 55 µmol, 39 %); δ_H (d_6-DMSO, 500 MHz) 9.46 (1H, s, OH), 9.16 (1H, s, OH), 9.06 (1H, s, OH), 8.80 (1H, br s, W_5), 8.74 (1H, br s, Z_2OH), 8.57 (1H, d, J = 5.3, W_7), 8.53 (1H, br s, W_4), 7.87 (1H, s, 6b), 7.65 (1H, br s, W_2), 7.64 (1H, s, 2b), 7.51 (1H, d, J = 8.2, 2f), 7.46 (1H, d, J = 8.1, 6f), 7.34 (1H, d, J = 8.1, 6e), 7.33-7.16 (2H, obs, $CONH_2$), 7.22 (1H, d, J = 8.2, 2e), 7.16 (1H, br s, 5b), 6.78 (1H, d, J = 8.9, 5f), 6.72 (1H, d, J = 8.9, 5e), 6.67 (1H, d, J = 11.5, W_6), 6.58 (1H, br s, W_3), 6.41 (1H, d, J = 1.7, 7d), 6.27 (1H, d, J = 1.9, 7f), 5.94 (1H, d, J = 5.1, Z_6OH), 5.83 (1H, d, J = 7.8, Z_2), 5.64 (1H, s,

X_4), 5.46 (1H, d, J = 5.4, 4b), 5.36 (1H, br s, V_4OH), 5.29 (1H, s, G_3OH), 5.27 (1H, br s, G_1), 5.23 (1H, br s, V_1), 5.17 (1H, br s, 4f), 5.13 (1H, d, J = 5.1, Z_6), 5.09 (1H, br s, G_4OH), 4.68 (1H, q, J = 6.3, V_5), 4.51 (1H, br s, X_3), 4.46 (1H, d, J = 7.4, X_5), 4.44 (1H, d, J = 5.3, X_7), 4.19 (1H, d, J = 11.5, X_6), 4.07 (1H, br s, G_6OH), 3.70 (1H, br d, J = 10.7, G_{6a}), 3.67-3.58 (1H, m, X_2), 3.59-3.50 (1H, m, $G_{6a'}$), 3.54 (1H, obs, G_2), 3.46 (1H, obs, G_3), 3.28 (1H, obs, G_4), 3.26 (1H, br s, G_5), 3.20 (1H, br s, V_4), 2.93-2.80 (1H, m, 3a), 2.13 (1H, dd, J = 16.0, 9.7, 3a'), 1.91 (1H, br d, J 13.2, V_{2ax}), 1.74 (1H, br d, J = 13.2, V_{2eq}), 1.31 (3H, s, V_7), 1.07 (3H, d, J = 6.3, V_6): δ_C (d_6-DMSO, 75 MHz) 172.5 (C), 172.5 (C), 169.9 (C), 169.2 (C), 168.5 (C), 167.8 (C), 157.9 (C), 157.2 (C), 156.6 (C), 155.1 (C), 152.7 (C), 151.2 (C), 149.7 (C), 148.3 (C), 142.6 (C), 139.1 (C), 136.0 (C), 135.8 (CH), 135.3 (C), 131.8 (CH), 128.6 (CH), 127.4 (CH), 127.2 (CH), 127.2 (CH), 126.9 (C), 126.4 (C), 126.1 (C), 125.4 (CH), 123.4 (CH), 121.6 (C), 118.1 (C), 116.2 (CH), 116.2 (CH), 107.4 (CH), 105.7 (CH), 104.6 (CH), 102.4 (CH), 101.2 (CH), 96.7 (CH), 78.1 (CH), 77.1 (CH), 76.8 (CH), 71.6 (CH), 70.6 (CH), 70.1 (CH), 63.1 (CH), 61.8 (CH), 61.2 (CH_2), 56.7 (CH), 54.8 (CH), 53.9 (C), 53.7 (CH), 53.5 (CH), 53.5 (CH), 51.4 (CH), 41.8 (CH_2), 33.2 (CH_2), 22.3 (CH_3), 16.9 (CH_3).

Data consistent with that reported in the William's paper and numbered as reported.[17]

By base cyclisation: Conditions for thiourea formation from Williams *et al.*,[17] the cleavage and cyclisation adapted from the work of Törnqvist *et al.*[19]

Phenyl isothiocyanate (9 µl, 74 µmol, 1.1eq) in DMF (100 µl) was added to a solution of vancomycin hydrochloride (100 mg, 67 µmol) in pyridine (0.4 ml) and water (0.4 ml). The mixture was then stirred at room temperature. After 24 hrs MS showed the vancomycin had been consumed and the mass ion, 1584 *m/z*, which corresponds to the thiourea, was present. The solution was evaporated to a paste, then dissolved in 1M $NaHCO_3$ solution (30 ml, excess) and stirred for 4.5 hrs at room temperature under N_2. The reaction mixture was then washed with ether (2 × 10 ml) and evaporated to dryness, using MeOH to azeotrope the water and prevent foaming. The resulting solid was then dissolved in MeOH and purified using HPLC, on a Discovery C-18 reverse phase column, with a gradient elution of 0 to 10 % CH_3CN in water with a 0.1 % TFA modifier. The fractions containing vancomycin hexapeptide dissolved in dilute aqueous CH_3CN were then combined and concentrated *in vacuo* to yield the title compound as an off-white solid (27 mgs, 20 µmol, 30 %); LCMS (method 1) *m/z* 662.2 ($M+2H^+$ ion), retention time 5.20 minutes. NMR consistant with data from above experiment.

One pot production: Phenyl isothiocyanate (16 µl, 134 µmol, 1 eq) in DMF (200 µl) was added to a solution of vancomycin hydrochloride (200 mg, 134 µmol) in pyridine (0.8 ml) and water (0.8 ml). The mixture was then stirred at room temperature. Observations by MS over 120 hrs showed that the vancomycin had been consumed and converted to the hexapeptide (58) ($M+H^+$ 1321 *m/z*) *via* the intermediate thiourea ($M+H^+$ 1584 *m/z*). The reaction mixture was diluted with MeOH (~4 ml) and then evaporated to dryness. The resultant paste was repeated azeotroped with MeOH (5 ml portions) to remove the remaining water. The crude solid was dissolved in DMSO and purified *via* HPLC, on a discovery C-18 reverse phase column, with a gradient elution of 0 to 10 % CH_3CN in water with a 0.1 % TFA modifier. The resulting fractions containing vancomycin hexapeptide dissolved in dilute aqueous CH_3CN were then combined and concentrated *in vacuo* to afford the title compound as a thick white gum (148 mg, 112 µmol, 83%); *m/z* (ES) 1323.5 ($M+H^+$, 100 %), 1178.5 (M–vancosamine+H^+, 15 %), 1016.4 (M–both sugars+H^+, 10 %). NMR consistant with data from above experiment.

Without HPLC: Adapted from the conditions of Nicolaou.[20]

Phenyl isothiocyanate (60 µl, 505 µmol, 1.5eq) was added to a solution of vancomycin hydrochloride (500 mg, 337 µmol) in pyridine (5 ml) and water (5 ml). The mixture was then stirred at room temperature. After 3 hrs MS showed the vancomycin had been consumed and the mass ion, 1584 *m/z*, which corresponds to the thiourea, was present. The solution was therefore evaporated to dryness. The resultant residue was dissolved in DCM (2.5 ml) and TFA (0.5 ml, 673 µmol, 20 eq) was added. The solution was stirred for 3 hrs, and then evaporated to dryness. The resultant solid was dissolved in MeOH (~10 ml) and precipitated by the addition of acetone (~50 ml). The precipitate was collected *via* centrifugation and the solids dissolved in water (~10 ml) and freeze-dried. This yielded the title compound as an off-white solid (389 mg, 294 µmol, 87 %); HPLC (composition indicated as a percentage by comparing relative peak areas) – peak 1: retention time, 19.8 minutes, 9 %; peak 2: retention time, 22.1 minutes, 78 %; peak 3: retention time, 26.5 minutes, 13 % (gradient 0 – 15 % CH_3CN over 30 minutes); *m/z* (ES) 661.3 (M+2H, 100 %), 1323.1 ($M+H^+$, 69 %), 681.8 (unknown, 50 %), 647.3 (unknown, 40 %), 263.0 (thiohydantoin, 35 %), 1178.5 (M–vancosamine+H^+, 20 %). Used without further purification in coupling reactions.

50 mg purified via HPLC for use during the testing and afforded 32 mg of fluffy white solid after freeze-drying (64 % recovery, 56 % yield from vancomycin); HPLC (single peak) – retention time, 22.6 minutes (gradient 0 – 15 % CH3CN over 30 minutes), retention time, 11.1 minutes (gradient 0 – 95 % CH3CN over 30 minutes); *m/z* (ES) Found M+, 1321.3334. $C_{59}H_{63}Cl_2N_8O_{23}$ requires M, 1321.3378.

4.5 Coupling of vancomycin hexapeptide and piperazine extenders

The analogues are named based on the terminating amino acid of the extender group and are numbered with an extension of the numbering system used in Pearce and Williams.[18]

This system numbers the amino acids of vancomycin sequentially from the *N*-terminus 1-7, and uses X to denote the α-protons and W to denote the protons on the amide nitrogens. Each proton of the residue is then denoted with the residue number and a letter. The extenders described here all have three amino acids (coloured red, blue and magenta in Figure 4.1) and are numbered sequentially from 8 to avoid confusion with the residues of vancomycin. The four methylenes of the piperazine ring have been numbered as substitutents of residue 8.

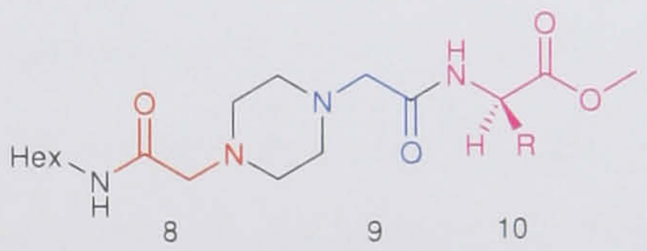

Figure 4.1. Naming convention for extending fragments.

Glycine analogue (58)

Coupling conditions adapted from Nicolaou.[20]

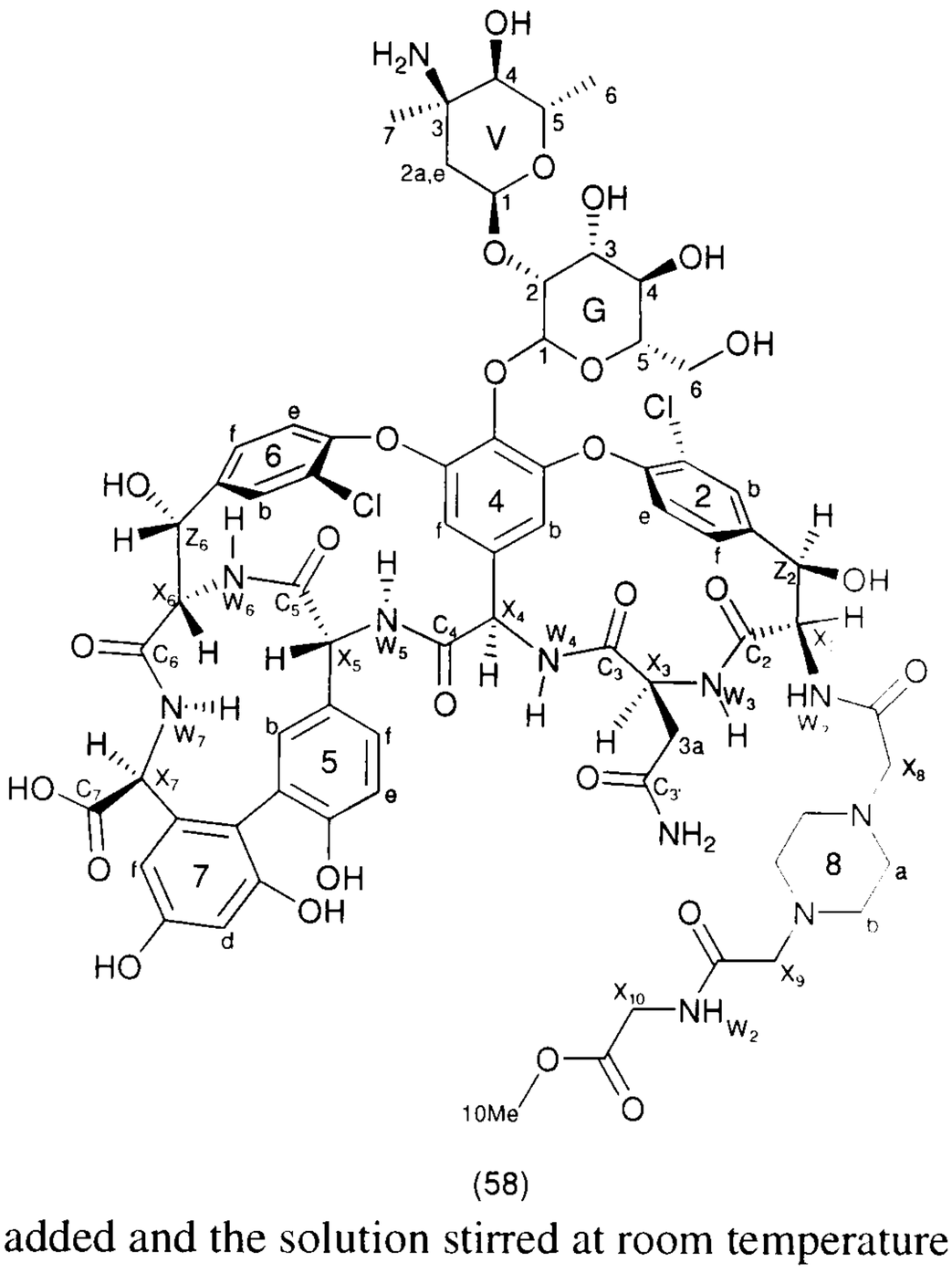

(58)

Piperazine (35) (41.5 mg, 126 mmol) was dissolved in TFA (3 ml, excess) and stirred for 4 hrs before being concentrated under vacuum and left under high vacuum for 14 hr to remove any residual TFA. Hexapeptide (50) (83.3 mg, 63 mmol, 0.5 eq) and HBTU (47.8 mg, 126 mmol, 1 eq) were added to the residue and the solids were put under vacuum for 15 minutes, then flushed with N_2, the exposure to vacuum and N_2 flush were repeated twice more and then the DMF (5 ml) and DIPEA (43.9 µl, 252 mmol, 2 eq) were added and the solution stirred at room temperature for 3 hrs. The reaction mixture was diluted with CH_3CN (50 ml); this precipitated the product, which was recovered *via* centrifuge. This solid was dissolved in water and purified by HPLC using a ThermoHypersil HyperPrep HS column and a gradient of 0 – 15 % CH_3CN over 30 minutes. The product fractions were then combined and concentrated under reduced pressure, this yielded a paste that was freeze dried to give the title compound as a cream solid (28.4 mg, 29 %); δ_H (d_6-DMSO, 500 MHz) 9.45 (1H, br s, OH), 9.16 (1H, s, OH), 9.11 (1H, s, OH), 8.69 (1H, d, J = 2.3, W_5), 8.46 (1H, d, J = 5.2, W_7), 8.04 (1H, s, W_4), 7.82 (1H, s, 6b), 7.73-7.52 (3H, m, 2b, W_2, W_{10}), 7.46 (1H, d, J = 8.4, 2f), 7.38-7.24 (3H, m, 6e, 6f, $CONH_2$), 7.20-7.11 (2H, m, 2e, 5b), 6.95 (1H, br s, W_3), 6.85 (1H, br s, $CONH_2$), 6.76 (1H, d, J = 8.5, 5f), 6.70 (1H, d, J = 8.5, 5e), 6.67 (1H, d, J = 11.6, W_6), 6.39 (1H, d, J = 1.8, 7d), 6.24 (1H, d, J = 1.8, 7f), 5.94 (2H, br s, Z_2-OH, Z_6-OH), 5.71 (1H, d, J = 7.9, X_4), 5.53 (1H, s, 4b), 5.45 (1H, br s, V_4-OH), 5.34 (1H, br s, G_4-OH), 5.28-5.15 (5H, m, 4f, G_1, V_1, Z_2, G_3-OH), 5.10 (1H, s, Z_6), 4.83-4.74 (1H, m, X_2), 4.67 (1H, q, J = 6.4, V_5), 4.50-4.33 (3H, m, X_3, X_5, X_7), 4.17 (1H, d, J = 11.6, X_6), 3.95-3.85 (3H, m, X_{10}, G_6-OH), 3.67 (1H, d, J = 10.7, G_{6a}), 3.67 (2H, obs, X_8, X_9), 3.62 (3H, s, 10Me), 3.60-2.52 (8H, m, 8a-b), 3.59-3.47 (3H, m, $G_{6a'}$, $X_{8'}$, $X_{9'}$), 3.37 (3H, obs, G_2, G_3, G_4), 3.27 (1H, s, G_5), 3.17 (1H, s, V_4), 2.43-2.32 (1H, m, 3a), 2.15 (1H, dd, J = 15.4,

4.4, 3a'), 1.90 (1H, d, J = 11.1, V_{2ax}), 1.72 (1H, d, J = 11.1, V_{2eq}), 1.28 (3H, s, V_7), 1.06 (3H, d, J = 6.4, V_6); δ_C ($CDCl_3$, 75 MHz) 172.5 (C), 172.5 (C), 171.2 (C), 170.5 (C), 170.5 (C), 170.1 (C), 170.1 (C), 169.6 (C), 169.1 (C), 167.8 (C), 167.2 (C), 157.2 (C), 156.6 (C), 155.1 (C), 152.3 (C), 151.3 (C), 150.1 (C), 148.3 (C), 142.5 (C), 139.5 (C), 136.1 (C), 135.7 (CH), 134.6 (C), 132.0 (CH), 128.8 (CH), 127.4 (CH), 127.4 (CH), 127.4 (CH), 126.3 (C), 126.3 (C), 126.1 (C), 125.6 (CH), 124.2 (CH), 123.4 (CH), 121.6 (C), 118.0 (C), 116.3 (CH), 107.3 (CH), 105.7 (CH), 104.7 (CH), 102.4 (CH), 101.3 (CH), 96.7 (CH), 78.2 (CH), 77.0 (CH), 76.7 (CH), 71.6 (CH), 70.7 (CH), 70.7 (CH), 70.2 (CH), 63.1 (CH), 61.8 (CH), 61.3 (CH_2), 61.3 (CH_2), 61.3 (CH_2), 58.8 (CH), 56.7 (CH), 54.9 (CH), 53.9 (C), 53.7 (CH), 51.8 (CH_3), 50.9 (CH), 40.5 (CH_2), 40.5 (CH_2), 33.2 (CH_3), 22.2 (CH_2), 16.7 (CH_3), (cross coupling in the HMQC also indicates presence of CH_2 signals obscured by solvent peak); HPLC (single peak) retention time, 24.8 minutes (gradient 0 – 15 % CH_3CN over 30 minutes); *m/z* (ES) 1432.9 (M–vancosamine+H^+, 100 %), 789.2 (M+2H^+, 69 %), 809.4 (unknown, 30 %), 1272.9 (M–both sugars+H^+, 28 %), 1577.9 (M+H^+, 22 %); (Found M^+, 1576.454, $C_{70}H_{80}Cl_2N_{11}O_{27}$ requires *M*, 1576.4597.

D-Phenylalanine analogue (61)

Coupling conditions adapted from Nicolaou.[20]

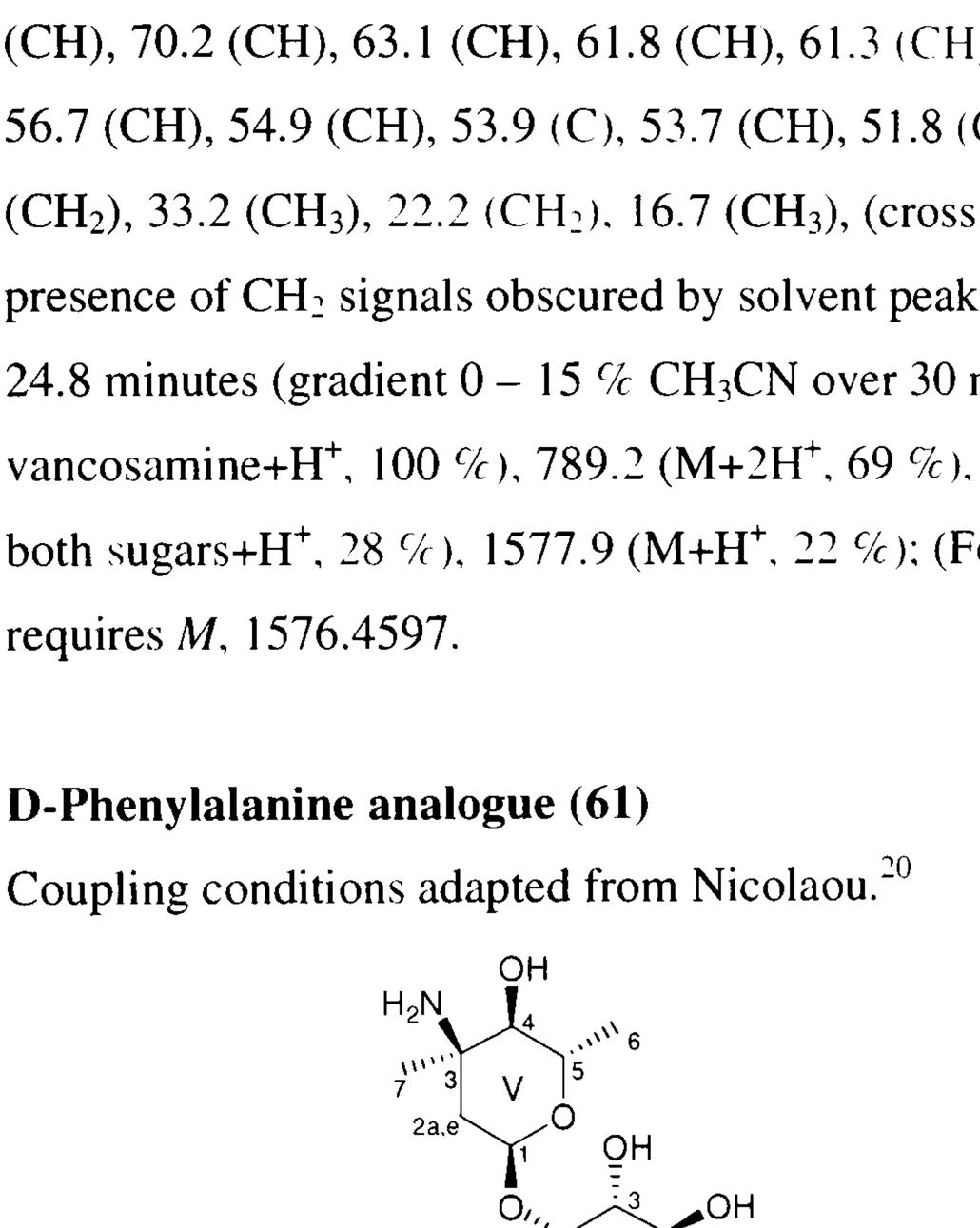

(61)

Piperazine (38) (127 mg, 303 µmol) was dissolved in TFA (4 ml, excess) and stirred for 3 hrs. The reaction mixture was then concentrated under vacuum and the sample left under high vacuum for 16 hr to remove any residual TFA. The residue and HBTU (115 mg, 303 µmol, 1 eq) were dissolved in DMF (4 ml). DIPEA (106 µl, 607 µmol, 2 eq) was added and the resultant solution was stirred for 15 minutes. The hexapeptide (50) (200 mg, 152 mmol, 0.5 eq) was put under vacuum for 15 minutes, while the above solution was stirred. The solution was then transferred *via* canular into the hexapeptide

and washed in with further DMF (3 ml). The resultant solution was stirred for 29 hrs, before being diluted with CH_3CN (50 ml); this precipitated the product, which was recovered *via* centrifuge. This solid was washed with further CH_3CN (2 × 50 ml), collecting *via* centrifuge each time. The crude solid was then dissolved in water and purified by HPLC using a ThermoHypersil HyperPrep HS column and a gradient of 0 – 40 % CH_3CN over 30 minutes. The product fractions were then combined and freeze dried to give the title compound as an off-white solid (55 mg, 33 μmol, 22 %): δ_H (d_6-DMSO, 500 MHz) 9.46 (1H, s, OH), 9.17 (1H, s, OH), 9.12 (1H, s, OH), 8.64 (1H, br s, W_5), 8.47 (1H, br s, W_7), 8.14 (1H, br s, W_4), 7.83 (1H, s, 6b), 7.65 (2H, br s, W_{10}, W_2), 7.46 (1H, d, J = 8.3, 6f), 7.35 (1H, obs, 2b), 7.34 (1H, obs, 6e), 7.29 (1H, obs, 10d), 7.27 (2H, obs, 10c), 7.21 (1H, obs, 10b), 7.20 (1H, obs, 2f), 7.16 (1H, obs, 2e), 7.16 (1H, br s, 5b), 7.06 (1H, br s, $CONH_2$), 6.77 (1H, br d, J = 8.3, 5f), 6.71 (1H, d, J = 8.3, 5e), 6.68 (1H, br s, W_6), 6.40 (1H, d, J = 2.0, 7d), 6.25 (1H, d, J = 2.0, 7f), 5.94 (1H, br s, Z_6OH), 5.94 (1H, br s, Z_2OH), 5.70 (1H, d, J = 8.0, X_4), 5.54 (1H, s, 4b), 5.46 (1H, br s, V_4OH), 5.36 (1H, br s, G_3OH), 5.27 (1H, obs, G_4OH), 5.25 (1H, obs, G1), 5.24 (1H, obs, V1), 5.21 (1H, obs, 4f), 5.21 (1H, obs, Z_2), 5.10 (1H, br s, Z_6), 4.79 (1H, br s, X_2), 4.68 (1H, q, J = 6.5, V_5), 4.61 (1H, td, J = 8.5, 5.1, X_{10}), 4.44 (1H, obs, X_5), 4.43 (1H, obs, X_7), 4.42 (1H, obs, X_3), 4.18 (1H, d, J = 10.7, X_6), 4.01 (1H, br s, G_6OH), 3.72-3.60 (1H, m, G_{6a}), 3.64 (3H, s, 10Me), 3.58-3.50 (1H, m, $G_{6a'}$), 3.50 (2H, obs, X_9), 3.50 (2H, obs, X_8), 3.54 (1H, obs, G_2), 3.43 (1H, obs, G_3), 3.26 (1H, obs, G_4), 3.27 (1H, br s, G_5), 3.16 (1H, br s, V_4), 3.11 (1H, dd, J = 13.7, 5.1, Z_{10}), 3.06-2.88 (1H, m, $Z_{10'}$), 2.69-2.21 (8H, obs, 8a-b), 2.39 (1H, obs, 3a), 2.15 (1H, br d, J = 13.3, 3a'), 1.91 (1H, br d, J 12.2, V_{2ax}), 1.73 (1H, br d, J = 12.2, V_{2eq}), 1.28 (3H, s, V_7), 1.07 (3H, d, J = 6.5, V_6); δ_C ($CDCl_3$, 75 MHz) 172.5 (C), 172.5 (C), 170.5 (C), 170.5 (C), 169.6 (C), 169.1 (C), 169.1 (C), 167.8 (C), 167.8 (C), 157.2 (C), 157.2 (C), 156.5 (C), 155.1 (C), 152.3 (C), 151.3 (C), 150.1 (C), 148.3 (C), 142.5 (C), 139.5 (C), 136.9 (C), 136.1 (C), 136.1 (C), 135.7 (CH), 134.6 (C), 132.0 (CH), 129.1 (CH), 129.1 (CH), 129.1 (CH), 128.8 (CH), 128.3 (CH), 128.3 (CH), 127.4 (CH), 127.4 (CH), 126.7 (C), 126.7 (CH), 126.2 (C), 126.1 (C), 125.5 (CH), 124.1 (CH), 123.4 (CH), 121.6 (C), 118.0 (C), 116.2 (CH), 107.3 (CH), 105.7 (CH), 104.7 (CH), 102.4 (CH), 101.3 (CH), 96.7 (CH), 78.2 (CH), 77.0 (CH), 76.7 (CH), 71.6 (CH), 70.7 (CH), 70.7 (CH), 70.2 (CH), 63.1 (CH), 61.8 (CH), 61.3 (CH_2), 61.3 (CH_2), 61.3 (CH_2), 58.6 (CH), 56.6 (CH), 54.9 (CH), 53.9 (C), 53.7 (CH), 52.8 (CH), 52.1 (CH_3), 50.9 (CH), 36.4 (CH_2), 36.4 (CH_2), 33.2 (CH_2), 22.2 (CH_3), 16.7 (CH_3), (cross coupling in the HMQC also indicates presence of CH_2 signals obscured by solvent peak); HPLC (single peak) retention time, 23.7 minutes (gradient 0

– 40 % CH_3CN over 30 minutes), retention time, 14.9 minutes (gradient 0 – 95 % CH_3CN over 30 minutes); *m/z* (ES) 834.5 (M+2H, 100 %), 854.9 (unknown, 31 %), 1668.2 ($M+H^+$, 5 %), 1523.3 (M–vancosamine+H^+, 4 %); (Found M^+. 1666.5238. $C_{77}H_{86}Cl_2N_{11}O_{27}$ requires *M* 1666.5066.

D-Phenylglycine analogue (63)

Coupling conditions adapted from Nicolaou.[20]

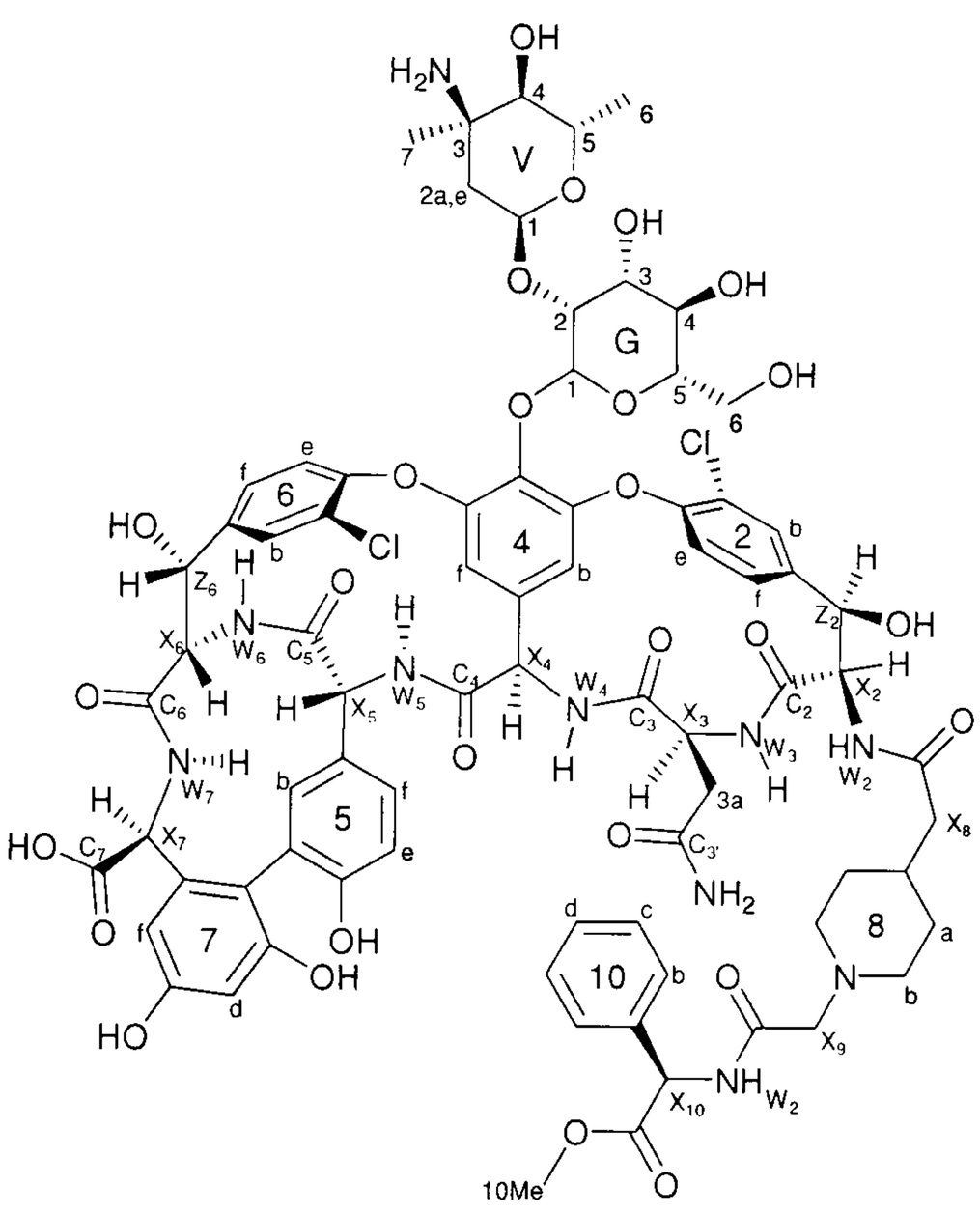

(63)

Piperazine (40) (83.4 mg, 206 µmol, 1.5 eq) was dissolved in TFA (2 ml, excess) and stirred for 3 hrs. The reaction mixture was then concentrated and the sample left under high vacuum for 16 hr to remove any residual TFA. The hexapeptide (50) (181 mg, 137 mmol) was put under vacuum for 1.5 hrs. The residue from the TFA cleavage and HBTU (72.8 mg, 303 µmol, 1.4 eq) were dissolved in DMF (6 ml). DIPEA (96 µl, 548 µmol, 4 eq) was added and the resultant solution was stirred for 45 minutes, whilst the hexapeptide was still under vacuum. The solution was then transferred *via* canular into the hexapeptide and washed in with further DMF (3 ml). The resultant solution was stirred for 19 hrs under N_2. The reaction mixture was diluted with CH_3CN (50 ml); this precipitated the crude product, which was recovered *via* centrifuge. This solid was washed with further CH_3CN (2 × 50 ml), collecting *via* centrifuge each time. The crude solid was then dissolved in water and purified by HPLC using a ThermoHypersil HyperPrep HS column and a gradient of 0 – 40 % CH_3CN over 30 minutes. The product fractions were then combined and freeze dried to give the title compound as an off-white solid (64 mg, 39 µmol, 28 %); δ_H (d_6-DMSO, 500 MHz) 9.46 (1H, s, OH), 9.17 (1H, s, OH), 9.15 (1H, s, OH), 8.62 (1H, s, W_5), 8.46 (1H, br d, *J* = 4.8, W_7), 8.19 (1H, s, W_4), 7.83 (1H, s, 6b), 7.80-7.52 (2H, m, W_2, W_{10}), 7.57 (1H, d, *J* = 7.9, 2f), 7.51 (1H, obs, 2b), 7.46 (1H, d, *J* = 8.5, 6f), 7.42-7.32 (5H, m, 10b-d), 7.32 (1H, d, *J* = 8.5, 6e), 7.21-7.13 (2H, m, 2e, 5b), 7.02 (1H, s, W_5), 6.85-6.74 (1H, m, 5f),

6.40 (1H, s, 7d), 6.24 (1H, s, 7f), 5.95 (1H, d, J = 5.9, Z_6-OH), 5.92 (1H, s, Z_2-OH), 5.71 (1H, d, J = 7.8, X_4), 5.53 (1H, s, 4b), 5.50-5.42 (2H, m, X_{10}, G_3-OH), 5.35 (1H, s, V_4-OH), 5.30-5.16 (4H, m, 4f, G_1, V_1, Z_2), 5.13-5.05 (2H, m, Z_6, G_4-OH), 4.67 (1H, q, J = 6.0, V_5), 4.52 (3H, m, X_3, X_5, X_7), 4.18 (1H, d, J = 11.1, X_6), 3.97 (1H, br s, G_6-OH), 3.64 (3H, obs, G_{6a}, X_8, X_9), 3.63 (3H, s, 10Me), 3.60-3.47 (3H, obs, $G_{6a'}$, $X_{8'}$, $X_{9'}$), 3.36 (3H, obs, G_2, G_3, G_4), 3.27 (1H, s, G_5), 3.17 (1H, d, J = 6.0, V_4), 2.98-2.40 (8H, m, 8a-b), 2.37-2.25 (1H, m, 3a), 2.13 (1H, dd, J = 14.8, 4.5, 3a'), 1.90 (1H, dd, J = 11.2, 3.5, V_{2ax}), 1.72 (1H, d, J = 11.2, V_{2eq}), 1.28 (3H, s, V_7), 1.06 (3H, d, J = 6.0, V_6); δ_C ($CDCl_3$, 75 MHz) 172.5 (C), 170.9 (C), 170.9 (C), 170.6 (C), 169.6 (C), 169.1 (C), 167.8 (C), 167.4 (C), 157.2 (C), 156.6 (C), 155.1 (C), 152.2 (C), 151.2 (C), 150.2 (C), 148.3 (C), 142.5 (C), 139.5 (C), 136.3 (C), 136.1 (C), 135.7 (CH), 134.6 (C), 132.0 (CH), 128.8 (CH), 128.8 (CH), 128.8 (CH), 128.3 (CH), 127.5 (CH), 127.5 (CH), 127.5 (CH), 127.4 (CH), 127.4 (CH), 126.8 (C), 126.3 (C), 126.1 (C), 125.6 (CH), 124.0 (CH), 123.5 (CH), 121.7 (C), 117.9 (C), 116.3 (CH), 107.2 (CH), 105.8 (CH), 104.7 (CH), 102.4 CH), 101.3 (CH), 96.8 (CH), 78.2 (CH), 77.0 (CH), 76.7 (CH), 71.6 (CH), 70.7(CH), 70.7(CH), 70.2 (CH), 63.1 (CH), 61.8 (CH), 61.3 (CH_2), 61.3 (CH_2), 61.3 (CH_2), 58.4 (CH), 56.7 (CH), 55.8 (CH), 54.8 (CH), 53.9 (CH), 52.4 (CH_3), 51.0 (CH), 37.8 (CH_2), 33.2 (CH_2), 22.2 (CH_3), 22.2 (CH_3), 16.7 (CH_3), (cross coupling in the HMQC also indicates presence of CH_2 signals obscured by solvent peak); HPLC (single peak) retention time, 21.0 minutes (gradient 0 – 40 % CH_3CN over 30 minutes), retention time, 12.9 minutes (gradient 0 – 95 % CH_3CN over 30 minutes); *m/z* (ES) 1510.1 (M–vancosamine+H^+, 100 %), 827.2 (M+2H^+, 67 %), 1655.4 (M+H^+, 45 %), 1347.9 (M–both sugars+H^+, 17 %); (Found M^+, 825.7420. $C_{76}H_{83}Cl_2N_{11}O_{27}$ requires M, 825.7424 (2+ ions).

4.6 Solid-phase synthesis of tripeptide (66)

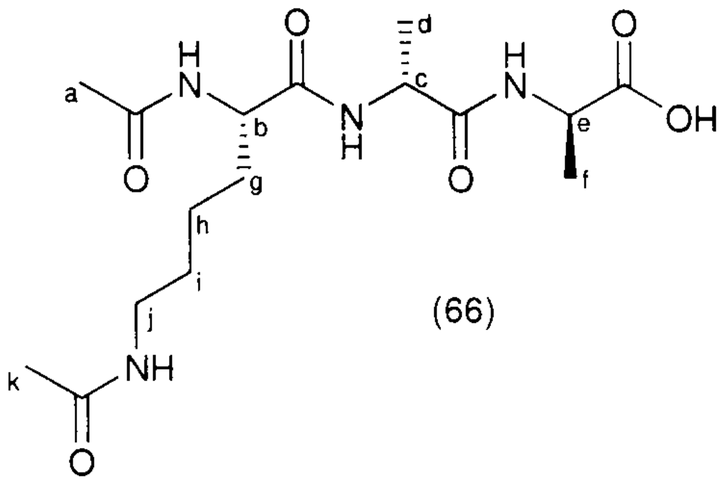

(66)

Wang resin pre-loaded with FMOC D-alanine (500 mg, 0.4 mmol) was coupled sequentially with FMOC D-alanine (249 mg, 0.8 mmol, 2 eq), then di-FMOC L-lysine (473 mg, 0.8 mmol, 2 eq). Removal of the FMOC protecting groups was accomplished with 20 % piperidine in DMF and each coupling used HATU (297 mg, 0.78 mmol, 1.95 eq) and DIPEA (279 µl, 1.6 mmol, 4 eq) dissolved in DMF. Conditions for the couplings, deprotections and washes as described in the Synthesis Notes section of the Novabiochem catolog.[21] After the final coupling the terminal amino groups of the lysine residue were deprotected with 20 % piperidine in DMF and then acylated by agitation with acetic anhydride (189 µl, 2 mmol, 5 eq) and pyridine (16 µl, 0.2 mmol, 0.5 eq) dissolved in DMF (3 ml) for 1 hr. The solution was drained and washed with DMF (3 × 3 ml). The resin then underwent a final wash with DCM (3x3 ml), 0.5 M aqueous acetic acid (3 × 3 ml), DMF (3 × 3 ml), DCM (3 × 3 ml), MeOH (2 × 3 ml) and was then dried over KOH under vacuum.

The peptide was then cleaved from the resin by agitation with TFA (5 ml) for 1 hr, followed by washing with TFA (2 × 3 ml) for 2 minutes per portion. The TFA was collected, combined and evaporated to 0.5 ml and then pipetted into ether (5 ml), which produced a precipitate. The precipitate was collected and purified by HPLC using a C-18 reverse phase column and 0-20 % CH_3CN gradient over 30 minutes. The resulting product fractions were combined and freeze-dried to give the title compound as an off-white solid (31 mg, 83 µmol, 21 %); HPLC (single peak) retention time, 17.3 minutes (gradient 0 – 20 % CH_3CN over 30 minutes), retention time, 9.4 minutes (gradient 0 – 95 % CH_3CN over 30 minutes); δ_H (D_2O, 300 MHz) 4.21 (1H, q, J = 7.4, H_c), 4.18 (1H, q, J = 7.2, H_e), 4.06 (1H, t, J = 7.2, H_b), 4.09 (1H, t, J = 6.8, H_j), 1.87 (3H, s, H_a), 1.82 (3H, s, H_k), 1.58 (1H, m, H_g), 1.37 (1H, quin, J = 7.1, H_i), 1.28 (3H, d, J = 7.4, H_d), 1.23 (3H, d, J = 7.2, H_e), 1.26-1.12 (1H, m, H_h); δ_C ($CDCl_3$, 75 MHz) 176.6 (C), 174.9 (C), 174.7 (C), 174.6 (C), 174.3 (C), 54.4 (CH), 49.8 (CH), 49.0 (CH), 39.5 (CH_2), 30.9 (CH_2), 28.2 (CH_2), 22.7 (CH_2), 22.2 (CH_3), 22.0 (CH_3), 16.8 (CH_3), 16.4 (CH_3); *m/z* (ES) (Found M^+, 373.2076. $C_{16}H_{29}N_4O_6$ requires M, 373.2082).

4.7 Testing

4.7.1 Nanoelectrospray ionisation – mass spectrometry (nano ESI-MS)[22]

The samples were analysed on an LCT Premier (Waters, Manchester, UK) equipped with a NanoMate (Advion Biosciences, Ithaca, NY, USA) automated injection and nano-electrospray ionisation interface. The solutions were prepared using HPLC grade solvents. Stock solutions (2 mM) were prepared and diluted 10-fold with 5 mM ammonium acetate buffer (pH 5.1). Equal volumes of each of the five glycopeptide solutions were then mixed separately with the tripeptide, this produced five separate solutions that each contained 100 μM of glycopeptide and 100 μM of tripeptide. An aliquot (5 microlitres) of the sample was injected with an electrospray voltage of 2kV. Data were acquired over the range *m/z* 500-3000, for 50 scans at a scan speed of 2.4 seconds per scan. A separate introduction of horse heart myoglobin was used to calibrate the spectra. The data were processed using MassLynx software by summing the 50 scans and producing a peak list with the profile data centred by mass. This list allowed the calculation of peak area as a measure of abundance for each ion. The peak areas for ions of each species were added together and used to calculate the concentration of each species; both peak area and concentration for each injection are shown in Table 4.2.

Glycopeptide	Species	Injection 1		Injection 2		Injection 3	
		Peak Area	Conc. (M)	Peak Area	Conc. (M)	Peak Area	Conc. (M)
hexapeptide	Free Drug	1.08 E+05	9.11E-05	1.06 E+05	9.15E-05	1.53 E+05	9.31E-05
	Complex	1.06 E+04	8.88E-06	9.92 E+03	8.55E-06	1.14 E+04	6.93E-06
	Total Drug	1.19 E+05	1.00E-04	1.16 E+05	1.00E-04	1.64 E+05	1.00E-04
vancomycin	Free Drug	8.40 E+04	3.08E-05	9.90 E+04	3.28E-05	1.05 E+05	3.55E-05
	Complex	1.89 E+05	6.92E-05	2.03 E+05	6.72E-05	1.91 E+05	6.45E-05
	Total Drug	2.73 E+05	1.00E-04	3.02 E+05	1.00E-04	2.96 E+05	1.00E-04
Glycine	Free Drug	4.91 E+04	2.63E-05	7.06 E+04	2.83E-05	7.50 E+04	2.89E-05
	Complex	1.38 E+05	7.37E-05	1.79 E+05	7.17E-05	1.85 E+05	7.11E-05
	Total Drug	1.87 E+05	1.00E-04	2.50 E+05	1.00E-04	2.60 E+05	1.00E-04
D-phenyl glycine	Free Drug	3.48 E+04	2.79E-05	1.37 E+05	2.96E-05	1.50 E+05	2.95E-05
	Complex	8.97 E+04	7.21E-05	3.25 E+05	7.04E-05	3.59 E+05	7.05E-05
	Total Drug	1.24 E+05	1.00E-04	4.62 E+05	1.00E-04	5.09 E+05	1.00E-04
D-phenyl alanine	Free Drug	5.23 E+04	2.13E-05	8.37 E+04	2.22E-05	7.89 E+04	2.19E-05
	Complex	1.93 E+05	7.87E-05	2.94 E+05	7.78E-05	2.82 E+05	7.81E-05
	Total Drug	2.45 E+05	1.00E-04	3.78 E+05	1.00E-04	3.61 E+05	1.00E-04

Table 4.2. Data from nano ESI-MS experiments.

4.7.2 Minimum inhibitory concentration (MIC)[23]

The MIC of antimicrobial agents were determined by broth microdilution in IsoSensitest broth (Oxoid, Basingstoke, UK) using and inoculum of 10^4 cells per ml for *Escherichia coli* or 10^6 cells per ml for *Staphylococcus aureus*. Antimicrobial agents were prepared in a two-fold dilution series in 50% DMSO (Sigma-Aldrich, Dorset, UK). Microwell plates with 96 wells (Nunc, Fisher Scientific, Loughborough, UK) containing the antimicrobial agent and bacterial suspension were incubated for 16h at 37°C in a Spectramax 384 plus microwell plate reader (Molecular Devices, Abingdon, UK), running SOFTmax PRO 3.1.1 software. Optical density readings (600nm) were taken at 10min intervals. Plates were shaken for 30 seconds before each reading. The MIC was taken as the lowest concentration of antimicrobial that prevented growth.

4.8 References

(1) Witiak, D. T.; Nair, R. V.; Schmid, F. A. Synthesis and Antimetastatic Properties of Stereoisomeric Tricyclic Bis(dioxopiperazines) in the Lewis Lung Carcinoma Model. *J. Med. Chem.* **1985**, *28*, (9), 1228-1234.

(2) Booij, L. H. D. J.; van der Broek, L. A. G. M.; Caulfield, W.; Dommerholt-Caris, B. M. G.; Clark, J. K.; van Egmond, J.; McGuire, R.; Muir, A. W.; Ottenheijm, H. C. J.; Rees, D. C. Non-depolarizing Neuromuscular Blocking Activity of Bisquaternary Amino Di- and Tripeptide Derivatives. *J. Med. Chem.* **2000**, *43*, (25), 4822-4833.

(3) Siebum, A. H. G.; Woo, W. S.; Lugtenburg, J. Preparation and Characterization of [5-^{13}C]-(2*S*,4*R*)-Leucine and [4-^{13}C]-(2*S*,3*S*)-Valine - Establishing Synthetic Schemes to Prepare Any Site-Directed Isotope of L-Leucine, L-Iisoleucine and L-Valine. *Eur. J. Org. Chem.* **2003**, 4664-4678.

(4) Horton, J. The Design and Synthesis of New and Selective Inhibitors of Bacterial MurD. In *Department of Chemistry*; University of Leeds: Leeds, 2003; pp 175.

(5) Mukaiyama, T.; Usui, M.; Schimada, E. A Convenient Method for the Synthesis of Carboxylic Esters. *Chem. Lett.* **1975**, *4*, (10), 1045-1048.

(6) Nozaki, S.; Kimura, A.; Muramatsu, I. Rapid Peptide Synthesis in Liquid Phase. Preparation of Angiotensin II as an Example. *Chem. Lett.* **1977**, 1057-1058.

(7) Nozaki, S.; Muramatsu, I. Rapid Peptide Synthesis in Liquid Phase. Preparation of Angiotensin II and Delta-sleep-inducing Peptide by the "Hold-in-Solution" Method. *Bull. Chem. Soc. Jpn.* **1982**, *55*, 2165-2168.

(8) Kataky, R.; Parker, D.; Teasdale, A.; Hutchinson, J. P.; Buschmann, H.-J. Binding Properties of Amide and Amide-Ester *N*-Functionalised Polyaza Macrocycles. *J. Chem. Soc., Perkin Trans. 2* **1992**, 1347-1351.

(9) Hulme, A. N.; Curley, K. S. Approaches to the synthesis of (2R,3S)-2-hydroxymethylpyrrolidin-3-ol (CYB-3) and its C(3) epimer: a cautionary tale. *J. Chem. Soc., Perkin Trans. 1* **2002**, *8*, 1083-1091.

(10) Almedida, J. F.; Anaya, J.; Martin, N.; Grande, M.; Moran, J. R.; Caballero, M. C. New Enantioselective Synthesis of 4-Hydroxy-2-Oxopyrolidine-*N*-Acetamide (Oxiracetam) from Malic Acid. *Tetrahedron: Asymmetry* **1992**, *3*, (11), 1431-1440.

(11) Webb, R. G.; Haskell, M. W.; Stammer, C. H. A Nuclear Magnetic Resonance Method for Distinguishing α-Amino Acids from β and γ Isomers. *J. Org. Chem.* **1969**, *34*, (3), 576-580.

(12) Nozaki, S. Efficient Amounts of Additives for Peptide Coupling Mediated by a Water-soluble Carbodiimide in Aqueous Media. *Chem. Lett.* **1997**, 1-2.

(13) Hsu, F.-L.; Hamada, A.; Booher, M. E.; Fuder, H.; Patil, P. N.; Miller, D. D. Optically Active Derivatives of Imidazolines. α-Adrenergic Blocking Properties. *J. Med. Chem.* **1980**, *23*, (11), 1232-1235.

(14) Carboni, C.; Quaedflieh, P. J. L. M.; Broxterman, Q. B.; Linda, P.; Gardossi, L. Quantative enzymatic protection of D-amino acid methyl esters by exploiting 'relaxed' enantioselectivity of penicillin-G amidase in organic solvent. *Tetrahedron Lett.* **2004**, *45*, 9649-9652.

(15) He, Y.; Chen, Y.; Du, H.; Schmid, L. A.; Lovely, C. J. A convenient synthesis of 1,4-disubstituted imiazoles. *Tetrahedron Lett.* **2004**, *45*, 5529-5532.

(16) Danila, G.; Cojocaru, Z.; Nechifor, M.; Dorneanu, V. 8-[4-(Phenyl-1-piperazinyl)methyl]theophylline: Romania, 1986, RO 88944.

(17) Booth, P. M.; Williams, D. H. Preparation and Conformational Analysis of Vancomycin Hexapeptide and Aglucovancomycin Hexapeptide. *J. Chem. Soc., Perkin Trans. 1* **1989**, 2335 - 2339.

(18) Pearce, C. M.; Williams, D. H. Complete Assignment of the ^{13}C NMR Spectrum of Vancomycin. *J. Chem. Soc., Perkin Trans. 2* **1995**, 153-157.

(19) Rydberg, P.; Lüning, B.; Wachtmeister, C. A.; Eriksson, L.; Törnqvist, M. Applicability of a Modified Edman Procedure for Measurement of Protein Adducts: Mechanisms of Formation and Degradation of Phenylthiohydantoins. *Chem. Res. Toxicol.* **2002**, *15*, (4), 570-581.

(20) Nicolaou, K. C.; Cho, S. Y.; Hughes, R.; Winssinger, N.; Smethurst, C.; Labischinski, H.; Endermann, R. Solid- and Solution-Phase Synthesis of Vancomycin and Vancomycin Analogues with Activity against Vancomycin-Resistant Bacteria. *Chem. Eur. J.* **2001**, *7*, (17), 3798 - 3823.

(21) Novobiochem Synthesis Notes. *The Fine Art of Solid-Phase Synthesis*, 2002/3 catalog.

(22) Jørgensen, T. J. D.; Roepstorff, P.; Heck , A. J. R. Direct Determination of Solution Binding Constants for Noncovalent Complexes between Bacterial Cell Wall Peptide Analogues and Vancomycin Group Antibiotics by Electrospray Ionization Mass Spectrometry. *Anal. Chem.* **1998**, *70*, (20), 4427-4432.

(23) Bostock, J. M. Institute for Molecular and Cellular Biology, Department of Biochemistry and Microbiology, University of Leeds, 2006.

Appendix A

HPLC trace of hexapeptide purified by precipitation

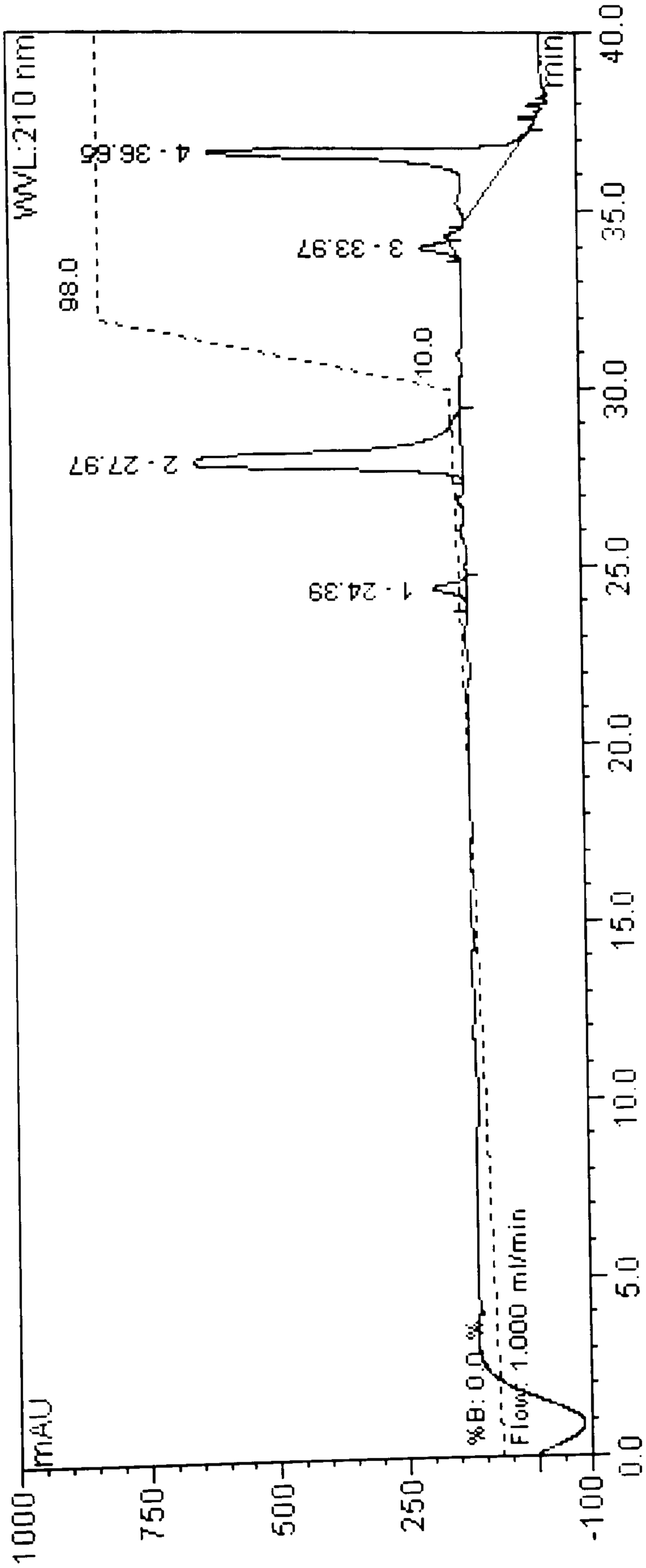

Appendix B

HPLC trace of vancomycin before HPLC purification